SPRINGER TRACTS
217 IN MODERN PHYSICS

Stefan Kehrein

The Flow Equation Approach to Many-Particle Systems

Springer

Springer Tracts in Modern Physics
Volume 217

Springer Tracts in Modern Physics

Springer Tracts in Modern Physics provides comprehensive and critical reviews of topics of current interest in physics. The following fields are emphasized: elementary particle physics, solid-state physics, complex systems, and fundamental astrophysics.
Suitable reviews of other fields can also be accepted. The editors encourage prospective authors to correspond with them in advance of submitting an article. For reviews of topics belonging to the above mentioned fields, they should address the responsible editor, otherwise the managing editor.
See also springer.com

Stefan Kehrein

The Flow Equation Approach to Many-Particle Systems

With 24 Figures

Springer

Stefan Kehrein
Ludwig-Maximilians-Universität München
Fakultät für Physik
Theresienstr. 37
80333 München
Germany
E-mail: stefan.kehrein@physik.lmu.de

Library of Congress Control Number: 2006925894

Physics and Astronomy Classification Scheme (PACS):
01.30.mm, 05.10.Cc, 71.10.-w

ISSN print edition: 0081-3869
ISSN electronic edition: 1615-0430
ISBN-10 3-540-34067-X Springer Berlin Heidelberg New York
ISBN-13 978-3-540-34067-6 Springer Berlin Heidelberg New York

Springer is a part of Springer Science+Business Media
springer.com

Printed in The Netherlands

Typesetting: by the author using a Springer LaTeX macro package
Cover concept: eStudio Calamar Steinen
Cover production: *design &production* GmbH, Heidelberg

Printed on acid-free paper SPIN: 10985205 56/techbooks 5 4 3 2 1 0

To Michelle

Preface

Over the past decade, the flow equation method has developed into a new versatile theoretical approach to quantum many-body physics. Its basic concept was conceived independently by Wegner [1] and by Głazek and Wilson [2, 3]: the derivation of a unitary flow that makes a many-particle Hamiltonian increasingly energy-diagonal. This concept can be seen as a generalization of the conventional scaling approaches in many-body physics, where some ultraviolet energy scale is lowered down to the experimentally relevant low-energy scale [4]. The main difference between the conventional scaling approach and the flow equation approach can then be traced back to the fact that the flow equation approach retains all degrees of freedom, i.e. the full Hilbert space, while the conventional scaling approach focusses on some low-energy subspace. One useful feature of the flow equation approach is therefore that it allows the calculation of dynamical quantities on all energy scales in one unified framework.

Since its introduction, a substantial body of work using the flow equation approach has accumulated. It was used to study a number of very different quantum many-body problems from dissipative quantum systems to correlated electron physics. Recently, it also became apparent that the flow equation approach is very suitable for studying quantum many-body nonequilibrium problems, which form one of the current frontiers of modern theoretical physics. Therefore the time seems ready to compile the research literature on flow equations in a consistent and accessible way, which was my goal in writing this book.

The choice of material presented here is necessarily subjective and motivated by my own research interests. Still, I believe that the work compiled in this book provides a pedagogical introduction to the flow equation method from simple to complex models while remaining faithful to its nonperturbative character. Most of the models and examples in this book come from condensed matter theory, and a certain familiarity with modern condensed matter theory will be helpful in working through this book.[1] Purposely, this book is focussed on the method and not on the physical background and motivation of the models discussed. By working through it, a student or researcher

[1] An excellent and highly recommended introduction is, for example, P.W. Anderson's classic textbook [4].

should become well equipped to investigate models of one's own interest using the flow equation approach. Most of the derivations are worked out in considerable detail, and I recommend to study them thoroughly to learn about the application and potential pitfalls of the flow equation approach.

The flow equation approach is under active development and many issues still need to be addressed and answered. I hope that this book will motivate its readers to contribute to these developments. I will try to keep track of such developments on my Internet homepage, and hope for e-mail feedback from the readers of this book. In particular, I am grateful for mentioning typos, which will be compiled on my homepage.

Both in my research on flow equations and in writing the present book, I owe debts of gratitude to numerous colleagues. First of all, I am deeply indebted to my Ph.D. advisor Franz Wegner, whose presentation of his new "flow equation scheme" in our Heidelberg group seminar in 1992 started both this whole line of research and my involvement in it. I also owe a very special acknowledgment to Andreas Mielke, with whom I have started my work on flow equations back in 1994. Our joint work has set the foundations of many of the developments presented in this book. During my work on flow equations, I have also profited greatly from many discussions with Dieter Vollhardt. I am particularly grateful to him for his continued interest and encouragement.

I also thank the participants of my flow equation lecture in Augsburg during the summer term 2005, which gave me the opportunity to test my presentation of the material that is compiled in this book. Among them I am especially thankful to Peter Fritsch, Lars Fritz, Andreas Hackl, Verena Körting, and Michael Möckel for proofreading parts of this manuscript.

The original idea to write this book is due to a suggestion by Peter Wölfle, and I am very grateful to him for starting me on this project and for his continued interest in the flow equation approach in general. This book project and a lot of the research compiled in it has only been possible due to a Heisenberg fellowship of the Deutsche Forschungsgemeinschaft (DFG). This gave me the necessary free time to pursue this project, and it is pleasure to acknowledge the DFG for this generous and unbureaucratic support through the Heisenberg program.

Finally, I thank my colleagues at the University of Augsburg for many valuable discussions, and everyone else not mentioned here by name with whom I have worked on flow equations in the past decade.

For everything else and much more, I thank Michelle.

Augsburg *Stefan Kehrein*
February 2006

References

1. F. Wegner, Ann. Phys. (Leipzig) **3**, 77 (1994)
2. S.D. Głazek and K.G. Wilson, Phys. Rev. D **48**, 5863 (1993)
3. S.D. Głazek and K.G. Wilson, Phys. Rev. D **49**, 4214 (1994)
4. P.W. Anderson: *Basic Notions of Condensed Matter Physics*, 6th edn (Addison-Wesley, Reading Mass. 1996)

Contents

1 Introduction

This introductory chapter provides a brief overview of the flow equation method and its relation to other methods in condensed matter theory. The aim of this chapter is to define the framework of the method, which will be filled out in more detail in the following chapters of this book.

1.1 Motivation

The fundamental challenge of condensed matter theory can be summed up by the observation that while we know all the relevant laws of nature for describing condensed matter systems, the number of degrees of freedom in such systems is typically much too large to allow a direct solution based on these laws. This observation is reflected in the multitude of phenomena that can be observed in condensed matter systems, from different kinds of ordering to phase transitions and novel states of matter like superconductivity and fractional Quantum Hall liquids. In order to arrive at a theoretical understanding of such complex phenomena, various stages of simplifications and suitable modeling are necessary. The resulting many-particle model then needs to be solved with a reliable theoretical method.

Theoretical methods for solving quantum many-particle problems can be broadly classified in three main categories:

1. Perturbative analytical expansions
2. Exact analytical solutions
3. Numerical solutions using computers

All these approaches have their specific advantages and shortcomings. Perturbative methods require the identification of a sufficiently small parameter that allows a reliable expansion. Exact analytical solutions like Bethe ansatz methods work only for very specific (integrable) Hamiltonians. Numerical solutions often have to be performed for system sizes that are far smaller than the experimentally relevant one, and therefore a (potentially difficult) extrapolation is necessary.

Many condensed matter systems are nowadays well-understood through the solution techniques developed in each of these approaches during the past decades. In this context, a special role has been played by renormalization and

Stefan Kehrein: *The Flow Equation Approach to Many-Body Problems*
STMP **217**, 1–9 (2006)

scaling ideas, which have led to the classification of microscopically very different systems into specific universality classes that show the same *universal* behavior. The behavior on large length scales or at sufficiently small energies turns out to be insensitive to the specific details of the microscopic interactions [1]. However, many condensed matter systems that involve strong electron correlations like in high temperature superconductors or heavy fermion materials have so far been out of our reach, and provide a major motivation for developing new theoretical tools.

This book introduces the reader to such a new analytical approach to quantum many-particle systems, the so-called *flow equation method* introduced by Wegner in 1994 [2]. The flow equation method has by now found many interesting applications in different fields of condensed matter physics. Independently, Głazek and Wilson developed similar ideas in the context of high-energy physics, the so-called *similarity renormalization scheme* [3, 4]. Essentially, both approaches are analytical methods that generalize scaling ideas in the sense that they generate a renormalized perturbative expansion. However, different from conventional scaling approaches one does not focus solely on the low-energy physics. Remarkably, these methods also turned out to be applicable in certain strong-coupling problems, where conventional perturbative scaling yields diverging coupling constants.

In this book we will be mainly interested in condensed matter systems and therefore use the original terminology *flow equations* introduced by Wegner in 1994 [2].

1.2 Flow Equations: Basic Ideas

Condensed matter systems are often characterized by very different energy scales: electronic band widths are typically of the order of a few eV, while temperatures in experiments can be two or more order of magnitude smaller. This implies that a theoretical calculation needs to yield reliable results on an energy scale that is much smaller than the intrinsic energy scales of the model. In such a situation one needs to do perturbation theory with respect to large energy differences first before proceeding to smaller energy differences, even if a small expansion parameter is present in the model [5].[1]

Scaling concepts in condensed matter theory embody this principle of *energy scale separation* by iteratively reducing an ultraviolet (UV)-cutoff Λ_{RG} from its initial value down to the experimentally relevant scale. This is achieved by performing a perturbative calculation with a *running coupling constant* that depends on the energy scale.

A schematic view of this procedure is depicted in Fig. 1.1a. The matrix denotes a many-particle Hamiltonian with single-particle energies on

[1] This situation is similar to atomic physics where one first calculates, e.g., the fine structure of the spectrum before deriving the hyperfine splittings based on these eigenstates calculated before.

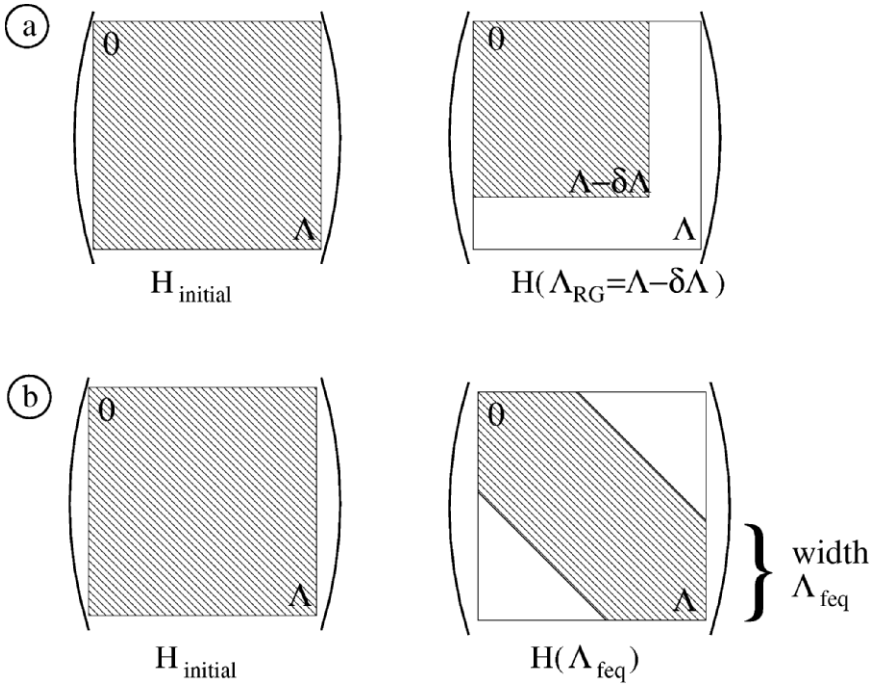

Fig. 1.1. Schematic view of different scaling approaches: (**a**) Conventional scaling methods successively reduce the high-energy cutoff $\Lambda_{\rm RG}$. (**b**) Flow equations make the Hamiltonian successively more band-diagonal with an effective band width $\Lambda_{\rm feq}$

the diagonal reaching from the lowest energy $E = 0$ to the UV-cutoff Λ.[2] The shaded off-diagonal matrix elements correspond to non-vanishing couplings between these various modes. In the conventional scaling approach, one then eliminates degrees of freedom with single-particle energies in the interval $[\Lambda - \delta\Lambda, \Lambda]$ by, e.g., integrating out these degrees of freedom in a path integral framework. Thereby one finds a Hamiltonian with a reduced cutoff $\Lambda_{\rm RG}$ and modified coupling constants that describes the same physics in the Hilbert space with the retained degrees of freedom $[0, \Lambda_{\rm RG}]$, where $\Lambda_{\rm RG} = \Lambda - \delta\Lambda$. The flow of the coupling constants is generated from the mode elimination and generally only accessible in perturbation theory. This leads to the scaling equations for the coupling constants upon varying $\Lambda_{\rm RG}$.

Let us for example consider a (renormalizable) theory with only one running dimensionless coupling $g(\Lambda_{\rm RG})$ and a single dimensionful parameter which is the cutoff $\Lambda_{\rm RG}$. One then finds the following scaling equation

[2] This is a highly simplified picture since an interacting many-body Hamiltonian cannot in general be represented as a simple matrix. However, we will see later on that the lessons learned from this picture apply for the general case as well.

$$\frac{\mathrm{d}g(\Lambda_{\mathrm{RG}})}{\mathrm{d}\ln\Lambda_{\mathrm{RG}}} = \beta\left(g(\Lambda_{\mathrm{RG}})\right) \ , \tag{1.1}$$

with a β-function that is usually determined in an expansion in the running coupling constant. The differential with respect to the logarithm on the left hand side of (1.1) appears naturally since the cutoff Λ_{RG} is the only dimensionful parameter.[3]

The fundamental property of the scaling approach is that the Hamiltonians $H[g(\Lambda_{\mathrm{RG}}), \Lambda_{\mathrm{RG}}]$ describe the same low-energy physics in the remaining low-energy Hilbert space when the coupling is varied according to the scaling equation (1.1). Although the β-function in (1.1) is typically only known perturbatively up to a certain power in g, the iterative procedure embodied by the differential scaling equation allows one to recover nonperturbative energy scales proportional to fractional powers of the coupling constant g^α with α not an integer, or energy scales behaving like $\exp(-1/g)$. Such non-analytic behavior in the coupling constant around the expansion point $g = 0$ renders naive perturbation theory for such energy scales in powers of g impossible.[4] A pragmatic way of thinking about scaling concepts is that they provide a tool to reorganize perturbation theory into a better-behaved convergent expansion by doing a perturbation expansion for the β-function instead of directly for the physical observable. Also, by analyzing the possible low-energy fixed points of the scaling flow one can identify universality classes and universal properties of such microscopic models. Here "*universal*" refers to the observation that only certain fixed points of the scaling flow are possible with properties that are largely independent from the details of the original bare interactions: Universality classes are typically determined by symmetries and dimensionality. The reader is referred to the extensive literature on this subject for more information about these beautiful concepts that have played a major role in modern condensed matter theory and beyond (see, for example, [1]).

The flow equation method depicted in Fig. 1.1b embodies the same principle of energy scale separation as the conventional scaling approach. However, the basic idea of the flow equation method is to *retain the full Hilbert space*. The Hamiltonian is made successively more energy-diagonal, that is band-diagonal in Fig. 1.1b. Another way of expressing this is to say that we iteratively reduce the *energy-diagonality parameter* Λ_{feq} of the Hamiltonian. Different from conventional scaling one does not lower some absolute UV-cutoff Λ_{RG}, but rather reduces the "cutoff" Λ_{feq} of the energy transfer of interaction matrix elements.

From the point of view of low-energy physics close to energy $E = 0$, we can consider both methods as effectively equivalent with $\Lambda_{\mathrm{feq}} \propto \Lambda_{\mathrm{RG}}$. One

[3] Furthermore, renormalizability ensures that the right hand side of (1.1) only depends on the coupling constant.

[4] A famous example is the Kondo temperature which behaves like $\exp(-1/\rho_F J)$, where $J > 0$ is the antiferromagnetic exchange coupling.

can see in Fig. 1.1b that excitations to high energies $E \gg \Lambda_{\rm feq}$ are suppressed by higher powers of the running coupling constant (which is as usual assumed to be small) in the flow equation procedure. In this way, the flow equation framework is a generalization of the conventional scaling approach with the additional feature of retaining the full Hilbert space. As we will see below, the price that we have to pay for this is a more complex set of scaling equations.

The benefit of this new approach is obviously that we keep information on all energy scales of our system. This is important in situations where we are interested in

- correlation functions on all energy scales
- systems that contain competing energy scales
- non-equilibrium models.

We will discuss examples for all these applications later on in this book. It should already be mentioned that in particular the analysis of non-equilibrium problems has recently emerged as a very interesting and promising direction for the flow equation approach. Non-equilibrium, either by preparing a non-equilibrium initial state or by continuously supplying the system with energy, is characterized by many energy scales that contribute to the low-temperature behavior. Therefore conventional scaling methods are problematic in such situations since one "loses" degrees of freedom during the scaling procedure. We will discuss examples for such applications in Sect. 5.2 and Sect. 5.3.

Our basic goal of implementing a scaling flow of the Hamiltonian while retaining the full Hilbert space effectively dictates the choice of the method for generating the Hamiltonians $H(\Lambda_{\rm feq})$. Clearly, the conventional elimination of degrees of freedom in a path integral framework is impossible. Since we want the spectrum of the flowing Hamiltonian to remain unchanged, we are naturally led to look for unitary transformations that connect the Hamiltonians $H(\Lambda_{\rm feq})$ in Fig. 1.1b. And since we need to respect energy scale separation to create a stable expansion, these transformations will be infinitesimal unitary transformations. During the early stages of the flow (for large $\Lambda_{\rm feq}$) we eliminate the off-diagonal matrix elements in Fig. 1.1b that couple modes with large energy differences, while during later stages of the flow we start eliminating couplings between more energy-degenerate states.

Any one-parameter family of unitarily equivalent Hamiltonians $H(B)$ can be generated by the solution of the differential equation (*flow equation*)

$$\frac{{\rm d}H(B)}{{\rm d}B} = [\eta(B), H(B)] \tag{1.2}$$

with an antihermitean *generator* $\eta(B)$

$$\eta(B) = -\eta^\dagger(B) \ . \tag{1.3}$$

All these Hamiltonians $H(B)$ are unitarily equivalent to the initial Hamiltonian $H(B = 0)$ if one can solve (1.2) exactly. However, an exact solution

of (1.2) is generally not possible for generic many-body problems. Therefore we want to create a systematic expansion where our Hamiltonians $H(B)$ are approximately unitarily equivalent to $H(B = 0)$ with an error that can be reduced by going to higher orders in the expansion. A stable way to create such a systematic expansion is by using energy scale separation as our guideline as depicted in Fig. 1.1b. The generator $\eta(B)$ should therefore first (for small B) eliminate interaction matrix elements that couple modes with large energy differences, while it decouples more degenerate states for larger values of the flow parameter B.

This *canonical generator* that eliminates the interaction matrix elements while respecting energy scale separation has been constructed by Wegner in the following manner [2]. We denote by H_0 the diagonal part of the Hamiltonian and by H_{int} the interaction part that we want to eliminate. Wegner's canonical generator is then defined via another commutator,

$$\eta(B) \stackrel{\text{def}}{=} [H_0(B), H_{\text{int}}(B)] \; . \tag{1.4}$$

It immediately follows that $\eta(B)$ is antihermitean from its construction as a commutator of two hermitean operators. $\eta(B)$ has dimension $(\text{Energy})^2$ since the Hamiltonian has dimension (Energy) and, consequently, the flow parameter B in (1.2) has dimension $(\text{Energy})^{-2}$. We will later see that the canonical generator (1.4) creates exactly the desired kind of energy scale separation in the Hamiltonian flow with the identification

$$\Lambda_{\text{feq}} = B^{-1/2} \; . \tag{1.5}$$

The interplay of the two equations (1.2) and (1.4) will be of central importance throughout this book and encodes the basic framework of the flow equation method. Since the Hamiltonian $H(B)$ eventually becomes diagonal (typically in a certain order of an expansion), the flow equation method is sometimes also denoted as *flow equation diagonalization*. However, different from exact diagonalization methods like the Bethe ansatz it can be used for generic non-integrable Hamiltonians. The purpose of the flow equation method is specifically not to compete with exact analytical diagonalization methods, but rather to be applicable to generic quantum many-body Hamiltonians and to diagonalize them in an approximate systematic expansion that is nonperturbative in nature.

The basic problem of the flow equation method follows from the observation that the system of equations (1.2) and (1.4) generates higher and higher order interaction terms if one starts with a generic many-body Hamiltonian $H(B = 0)$. Therefore one needs to find a systematic truncation scheme that renders this system of equations solvable. Typically this will be the running coupling constant like in conventional scaling approaches. However, in Sect. 5.1 we will discuss examples where the expansion parameter of the flow equation method is actually not the running coupling constant, but a parameter that remains finite even in certain strong-coupling models where

conventional scaling leads to diverging coupling constants. This has opened the exciting perspective to solve such strong-coupling models like the Kondo model, which play a central role in modern condensed matter theory, in a controlled analytical way without relying on integrability. Based on this flow equation solution one can then also study deviations away from the integrable point, like couplings to other degrees of freedom.[5]

Once a many-particle Hamiltonian is diagonalized with the flow equation method, the next step is to discuss expectation values of observables and correlation functions. Since $H(B=\infty)$ is diagonal it generates a very simple time evolution $\mathrm{e}^{-\mathrm{i}H(B=\infty)t}$. However, this simple time evolution acts on the unitarily transformed observables. If we are interested in an observable O, we need to solve the differential equation

$$\frac{\mathrm{d}O(B)}{\mathrm{d}B} = [\eta(B), O(B)] \tag{1.6}$$

with the same generator $\eta(B)$ that has been employed to diagonalize the Hamiltonian. The initial condition of (1.6) is $O(B=0)=O$. The time evolution $\mathrm{e}^{-\mathrm{i}H(B=\infty)t}$ then acts on the transformed observable $O(B=\infty)$. The solution of (1.6) typically leads to transformed operators $O(B=\infty)$ that have a very complicated structure, while the Hamiltonian $H(B=\infty)$ has become very simple. Still, the time evolution is straightforward and can be used to discuss correlation functions on all energy scales as will be explored later in this book.

From this first presentation of the basic ideas of the flow equation method, we will now proceed to a systematic and more mathematical discussion in the subsequent chapters.

1.3 Outline and Scope of this Book

The main purpose of this book is to give the reader a good working knowledge of the flow equation method, so that it can be applied successfully to one's own problems. We will first discuss the fundamental technical aspects of the flow equation method in Chaps. 2 and 3, and then work out various applications to important many-body problems in Chap. 4. This core part of the book should provide a good basis from which the reader can understand the method with respect to both its advantages and its limitations. Chapter 5 then contains some more recent developments like strong-coupling models and non-equilibrium problems. Along the way, we will work out in detail many solutions of model Hamiltonians to illustrate the method. However, since our focus is to learn how to use the flow equation method, we will be more interested in the technical aspects of the flow equation method than in the

[5] An interesting example for this is provided by a model of Ising-coupled Kondo impurities which exhibits a remarkable quantum phase transition discussed in [6].

physical motivation behind these model Hamiltonians. For the latter we refer the reader to textbooks on condensed matter theory.

Chapter 2 contains the basic framework of the flow equation method as a tool to diagonalize many-body Hamiltonians and to derive flow equations with respect to the energy-diagonality parameter Λ_{feq} in Fig. 1.1b. These ideas are illustrated in Sect. 2.1.1, where we work out the flow equation solution of the potential scattering model very pedagogically and in all detail. While this model is trivial from a many-body point of view, its solution is an ideal stepping stone for the more complex problems encountered later on and highly recommended for detailed study.

Chapter 3 then deals with the transformation of observables under the unitary flow of the method. This is of central importance for practical applications of the flow equation method. It also shows one of its key advantages as compared to other scaling methods, namely the possibility to evaluate physical quantities on all energy scales in one unified framework. However, the transformation of observables is frequently the most confusing part of this method for readers familiar with conventional, e.g. diagrammatic, many-body techniques. The reason is that observables often change their form completely under the unitary flow. This somehow unfamiliar concept turns out to be a key point of the flow equation method. We illustrate this transformation of observables with a simple example (the resonant level model) in Sect. 3.3.2. Again this simple example is an ideal stepping stone before studying the more complex problems later on and recommended for detailed study.

Chapter 4 contains the application of the flow equation method to various interacting many-body problems that exhibit the complexity of generic interacting many-body Hamiltonians. We analyze the Kondo model in Sect. 4.2, where its flow equation solution is worked out in pedagogical detail in an expansion in the running coupling constant to third order. As an example of a bosonic model, we then study the spin–boson model in Sect. 4.3. This also helps us to better understand how dissipative effects emerge in a purely unitary Hamiltonian framework like the flow equation method.

Fermi liquid theory is the cornerstone of the modern theoretical understanding of interacting electron systems. In Sect. 4.4 we will work out the connection between it and the flow equation approach. In fact, the canonical application of the flow equation approach leads to Fermi liquid theory and can serve as one of its microscopic foundations. In particular, we will see how Landau's quasiparticles with a finite lifetime are related to the transformation of the fermionic creation and annihilation operators under this unitary flow.

Section 4.5.1 discusses a somehow different application of flow equations, namely the derivation of effective Hamiltonians. We re-analyze the famous Fröhlich unitary transformation [7] from the point of view of the flow equation method, and find a remarkably different result as first pointed out by Lenz and Wegner [8]. We will see how this is related to the fact that the flow

equation effective electron-electron interaction shows retardation effects in a Hamiltonian framework, which are very important for obtaining the correct superconducting transition temperature for many materials.

In Chap. 5 we then look at two aspects of the flow equation method that seem particularly promising for future research, namely strong-coupling problems in Sect. 5.1 and non-equilibrium problems in Sect. 5.2 and Sect. 5.3. For such problems traditional scaling methods face severe limitations, some of which can be overcome with the flow equation approach.

In Sect. 5.1 we investigate the sine–Gordon model. The sine–Gordon model is a one-dimensional strong-coupling model of paradigmatic importance in many low-dimensional quantum systems. In its strong-coupling phase the conventional scaling approach eventually breaks down due to a diverging running coupling constant. Using flow equations one can identify an expansion parameter that is different from the running coupling constant, and thereby generate a systematic controlled expansion even in the strong-coupling phase. This allows one to study the full crossover from weak-coupling to strong-coupling physics in this model.

In Sect. 5.2 we then look at stationary non-equilibrium problems, here specifically the Kondo model with an applied voltage bias. The current-carrying steady state of this system is characterized by many energy scales that contribute to the low-temperature behavior. The fact that the flow equation method retains all degrees of freedom in the Hilbert space (as opposed to conventional scaling approaches) will turn out to be very important in such non-equilibrium models. A different application of the flow equation method to non-equilibrium problems is then discussed in Sect. 5.3, namely the real time evolution of a quantum system that is not prepared in its ground state. Again it is of key importance to retain the full Hilbert space and not only low-lying excitations close to the equilibrium ground state.

Section 5.4 concludes this book with an outlook into the future perspectives of the flow equation method and open questions.

References

1. P.W. Anderson: *Basic Notions of Condensed Matter Physics*, 6th edn (Addison-Wesley, Reading Mass. 1996)
2. F. Wegner, Ann. Phys. (Leipzig) **3**, 77 (1994)
3. S.D. Głazek and K.G. Wilson, Phys. Rev. D **48**, 5863 (1993)
4. S.D. Głazek and K.G. Wilson, Phys. Rev. D **49**, 4214 (1994)
5. K.G. Wilson, Rev. Mod. Phys. **47**, 773 (1975)
6. M. Garst, S. Kehrein, Th. Pruschke, A. Rosch, and M. Vojta, Phys. Rev. B **69**, 214413 (2004)
7. H. Fröhlich, Proc. Roy. Soc. A **215**, 291 (1952)
8. P. Lenz and F. Wegner, Nucl. Phys. B[FS] **482**, 693 (1996)

2 Transformation of the Hamiltonian

In this chapter we set up the basic framework of the flow equation approach to many-particle systems. We will do this by first clarifying the importance of energy scale separation in many-particle systems, and then use this as a guiding principle to develop the flow equation method. The fundamental ideas of the flow equation approach are summed up in Sect. 2.2.4. As a first example for the flow equation approach we solve a simple model in Sect. 2.3 and compare the flow equation solution with the conventional scaling approach.

2.1 Energy Scale Separation

Many of the most intriguing problems in condensed matter physics are characterized by vastly different energy scales: electron band widths or Coulomb energies are of the order of eV, while we are usually interested in excitations around the Fermi surface with an energy determined by the temperature. Even at room temperature these energy scales typically differ by two orders of magnitude. In a situation like this naive use of perturbation theory can lead to results that are entirely misleading even for small expansion parameters. This makes it necessary to organize perturbation expansions in a clever way to obtain accurate results. The well-established way to do this is by combining perturbation theory with scaling arguments. One first performs a perturbation expansion with respect to high-energy excitations, and then successively moves down in energy until one reaches the energy scale that one is experimentally or theoretically interested in. The flow equation method follows the same philosophy. However, we will see that it looks at energy differences (more precisely, at the energy transfer of interaction matrix elements) and not at absolute excitation energies above some ground state.

In this chapter, we introduce and discuss two important models that exemplify this observation of the breakdown of naive perturbation theory and the need to reorganize it using scaling arguments. The first model is the potential scattering model, which describes a potential scatterer in an electron gas. This leads to a quadratic Hamiltonian that can be solved exactly. However, even in this very simple model perturbation theory needs to be reorganized using scaling methods. In interacting (that is non-quadratic) problems

Stefan Kehrein: *The Flow Equation Approach to Many-Body Problems*
STMP **217**, 11–41 (2006)

this will generally be the only feasible procedure available for an analytical solution.

The potential scattering model allows us to study these tools in a controlled environment where everything can be checked explicitly and exactly. We will then revisit this model again in Sect. 2.3 and solve it using the flow equation method. A thorough understanding of the various approaches to this simple model is extremely helpful for studying more complex models. In fact, we will later see that we can even study strong-coupling behavior in this model.

A more challenging strong-coupling model is the Kondo model that we discuss afterwards. The Kondo model contains the full complexity of an interacting many-body problem and has become of paradigmatic importance in correlated electron physics. We will make the same observations regarding perturbation theory as in the potential scattering model. In Sect. 4.2 we will revisit the Kondo model and analyze it using the flow equation method. Understanding the various approaches to the Kondo model serves as a good basis for applying the flow equation approach to other problems in modern condensed matter theory.

2.1.1 Potential Scattering Model

One realization of the potential scattering model is a gas of spinless electrons interacting with an impurity potential $V(\boldsymbol{x})$. The Hamiltonian of this system is

$$H = \sum_{\boldsymbol{p}} \epsilon_{\boldsymbol{p}} c^\dagger_{\boldsymbol{p}} c_{\boldsymbol{p}} + \int \mathrm{d}\boldsymbol{x}\, V(\boldsymbol{x})\, c^\dagger(\boldsymbol{x}) c(\boldsymbol{x}) \ . \tag{2.1}$$

For the scattering potential we use a δ-function of strength g,

$$V(\boldsymbol{x}) = g\, \delta(\boldsymbol{x}) \ . \tag{2.2}$$

For spherical symmetry the Hamiltonian is effectively one-dimensional in terms of s-waves around the origin. The corresponding electron creation and annihilation operators are denoted by c_k and $c^\dagger_k$ with the fermionic anticommutation relation $\{c_k, c^\dagger_{k'}\} = \delta_{kk'}$. We discretize the system using N band states and the Hamiltonian takes the form

$$H = \sum_k \epsilon_k c^\dagger_k c_k + \frac{g}{N} \sum_{k,k'} c^\dagger_{k'} c_k \ . \tag{2.3}$$

We are interested in the thermodynamic limit $N \to \infty$ with the density of states

$$\rho(\epsilon) \stackrel{\mathrm{def}}{=} \sum_k \delta(\epsilon - \epsilon_k) \tag{2.4}$$

determined by the original problem (2.1). For simplicity we will use a constant density of states in a band of energy width D:

$$\rho(\epsilon) = \begin{cases} 1/D & \text{for } 0 < \epsilon < D \\ 0 & \text{otherwise.} \end{cases} \tag{2.5}$$

This density of states mimics the density of states of a two-dimensional tight-binding square lattice, which also exhibits a discontinuity of $\rho(\epsilon)$ at the band edge. This discontinuity turns out to be responsible for the nonperturbative behavior in the coupling constant g that we will find below.

Exact solution

For reference we first work out the exact solution for the spectrum of (2.3). This is an easy problem for this quadratic Hamiltonian. Of course, for interacting non-quadratic problems we will generally have to resort to perturbation theory. The Hamiltonian (2.3) can be written as an $N \times N$ matrix with

$$H = H_0 + H_{\text{int}} \tag{2.6}$$

and the diagonal part

$$H_0 = \begin{pmatrix} \epsilon_1 & 0 & \dots\dots\dots & 0 \\ 0 & \epsilon_2 & 0 & \dots\dots & 0 \\ 0 & 0 & \epsilon_3 & 0 & \dots & 0 \\ \dots & \dots & \dots & \dots & \dots & \dots \\ 0 & 0 & \dots\dots\dots & \epsilon_N \end{pmatrix} , \tag{2.7}$$

where $\epsilon_i = (i-1)\Delta\epsilon$, $\Delta\epsilon = D/(N-1)$. The interaction part is given by

$$H_{\text{int}} = \frac{g}{N} \begin{pmatrix} 1 & 1 & 1 & \dots\dots & 1 \\ 1 & 1 & 1 & \dots\dots & 1 \\ 1 & 1 & 1 & \dots\dots & 1 \\ \dots & \dots & \dots & \dots & \dots \\ 1 & 1 & 1 & \dots\dots & 1 \end{pmatrix} . \tag{2.8}$$

For an eigenvector $\boldsymbol{v} = (v_1, \dots, v_N)$ with eigenvalue E we can write

$$H\,\boldsymbol{v} = E\,\boldsymbol{v} \tag{2.9}$$

$$\Rightarrow \quad \forall i \quad E\,v_i = \epsilon_i\,v_i + \frac{g}{N}\sum_j v_j$$

$$\Rightarrow \quad v_i = \frac{g}{E-\epsilon_i}\,\frac{1}{N}\sum_j v_j \ . \tag{2.10}$$

Summing the left hand side of this equation over i allows us to eliminate the v_i's, and yields the following condition for the eigenvalue E:

$$\frac{1}{N}\sum_{i=1}^{N}\frac{1}{E-\epsilon_i} = \frac{1}{g} \ . \tag{2.11}$$

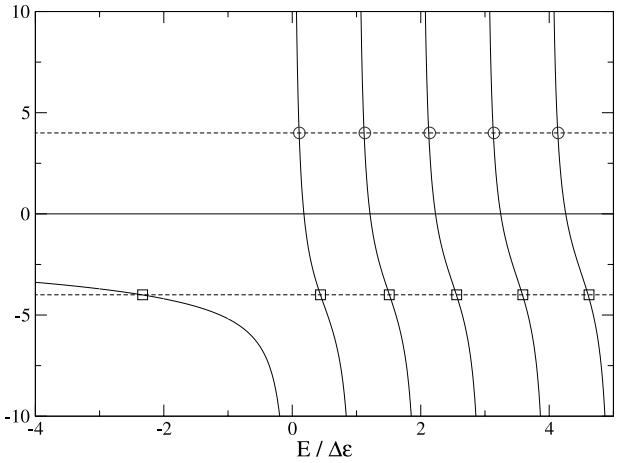

Fig. 2.1. Left hand side of (2.12). The circles denote solutions for a repulsive potential with $g > 0$ and the squares show solutions for an attractive potential with $g < 0$ (always $N = 100$)

The summation over i can be performed in closed form and leads to ψ-functions,

$$\psi\left(-\frac{E}{\Delta\epsilon}\right) - \psi\left(-\frac{E}{\Delta\epsilon} + N\right) = \frac{1}{\rho\, g} \ . \tag{2.12}$$

We will focus our attention on energies much smaller than the bandwidth $E \ll D$ and we are interested in the thermodynamic limit $N \to \infty$. A graphical solution can be obtained from plotting the left hand side of (2.12), compare Fig. 2.1. It is convenient to express each eigenvalue E_j as a shift of the corresponding diagonal element of H_0: $E_j = \epsilon_j + \Delta\epsilon_j$. The expansion of the ψ-functions for large N and for a fixed eigenenergy $E > 0$ (i.e., for $j \to \infty$ but j/N fixed) yields

$$\frac{D}{N\,\Delta\epsilon_j} + \ln j - \ln N + O(N^0) = \frac{1}{\rho g} \ , \tag{2.13}$$

or equivalently

$$\Delta\epsilon_j = \frac{1}{N}\,\frac{g}{1 + \rho g \ln(D/\epsilon_j)} \ . \tag{2.14}$$

In the above limit this relation holds except for the eigenvalue $E_1 < 0$ in the case of attractive potential scattering $g < 0$. From Fig. 2.1 it is clear that in this case the $\psi(x)$-function in (2.12) has to be expanded for large positive arguments x in the limit $N \to \infty$. This leads to the following relation instead of (2.13):

$$\ln\left(\frac{-\Delta\epsilon_1\, N}{D}\right) - \ln N + O(N^0) = \frac{1}{\rho g} \ . \tag{2.15}$$

The lowest lying eigenvalue is therefore given by

$$E_1 = \Delta\epsilon_1 = -D \exp\left(\frac{1}{\rho g}\right) . \tag{2.16}$$

This can be a very small energy scale for weakly attractive potentials $|\rho g| \ll 1$, $g < 0$. The corresponding eigenstate is a localized state that forms below the continuum of band states. Its energy shift is of order N^0 in the thermodynamic limit $N \to \infty$ unlike the other energy shifts in (2.14). We will return to this intriguing situation for attractive potentials later on in more detail when we discuss the flow equation solution of this model.

For the rest of this chapter we focus on the repulsive case $g > 0$, where we can use (2.14) and all band energies are shifted by an impurity contribution proportional to $1/N$. We will always assume a small coupling, $|\rho g| \ll 1$, so that band edge effects are unimportant. From (2.14) we can deduce that all band energies are shifted to higher energies with a shift

- that is determined by the coupling constant g at large energies (i.e., energies not much smaller than the bandwidth) and
- that vanishes as $1/\ln(D/\epsilon)$ for small energies.

These energy shifts determine (among other quantities) the impurity contribution ΔE_{imp} to the total energy of the system at zero temperature. For a conduction band filled with electrons up to the chemical potential μ we find

$$\begin{aligned} \Delta E_{\mathrm{imp}} &= \sum_{\epsilon_k < \mu} \Delta\epsilon_k \\ &= \rho \int_0^\mu \mathrm{d}\epsilon \frac{g}{1 + \rho g \ln(D/\epsilon)} . \end{aligned} \tag{2.17}$$

For small filling $\mu \ll D \exp(-1/\rho g)$ this gives

$$\Delta E_{\mathrm{imp}} = \mu \frac{1}{\ln(D/\mu)} , \tag{2.18}$$

while for $\mu \gg D \exp(-1/\rho g)$ one finds

$$\Delta E_{\mathrm{imp}} = \mu \rho g . \tag{2.19}$$

Perturbation Theory

For a general many-body Hamiltonian we usually have to resort to perturbation expansions to gain analytical insights. Therefore we next perform conventional second perturbation theory for the potential scattering Hamiltonian (2.3). We will learn some important lessons about perturbation expansions in general by comparison with the exact result.

Our starting point is the standard perturbative expansion for the eigenenergies in second order:

$$E_j^{(2pt)} = \epsilon_j + \langle j|H_{\rm int}|j\rangle + \sum_{i\neq j} \frac{\langle j|H_{\rm int}|i\rangle\ \langle i|H_{\rm int}|j\rangle}{\epsilon_j - \epsilon_i}\ . \tag{2.20}$$

This yields

$$\begin{aligned} E_j^{(2pt)} &= \epsilon_j + \frac{g}{N} + \frac{g^2}{N^2} \sum_{i\neq j} \frac{1}{\epsilon_j - \epsilon_i} \\ &= \epsilon_j + \frac{g}{N} - \frac{\rho g^2}{N}\ \ln\left(\frac{D-\epsilon_j}{\epsilon_j}\right)\ , \end{aligned} \tag{2.21}$$

where we have replaced the summation by an integral (which is possible for $N \to \infty$). For eigenenergies much smaller than the bandwidth D the energy shift in second order perturbation theory is therefore given by

$$\begin{aligned} \Delta\epsilon_j^{(2pt)} &= E_j^{(2pt)} - \epsilon_j \\ &= \frac{1}{N}\ \Big(g - \rho g^2\ \ln\Big(D/\epsilon_j\Big)\Big)\ . \end{aligned} \tag{2.22}$$

This should be compared with the exact expression (2.14). In fact, it is just the expansion of the exact expression in powers of the coupling constant.

However, this expansion is only possible for $|\rho\, g\, \ln(D/\epsilon_j)| \ll 1$. For energies very close to the lower band edge, $\epsilon_j \ll D\, \exp(-1/|\rho g|)$, the perturbative results breaks down and even predicts a negative energy shift as opposed to the correct result. We find a low-energy regime where perturbation theory breaks down even for a small coupling constant where one would expect to have a reliable expansion parameter. For example, the second order perturbation theory result for the impurity contribution to the total energy is

$$\Delta E_{\rm imp}^{(2pt)} = \mu\, \rho\, g \left(1 - \rho g\ \ln\left(\frac{D}{\mu}\right)\right)\ . \tag{2.23}$$

We notice that this is quite wrong for small fillings $\mu \ll D\, \exp(-1/|\rho g|)$ by comparison with the exact result (2.18).

From the exact expression (2.14) we can also deduce that going to higher powers in the perturbative expansion in the coupling constant cannot cure this problem. In fact, this produces even more uncontrolled terms in the low-filling limit. Notice that these observations hold for both repulsive and attractive potential scattering.

Scaling Theory

We have seen that perturbation theory can break down even for a simple quadratic Hamiltonian with a small expansion parameter. The conventional approach to overcome this problem is to reorganize the perturbation expansion using scaling theory. The fundamental idea is to first treat the effect of

high-lying states on the low-energy physics, and then to successively move to lower and lower energies. We will see that this principle of *energy scale separation* leads to a more stable expansion.

There are various ways to accomplish this goal using diagrammatic methods, path integral methods, etc. We refer the reader to the extensive literature on this subject (see, e.g., [1]). We will here use a method based on constructing low-energy effective Hamiltonians in order to focus our discussion on the essential points.[1] The basic idea is to split up the Hilbert space $\mathcal{H}$ of our system into two parts by using projection operators P and Q, $P + Q = 1$. $\mathcal{H}_P = P\mathcal{H}P$ denotes a low-energy Hilbert space and $\mathcal{H}_Q = Q\mathcal{H}Q$ is the complementary high-energy Hilbert space. Let $|\Psi\rangle$ be an eigenstate of the Hamiltonian:

$$H\,|\Psi\rangle = E\,|\Psi\rangle\ . \tag{2.24}$$

We can split up $|\Psi\rangle$ in a part that lives in $\mathcal{H}_P$ and one that lives in $\mathcal{H}_Q$,

$$|\Psi_P\rangle \stackrel{\text{def}}{=} P\,|\Psi\rangle\ , \quad |\Psi_Q\rangle \stackrel{\text{def}}{=} Q\,|\Psi\rangle\ . \tag{2.25}$$

The eigenvalue condition (2.24) then takes the following form:

$$\begin{pmatrix} PHP\ PHQ \\ QHP\ QHQ \end{pmatrix} \begin{pmatrix} |\Psi_P\rangle \\ |\Psi_Q\rangle \end{pmatrix} = E \begin{pmatrix} |\Psi_P\rangle \\ |\Psi_Q\rangle \end{pmatrix}\ . \tag{2.26}$$

We eliminate the component of the eigenstate in the high-energy Hilbert space,

$$|\Psi_Q\rangle = \frac{1}{E - QHQ}\,QHP\,|\Psi_P\rangle\ , \tag{2.27}$$

and express the eigenvalue equation (2.24) in terms of the low-energy Hilbert $\mathcal{H}_P$ space only:

$$PHP\,|\Psi_P\rangle + PHQ\,\frac{1}{E - QHQ}\,QHP\,|\Psi_P\rangle = E\,|\Psi_P\rangle\ . \tag{2.28}$$

In most applications one is interested in eigenenergies E close to the ground state energy E_{gs}, which are by definition much smaller than the energies in the high-energy Hilbert space $\mathcal{H}_Q$. In this situation we can approximate the left hand side of (2.28) by an effective Hamiltonian H_{eff},

$$H_{\text{eff}} = PHP + PHQ\,\frac{1}{E_{\text{gs}} - QHQ}\,QHP\ . \tag{2.29}$$

The eigenvalue equation (2.24) reduces to an eigenvalue equation for H_{eff} in the low-energy Hilbert space $\mathcal{H}_P$:

[1] This is not the best method if one is interested in higher orders of the scaling expansion, but it is a particularly pedagogical approach for working out the fundamental idea of the scaling approach.

$$H_{\text{eff}} \, |\Psi_P\rangle = E \, |\Psi_P\rangle \ . \tag{2.30}$$

The basic idea of scaling theory is to repeat this construction of low-energy effective Hamiltonians by successively eliminating high-energy degrees of freedom from the original system. We denote the original high-energy cutoff with Λ. Scaling theory then generates a sequence of effective Hamiltonians

$$H \longrightarrow H_{\text{eff}}(\Lambda_1) \longrightarrow H_{\text{eff}}(\Lambda_2) \longrightarrow \ldots \longrightarrow H_{\text{eff}}(\Lambda_{\text{IR}}) \tag{2.31}$$

with $\Lambda > \Lambda_1 > \Lambda_2 > \ldots > \Lambda_{\text{IR}}$. Here Λ_{IR} is the low-energy scale (infrared scale) that we are interested in.

In practice, the sequence (2.31) is constructed by infinitesimal steps with each step based on (2.29). Typically, the construction of the low-energy effective Hamiltonians needs to be done perturbatively in order to keep this sequence tractable. Still, this provides a reorganization of the perturbation expansion that respects energy scale separation and turns out to be much more stable than naive perturbation theory.

As an explicit example we now look at the potential scattering Hamiltonian (2.3). Let $\mathcal{H}_Q$ consist of band states close to the upper band edge with energies $\epsilon \in [D - \delta D, D]$, $\delta D \ll D$. The effective Hamiltonian with the reduced band width $D - \delta D$ then takes the following form

$$\begin{aligned} H_{\text{eff}}(D - \delta D) = & \sum_{k:\epsilon_k < D-\delta D} \epsilon_k c_k^\dagger c_k + \frac{g}{N} \sum_{k,k':\epsilon_k,\epsilon_{k'} < D-\delta D} c_k^\dagger c_{k'} \\ & + \sum_{k,k':\epsilon_k,\epsilon_{k'} < D-\delta D} \sum_{q:\epsilon_q > D-\delta D} c_{k'}^\dagger \, \frac{g}{N} \, \frac{1}{-\epsilon_q} \, \frac{g}{N} \, c_k + O(g^3) \ . \end{aligned} \tag{2.32}$$

We can rewrite this in terms of a potential scattering Hamiltonian with a reduced band width and a different scattering strength:

$$H_{\text{potscat}}(D_{\text{eff}}, g_{\text{eff}}) = \sum_{k:\epsilon_k < D_{\text{eff}}} \epsilon_k c_k^\dagger c_k + \frac{g_{\text{eff}}}{N} \sum_{k,k':\epsilon_k,\epsilon_{k'} < D_{\text{eff}}} c_k^\dagger c_{k'} \ . \tag{2.33}$$

Here the new coupling constant is given by

$$\begin{aligned} g_{\text{eff}} &= g - \frac{g^2}{N} \sum_{q:\epsilon_q > D-\delta D} \frac{1}{\epsilon_q} + O(g^3) \\ &= g - \rho g^2 \, \frac{\delta D}{D_{\text{eff}}} + O(g^3) \ . \end{aligned} \tag{2.34}$$

In this way we have constructed a sequence of effective Hamiltonians (2.33) that describe the same low-energy physics as the original problem if the effective scattering strength obeys the following *scaling equation* derived from (2.34):

$$\frac{\mathrm{d}g_{\mathrm{eff}}}{\mathrm{d}D_{\mathrm{eff}}} = \frac{\rho\, g_{\mathrm{eff}}^2}{D_{\mathrm{eff}}} \tag{2.35}$$

or equivalently

$$\frac{\mathrm{d}g_{\mathrm{eff}}}{\mathrm{d}\ln D_{\mathrm{eff}}} = \rho\, g_{\mathrm{eff}}^2 \ . \tag{2.36}$$

Notice that we have neglected all higher order terms in the coupling constant. This scaling approach with the *running coupling constant* $g_{\mathrm{eff}}(D_{\mathrm{eff}})$ is therefore a resummation of second order perturbation theory.

Equation (2.36) can be solved easily with the initial condition $g_{\mathrm{eff}}(D) = g$:

$$g_{\mathrm{eff}}(D_{\mathrm{eff}}) = \frac{g}{1 + \rho g\, \ln(D/D_{\mathrm{eff}})} \ . \tag{2.37}$$

The scattering strength becomes effectively weaker close to the lower band edge for a repulsive potential $g > 0$. For attractive scattering, however, the modulus of the running coupling constant grows and g_{eff} eventually diverges. This signals the formation of the bound state discussed before in the exact solution. We return to this issue later and for now focus on the repulsive case.

We now work out the shift of the eigenenergies on an energy scale ϵ_j using (2.20):

$$\Delta\epsilon_j = \langle j \,|\, H_{\mathrm{int}}(D_{\mathrm{eff}} = \epsilon_j) \,|\, j \rangle + O(g_{\mathrm{eff}}^2) \ , \tag{2.38}$$

where $H_{\mathrm{int}}(D_{\mathrm{eff}} = \epsilon_j)$ is the interaction part of the effective Hamiltonian scaled to the energy scale ϵ_j. This gives

$$\Delta\epsilon_j = \frac{1}{N} \frac{g}{1 + \rho g \ln(D/\epsilon_j)} + O(g_{\mathrm{eff}}^2) \tag{2.39}$$

with $g_{\mathrm{eff}} = g/(1 + \rho g \ln(D/\epsilon_j))$. This is in perfect agreement with the exact result (2.14). From the exact result we even know that there are no higher order terms on the right hand side of (2.39). However, this is a specific property of the potential scattering model and does not hold generally.

However, what is generally true is that scaling theory allows us to resum perturbation theory in such a way that we recover the correct behavior also at low energies. Figure 2.2 shows the impurity contribution to the total energy calculated with these various approaches and demonstrates the importance of energy scale separation embodied in the scaling approach.

2.1.2 Kondo Model

The potential scattering model is described by a quadratic Hamiltonian and can be solved exactly with elementary methods. We next introduce the Kondo model, which is a genuine interacting many-body problem of paradigmatic importance for strongly correlated electron systems. While there is an exact solution for its thermodynamic properties based on the Bethe ansatz [2, 3],

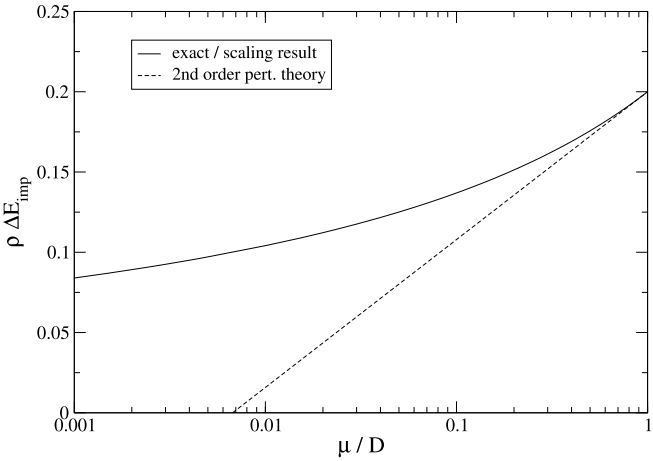

Fig. 2.2. Impurity contribution to the total energy $\Delta E_{\rm imp}$ for a repulsive potential scattering model (here $\rho\, g = 0.2$) as a function of the chemical potential μ. The full line depicts the exact/scaling theory result (2.18) and (2.39), while the dashed line shows the result in unrenormalized second order perturbation theory (2.23)

this solution relies on integrability. It cannot be generalized to an arbitrary conduction band density of states or to the evaluation of correlation functions beyond the low-energy limit, etc.[2]

The Kondo model is similar to the potential scattering model (2.3) in that it describes potential scattering of electrons. However, the potential scattering is generated by a quantum mechanical spin-1/2 degree of freedom $\boldsymbol{S}$ that obeys its own dynamics. The Kondo Hamiltonian has the form

$$H = \sum_{k,\alpha} \epsilon_k \, c^\dagger_{k\alpha} c_{k\alpha} + J \, \frac{1}{2} \, \boldsymbol{S} \cdot \sum_{k,k',\alpha,\beta} c^\dagger_{k'\alpha} \, \boldsymbol{\sigma}_{\alpha\beta} \, c_{k\beta} \ , \tag{2.40}$$

where J is an antiferromagnetic exchange coupling, $J > 0$. In correlated electron systems one thinks of $\boldsymbol{S}$ as describing the spin of an electron in a strongly correlated singly occupied orbital. The naive twofold ground state degeneracy of the system is screened by many-particle processes that effectively screen the impurity spin below an energy scale set by the *Kondo temperature* $T_K \propto D \, \exp(-1/\rho J)$. The impurity spin susceptibility becomes finite in the zero temperature limit and the Fermi sea responds to the formation of this screened Kondo singlet with an increased density of states at the Fermi level. This increased density of states in turn leads to an increased impurity contribution to the specific heat. The Kondo problem has triggered

[2]Especially the development of dynamical mean field theory for strongly correlated electron systems [5, 4] has led to renewed interest in reliable analytical and numerical methods that can solve the Kondo model for an arbitrary (in fact, self-consistently determined) conduction band density of states.

many developments in modern condensed matter theory and will be a useful test case for the flow equation method later on. For more details about the Kondo problem the reader should consult the extensive literature on this subject, e.g. [6].

We next analyze the Kondo model using scaling methods in the spirit of (2.31). We assume that the conduction band is symmetric around the Fermi surface $\epsilon_F = 0$ with band width $2D$: $\epsilon_k \in [-D, D]$. The projection operator Q is defined as projecting on states with energies $|\epsilon_q| \in [D - \delta D, D]$. Equation (2.29) then yields the following contribution to the low-energy interaction:

$$\begin{aligned} & PHQ \, \frac{1}{-QHQ} \, QHP \\ & = \frac{J^2}{4} \sum_{k',k:\epsilon_k,\epsilon_{k'} \in \mathcal{H}_P} \; \sum_{q:\epsilon_q \in \mathcal{H}_Q} \Big(c^\dagger_{k'\alpha} \, \boldsymbol{S} \cdot \boldsymbol{\sigma}_{\alpha\beta} \, c_{q\gamma} \, \frac{1}{-\epsilon_q} \, c^\dagger_{q\gamma} \, \boldsymbol{S} \cdot \boldsymbol{\sigma}_{\gamma\beta} \, c_{k\beta} \\ & \qquad + c^\dagger_{q\gamma} \, \boldsymbol{S} \cdot \boldsymbol{\sigma}_{\gamma\beta} \, c_{k\beta} \, \frac{1}{-\epsilon_q} \, c^\dagger_{k'\alpha} \, \boldsymbol{S} \cdot \boldsymbol{\sigma}_{\alpha\gamma} \, c_{q\gamma} \Big) \; . \end{aligned} \tag{2.41}$$

We use the standard relation for the spin-1/2 SU(2)-algebra,

$$S^i \, S^j = \frac{1}{4} \, \delta_{ij} + \frac{\mathrm{i}}{2} \sum_k \epsilon_{ijk} \, S^k \; . \tag{2.42}$$

The occupation numbers are given by

$$n(q) \stackrel{\mathrm{def}}{=} \langle FS | c^\dagger_{q\beta} \, c_{q\beta} | FS \rangle \; , \tag{2.43}$$

where $|FS\rangle$ denotes the non-interacting Fermi sea (no summation over β is implied in (2.43)). The right hand side of (2.41) can then be simplified to the following contribution to the interaction term in $\mathcal{H}_P$:

$$\frac{J^2}{4} \sum_{k',k:\epsilon_k,\epsilon_{k'} \in \mathcal{H}_P} \; \sum_{q:\epsilon_q \in \mathcal{H}_Q} \frac{1}{\epsilon_q} \Big((1 - 2n(q)) \, c^\dagger_{k'\alpha} \, \boldsymbol{S} \cdot \boldsymbol{\sigma}_{\alpha\beta} \, c_{k\beta} \Big) \; . \tag{2.44}$$

We have ignored an uninteresting constant that contributes to the ground state energy. The scaling equation for the spin-spin interaction then reads

$$\frac{\mathrm{d}J}{\mathrm{d}D} = -\frac{\rho J^2}{2D} \big(1 - 2n(D) - (1 - 2n(-D)) \big) \tag{2.45}$$

or

$$\frac{\mathrm{d}J}{\mathrm{d} \ln D} = \rho J^2 \big(n(D) - n(-D) \big) \; . \tag{2.46}$$

At zero temperature the occupation number is given by $n(\epsilon) = \Theta(-\epsilon)$ and (2.46) takes the same structure as the scaling equation for the potential scattering model (2.36) except for a minus sign:

$$\frac{\mathrm{d}J}{\mathrm{d}\ln D} = -\rho J^2 \ . \tag{2.47}$$

Since the spin-spin coupling is generally antiferromagnetic, $J > 0$, the solution is

$$J_{\mathrm{eff}}(D_{\mathrm{eff}}) = \frac{J}{1 - \rho J \ln(D/D_{\mathrm{eff}})} \tag{2.48}$$

or

$$\rho J_{\mathrm{eff}}(D_{\mathrm{eff}}) = \frac{1}{\ln(D_{\mathrm{eff}}/T_K)} \ . \tag{2.49}$$

Here we have introduced the Kondo temperature

$$T_K \stackrel{\mathrm{def}}{=} D \exp\left(-\frac{1}{\rho J}\right) \ . \tag{2.50}$$

The scaling approach breaks down when the effective band width reaches the Kondo temperature since then the expansion parameter ρJ_{eff} diverges. The Kondo model therefore exhibits *strong-coupling* behavior similar to the attractive potential scattering model.[3]

Still, the scaling approach provides a useful tool to resum perturbation theory since it identifies the low-energy scale T_K of the Kondo model. Screening of the magnetic impurity moment sets in for temperatures below T_K. It is clearly not possible to identify T_K from perturbation theory even for small coupling constants J since (2.50) does not have a convergent Taylor expansion around $\rho J = 0$.

2.2 Flow Equation Approach

2.2.1 Motivation

The flow equation approach is a new way to implement the important principle of energy scale separation discussed above. The flow equation approach goes back to publications by Głazek and Wilson [7, 8] and Wegner [9] in 1993-94, who have independently proposed this scheme. Głazek and Wilson suggested it in the context of high-energy physics under the name *similarity renormalization scheme*, while Wegner developed it in the context of condensed matter theory under the name *flow equations*. Since we are interested in solid state systems in this book, we will generally follow Wegner's notation, see also [10, 11, 12, 13] For further information on the similarity renormalization scheme the reader can consult [14, 15, 16].

[3] This similarity is not accidental. Ultimately, in both the Kondo model and the potential scattering model the strong-coupling behavior is due to a discontinuity: the zero temperature discontinuity of the occupation number $n(\epsilon)$ at the Fermi level in the Kondo model, or the discontinuous band density of states at the lower band edge in the potential scattering model.

The fundamental difference between flow equations and the conventional scaling approach is summed up in Fig. 1.1. Instead of eliminating highly excited states with an energy $|E| \in [\Lambda_{\rm RG} - \delta\Lambda_{\rm RG}, \Lambda_{\rm RG}]$, the flow equation approach eliminates matrix elements that couple states an *energy difference* $|\Delta E| \in [\Lambda_{\rm feq} - \delta\Lambda_{\rm feq}, \Lambda_{\rm feq}]$. From the point of view of low-energy physics both approaches look similar once $\Lambda_{\rm feq}, \Lambda_{\rm RG} \ll D$: an excitation to a higher energy $\gg \Lambda_{\rm feq}$ in the flow equation approach requires multiple interaction processes with a coupling constant that we have assumed to be small. For low-energy excitations above the ground state both methods therefore yield the same scaling flow with the identification $\Lambda_{\rm RG} = \Lambda_{\rm feq}$. *In this sense the flow equation method contains the conventional scaling approach as a limiting case.* However, in the flow equation approach the Hilbert space remains unchanged so that we can also get information about, for example, correlation functions at higher energies.

Since the original proposal in 1994, various other applications of the flow equation approach have been worked out, for example in non-equilibrium models where one cannot focus on the ground state in the first place. We will mention both the similarities and the differences of the flow equation approach as compared to the conventional scaling approach as we discuss various models later on. This should allow the reader to choose the suitable method for a given problem that one is interested in.

2.2.2 Infinitesimal Unitary Transformations

From Fig. 1.1 it is obvious that we need to develop new tools to achieve the flow $\Lambda_{\rm feq} \to \Lambda_{\rm feq} - \delta\Lambda_{\rm feq}$. Elimination of a part of the Hilbert space is here clearly not the appropriate procedure. Since we require our Hamiltonians to be unitarily equivalent under the flow, we are led to consider infinitesimal unitary transformations that eliminate interaction matrix elements that couple states with an energy transfer $|\Delta E| \in [\Lambda_{\rm feq} - \delta\Lambda_{\rm feq}, \Lambda_{\rm feq}]$. Let us for example think of a diagonal Hamiltonian

$$H_0 = \sum_n \epsilon_n \, c_n^\dagger c_n \tag{2.51}$$

and a specific (hermitean) interaction matrix element M that we want to eliminate from the total interaction term $H_{\rm int}$:

$$M = g \, (c_{m_1'}^\dagger c_{m_2'}^\dagger c_{m_1} c_{m_2} + \text{h.c.}) \; . \tag{2.52}$$

We assume that all interaction terms are proportional to a small coupling constant g. Then we construct a new Hamiltonian $\tilde{H}$ via a unitary transformation U ($U^{-1} = U^\dagger$),

$$\tilde{H} = U \, H \, U^\dagger \; , \tag{2.53}$$

where $U = {\rm e}^\eta$ with an antihermitean generator η. In our case we choose

$$\eta = \frac{g}{\epsilon_{m_1'} + \epsilon_{m_2'} - \epsilon_{m_1} - \epsilon_{m_2}} \left(c^\dagger_{m_1'} c^\dagger_{m_2'} c_{m_1} c_{m_2} - \text{h.c.}\right) \tag{2.54}$$

and find

$$\begin{aligned} \tilde{H} &= \mathrm{e}^{\eta} \left(H_0 + H_{\text{int}}\right) \mathrm{e}^{-\eta} && (2.55)\\ &= H_0 + H_{\text{int}} + [\eta, H_0 + H_{\text{int}}] + \frac{1}{2}[\eta, [\eta, H_0 + H_{\text{int}}]] + \text{higher orders} \\ &= H_0 + H_{\text{int}} - M + [\eta, H_{\text{int}}] + \frac{1}{2}[\eta, [\eta, H_0 + H_{\text{int}}]] + \text{higher orders} \\ &= H_0 + (H_{\text{int}} - M) + O(g^2) \ . && (2.56) \end{aligned}$$

We have therefore eliminated the interaction term M to first order in the coupling constant from the total interaction term.

We now want to repeat this procedure iteratively by looking at smaller and smaller energy differences $\Delta E = \epsilon_{m_1'} + \epsilon_{m_2'} - \epsilon_{m_1} - \epsilon_{m_2}$. A convenient way to do this for general interaction terms has been suggested by Wegner [9]. We label the one-parameter family of unitarily equivalent Hamiltonians with some flow parameter B [4] and consider the differential equation

$$\frac{\mathrm{d}H(B)}{\mathrm{d}B} = [\eta(B), H(B)] \ , \tag{2.57}$$

where $\eta(B) = -\eta^\dagger(B)$ is an antihermitean generator.

Let us first of all verify that the solution of (2.57) generates Hamiltonians $H(B)$ that are unitarily equivalent to the initial Hamiltonian $H(B = 0)$. We claim that the solution $H(B)$ of (2.57) is given by

$$H(B) = U(B)\, H(B = 0)\, U^\dagger(B) \ , \tag{2.58}$$

where $U(B)$ is defined as

$$\begin{aligned} U(B) &= T_B \, \exp\left(\int_0^B \mathrm{d}B' \, \eta(B')\right) && (2.59)\\ &= 1 + \sum_{n=1}^{\infty} \frac{1}{n!} \int_0^B \mathrm{d}B_1 \, \ldots \, dB_n \, T_B\{\eta(B_1) \ldots \eta(B_n)\} \ . && (2.60) \end{aligned}$$

Here $T_B\{\ldots\}$ denotes *B-ordering* defined in the same way as the usual time ordering. The generator $\eta(B_i)$ with the largest B_i is commuted to the left etc.,

$$T_B\{\eta(B_1) \ldots \eta(B_n)\} \stackrel{\text{def}}{=} \eta(B_{\pi(1)}) \ldots \eta(B_{\pi(n)}) \ , \tag{2.61}$$

[4] The flow parameter is often also denoted by ℓ. In order to avoid confusion with the common notation where ℓ is the logarithm of the change in length scale in conventional scaling equations, we use B instead of ℓ in this book.

with the permutation $\pi \in S_n$ such that $B_{\pi(1)} \geqq B_{\pi(2)} \geqq \ldots \geqq B_{\pi(n)}$. One can easily check that $U(B)$ is a unitary operator, $U(B)\,U^\dagger(B) = 1$. Also:

$$\begin{aligned} &\frac{\mathrm{d}}{\mathrm{d}B}\,\big(U(B)\,H(B=0)\,U^\dagger(B)\big) \\ &= \frac{\mathrm{d}U(B)}{\mathrm{d}B}\,U^\dagger(B)H(B) + H(B)U(B)\,\frac{\mathrm{d}U^\dagger(B)}{\mathrm{d}B}\ . \end{aligned} \tag{2.62}$$

With our definition (2.59) one finds

$$\frac{\mathrm{d}U(B)}{\mathrm{d}B}\,U^\dagger(B) = \eta(B)\,U(B)\,U^\dagger(B) = \eta(B)\ , \tag{2.63}$$

and therefore

$$\frac{\mathrm{d}}{\mathrm{d}B}\,\big(U(B)\,H(B=0)\,U^\dagger(B)\big) = [\eta(B), H(B)]\ . \tag{2.64}$$

This shows that $H(B)$ defined by $H(B) = U(B)\,H(B=0)\,U^\dagger(B)$ obeys the differential equation (2.57). The correct initial condition is also fulfilled since $U(B=0) = 1$. Therefore $H(B)$ from (2.58) is the solution of (2.57).

After showing unitary equivalence, we next need to construct a suitable antihermitean generator $\eta(B)$ that implements (2.56) in an energy scale separated way.

2.2.3 Choice of Generator

The choice of the generator η that implements Fig. 1.1 is at the heart of the flow equation method. For a Hamiltonian that can be split up in a diagonal and an interaction part

$$H(B) = H_0(B) + H_{\mathrm{int}}(B)\ , \tag{2.65}$$

Wegner suggested the following *canonical generator*[5]

$$\eta(B) \stackrel{\mathrm{def}}{=} [H_0(B), H_{\mathrm{int}}(B)]\ . \tag{2.66}$$

With this choice $\eta(B)$ is antihermitean as required since it is the commutator of two hermitean operators. $\eta(B)$ has dimension (Energy)^2 and as a consequence the flow parameter B has the dimension (Energy)$^{-2}$. Let us see what this means for a typical interacting fermion model with a kinetic energy given by

$$H_0(B) = \sum_n \epsilon_n(B)\,c_n^\dagger c_n \tag{2.67}$$

and a two-particle interaction term

[5] Similar ideas called *double bracket flow* and *isospectral flow* have independently been developed in numerical mathematics [17, 18, 19].

$$H_{\rm int}(B) = \sum_{m_1',m_2',m_1,m_2} g_{m_1'm_2'm_1m_2}(B)\, c^\dagger_{m_1'} c^\dagger_{m_2'} c_{m_1} c_{m_2} \ . \tag{2.68}$$

Equation (2.66) yields the canonical generator

$$\eta(B) = \sum_{m_1',m_2',m_1,m_2} g_{m_1'm_2'm_1m_2}(B)\,(\epsilon_{m_1'}(B) + \epsilon_{m_2'}(B) - \epsilon_{m_1}(B) - \epsilon_{m_2}(B)) \times c^\dagger_{m_1'} c^\dagger_{m_2'} c_{m_1} c_{m_2} \tag{2.69}$$

and this in turn the *flow equation* (2.57):

$$\begin{aligned}\frac{{\rm d}H(B)}{{\rm d}B} &= [\eta(B), H_0(B)] + [\eta(B), H_{\rm int}(B)] \\ &= -\sum_{m_1',m_2',m_1,m_2} g_{m_1'm_2'm_1m_2}(B)\, \Big(\epsilon_{m_1'}(B) + \epsilon_{m_2'}(B) - \epsilon_{m_1}(B) - \epsilon_{m_2}(B)\Big)^2 \\ &\qquad \times c^\dagger_{m_1'} c^\dagger_{m_2'} c_{m_1} c_{m_2} + O(g^2) \ .\end{aligned} \tag{2.70}$$

One can easily verify that the structure of these equations is generic for all interaction terms:

- In the generator the interaction coefficient is multiplied by the energy transfer of the scattering process.
- In the flow equation the interaction coefficient is multiplied by the square of the energy transfer of the scattering process, and the overall sign is negative.

Identification of the same interaction terms on the left hand and right hand side of (2.70) leads to the differential equation

$$\frac{{\rm d}g_{m_1'm_2'm_1m_2}}{{\rm d}B} = -\Big(\epsilon_{m_1'}(B) + \epsilon_{m_2'}(B) - \epsilon_{m_1}(B) - \epsilon_{m_2}(B)\Big)^2 g_{m_1'm_2'm_1m_2}(B) + O(g^2) \ . \tag{2.71}$$

As long as we can neglect the coupling constant in comparison with the energy transfer, we can use the approximate *linearized* solution:

$$g_{m_1'm_2'm_1m_2}(B) = g_{m_1'm_2'm_1m_2}(0)\, {\rm e}^{-B\,(\epsilon_{m_1'}(B)+\epsilon_{m_2'}(B)-\epsilon_{m_1}(B)-\epsilon_{m_2}(B))^2} \ . \tag{2.72}$$

This shows that the canonical choice of the generator (2.66) achieves the desired decoupling of interaction matrix elements in an energy scale separated way as indicated in Fig. 1.1. For dimensional reasons we have the identification

$$\Lambda_{\rm feq} = B^{-1/2} \ , \tag{2.73}$$

i.e. in the initial phase of the flow (for small B) one removes interaction matrix elements with large energy differences from the interaction term. In the later stages of the flow (for larger values of the flow parameter B) one then starts decoupling more and more energetically degenerate states. We will later see that the interesting scaling properties enter through the term in $O(g^2)$ in (2.71).

Let us go back to the initial split-up of the Hamiltonian in a diagonal and an interaction part in (2.66). There is of course a certain arbitrariness in such a separation. From a fundamental point of view we do not know a priori what the "correct" diagonal part of a Hamiltonian is. However, if one makes the "wrong" choice, one typically runs into coupling constants and expansion parameters in the flow equation approach that become large and therefore uncontrolled during the flow. A flow equation solution based on a specific choice of the generator becomes justified *a posteriori* if its expansion parameter remains small during the flow.

Still, we can identify two conditions that should be met so that the canonical generator has a chance of achieving its goal of making the Hamiltonian increasingly energy diagonal. These conditions are

$$\mathrm{Tr}\left(H_0(B)\, H_{\mathrm{int}}(B)\right) = 0 \tag{2.74}$$

and

$$\mathrm{Tr}\left(\frac{\mathrm{d}H_0(B)}{\mathrm{d}B}\, H_{\mathrm{int}}(B)\right) = 0\ . \tag{2.75}$$

Here the trace is taken over all states in the Hilbert space. Notice that these conditions are always fulfilled if

- the diagonal part contains all terms which do not change the quantum numbers of a quantum state: this is e.g. true if $H_0(B)$ can be expressed as a sum over number operators like the kinetic energy (2.67)
- and if the interaction term $H_{\mathrm{int}}(B)$ contains only scattering processes which change at least one quantum number.

The product of $H_0(B)$ and $H_{\mathrm{int}}(B)$ in (2.74) and (2.75) then necessarily changes at least one quantum number of any state that it acts on. This implies that the traces (2.74) and (2.75) vanish.

If (2.74) and (2.75) are fulfilled, the canonical generator reduces the interaction part of the Hamiltonian in the sense that

$$\frac{\mathrm{d}}{\mathrm{d}B}\,\mathrm{Tr}(H_{\mathrm{int}}^2(B)) \leqq 0\ . \tag{2.76}$$

This is the property that we want to prove now. We first use (2.75) to show

$$\begin{aligned}\frac{\mathrm{d}}{\mathrm{d}B}\,\mathrm{Tr}\left(H_{\mathrm{int}}^2(B)\right) &= 2\,\mathrm{Tr}\left(H_{\mathrm{int}}(B)\,\frac{\mathrm{d}H_{\mathrm{int}}(B)}{\mathrm{d}B}\right)\\ &= 2\,\mathrm{Tr}\left(H_{\mathrm{int}}(B)\,\frac{\mathrm{d}H(B)}{\mathrm{d}B}\right)\ .\end{aligned} \tag{2.77}$$

Next we employ the definition of the flow equation (2.57) and the possibility for cyclic exchange under the trace:

$$\begin{aligned}\frac{\mathrm{d}}{\mathrm{d}B}\,\mathrm{Tr}\left(H_{\mathrm{int}}^2(B)\right) &= 2\,\mathrm{Tr}\Big(H_{\mathrm{int}}(B)\,[\eta(B),H(B)]\Big)\\ &= 2\,\mathrm{Tr}\Big(\eta(B)\left(H(B)\,H_{\mathrm{int}}(B)-H_{\mathrm{int}}(B)\,H(B)\right)\Big)\end{aligned} \tag{2.78}$$

We use the definition of the canonical generator (2.66) and the fact that it can equivalently be expressed as

$$\eta(B) = [H(B), H_{\mathrm{int}}(B)]\ . \tag{2.79}$$

Therefore (2.78) is equivalent to

$$\begin{aligned}\frac{\mathrm{d}}{\mathrm{d}B}\,\mathrm{Tr}\left(H_{\mathrm{int}}^2(B)\right) &= 2\,\mathrm{Tr}\left(\eta^2(B)\right)\\ &= -2\,\mathrm{Tr}\Big(\eta^\dagger(B)\,\eta(B)\Big)\\ &\leqq 0\ ,\end{aligned} \tag{2.80}$$

since $\eta^\dagger(B)\,\eta(B)$ is a positive semi-definite operator. This implies that the flow makes the Hamiltonian "more diagonal" as long as the generator $\eta(B)$ itself does not vanish. However, if this happens $H_0(B)$ and $H_{\mathrm{int}}(B)$ commute and can be diagonalized in a simultaneous eigenbasis. Therefore the canonical choice of the generator according to Wegner [9] fulfills our requirements of generating a more and more energy diagonal unitarily equivalent Hamiltonian as $B \to \infty$.

However, at this point a word of caution is in order. While (2.80) is a very desirable property, we should remember that in a many-body Hamiltonian such traces are typically divergent in the thermodynamic limit. Also we will generically be forced to use some approximations for the flow of a many-body Hamiltonian, while (2.80) holds for the exact unitary flow. These complications non-withstanding, the canonical generator turns out to be a remarkably good choice with the desired properties in a large number of many-body problems.

2.2.4 Flow Equations

Let us sum up the main ingredients of the flow equation method that we have developed so far.

I. The unitary flow of the Hamiltonian is generated by the flow equation

$$\frac{\mathrm{d}H(B)}{\mathrm{d}B} = [\eta(B), H(B)]\ , \tag{2.81}$$

where $H(B=0)$ is the initial Hamiltonian and $H(B=\infty)$ is the final energy-diagonal Hamiltonian. We want to achieve this flow in an energy scale separated way as indicated in Fig. 1.1 with the identification $\Lambda_{\rm feq} = B^{-1/2}$. $\eta(B)$ is an antihermitean operator that generates this flow.

II. The canonical generator is defined as the commutator of the diagonal part with the interaction part of the Hamiltonian:

$$\eta(B) \stackrel{\rm def}{=} [H_0(B), H_{\rm int}(B)] \ . \tag{2.82}$$

This choice makes the flowing Hamiltonian more energy-diagonal in an energy scale separated way as can be seen from (2.80).

III. An interaction matrix element $g_{\Delta E}$ with energy transfer ΔE (as measured with respect to H_0) decays like

$$g_{\Delta E}(B) = g_{\Delta E}(B=0)\, {\rm e}^{-B(\Delta E)^2} + O(g^2) \tag{2.83}$$

for the canonical choice of the generator. The higher order terms in this equation will turn out to be responsible for nontrivial scaling properties, i.e. nontrivial β-functions. The analysis of such higher order terms will comprise the main part of this book.

Some remarks are in order concerning this general methodology.

1. The main challenge of the flow equation approach lies in the generation of higher and higher order interaction terms during the flow. This is apparent from looking at the differential equation (2.81). If the original interaction contains two-particle interaction terms, that is terms with two fermion creation and two fermion annihilation operators, then η has the same structure. The commutator of η with the interaction Hamiltonian on the right hand side of (2.81) then produces a term with three creation and three annihilation operators. This makes the generator more complicated and this progression of higher order terms continues indefinitely. In Chap. 4 we will discuss possibilities to truncate this infinite sequence to produce a systematic expansion.
2. If our initial Hamiltonian commutes with some symmetry operator S

$$[H(0), S] = 0 \ , \tag{2.84}$$

then the canonical generator also commutes with S.[6] Consequently, the flow preserves this symmetry:

$$[H(B), S] = 0 \quad \forall B \ . \tag{2.85}$$

One can only destroy this symmetry by making an approximation on the right hand side of (2.81) that does not respect the symmetry.

[6] Notice that $[H_0, S] = 0$ holds trivially in all realistic examples.

3. The canonical choice of the generator (2.82) is particularly well-behaved as we have seen in the previous chapter. *As a general rule I recommend working with the canonical generator since this choice is very robust.* However, there can be situations where other choices of the generator turn out to be more convenient in the sense that they simplify the structure of differential equations during the flow.[7] Different choices of the generator amount to different ways of doing the expansion around the noninteracting model. A particular choice of the generator can be justified a posteriori if the resulting expansion has a small expansion parameter during the flow since we typically have to neglect certain higher orders in our expansion parameter on the right hand side of (2.81).
   The freedom to choose different generators in the flow equation approach is therefore nothing "uncontrolled" about this approach. It is simply a reflection of the fact that different expansions are possible. If one can go to higher orders in these expansions and if these expansions are convergent, then the resulting observable quantities will be the same. The key trick is to find an expansion that already encompasses as much as possible in low orders so that we can actually manage the calculation.[8] This is just another way of saying that our expansion parameter should be small during the entire flow.
   There are specific cases where a different generator than the canonical generator can be useful. One should, however, always remember the importance of energy scale separation. Energy scale separation is respected if the coefficient multiplying an interaction term in η vanishes at least linearly with the energy transfer ΔE of this interaction term.[9] We will generally work with the canonical generator throughout this book since it robustly generates stable expansions due to the property (2.80), except for some specific situations like strong-coupling models.
4. One can ask the question whether it is useful to reconstruct the full unitary transformation $U(B = \infty)$ from the infinitesimal steps using (2.59). As a general rule such an endeavor is both difficult and not helpful. In many-body problems the generator at different B-values does generally not commute, $[\eta(B_1), \eta(B_2)] \neq 0$. This makes the evaluation of the B-ordered exponential in (2.59) difficult. Also, the full unitary transformation $U(B = \infty)$ completely hides the fact that it can be expressed as such an B-ordered exponential, and hence that is generated by infinitesimal

[7] We will discuss an example for this in Sect. 4.3.

[8] Notice that the complexity of such calculations typically grows considerably with every order.

[9] A generator that does not respect energy scale separation does not automatically make the approach uncontrolled. Energy scale separation is not important in all interactions as one knows from the many successful applications of conventional perturbation theory. However, one needs to be extra careful with a generator that does not respect energy scale separation and make sure that this does not lead to uncontrolled errors in higher orders.

steps that respect energy scale separation. It is therefore more natural to work with the infinitesimal formulation. One can only properly motivate the unavoidable approximations for a generic many-body problem in this infinitesimal formulation.

2.3 Example: Potential Scattering Model

As a first example we now discuss the application of the flow equation method to the potential scattering model (2.3) in full pedagogical detail. In this way one can gain some first familiarity with the method and see how it works. Of course, the potential scattering model is trivial from a many-particle point of view. Still, it is nontrivial from the scaling point of view as we have seen before. In Chap. 4 we will then discuss applications of the flow equation method to models that are both non-trivial from the scaling and the many-particle point of view.

2.3.1 Setting up the Flow Equations

The basic idea of the flow equation approach is to make the interaction increasingly energy-diagonal. The ansatz for the flowing Hamiltonian should reflect this. For the potential scattering model (2.3) we write

$$H(B) = \sum_k (\epsilon_k + g_{kk}(B))\, c_k^\dagger c_k + \sum_{k,k':k\neq k'} g_{k'k}(B)\, c_{k'}^\dagger c_k \tag{2.86}$$

with the initial condition

$$g_{k'k}(B=0) = \frac{g}{N}\ . \tag{2.87}$$

The appropriate separation of diagonal and interaction part of the Hamiltonian is obvious:

$$H(B) = H_0(B) + H_{\rm int}(B) \tag{2.88}$$

with

$$H_0(B) = \sum_k E_k(B)\, c_k^\dagger c_k \tag{2.89}$$

$$H_{\rm int}(B) = \sum_{k,k':k\neq k'} g_{k'k}(B)\, c_{k'}^\dagger c_k\ . \tag{2.90}$$

Here we have introduced the abbreviation $E_k(B) \stackrel{\rm def}{=} \epsilon_k + g_{kk}(B)$.

Next we construct the canonical generator (2.82). It is worthwhile to calculate the basic commutators first and then to plug them into the various

commutators that generate the flow.[10] In the potential scattering model we therefore need to calculate

$$[c_{1'}^\dagger c_1, c_{2'}^\dagger c_2] =? \ . \tag{2.91}$$

Let us first think of potential scattering for fermions with the basic anticommutation relations

$$\{c_1, c_{1'}^\dagger\} = \delta_{1'1} \ , \quad \{c_{1'}^\dagger, c_{2'}^\dagger\} = \{c_1, c_2\} = 0 \ . \tag{2.92}$$

We use the following expression that holds generally for all operators A, B, C, D:

$$\begin{aligned}[AB, CD] &= ABCD - CDAB \\ &= A\{B, C\}D - C\{D, A\}B + CA\{B, D\} - \{C, A\}BD\end{aligned} \tag{2.93}$$

With this expression it is straightforward to evaluate (2.91):[11]

$$[c_{1'}^\dagger c_1, c_{2'}^\dagger c_2] = \delta_{2'1} c_{1'}^\dagger c_2 - \delta_{1'2} c_{2'}^\dagger c_1 \ . \tag{2.94}$$

Alternatively, one can consider potential scattering of bosonic particles. Then we have the basic commutation relations:

$$[c_1, c_{1'}^\dagger] = \delta_{1'1} \ , \quad [c_{1'}^\dagger, c_{2'}^\dagger] = [c_1, c_2] = 0 \ . \tag{2.95}$$

Here we can use the following expression that also holds generally for all operators A, B, C, D:

$$[AB, CD] = A[B, C]D - C[D, A]B + CA[B, D] - [C, A]BD \ . \tag{2.96}$$

Remarkably, we see by comparison with (2.93) that only the anticommutators are replaced by commutators. Hence we also find for bosonic particles

$$[c_{1'}^\dagger c_1, c_{2'}^\dagger c_2] = \delta_{2'1} c_{1'}^\dagger c_2 - \delta_{1'2} c_{2'}^\dagger c_1 \ . \tag{2.97}$$

Since all commutators in the flow equation solution of the potential scattering model can be traced back to this expression, our calculation holds for both the fermionic and the bosonic case.

The canonical generator of the flow equation approach (2.82) is given by

$$\begin{aligned}\eta(B) &= [H_0(B), H_{\rm int}(B)] \\ &= \sum_{p,p'} \eta_{p'p} c_{p'}^\dagger c_p\end{aligned} \tag{2.98}$$

[10] I highly recommend this procedure especially for more complex many-body problems since it i) structures the calculation and ii) makes it much easier to identify mistakes and to trace them back to some basic commutator.

[11] Sometimes the fact that a commutator bilinear in fermions can be expressed in terms of basic fermionic anticommutation relation comes as a surprise. I recommend to take a moment to check (2.93) explicitly.

with

$$\eta_{p'p} = (E_{p'} - E_p)\, g_{p'p} \ . \tag{2.99}$$

Here we have used (2.94). We will usually not explicitly denote the B-dependence of the parameters in order to keep the expressions shorter. It is understood that during the flow all couplings depend on B anyway.

Next we need to work out the commutator of $\eta(B)$ with the Hamiltonian $H(B)$ in order to obtain the right hand side of the fundamental flow equation (2.57). It is convenient to do this in two steps. First we work out the (generally simple) commutator $[\eta(B), H_0(B)]$, and then the commutator $[\eta(B), H_{\rm int}(B)]$. We will later see that the evaluation of this second commutator is the key calculation in the flow equation approach for genuine many-particle models. Again using (2.94) we find

$$\begin{aligned}[\eta(B), H_0(B)] &= \sum_{p,p'} \eta_{p'p}(E_p - E_{p'})\, c^\dagger_{p'} c_p \\ &= -\sum_{p,p'} (E_p - E_{p'})^2\, g_{p'p}\, c^\dagger_{p'} c_p \end{aligned} \tag{2.100}$$

and

$$\begin{aligned}[\eta(B), H_{\rm int}(B)] &= \sum_{p,p'} \Big(\eta_{p'p} g_{pk}\, c^\dagger_{p'} c_k - \eta_{p'p} g_{k'p'}\, c^\dagger_{k'} c_p \Big) \\ &= \sum_{k,k',p} (E_{k'} + E_k - 2E_p)\, g_{k'p} g_{pk}\, c^\dagger_{k'} c_k \ . \end{aligned} \tag{2.101}$$

We are now ready to compare the coefficients of the operators on the left and and the right hand side of the fundamental flow equation

$$\frac{{\rm d}H}{{\rm d}B} = [\eta(B), H(B)] \ . \tag{2.102}$$

We find

$$\begin{aligned}\frac{{\rm d}g_{k'k}}{{\rm d}B} &= -(E_{k'} - E_k)^2\, g_{k'k} \\ &\quad + \sum_p (E_{k'} + E_k - 2E_p)\, g_{k'p} g_{pk} \ . \end{aligned} \tag{2.103}$$

Very similar structures of differential equations will appear later again and again for interacting many-particle systems. One can immediately see that the flow equations achieve the desired diagonalization from the part of (2.103) that is linear in the coupling constant:

$$g_{k'k}(B) \propto g_{k'k}(0)\, {\rm e}^{-B(E_{k'} - E_k)^2} \tag{2.104}$$

with $B \propto \Lambda_{\rm feq}^{-2}$ (see Fig. 1.1). Also notice that the shift of the single-particle energies $\Delta\epsilon_k$ calculated in the exact solution (2.14) is given by

$$\Delta\epsilon_k = g_{kk}(B = \infty) \ , \tag{2.105}$$

since all other couplings with $k' \neq k$ vanish for $B \to \infty$ according to (2.104).

2.3.2 Methods of Solution

Equation (2.103) together with the initial condition (2.87) encodes the flow equation solution of the potential scattering model. We will now go through three different ways of solving these systems of coupled differential equations that are characteristic also for interacting many-particle systems:

1. Exact solution based on numerical implementation on a computer.
2. Diagonal parametrization of the running coupling constant.
3. IR-parametrization of the running coupling constant.

The exact solution solves the system of flow equations without further approximations and is useful when one needs quantitative results. The IR-parametrization reduces the system of flow equations to a small set of (here in fact only one) differential equations that can be solved analytically and allow immediate analytical insights into the low-energy physics. The price that one pays for this are quantitative (but usually not qualitative) errors as compared to the exact solution. The diagonal parametrization is somewhere in between these two methods. It reduces the set of differential equations to a number that grows linearly with the number of band states.

In a genuine many-particle system one usually starts with working out the IR-parametrization, and then proceeds to more accurate solution methods. For pedagogical reasons and in order to assess the accuracy of the various methods, we will here start in reverse order and look at the behavior of the exact solution first.

Exact Solution

For the numerical solution of (2.103) one needs to implement these systems of differential equations on a computer. In practice, a good algorithm is an adaptive step-size 5th order Runge-Kutta algorithm that can be found in many compilations of numerical algorithms (see, e.g., [20]). The conduction band is discretized with N states and for the potential scattering model we then end up with N^2 coupled differential equations. It is fairly easy to solve systems up to 500×500 coupled equations on a standard workstation in a few hours. Two hints for a successful implementation:

– Consider the differential equation for a coupling constant $g_{k'k}(B)$ for given k', k. Once the flow has proceeded to values of B such that $B\,(\epsilon_{k'} - \epsilon_k)^2 \gtrsim 5$, the coupling $g_{k'k}(B)$ has decayed to values that are typically only $\mathrm{e}^{-5} \approx 0.007$ of its initial value (i.e. less than 1%). It is then quite appropriate to set $g_{k'k}(B) \equiv 0$ for larger values of B since the accuracy of the numerical solution will be limited anyway. This procedure reduces the number of differential equations during later stages of the flow considerably. It also ensures that the numerical algorithm finds the appropriate stepsize for large values of B.

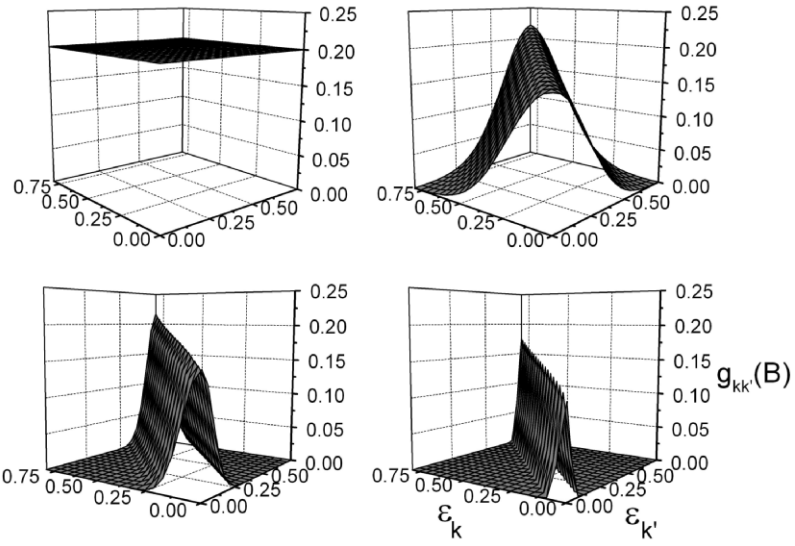

Fig. 2.3. Flow of the coupling constants $g_{kk'}(B)$ according to (2.103) for a repulsive potential scattering model with $\rho g = 0.2$ and band energies $\epsilon_k \in [0, 1]$. The diagrams show the coupling constants for flow parameters $B = 0$ (*upper left*), $B = 5$ (*upper right*), $B = 50$ (*lower left*) and $B = 500$ (*lower right*). One can observe how the banded structure of the flowing Hamiltonian evolves. Only diagonal couplings ($\epsilon_k = \epsilon_{k'}$) remain nonzero for $B \to \infty$. Notice that the nonperturbative scaling aspects are most noticeable at the lower band edge ($\epsilon_k = \epsilon_{k'} = 0$)

– Often the interesting low-energy scale is much smaller than the bandwidth of the system, e.g. like the Kondo temperature T_K (2.50) for small couplings. It is then advantageous to use a discretization mesh that becomes finer at the relevant low-energy scale in order to resolve such energies and to safe computer time. For example, one possibility is to use some variant of logarithmic discretization known from numerical renormalization group (NRG) [21] (e.g., $\epsilon_{i-1}/\epsilon_i = \Lambda$ with $\Lambda > 1$; the low-energy limit is reached for $i \to \infty$). Of course, one can also create a finer mesh around some nonzero energy scale if one is interested in it.[12]

Figure. 2.3 shows the typical flow of the coupling constants for the repulsive potential scattering model. One finds very similar pictures for interacting many-body systems, which makes it worthwhile to study the model here in some detail. One can see that the Hamiltonian $H(B)$ becomes increasingly

[12]Notice that logarithmic discretization amounts to an approximation in NRG that is essential to make the method work. On the other hand, in the numerical implementation of the flow equations a finer mesh is only a numerical trick to make our solution of the flow equations more efficient: in principle one can and often does take the limit $\Lambda \to 1$.

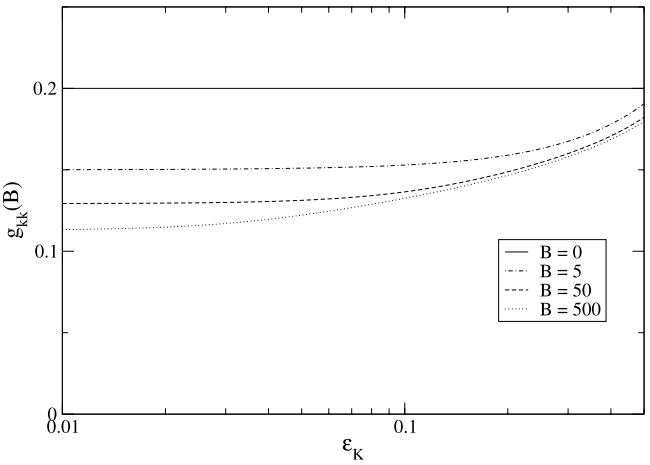

Fig. 2.4. Flow of the diagonal coupling constants $g_{kk}(B)$ according to (2.103) for a repulsive potential scattering model with the same parameters as in Fig. 2.3 ($\rho\, g = 0.2$, band energies $\epsilon_k \in [0, 1]$). Notice that the nonperturbative scaling effects are largest at the lower band edge $\epsilon_k = 0$ and eventually drive $g_{00}(B)$ to zero for $B \to \infty$

energy-diagonal for larger values of B as expected in the flow equation framework. Only the diagonal couplings with $\epsilon_k = \epsilon_{k'}$ remain nonzero for $B \to \infty$. The banded structure of the flowing Hamiltonian as opposed to the reduced size of the Hilbert space in the conventional scaling approach is immediately apparent, compare Fig. 1.1. In Figs. 2.3 and 2.4 one can also notice the "renormalization" of the diagonal couplings that reflects the non-perturbative scaling properties of our model. Obviously, the numerical solution for $B = \infty$ agrees with the exact solution from Sect. 2.1.1 and the diagonal couplings $g_{kk}(B = \infty)$ yield the exact shift of the single-particle energy levels according to (2.105) and (2.14).

Diagonal Parametrization

Figures 2.3 and 2.4 motivate an *approximate* parametrization of the $N \times N$ coupling constants in terms of its N diagonal entries by solving the linear part of the differential equation (2.103). For easier notation we define $g_k(B) \stackrel{\text{def}}{=} g_{kk}(B)$ and define $p = \overline{k'k}$ as the arithmetic average $\epsilon_p = (\epsilon_{k'} + \epsilon_k)/2$:

$$\epsilon_{\overline{k'k}} \stackrel{\text{def}}{=} \frac{\epsilon_{k'} + \epsilon_k}{2} \ . \tag{2.106}$$

The *diagonal parametrization* then amounts to the ansatz

$$g_{k'k}(B) = g_{\overline{k'k}}(B)\, \mathrm{e}^{-B(\epsilon_{k'} - \epsilon_k)^2} \ . \tag{2.107}$$

Equation (2.107) is obviously an approximation, but we will later see that it compares very favorably with the exact solution. Let us first work out its implications for the system of flow equations (2.103). We now only have differential equations for the diagonal couplings:

$$\frac{\mathrm{d}g_k}{\mathrm{d}B} = 2\sum_p (E_k - E_p)\,(g_{\overline{kp}})^2\,\mathrm{e}^{-2B(\epsilon_k-\epsilon_p)^2}\ . \tag{2.108}$$

We can use the observation that the energy levels are only shifted in order $1/N$ in the repulsive case as expected for an impurity model. Therefore we can replace $(E_k - E_p)$ by $(\epsilon_k - \epsilon_p)$ in the thermodynamic limit $N \to \infty$.

In order to work out an analytical solution we next use an approximation where we replace $g_{\overline{kp}}$ by g_k in (2.108). This is justified because $g_k(B)$ depends only weakly on k in the energy range where the exponential factor in (2.108) does not anyway suppress it completely, compare Fig. 2.3. Therefore we can write

$$\frac{\mathrm{d}g_k}{\mathrm{d}B} = 2g_k^2\,N\,\rho\int_0^D \mathrm{d}\epsilon\,(\epsilon_k-\epsilon)\,\mathrm{e}^{-2B(\epsilon_k-\epsilon)^2} \tag{2.109}$$

$$= \frac{\rho\,N\,g_k^2}{2B}\,\left(\mathrm{e}^{-2B(\epsilon_k-D)^2} - \mathrm{e}^{-2B\epsilon_k^2}\right)\ . \tag{2.110}$$

The behavior of this equation is regular in the limit $B \to 0$: the flow of g_k is effectively negligible for $B \lesssim D^{-2}$. Hence we can replace (2.110) by the following simpler equation:

$$\frac{\mathrm{d}g_k}{\mathrm{d}B} = -\frac{\rho\,N\,g_k^2}{2B}\,\mathrm{e}^{-2B\epsilon_k^2} \tag{2.111}$$

with the initial condition now posed at $B = D^{-2}$:

$$g_k(B = D^{-2}) = \frac{g}{N}\ . \tag{2.112}$$

This equation can be integrated easily

$$\frac{1}{N}\,\left(\frac{1}{g_k(B)} - \frac{1}{g_k(D^{-2})}\right) = \frac{\rho}{2}\int_{D^{-2}}^B \mathrm{d}B'\,\frac{\exp(-2B'\epsilon_k^2)}{B'} \tag{2.113}$$

yielding

$$g_k(B=\infty) = \frac{1}{N}\,\frac{g}{1+\rho g\,\mathrm{Ei}(1,2\epsilon_k^2/D^2)/2}\ . \tag{2.114}$$

Here the exponential integral $\mathrm{Ei}(1,x)$ appears in the denominator. Notice that its series expansion for small arguments is given by $\mathrm{Ei}(1,x) = -\gamma - \ln x + O(x)$, which makes the result (2.114) agree with the exact result (2.14) in the low-energy limit $\epsilon_k \ll D$. From (2.114) we see that the $B \to \infty$ limit of the diagonal elements of the coupling constant $g_{k'k}(B)$ is just the energy scale dependent running coupling constant.

IR-Parametrization

The approximation that is closest to the conventional scaling approach is to focus only on the infrared limit in the flow equations (2.103). We use the following parametrization

$$g_{k'k}(B) = \frac{g_{\mathrm{IR}}(B)}{N}\, \mathrm{e}^{-B(\epsilon_{k'}-\epsilon_k)^2} \ , \tag{2.115}$$

and derive the scaling equation for $g_{\mathrm{IR}}(B)$ by putting it into the flow equation (2.103) for $k' = k = 0$. This gives

$$\frac{\mathrm{d}g_{\mathrm{IR}}}{\mathrm{d}B} = -2g_{\mathrm{IR}}^2\, \rho \int_0^D \mathrm{d}\epsilon\, \epsilon\, \mathrm{e}^{-2B\epsilon^2} \tag{2.116}$$

leading to

$$\frac{\mathrm{d}g_{\mathrm{IR}}}{\mathrm{d}B} = -\frac{\rho g_{\mathrm{IR}}^2}{2B} \tag{2.117}$$

with the initial condition posed at $B = D^{-2}$:

$$g_{\mathrm{IR}}(B = D^{-2}) = \frac{g}{N} \ . \tag{2.118}$$

This is exactly the scaling equation derived from a conventional scaling analysis (2.36) with the identification $B = D_{\mathrm{eff}}^{-2}$. It therefore agrees with the exact solution.

The observation that a flow equation parametrization like (2.115) that focuses on the IR-limit reproduces the conventional scaling equation is generic also for interacting quantum many-body systems. One can understand this by noticing that the infrared limit of the flow equation Hamiltonian becomes equivalent to the conventional scaling Hamiltonian. Although $H(\Lambda_{\mathrm{feq}})$ in Fig. 1.1 contains higher energy excitations than $H(\Lambda_{\mathrm{RG}})$, these can only be reached through higher-order processes in the coupling constant that is assumed to be small.

Finally it is worthwhile to observe that we can recover the result of the diagonal parametrization in the previous section with the relation

$$g_k(B = \infty) = g_{\mathrm{IR}}(B = \epsilon_k^{-2}) \ , \tag{2.119}$$

since the flow on the energy scale ϵ_k effectively stops at the corresponding B-scale of the running coupling constant in the infrared limit. However, a simple relation like (2.119) does not always hold in interacting many-body systems. It is generally useful to perform an analysis based on the diagonal parametrization after getting some first insights based on the infrared parametrization.[13]

[13] Typical examples where one needs to be careful are models with another intrinsic energy scale like the Kondo model with a magnetic field or a nontrivial density of states.

2.3.3 Strong-Coupling Case

Our analysis has so far focussed on the case of repulsive potential scattering. As we had noticed in the exact solution in Sect. 2.1.1, for attractive scattering $g < 0$ a bound state with energy

$$E_B = -D \exp\left(\frac{1}{\rho g}\right) \tag{2.120}$$

forms below the lower band edge. In the scaling approach this bound state is indicated by the strong-coupling divergence of the running coupling constant (2.37)

$$\rho\, g_{\rm eff}(D_{\rm eff}) = \frac{1}{\ln(D_{\rm eff}/|E_B|)}\ . \tag{2.121}$$

This indicates the breakdown of the scaling approach as an expansion in the running coupling. It is interesting to see how the flow equation approach fares in this situation. As a cautionary remark one should mention that while the weak-coupling observations in the previous section can be carried over rather generally to interacting many-body systems, the flow equation analysis of the strong-coupling potential scattering model seems not to be generalizable to strong-coupling interacting many-body systems. We will later see this explicitly for the case of the Kondo model. However, the flow equation analysis of the attractive potential scattering model provides some interesting insights into the method.

Our starting point is the exact numerical solution of the flow equations (2.103). Figure 2.5 shows the behavior of the single-particle energies $E_k(B) = \epsilon_k + g_{kk}(B)$ during the flow. As indicated by the analytical solution of the scaling equation, the couplings $g_{kk}(B)$ at the lower band edge become very large during the flow. In fact, the shift of the single particle energies E_k at the lower band edge is no longer of order $1/N$. Putting it otherwise: if we take the thermodynamic limit $N \to \infty$ in the full flow equations (2.103) and replace the E_k's by the ϵ_k's, the system of differential equations does not converge anymore in the limit $B \to \infty$. The strong-coupling behavior of the scaling equations in the attractive potential scattering model is therefore due to taking the thermodynamic limit before the $B \to \infty$ scaling limit. .

The full flow equations for finite N, however, reproduce the exact solution as shown in Fig. 2.5 and show the development of the bound state below the continuum. Of course, it should be expected that the flow equation approach always works for a quadratic Hamiltonian if we work with the full system of differential equations. For an interesting discussion of the scaling flow of this quadratic Hamiltonian within Głazek and Wilson's similarity renormalization scheme and its relation to asymptotic freedom the reader should also consult [22]. A fascinating model which is quite similar to the Hamiltonian discussed here but which exhibits limit–cycle behavior is discussed in [23, 24].

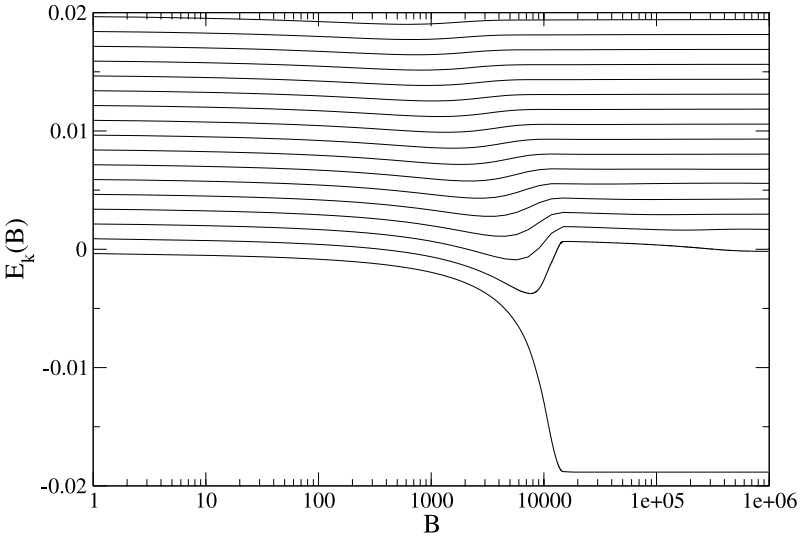

Fig. 2.5. Flow of the single-particle energies $E_k(B)$ for an attractive potential scattering model with $\rho\, g = -0.25$. Here $N = 500$ equidistant band states are used (with $\epsilon_k \in [0, 1]$) in the numerical solution of the flow equations. Notice the development of the bound state below the lower band edge

References

1. P.W. Anderson: *Basic Notions of Condensed Matter Physics*, 6th edn (Addison-Wesley, Reading Mass. 1996)
2. N. Andrei, K. Furuya, and J.H. Lowenstein, Rev. Mod. Phys. **55**, 331 (1983)
3. A.M. Tsvelick and P.B. Wiegmann, Adv. Phys. **32**, 453 (1983)
4. W. Metzner and D. Vollhardt, Phys. Rev. Lett. **62**, 324 (1989)
5. A. Georges, G. Kotliar, W. Krauth, and M.J. Rozenberg, Rev. Mod. Phys. **68**, 13 (1996)
6. A.C. Hewson: *The Kondo Problem to Heavy Fermions*, 1st edn (Cambridge University Press, Cambridge 1993)
7. S.D. Głazek and K.G. Wilson, Phys. Rev. D **48**, 5863 (1993)
8. S.D. Głazek and K.G. Wilson, Phys. Rev. D **49**, 4214 (1994)
9. F. Wegner, Ann. Phys. (Leipzig) **3**, 77 (1994)
10. F. Wegner, Phil. Mag. B **77**, 1249 (1998)
11. F. Wegner, Phys. Rep. **348**, 77 (2001)
12. F. Wegner, Nucl. Phys. B (Proc. Suppl.) **90**, 141 (2000)
13. F. Wegner, cond-mat/0511660
14. S.D. Głazek, Renormalization of Hamiltonians. In: *Lecture Notes of the First International School on Light–Cone Quantization* (Iowa State University Press, Ames 1997)
15. T.S. Walhout, Phys. Rev. D **59**, 065009 (1999)
16. S.D. Głazek, Acta Phys. Polon. B **31**, 909 (2000)
17. M.T. Chu and K.R. Driessel, SIAM J. Numer. Anal. **27**, 1050 (1990)

18. M.T. Chu, Fields Institute Communications **3**, 87 (1994)
19. R.W. Brockett, Lin. Alg. and its Appl. **146**, 79 (1991)
20. W.H. Press, S.A. Teukolsky, W.T. Vetterling, and B.P. Flannery: *Numerical Recipes in C*, 2nd edn (Cambridge University Press, Cambridge 1992)
21. K.G. Wilson, Rev. Mod. Phys. **47**, 773 (1975)
22. S.D. Głazek and K.G. Wilson, Phys. Rev. D **57**, 3558 (1998)
23. S.D. Głazek and K.G. Wilson, Phys. Rev. Lett. **89**, 230401 (2002); Erratum Phys. Rev. Lett. **92**, 139901 (2004)
24. S.D. Głazek and K.G. Wilson, Phys. Rev. B **69**, 094303 (2004)

3 Evaluation of Observables

The evaluation of observables in the flow equation framework is the concept that tends to be most unfamiliar by comparison with traditional many-body methods. It introduces novel ideas that take some time getting used to, but this is well worth the effort. In fact, the flow equation approach is particularly useful for evaluating observables like correlation functions. In this chapter we introduce the necessary tools, and then use them to discuss two simple models in Sect. 3.3 in full pedagogical detail.

3.1 Expectation Values

3.1.1 Zero Temperature

We consider a hermitean observable O and are interested in its ground state (zero temperature) expectation value

$$\langle O\rangle_{\rm gs} = \langle \Psi_{\rm gs}|O|\Psi_{\rm gs}\rangle \ . \tag{3.1}$$

Here $|\Psi_{\rm gs}\rangle$ is the ground state of the full interacting Hamiltonian $H = H_0 + H_{\rm int}$

$$H\,|\Psi_{\rm gs}\rangle = E_{\rm gs}\,|\Psi_{\rm gs}\rangle \tag{3.2}$$

with the ground state energy $E_{\rm gs}$. How do we proceed to evaluate (3.1) in the flow equation framework?

In the previous chapter we have learned how to diagonalize the interacting Hamiltonian. At least in principle we therefore know how to construct the unitary transformation $U(B=\infty)$ from (2.59) that achieves this goal:

$$H(B=\infty) = U(B=\infty)\,H\,U^\dagger(B=\infty) \tag{3.3}$$

is diagonal. This makes it easy to find the ground state in this transformed basis. One just needs to construct the eigenstate with the smallest eigenenergy of $H(B=\infty)$, which is usually a trivial task:

$$H(B=\infty)\,|\tilde{\Psi}_{\rm gs}\rangle = E_{\rm gs}\,|\tilde{\Psi}_{\rm gs}\rangle \ . \tag{3.4}$$

From this one immediately finds $|\Psi_{\rm gs}\rangle$ which fulfills (3.2):

Stefan Kehrein: *The Flow Equation Approach to Many-Body Problems*
STMP **217**, 43–61 (2006)

$$|\Psi_{\rm gs}\rangle = U^\dagger(B=\infty)\,|\tilde{\Psi}_{\rm gs}\rangle\ . \tag{3.5}$$

We can rewrite (3.1) in the following way

$$\langle O\rangle_{\rm gs} = \langle\tilde{\Psi}_{\rm gs}|\tilde{O}|\tilde{\Psi}_{\rm gs}\rangle \tag{3.6}$$

with the *transformed observable*

$$\tilde{O} \stackrel{\rm def}{=} U(B=\infty)\,O\,U^\dagger(B=\infty)\ . \tag{3.7}$$

The key challenge lies in the fact that while the ground state wave function $|\tilde{\Psi}_{\rm gs}\rangle$ is usually trivial in (3.1), the transformed observable $\tilde{O}$ is typically very complicated. After all we have chosen the unitary transformation $U(B=\infty)$ such that it diagonalizes the Hamiltonian (3.3) without caring about what it does with the observable in (3.7).

However, given the structure (3.7) we can rewrite the problem of finding the transformed observable in a differential form similar to the flow equation for the Hamiltonian itself:

$$\frac{{\rm d}O(B)}{{\rm d}B} = [\eta(B), O(B)]\ . \tag{3.8}$$

Here the initial condition $O(B=0)=O$ is given by the observable in the original basis. $\tilde{O}=O(B=\infty)$ is the transformed operator that we need to insert in (3.6).

In a many-body problem it can be very difficult to solve (3.8), and we again have to find reliable approximation and truncation schemes for this differential equation. This will be discussed later for some important many-body models in Chap. 4. For now we just assume that this task can be done. This means that we know how to express $\tilde{O}$ as a sum over a usually infinite number of operators T_a that each contain a specific combination of creation and annihilation operators:

$$O(B=\infty) = \sum_a t_a(O)\,T_a\ . \tag{3.9}$$

The coefficients $t_a(O)$ in this expansion depend on the observable. We can choose each T_a such that it consists of a specific combination of creation and annihilation operators such that

$$[H(B=\infty), T_a] = \Omega_a\,T_a \tag{3.10}$$

since $H(B=\infty)$ is diagonal. The transformed observable can therefore be expressed as a sum over operators T_a that act like ladder operators for the diagonalized Hamiltonian. For example, in the interacting fermion model (2.68) one finds the structure

$$\tilde{c}_m = \sum_n t_n(m)\,c_n + \sum_{n_1',n_1,n_2} t_{n_1'n_1n_2}(m)\,c^\dagger_{n_1'}c_{n_1}c_{n_2} + \text{ higher order terms.} \tag{3.11}$$

The diagonal Hamiltonian takes the form

$$H(B=\infty) = \sum_n E_n \, c_n^\dagger \, c_n \tag{3.12}$$

and this implies

$$\begin{aligned} \Omega_n(m) &= -E_n \\ \Omega_{n_1' n_1 n_2}(m) &= E_{n_1'} - E_{n_1} - E_{n_2} \ . \end{aligned} \tag{3.13}$$

The ground state expectation value of O can then be expressed as a sum over expectation values with respect to the "trivial" state $|\tilde{\Psi}_{\rm gs}\rangle$,

$$\langle O \rangle_{\rm gs} = \sum_a t_a(O) \, \langle \tilde{\Psi}_{\rm gs} | T_a | \tilde{\Psi}_{\rm gs} \rangle \ , \tag{3.14}$$

which can usually be performed easily. The key problem in the calculation lies in finding the expansion (3.9), i.e. in solving the *flow equation for the observable* (3.8). Notice that only operators with $\Omega_a = 0$ can contribute in (3.14).

Readers familiar with the evaluation of the asymptotic behavior of correlation functions using Bethe ansatz methods will notice a certain similarity. There the evaluation of correlation functions can be an even harder task than the original diagonalization of the Hamiltonian. In particular, in the flow equation framework we need to solve a differential equation of the type (3.8) for *each* observable that we are interested in. It is also already worthwhile to mention that in realistic models some transformed observables might be obtained with good accuracy because the solution of their differential equation (3.8) is easy, while other observables in the same model can pose a much harder task.

At this point the natural question arises why one does not "simply" focus on finding the interacting ground state in the original basis, i.e. why one does not evaluate (3.5) explicitly. However, experience in interacting many-body problems has taught us that there is no good guiding principle for the unavoidable approximations in this calculation because of the B-ordered exponential that defines $U(B=\infty)$.

On the other hand, the truncation to the first few orders in an expansion like (3.11) often works very well. This is maybe not too surprising considering the fact that the full interacting ground state in the original basis contains all the information about this quantum state, while the transformed observables only extract a limited amount of information about this quantum state. The expansion of the full interacting ground state in the original basis will therefore be a more complicated expression than the corresponding expansion for a specific observable that we are interested in.

3.1.2 Nonzero Temperature

In the previous section we have looked at the evaluation of ground state expectation values in the flow equation framework. These ideas are straightforwardly generalized to the evaluation of thermal expectation values at nonzero temperature $T \neq 0$,

$$\langle O \rangle_\beta = \mathrm{Tr}(\rho(\beta)\, O) \ . \tag{3.15}$$

Here the trace is taken over all the states in the Hilbert space. $\rho(\beta)$ is the density matrix defined via the Boltzmann weights with respect to the full interacting Hamiltonian,

$$\rho(\beta) = \frac{1}{Z(\beta)}\, \mathrm{e}^{-\beta H} \ . \tag{3.16}$$

$\beta = 1/T$ is the inverse temperature and $Z(\beta)$ is the partition function,

$$Z(\beta) \stackrel{\mathrm{def}}{=} \mathrm{Tr}\, \mathrm{e}^{-\beta H} \ . \tag{3.17}$$

Since the trace over all Hilbert space states $|n\rangle$ is invariant under cyclic exchange of the operators, one can insert the unitary transformation $U(B = \infty)$ in the following way:

$$\begin{aligned}
\langle O \rangle_\beta &= \frac{1}{Z(\beta)} \sum_n \langle n | U(B=\infty)\, \mathrm{e}^{-\beta H} O U^\dagger(B=\infty) | n \rangle \\
&= \frac{1}{Z(\beta)} \sum_n \langle n | U(B=\infty)\, \mathrm{e}^{-\beta H} U^\dagger(B=\infty) U(B=\infty)\, O\, U^\dagger(B=\infty) | n \rangle \\
&= \frac{1}{\tilde{Z}(\beta)} \sum_n \langle n |\, \mathrm{e}^{-\beta H(B=\infty)}\, \tilde{O}\, | n \rangle \ .
\end{aligned} \tag{3.18}$$

For convenience, the partition function is here also expressed with respect to the transformed Hamiltonian:

$$Z(\beta) = \tilde{Z}(\beta) \stackrel{\mathrm{def}}{=} \sum_n \langle n |\, \mathrm{e}^{-\beta H(B=\infty)}\, | n \rangle \ . \tag{3.19}$$

Since the trace can be taken over an arbitrary basis in (3.18) and (3.19), it is most convenient to choose the trivial eigenbasis of the diagonal Hamiltonian $H(B = \infty)$

$$H(B=\infty)\, |n\rangle = E_n\, |n\rangle \ , \tag{3.20}$$

where all states are orthonormal

$$\langle n | m \rangle = \delta_{nm} \ . \tag{3.21}$$

In this way we arrive at the finite temperature generalization of (3.14)

$$\langle O\rangle_\beta = \frac{1}{\tilde{Z}(\beta)} \sum_a t_a(O) \sum_n \mathrm{e}^{-\beta E_n} \langle n| T_a |n\rangle \tag{3.22}$$

with

$$\tilde{Z}(\beta) = \sum_n \mathrm{e}^{-\beta E_n} \ . \tag{3.23}$$

Notice that again only operators with $\Omega_a = 0$ can contribute in (3.22).[1]

3.2 Correlation Functions

3.2.1 Zero Temperature

Next we want to evaluate a zero temperature correlation function of two observables O_1 and O_2:

$$C_{\mathrm{gs}}(t_1, t_2) = \langle O_1(t_1)\, O_2(t_2)\rangle_{\mathrm{gs}} \ . \tag{3.24}$$

Here $O_i(t_i)$ are the operators in the Heisenberg picture:

$$O_i(t_i) = \mathrm{e}^{\mathrm{i}Ht_i}\, O_i\, \mathrm{e}^{-\mathrm{i}Ht_i} \ . \tag{3.25}$$

We can use the same trick as before in (3.6) and insert the unitary transformation as an identity:

$$\begin{aligned} C_{\mathrm{gs}}(t_1, t_2) &= \langle\tilde{\Psi}_{\mathrm{gs}}|\, \mathrm{e}^{\mathrm{i}H(B=\infty)t_1}\, \tilde{O}_1\, \mathrm{e}^{-\mathrm{i}H(B=\infty)(t_1-t_2)}\, \tilde{O}_2\, \mathrm{e}^{-\mathrm{i}H(B=\infty)t_2}\, |\tilde{\Psi}_{\mathrm{gs}}\rangle \\ &= \langle\tilde{\Psi}_{\mathrm{gs}}|\, \tilde{O}_1\, \mathrm{e}^{\mathrm{i}(H(B=\infty)-E_{\mathrm{gs}})(t_2-t_1)}\, \tilde{O}_2\, |\tilde{\Psi}_{\mathrm{gs}}\rangle \ . \end{aligned} \tag{3.26}$$

We employ the expansion (3.9) for the transformed observables that we have used before and commute T_{a_2} past $H(B=\infty)$:

$$\begin{aligned} C_{\mathrm{gs}}(t_1, t_2) &= \sum_{a_1,a_2} t_{a_1}(O_1)\, t_{a_2}(O_2)\, \langle\tilde{\Psi}_{\mathrm{gs}}|\, T_{a_1}\, \mathrm{e}^{-\mathrm{i}(H(B=\infty)-E_{\mathrm{gs}})(t_1-t_2)}\, T_{a_2}\, |\tilde{\Psi}_{\mathrm{gs}}\rangle \\ &= \sum_{a_1,a_2} t_{a_1}(O_1)\, t_{a_2}(O_2)\, \mathrm{e}^{-\mathrm{i}\Omega_{a_2}(t_1-t_2)}\, \langle\tilde{\Psi}_{\mathrm{gs}}|\, T_{a_1}\, T_{a_2}\, |\tilde{\Psi}_{\mathrm{gs}}\rangle \ . \end{aligned} \tag{3.27}$$

Notice that only the matrix elements with $\Omega_{a_1} = -\Omega_{a_2}$ are nonvanishing. Therefore we can also write

$$C_{\mathrm{gs}}(t_1, t_2) = \sum_{a_1,a_2} t_{a_1}(O_1)\, t_{a_2}(O_2)\, \mathrm{e}^{\mathrm{i}\Omega_{a_1}(t_1-t_2)}\, \langle\tilde{\Psi}_{\mathrm{gs}}|\, T_{a_1}\, T_{a_2}\, |\tilde{\Psi}_{\mathrm{gs}}\rangle \ , \tag{3.28}$$

[1] As a side remark we should already mention that the coefficients $t_a(O)$ typically explicitly depend on temperature in an interacting many-body problem, which introduces another β-dependence in (3.22). We will return to this issue in Chap. 4 when we discuss interacting quantum many-body problems.

which can equally be obtained by commuting T_{a_1} past $H(B = \infty)$ in (3.27).

Equations (3.27) and (3.28) form the basis for the evaluation of correlation functions in the flow equation approach. Notice that once we have the expansion (3.9) for an observable, it is an easy task to calculate all kinds of correlation functions.[2] *The main reason for this is that it is trivial to solve the Heisenberg equations of motion for our transformed observables.* This is a somehow unusual concept by comparison with conventional many-body methods. Also notice that the correlation function only depends on the time difference $\tau = t_1 - t_2$ as expected in equilibrium.

One frequently needs the symmetrized correlation function for the special case $O_1 = O_2$. For later reference we will give the expression here which follows immediately from (3.27). The symmetrized correlation function is real

$$\begin{aligned} C^{(\mathrm{sym})}_{\mathrm{gs}}(t_1,t_2) &\stackrel{\mathrm{def}}{=} \frac{1}{2}\langle\{O(t_1),O(t_2)\}\rangle_{\mathrm{gs}} \\ &= \sum_{a_1,a_2} t_{a_1}(O)\, t_{a_2}(O)\, \cos(\Omega_{a_2}(t_1-t_2))\, \langle\tilde{\Psi}_{\mathrm{gs}}|\, T_{a_1}\, T_{a_2}\, |\tilde{\Psi}_{\mathrm{gs}}\rangle\ , \end{aligned} \tag{3.29}$$

and Fourier transformation with respect to the time difference τ yields:

$$\begin{aligned} C^{(\mathrm{sym})}_{\mathrm{gs}}(\omega) &= \int \mathrm{d}\tau\, \mathrm{e}^{\mathrm{i}\omega\tau}\, C^{(\mathrm{sym})}_{\mathrm{gs}}(\tau) \\ &= \pi \sum_{a_1,a_2} t_{a_1}(O)\, t_{a_2}(O)\, \langle\tilde{\Psi}_{\mathrm{gs}}|\, T_{a_1}\, T_{a_2}\, |\tilde{\Psi}_{\mathrm{gs}}\rangle \times (\delta(\omega-\Omega_{a_2}) + \delta(\omega+\Omega_{a_2}))\ . \end{aligned} \tag{3.30}$$

Likewise one finds for the response function

$$R_{\mathrm{gs}}(t_1,t_2) \stackrel{\mathrm{def}}{=} -\mathrm{i}\,\Theta(t_1-t_2)\,\langle[O(t_1),O(t_2)]\rangle_{\mathrm{gs}} \tag{3.31}$$

the following imaginary part of its Fourier transform:

$$\begin{aligned} \mathrm{Im}\, R_{\mathrm{gs}}(\omega) = \pi \sum_{a_1,a_2} & t_{a_1}(O)\, t_{a_2}(O)\, \langle\tilde{\Psi}_{\mathrm{gs}}|\, T_{a_1}\, T_{a_2}\, |\tilde{\Psi}_{\mathrm{gs}}\rangle \\ & \times (\delta(\omega-\Omega_{a_2}) - \delta(\omega+\Omega_{a_2}))\ . \end{aligned} \tag{3.32}$$

Another important quantity to make contact with conventional many-body schemes are retarded Green's functions, which we will write down explicitly for fermions. One defines

$$G^{+}_{kk'}(\tau) \stackrel{\mathrm{def}}{=} -\mathrm{i}\,\Theta(\tau)\,\langle\{c_k(\tau), c^{\dagger}_{k'}(0)\}\rangle_{\mathrm{gs}} \tag{3.33}$$

[2] It is trivial to extend the above derivation to three and higher point correlation functions.

which gives via Fourier transformation

$$G_{kk'}(\omega^+) = \sum_{a_1,a_2} t_{a_1}(k)\, t^*_{a_2}(k')\, \frac{\langle\tilde{\Psi}_{\rm gs}|\,\{T_{a_1}, T^\dagger_{a_2}\}\,|\tilde{\Psi}_{\rm gs}\rangle}{\omega - \Omega_{a_2} + {\rm i}\epsilon}\ . \tag{3.34}$$

Here $\epsilon > 0$ is the usual infinitesimal shift away from the real axis. We have used the notation

$$\tilde{c}_k = \sum_a t_a(k)\, T_a \tag{3.35}$$

for the transformed fermion annihilation operators. The creation operators follow immediately through hermitean conjugation.[3] Notice that the Green's function (3.34) is independent from the specific form of the ground state if the transformed fermion operators remain linear in either creation or annihilation operators in (3.35).

3.2.2 Nonzero Temperature

The generalization of the previous results to nonzero temperature is straightforward and follows the same lines as in Sect. 3.1.2. We only give the results here. The finite temperature correlation function is defined by

$$C_\beta(t_1,t_2) = \frac{1}{Z(\beta)}\,{\rm Tr}\big(\rho(\beta)\, O_1(t_1)\, O_2(t_2)\big)\ , \tag{3.36}$$

which leads to

$$C_\beta(t_1,t_2) = \frac{1}{\tilde{Z}(\beta)} \sum_n \sum_{a_1,a_2} t_{a_1}(O_1)\, t_{a_2}(O_2)\, {\rm e}^{-\beta E_n - {\rm i}\Omega_{a_2}(t_1-t_2)}\, \langle n|\, T_{a_1}\, T_{a_2}\, |n\rangle \tag{3.37}$$

Here the first sum runs over all eigenstates $|n\rangle$ of $H(B=\infty)$. The symmetrized correlation function takes the following form at nonzero temperature:

$$C^{(\rm sym)}_\beta(\omega) = \frac{\pi}{\tilde{Z}(\beta)} \sum_n \sum_{a_1,a_2} t_{a_1}(O)\, t_{a_2}(O)\, {\rm e}^{-\beta E_n}\, \langle n|\, T_{a_1}\, T_{a_2}\, |n\rangle \times \big(\delta(\omega - \Omega_{a_2}) + \delta(\omega + \Omega_{a_2})\big)\ . \tag{3.38}$$

The response function is given by

$$\mathrm{Im}\, R_\beta(\omega) = \frac{\pi}{\tilde{Z}(\beta)} \sum_n \sum_{a_1,a_2} t_{a_1}(O)\, t_{a_2}(O)\, {\rm e}^{-\beta E_n}\, \langle n|\, T_{a_1}\, T_{a_2}\, |n\rangle \times \big(\delta(\omega - \Omega_{a_2}) - \delta(\omega + \Omega_{a_2})\big)\ . \tag{3.39}$$

[3] If the Hamiltonian contains only real couplings then all the coefficients t_a are real for the canonical choice of the generator.

3.2.3 Fluctuation–Dissipation Theorem

The fluctuation–dissipation theorem is the fundamental relation which connects equilibrium fluctuations and dissipation in a quantum many-body system. It can be expressed in the following way as a relation between the symmetrized correlation function and the response function [1]:

$$C_\beta^{(\mathrm{sym})}(\omega) = \coth\left(\frac{\beta\omega}{2}\right) \operatorname{Im} R_\beta(\omega) \ . \tag{3.40}$$

We want to verify that this fundamental relation is fulfilled even if we have to make approximations in the transformation of the observable. Putting it otherwise, we want to verify that the fluctuation–dissipation theorem also holds if we have made approximations in deriving the coefficients $t_a(O)$, e.g. by truncating the flow equation for the observable.

We first discuss zero temperature where the fluctuation–dissipation relation takes the simple form

$$C_{\mathrm{gs}}^{(\mathrm{sym})}(\omega) = \operatorname{sgn}(\omega) \operatorname{Im} R_{\mathrm{gs}}(\omega) \ . \tag{3.41}$$

Now this follows immediately from the flow equation formulation (3.30) and (3.32) because of the following observation:

$$\Omega_{a_2} < 0 \quad \Rightarrow \quad T_{a_2} |\tilde{\Psi}_{\mathrm{gs}}\rangle = 0 \ . \tag{3.42}$$

This holds because otherwise $T_{a_2} |\tilde{\Psi}_{\mathrm{gs}}\rangle$ would be an eigenstate of $H(B=\infty)$ with a lower energy than the ground state energy. Therefore only the first δ-function on the right hand side of (3.30) or (3.32) contributes for positive ω. Likewise, for negative ω only the second δ-function on the right hand side of (3.30) or (3.32) can contribute. This just produces the sign-function in (3.41).

At finite temperature we insert a complete set of eigenstates in (3.38):

$$\begin{aligned} C_\beta^{(\mathrm{sym})}(\omega) &= \frac{\pi}{\tilde{Z}(\beta)} \sum_{n,m} \sum_{a_1,a_2} t_{a_1}(O)\, t_{a_2}(O)\, \mathrm{e}^{-\beta E_n} \langle n| T_{a_1} |m\rangle\langle m| T_{a_2} |n\rangle \\ &\qquad \times \left(\delta(\omega - \Omega_{a_2}) + \delta(\omega + \Omega_{a_2})\right) \qquad (3.43) \\ &= \frac{\pi}{\tilde{Z}(\beta)} \sum_{n,m} \sum_{a_1,a_2} \Big(t_{a_1}(O)\, t_{a_2}(O) \mathrm{e}^{-\beta E_n} \langle n| T_{a_1} |m\rangle\langle m| T_{a_2} |n\rangle \delta(\omega - E_m + E_n) \\ &\qquad + t_{a_1}(O)\, t_{a_2}(O)\, \mathrm{e}^{-\beta E_n} \langle n| T_{a_1} |m\rangle\langle m| T_{a_2} |n\rangle\, \delta(\omega + E_m - E_n) \Big) \ . \end{aligned}$$

Next we exchange both $n \leftrightarrow m$ and $a_1 \leftrightarrow a_2$ in the second term. This yields

$$\begin{aligned} C_\beta^{(\mathrm{sym})}(\omega) = \frac{\pi}{\tilde{Z}(\beta)} \sum_{n,m} &\left(\mathrm{e}^{-\beta E_n} + \mathrm{e}^{-\beta E_m}\right) \\ &\times \left(\sum_{a_1,a_2} t_{a_1}(O)\, t_{a_2}(O) \langle n| T_{a_1} |m\rangle\langle m| T_{a_2} |n\rangle \delta(\omega - E_m + E_n) \right) \end{aligned}$$

$$= \frac{\pi}{\tilde{Z}(\beta)} \sum_{n,m} \left(\mathrm{e}^{-\beta E_n} + \mathrm{e}^{-\beta(\omega+E_n)} \right)$$
$$\times \left(\sum_{a_1,a_2} t_{a_1}(O)\, t_{a_2}(O) \langle n| \, T_{a_1} \, |m\rangle \langle m| \, T_{a_2} \, |n\rangle \delta(\omega - E_m + E_n) \right)$$
$$= \frac{\pi}{\tilde{Z}(\beta)} \left(1 + \mathrm{e}^{-\beta\omega}\right) \sum_{n,m} \mathrm{e}^{-\beta E_n} \tag{3.44}$$
$$\times \left(\sum_{a_1,a_2} t_{a_1}(O)\, t_{a_2}(O) \langle n| \, T_{a_1} \, |m\rangle \langle m| \, T_{a_2} \, |n\rangle \delta(\omega - E_m + E_n) \right)$$

Likewise one shows

$$\operatorname{Im} R_\beta(\omega) = \frac{\pi}{\tilde{Z}(\beta)} \left(1 - \mathrm{e}^{-\beta\omega}\right) \sum_{n,m} \mathrm{e}^{-\beta E_n} \tag{3.45}$$
$$\times \left(\sum_{a_1,a_2} t_{a_1}(O)\, t_{a_2}(O) \langle n| \, T_{a_1} \, |m\rangle \langle m| \, T_{a_2} \, |n\rangle \delta(\omega - E_m + E_n) \right)$$

and together with (3.44) this proves the fluctuation–dissipation relation (3.40).

We have thereby arrived at the important conclusion that while approximations in the flow equation transformation will lead to deviations from the exact result, the fluctuation–dissipation relation between such an approximate correlation function and the corresponding approximate response function still holds exactly. Approximations in the transformation of the observables do not destroy the fluctuation–dissipation relation as long as we evaluate the matrix elements $\langle n| \, T_{a_1} \, T_{a_2} \, |n\rangle$ in (3.38) and (3.39) exactly without further approximations.

3.3 Examples

In order to practice the calculation of observables in the flow equation approach, we discuss two examples in this chapter: the potential scattering model and the resonant level model. Both models are "trivial" in the sense that the Hamiltonian is quadratic and can be solved easily, e.g. using equations of motion techniques. However, they provide a good opportunity to study the transformation of observables without additional complications. As mentioned previously, the transformation of observables is often the topic that is most difficult to get used to initially because it is unfamiliar by comparison with conventional many-body techniques. Many of the observations that we make here in these very simple models will later reappear in very nontrivial models, and it is worthwhile to study these examples in pedagogical detail.

3.3.1 Potential Scattering Model

We have already worked out the flow equations for the potential scattering Hamiltonian

$$H = \sum_k \epsilon_k c_k^\dagger c_k + \frac{g}{N} \sum_{k,k'} c_{k'}^\dagger c_k \ . \tag{3.46}$$

in Sect. 2.1.1. For simplicity we focus on the case without a bound state, i.e. on repulsive potentials. Let us say that we are interested in calculating the retarded Green's function

$$G^+_{kk'}(\tau) \stackrel{\text{def}}{=} -\mathrm{i}\,\Theta(\tau)\,\langle\{c_k(\tau), c_{k'}^\dagger(0)\}\rangle_{\text{gs}} \ , \tag{3.47}$$

or more conveniently the T-matrix defined by

$$G_{kk'}(\epsilon^+) = G^{(0)}_{kk'}(\epsilon^+) + \sum_{p,p'} G^{(0)}_{kp'}(\epsilon^+)\, T_{p'p}(\epsilon^+)\, G^{(0)}_{pk'}(\epsilon^+) \ . \tag{3.48}$$

Here $G^{(0)}_{kk'}(\epsilon^+)$ is the noninteracting Green's function

$$G^{(0)}_{kk'}(\epsilon^+) = \frac{\delta_{kk'}}{\epsilon^+ - \epsilon_k} \ . \tag{3.49}$$

In order to calculate the T-matrix we need to find the transformation of the fermion creation or annihilation operators under the unitary flow according to (3.8). It is easy to verify that the following ansatz is closed under the flow since η from (2.98) is bilinear in the fermion operators:

$$c_p^\dagger(B) = \sum_u t_u(p)\, c_u^\dagger \tag{3.50}$$

with $t_u(p)(B=0) = \delta_{pu}$. The flow equation for the operator takes the form:

$$\begin{aligned} \frac{\mathrm{d}c_p^\dagger(B)}{\mathrm{d}B} &= [\eta(B), c_p^\dagger(B)] \\ &= \sum_{q',q} (E_{q'} - E_q)\, g_{q'q}\, t_q(p)\, c_{q'}^\dagger \ . \end{aligned} \tag{3.51}$$

By comparing coefficients on the right hand side this yields

$$\frac{\mathrm{d}t_u(p)}{\mathrm{d}B} = \sum_q (E_u - E_q)\, g_{uq}\, t_q(p) \ . \tag{3.52}$$

Notice that one immediately concludes

$$\begin{aligned} & \frac{\mathrm{d}}{\mathrm{d}B} \left(\sum_q t_q(p')\, t_q(p) \right) = 0 \\ \Rightarrow \quad \forall B \quad & \sum_q t_q(p')(B)\, t_q(p)(B) = \sum_q t_q(p')(B=0)\, t_q(p)(B=0) \\ & = \delta_{pp'} \ , \end{aligned} \tag{3.53}$$

which is another way of saying that the anticommutator remains invariant under the unitary flow (as it should):

$$\{c_p(B), c_{p'}^\dagger(B)\} = \delta_{pp'} \ . \tag{3.54}$$

Similar *sum rules* are often important when looking at the transformation of observables in the flow equation framework, particularly when approximations are unavoidable in many-body problems. We will return to this issue later in Chap. 4.

Next we have to solve (3.52). We choose the diagonal parametrization (2.107) and first integrate from $B = 0$ to $B = \infty$ with the initial condition $t_q(p)(B = 0) = \delta_{pq}$:

$$t_p(p)(B = \infty) = 1 \tag{3.55}$$

$$\begin{aligned} \forall u \neq p \quad t_u(p)(B = \infty) &= \int_0^\infty \mathrm{d}B' \, (\epsilon_u - \epsilon_p) \, g_{\overline{up}}(B') \, \mathrm{e}^{-B'(\epsilon_u - \epsilon_p)^2} \\ &= g_{\overline{up}}(B = \infty) \, \frac{1}{\epsilon_u - \epsilon_p} + O\left(N \, g_{\overline{up}}^2(B = \infty)\right) \ . \end{aligned} \tag{3.56}$$

Here we have neglected the feedback of the flow of the coefficients $t_q(p)(B)$ into the system of differential equations. This amounts to neglecting higher powers of the running coupling constant. Therefore (3.56) is correct in leading order of the running coupling constant. Because of the slow logarithmic dependence of the coupling constant on the energy scale according to (2.114), we could also ignore its B'-dependence in (3.56) and replace it by its asymptotic $B = \infty$ value. Also, strictly speaking, our results only hold in the thermodynamic limit.[4]

Next we plug (3.56) into the expression (3.34) for the retarded Green's function:

$$\begin{aligned} G_{kk'}(\epsilon^+) &= \delta_{kk'} \, \frac{1}{\epsilon^+ - \epsilon_k} + t_{k'}(k)(B = \infty) \, \frac{1}{\epsilon^+ - \epsilon_{k'}} + t_k(k')(B = \infty) \, \frac{1}{\epsilon^+ - \epsilon_k} \\ &\quad + \sum_{q \neq k,k'} t_q(k')(B = \infty) \, t_q(k)(B = \infty) \, \frac{1}{\epsilon^+ - \epsilon_q} \\ &= \delta_{kk'} \, \frac{1}{\epsilon^+ - \epsilon_k} + g_{\overline{kk'}}(B = \infty) \, \frac{1}{\epsilon_{k'} - \epsilon_k} \left(\frac{1}{\epsilon^+ - \epsilon_{k'}} - \frac{1}{\epsilon^+ - \epsilon_k} \right) \\ &\quad + O\left(N \, g_{\overline{kk'}}^2(B = \infty)\right) \\ &= \delta_{kk'} \, \frac{1}{\epsilon^+ - \epsilon_k} + g_{\overline{kk'}}(B = \infty) \, \frac{1}{\epsilon^+ - \epsilon_{k'}} \, \frac{1}{\epsilon^+ - \epsilon_k} \\ &\quad + O\left(N \, g_{\overline{kk'}}^2(B = \infty)\right) \ . \end{aligned} \tag{3.57}$$

[4] More accurately, for $|\epsilon_u - \epsilon_p| \gg D/N$. One can check this easily from the $1/N$-normalization of the coupling constant.

By comparison with (3.48) we can read off the T-matrix to leading order in the running coupling constant (2.114):

$$T_{p'p}(\epsilon^+) = g_{\overline{p'p}}(B = \infty) \ . \tag{3.58}$$

We have therefore achieved a resummation of the conventional perturbative expansion in the bare coupling constant for the T-matrix and arrived at the correct renormalized expression (3.58).

3.3.2 Resonant Level Model

In the example in the previous section we could evaluate observables in a straightforward way using the flow equation formalism and were able to capture nontrivial scaling aspects with this calculation. We now look at another simple (i.e. quadratic) Hamiltonian that will teach us some new lessons about the flow equation method, namely the resonant level model. The resonant level model ($U = 0$ Anderson impurity model) is defined by the Hamiltonian

$$H = \sum_k \epsilon_k c_k^\dagger c_k + \epsilon_d d^\dagger d + \sum_k V_k \left(c_k^\dagger d + d^\dagger c_k \right) \ . \tag{3.59}$$

Here d is a fermionic impurity orbital that hybridizes via the hybridization matrix elements V_k with the conduction band described by the operators $c_k^\dagger, c_k$. The hybridization matrix elements scale with $1/\sqrt{N}$ where N is the number of band states.

Unlike the potential scattering model, the resonant level model does not exhibit interesting nonperturbative scaling behavior. However, its new feature is the coupling of a localized state (the d-impurity orbital) with a continuum of band states. Conventional many-body techniques can deal with this situation easily. Unfortunately, in the flow equation method one needs to put in a lot of work for the same results. Still, we will later encounter interacting many-body problems where both aspects of nonperturbative scaling and coupling of a small system to an environment are important. In such situations flow equations can be advantageous compared to conventional methods. So while it is exaggerated to use our sophisticated machinery for the simple model in this section, we will later use the same machinery with little change in much more complicated problems. This is the main motivation for studying the resonant level model in pedagogical detail.

Our goal is to calculate the impurity orbital density of states $\rho_d(\omega)$,

$$\rho_d(\omega) = -\frac{1}{\pi} \operatorname{Im} G_d(\omega^+) \ , \tag{3.60}$$

where $G_d(\omega^+)$ is the impurity orbital Green's function,

$$G_d^+(\tau) = -\mathrm{i}\, \Theta(\tau) \left\langle \{ d(\tau), d^\dagger(0) \} \right\rangle \ . \tag{3.61}$$

The exact answer is (e.g. obtained using equations of motion [2])

$$\rho_d(\omega) = \frac{\Delta(\omega)}{\Big(\omega - \epsilon_d - \Lambda(\omega)\Big)^2 + \pi^2\,\Delta^2(\omega)}\ , \tag{3.62}$$

where $\Lambda(\omega)$ and $\Delta(\omega)$ are the real and imaginary parts of

$$\sum_k \frac{V_k^2}{\omega^+ - \epsilon_k} = \Lambda(\omega) + \mathrm{i}\pi\Delta(\omega), \tag{3.63}$$

respectively. $\Delta(\omega)$ is usually called the hybridization function.

In order to find this result in our framework, we first need to set up the flow equations for diagonalizing the Hamiltonian (3.59). The procedure is very similar to the calculation in Sect. 2.3. The diagonal part of the Hamiltonian is

$$H_0(B) = \sum_k \epsilon_k c_k^\dagger c_k + \epsilon_d d^\dagger d\ . \tag{3.64}$$

When one starts evaluating the commutator $[\eta, H]$, one notices immediately that new terms $\omega_{k'k} c_{k'}^\dagger c_k$ are generated which are not present in the original Hamiltonian (3.59). This makes a more general parametrization of $H_{\mathrm{int}}(B)$ that includes these new terms necessary to close the flow equations:

$$H_{\mathrm{int}}(B) = \sum_k V_k\,(c_k^\dagger d + d^\dagger c_k) + \sum_{k'\neq k} \omega_{k'k} c_{k'}^\dagger c_k\ . \tag{3.65}$$

Here V_k and $\omega_{k'k}$ depend on B and $\omega_{k'k} = \omega_{kk'}$ for hermiticity. One easily checks that the parametrization (3.65) remains form invariant under the flow induced by the canonical generator. Working out the flow equations is left as an exercise to the reader. The canonical commutator has the structure:

$$\begin{aligned}\eta &= [H_0, H_{\mathrm{int}}] \\ &= \sum V_k\,(\epsilon_k - \epsilon_d)\,(c_k^\dagger d - d^\dagger c_k) + \sum \omega_{k'k}\,(\epsilon_{k'} - \epsilon_k)\,c_{k'}^\dagger c_k\ .\end{aligned} \tag{3.66}$$

With it one finds the following set of flow equations:

$$\frac{\mathrm{d}V_k}{\mathrm{d}B} = -(\epsilon_k - \epsilon_d)^2 V_k\ - \sum_q (2\epsilon_q - \epsilon_k - \epsilon_d) V_q\ \omega_{qk} \tag{3.67}$$

$$\begin{aligned}\frac{\mathrm{d}\omega_{k'k}}{\mathrm{d}B} &= -(\epsilon_{k'} - \epsilon_k)^2 \omega_{k'k} + (\epsilon_{k'} + \epsilon_k - 2\epsilon_d) V_{k'}\, V_k \\ &\quad + \sum_q (\epsilon_{k'} + \epsilon_k - 2\epsilon_q)\omega_{k'q}\,\omega_{qk}\end{aligned} \tag{3.68}$$

$$\frac{\mathrm{d}\epsilon_d}{\mathrm{d}B} = 2\sum_q (\epsilon_d - \epsilon_q) V_q^2 \tag{3.69}$$

$$\frac{\mathrm{d}\epsilon_k}{\mathrm{d}B} = 2(\epsilon_k - \epsilon_d) V_k^2 + 2\sum_q (\epsilon_k - \epsilon_q)\omega_{kq}^2\ . \tag{3.70}$$

The general structure of these equations is already familiar from the potential scattering model:

- The interaction terms V_k and $\omega_{k'k}$ are eliminated by differential equations that are proportional to minus the respective energy transfer squared (in linear order).
- The band energies are shifted in order $1/N$, while the single-particle energy of the impurity orbital in shifted in order N^0. This is expected in an impurity model.

A new feature is that the potential scattering terms $\omega_{k'k}$ are generated during the flow according to (3.68), even if they are not present in the original Hamiltonian.[5] Notice that these terms are generated in order $1/N$ as expected for potential scattering, compare (2.87).

Before proceeding with analyzing the solution of these equations, let us find the flow equations for the transformation of the impurity orbital creation and annihilation operators $d^\dagger$ and d that we will need for calculating $\rho_d(\omega)$. The following ansatz is immediately plausible:

$$d^\dagger(B) = h(B)\, d^\dagger + \sum_p t_p(B)\, c_p^\dagger \ . \tag{3.71}$$

The commutator with the generator takes the following structure:

$$\begin{aligned}[\eta, d^\dagger(B)] = &\sum V_k\, (\epsilon_k - \epsilon_d)\, h\, c_k^\dagger - \sum V_k\, (\epsilon_k - \epsilon_d)\, t_k\, d^\dagger \\ &+ \sum \omega_{k'k} (\epsilon_{k'} - \epsilon_k)\, t_k\, c_{k'}^\dagger \ .\end{aligned} \tag{3.72}$$

This leads to the following set of differential equations that determine the flow of $d^\dagger(B)$:

$$\frac{\mathrm{d}h}{\mathrm{d}B} = -\sum_k V_k\ (\epsilon_k - \epsilon_d)\, t_k \tag{3.73}$$

$$\frac{\mathrm{d}t_k}{\mathrm{d}B} = V_k\, (\epsilon_k - \epsilon_d)\, h + \sum_q \omega_{kq} (\epsilon_k - \epsilon_q)\, t_q \ . \tag{3.74}$$

Very similar sets of differential equations will appear later in more complicated models. As in the previous section, a first check of the calculation is

[5] A careful reader will notice that it is possible to modify the generator η by introducing new terms $\sum_{k',k} \eta^{(2)}_{k'k}(B)\, c^\dagger_{k'} c_k$ in such a way that the terms $\omega_{k'k}$ are not generated during the flow. In fact, similar modifications of the canonical generator have been used in some of the flow equation literature [3]. However, this procedure introduces energy denominators into the generator that violate our conditions from Sect. 2.2.4 and can potentially be dangerous. For pedagogical reasons we work with the canonical choice of the generator in this introductory chapter. For more details on alternative choices consult the outlook and open questions in Sect. 5.4.

to verify that the anticommutation relation of $d^\dagger(B)$ and $d(B)$ is preserved under the unitary flow. This is equivalent to

$$\forall B \quad h^2(B) + \sum_k t_k^2(B) = 1 \ , \tag{3.75}$$

which follows from the initial condition $h(B=0)=1$, $t_k(B=0)=0$ and

$$\frac{\mathrm{d}}{\mathrm{d}B}\left(h^2(B) + \sum_k t_k^2(B)\right) = 0 \tag{3.76}$$

according to (3.73) and (3.74).

We first look at the case where all the hybridization matrix elements are constant, $V_k = V$, in order to focus on the key issues. We also require that the conduction band density of states is constant, $\rho(\epsilon) = \rho$. Notice that this implies $\Delta(\omega) = \Delta = \rho V^2$ and $\Lambda(\omega) = 0$ in the exact solution (3.62). We take the hybridization matrix elements V as small parameters and solve the differential equations to leading order in V. First

$$V_k(B) = V\,\mathrm{e}^{-B(\epsilon_k - \epsilon_d)^2} \tag{3.77}$$

and with this

$$\frac{\mathrm{d}t_k}{\mathrm{d}B} = V\,\mathrm{e}^{-B(\epsilon_k-\epsilon_d)^2}\,(\epsilon_k - \epsilon_d)\,h + O(V^3) \ . \tag{3.78}$$

The initial deviation of $h(B)$ from 1 is $O(V^2)$, so we can try to set $h(B) = 1$ in (3.78) and find

$$\begin{aligned} t_k(B) &= \frac{V}{\epsilon_k - \epsilon_d}\left(1 - \mathrm{e}^{-B(\epsilon_k-\epsilon_d)^2}\right) \\ \Rightarrow \quad t_k(B=\infty) &= \frac{V}{\epsilon_k - \epsilon_d} \ . \end{aligned} \tag{3.79}$$

This result can only be trusted if $h(B)$ is still sufficiently close to 1 on the B-scale where the main contributions to $t_k(B=\infty)$ come from, that is for $B \lesssim (\epsilon_k - \epsilon_d)^{-2}$. We can check this by plugging our approximate solution for $t_k(B)$ into the differential equation for $h(B)$, or, equivalently, into (3.75):

$$\begin{aligned} 1 - h^2(B) &= \sum_k \frac{V^2}{(\epsilon_k - \epsilon_d)^2}\left(1 - \mathrm{e}^{-B(\epsilon_k-\epsilon_d)^2}\right)^2 \\ &\propto O(\rho V^2)\, B^{1/2} \ . \end{aligned} \tag{3.80}$$

This implies that we can trust (3.79) for $|\epsilon_k - \epsilon_d| \gg \Delta$. The impurity orbital density of states follows immediately according to (3.34):

$$\rho_d(\omega) = \rho\, t_\omega^2(B=\infty) + h^2(B=\infty)\,\delta\big(\omega - \epsilon_d(B=\infty)\big)\ . \tag{3.81}$$

Here t_ω denotes the coefficient t_k with $\epsilon_k = \omega$. One sees that (3.79) is indeed correct to leading order in the hybridization for $|\omega - \epsilon_d| \gg \Delta$ by comparison with the exact result (3.62). Also notice that in our case $\epsilon_d(B=\infty) = \epsilon_d(B=0)$ since the hybridization matrix elements are constant.

Next we also want to learn something about $\rho_d(\omega)$ for $|\omega - \epsilon_d| \lesssim \Delta$. This is unfortunately quite difficult in the flow equation framework.[6] In order to proceed we first need to learn more about the solution of the flow equations for the Hamiltonian (3.67)–(3.70). We use the following approximate parametrization for the flowing coupling constants $V_k(B)$ in the same spirit as for the IR-parametrization in Sect. 2.3.2:

$$V_k(B) = V_d(B)\,\mathrm{e}^{-B(\epsilon_k-\epsilon_d)^2}\ . \tag{3.82}$$

Notice that the coupling constant $V_d(B)$ is never suppressed by an exponential term. One can verify numerically that this approximation is very accurate and can be used safely for our purposes. With this parametrization one easily derives

$$\omega_{qd}(B) = (\epsilon_q - \epsilon_d)\,\mathrm{e}^{-B(\epsilon_q-\epsilon_d)^2} \int_0^B \mathrm{d}B'\, V_d^2(B')\ , \tag{3.83}$$

where we have neglected terms in order V_d^4. This leads to

$$\begin{aligned}\frac{\mathrm{d}V_d}{\mathrm{d}B} &= -2V_d(B)\sum_q (\epsilon_q-\epsilon_d)^2 \mathrm{e}^{-2B(\epsilon_q-\epsilon_d)^2} \int_0^B \mathrm{d}B'\, V_d^2(B') \\ &= -\frac{\sqrt{2\pi}}{4}\,\rho\, V_d(B)\, B^{-3/2} \int_0^B \mathrm{d}B'\, V_d^2(B')\ .\end{aligned} \tag{3.84}$$

The full solution is a cumbersome expression and we can restrict our analysis to the asymptotic behavior: for large B one finds an algebraic decay with a universal exponent $-1/4$,

$$V_d(B) = \frac{1}{(8\pi\rho^2\, B)^{1/4}}\ . \tag{3.85}$$

This decay sets in once the flow equation scaling parameter is of order the hybridization parameter, $B^{-1/2} \propto \rho V^2 = \Delta$. For smaller values of B the coupling $V_d(B)$ remains essentially unchanged. Figure 3.1 shows this behavior of the hybridization matrix elements during the flow obtained from the full numerical solution of the differential equations.

Next we use this information to analyze the flow of $h(B)$ according to (3.73) and (3.74). In the initial phase of the flow we can neglect the ω_{kq}-terms

[6] It would be very desirable to have suitable mathematical tools that allow us to analytically solve systems like (3.73)–(3.74) for general coupling constants. At the time of writing this book, however, no such approach has yet been found.

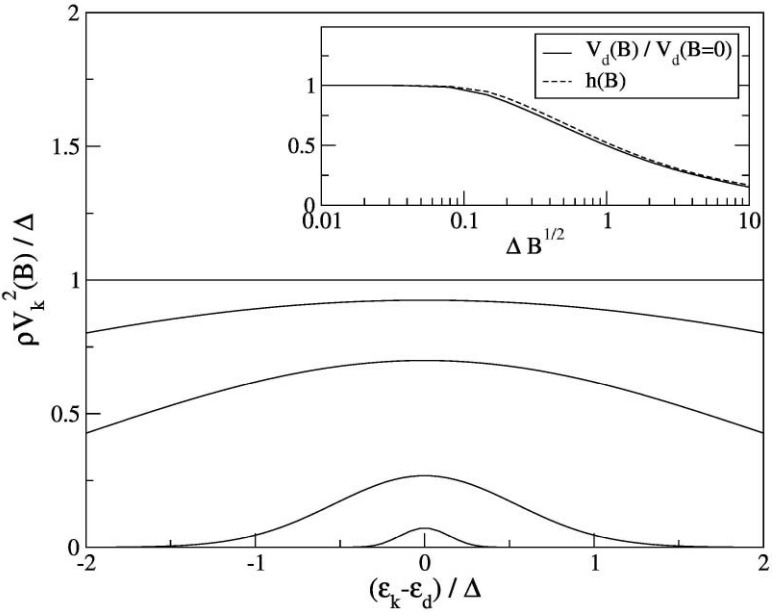

Fig. 3.1. Decay of hybridization couplings $V_k(B)$ during various stages of the flow from the exact numerical solution of the flow equations. Curves are for $B^{-1/2}/\Delta = \infty, 10, 4, 1, 0.25$ from top to bottom. The inset depicts the flow of the coupling $V_d(B)$ and $h(B)$ describing the transformation of the observable (3.73)

in (3.74) since they contribute in $O(V^3)$.[7] Integrating up (3.74) therefore yields

$$t_k(B) = (\epsilon_k - \epsilon_d) \int_0^B \mathrm{d}B' \, \mathrm{e}^{-B'(\epsilon_k - \epsilon_d)^2} \, V_d(B') \, h(B') \; . \tag{3.86}$$

First we will show that a nonvanishing asymptotic value $h(B = \infty) > 0$ is inconsistent with the properties of these equations. With the solution (3.85) for $V_d(B')$ one immediately derives

$$t_K(B = \infty) \propto h(B = \infty) \, \mathrm{sgn}(\epsilon_k - \epsilon_d) \, |\epsilon_k - \epsilon_d|^{-1/2} \; , \tag{3.87}$$

which leads to a divergent sum $\sum_k t_k^2(B = \infty)$ that is inconsistent with (3.75). *From this we make the important observation that the operator $d^\dagger$ decays completely into bath modes under the unitary flow.*

We will see later on that this is the typical behavior for a degree of freedom that is coupled to a thermodynamically large environment with a continuum of quasi-resonant modes. In particular, this implies that no coherent δ-function term remains in (3.81). The complete transformation of a degree

[7] However, this approximation is not accurate in the later phase of the flow though it gives the qualitatively correct behavior.

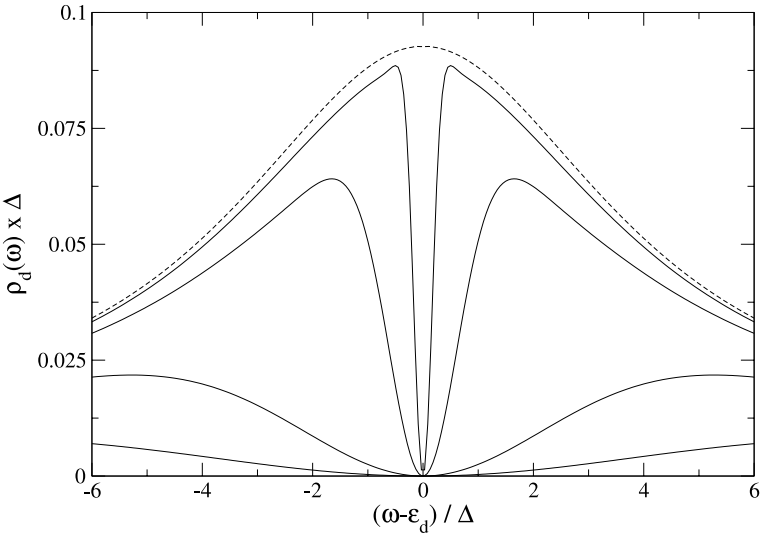

Fig. 3.2. Impurity orbital density of states at various stages of the flow from the exact numerical solution. The curves show $\rho_d(\omega;B) \stackrel{\text{def}}{=} \rho\, t_\omega^2(B)$ for $B^{-1/2}/\Delta = 10, 4, 1, 0.25$ from bottom to top. The dashed line depicts the exact solution (3.62) that is approached in the limit $B \to \infty$. Notice that the curves for finite B are not normalized since the δ-contribution for $h(B) \neq 0$ is not included in the definition of $\rho_d(\omega;B)$

of freedom into a different form is rather unusual from a standard many-body point of view. However, it is an essential and unavoidable consequence of the flow equation goal to generate a diagonal Hamiltonian.

Inserting the expression (3.86) into the differential equation for $h(B)$ leads to

$$\frac{\mathrm{d}h}{\mathrm{d}B} = -\frac{\sqrt{\pi}}{2}\,\rho\, V_d(B) \int_0^B \mathrm{d}B'\,(B+B')^{-3/2}\, V_d(B')\, h(B')\ . \tag{3.88}$$

One notices the similarity to the differential equation (3.84) for $V_d(B)$ which motivates using a similar solution with $h(B) \propto V_d(B)$. It is easy to verify that this ansatz in fact fulfills (3.88) for large values of B. The full numerical solution confirms that the proportionality $h(B) \propto V_d(B)$ indeed holds with very good accuracy during the entire flow, see Fig. 3.1.

With this information it is now straightforward to obtain the coefficients $t_k(B=\infty)$ for $|\epsilon_k - \epsilon_d| \ll \Delta$:

$$\begin{aligned} t_k(B=\infty) &\propto \frac{1}{V_d(0)}\,(\epsilon_k - \epsilon_d) \int_0^{(\epsilon_k-\epsilon_d)^{-2}} \mathrm{d}B'\, V_d^2(B') \\ &\propto \frac{1}{\rho V_d(0)}\,\mathrm{sgn}(\epsilon_k - \epsilon_d)\ . \end{aligned} \tag{3.89}$$

This yields the qualitatively correct behavior of $\rho_d(\omega)$ in the vicinity of the impurity orbital energy:

$$\rho_d(\omega) \propto \frac{1}{\Delta} \; , \tag{3.90}$$

which smoothly connects with the off-resonance behavior from (3.79).

However, in order to get quantitative results for $\rho_d(\omega)$ one has to resort to the numerical solution of (3.73) and (3.74). The results that demonstrate the buildup of $\rho_d(\omega)$ during the flow are shown in Fig. 3.2. One can make the following important observation from these curves: Since $t_k(B)$ necessarily changes its sign at $\epsilon_k = \epsilon_d$ according to (3.74), the function $\rho_d(\omega)$ always displays a dip at $\omega = \epsilon_d$ for finite B. This dip only closes asymptotically for $B \to \infty$. *It is worthwhile to emphasize again that the finite width of the spectral function is obtained with a hermitean diagonal Hamiltonian due to the complete decay of the observable into bath degrees of freedom.*

A final remark regarding the changes for a nonflat hybridization function $\Delta(\omega)$. The main new feature is a nontrivial flow of the impurity orbital energy $\epsilon_d(B)$ according to (3.69). It is precisely this flow which mimics the effect of $\Lambda(\omega)$ in (3.62), and one can show:

$$\epsilon_d(B = \infty) = \epsilon_d(B = 0) + \Lambda(\epsilon_d(B = 0)) \; . \tag{3.91}$$

References

1. H.B. Callen and T.A. Welton, Phys. Rev. **83**, 34 (1951)
2. A.C. Hewson: *The Kondo Problem to Heavy Fermions*, 1st edn (Cambridge University Press, Cambridge 1993)
3. S. Kehrein and A. Mielke, Ann. Phys. (NY) **252**, 1 (1996)

4 Interacting Many-Body Systems

In the previous chapters we have discussed various applications of the flow equation method for simple Hamiltonians. These applications were meant to familiarize the reader with the method in a pedagogical way. However, the flow equation method is designed as an analytical tool for solving nonperturbative interacting many-body problems that are much more complicated than the Hamiltonians in these previous examples. In order to look at such problems, we first need to introduce another ingredient for realistic flow equation applications, namely the concept of *normal-ordering*. Then we will discuss three examples of flow equation solutions that highlight different aspects of such many-body applications: the Kondo model as a fermionic impurity model in Sect. 4.2, the spin–boson model as a bosonic impurity model in Sect. 4.3, and Fermi liquid theory in Sect. 4.4.

4.1 Normal-Ordering

The fundamental problem in applications of the flow equation method to interacting systems can be understood by looking at a simple fermionic model:

$$H = \sum_n \epsilon_n c_n^\dagger c_n + \sum_{m_1', m_1, m_2', m_2} g(m_1', m_1, m_2', m_2)\, c_{m_1'}^\dagger c_{m_1} c_{m_2'}^\dagger c_{m_2} \ . \quad (4.1)$$

The canonical generator takes the structure

$$\eta = \sum g(m_1', m_1, m_2', m_2)\, (\epsilon_{m_1'} + \epsilon_{m_2'} - \epsilon_{m_1} - \epsilon_{m_2})\, c_{m_1'}^\dagger c_{m_1} c_{m_2'}^\dagger c_{m_2} \ . \quad (4.2)$$

We denote the kinetic energy part of (4.1) by H_0. It is easy to work out

$$[\eta, H_0] = -\sum g(m_1', m_1, m_2', m_2)\, (\epsilon_{m_1'} + \epsilon_{m_2'} - \epsilon_{m_1} - \epsilon_{m_2})^2\, c_{m_1'}^\dagger c_{m_1} c_{m_2'}^\dagger c_{m_2} \ . \quad (4.3)$$

However, the full flow equation for the Hamiltonian also requires the commutator of η with the interaction part. This leads to a commutator of a two-particle interaction term with another two-particle interaction term, i.e.

$$\begin{aligned} [\, c_{1'}^\dagger c_1 c_{2'}^\dagger c_2 \,,\, c_{3'}^\dagger c_3 c_{4'}^\dagger c_4 \,] &= c_{1'}^\dagger c_1 \,[\, c_{2'}^\dagger c_2 \,,\, c_{3'}^\dagger c_3 \,]\, c_{4'}^\dagger c_4 + \text{ other permutations} \\ &= \delta_{23'}\, c_{1'}^\dagger c_1 c_{2'}^\dagger c_3 c_{4'}^\dagger c_4 - \delta_{2'3}\, c_{1'}^\dagger c_1 c_{3'}^\dagger c_2 c_{4'}^\dagger c_4 \\ &\quad + \text{other permutations}, \end{aligned} \quad (4.4)$$

Stefan Kehrein: *The Flow Equation Approach to Many-Body Problems*
STMP **217**, 63–135 (2006)

where we have used (2.94). We see that this commutator produces a three-particle interaction term that is not originally contained in the Hamiltonian (4.1). Taking this new term into account, the canonical generator will also acquire a three-particle structure. This in turn produces even higher-order interactions in the commutator with $H_{\rm int}(B)$. This proliferation of higher-order terms is the fundamental "problem" of the flow equation method, as it is in one way or another of all analytical many-particle approaches that do not require integrability of the Hamiltonian. In order to turn the flow equation method into a useful nonperturbative tool, we first need to introduce a way of organizing these higher-order interactions into such a form that this series becomes well-behaved and can be truncated. This tool will be the normal-ordering prescription introduced in the next subsection.[1]

4.1.1 Bosons

Normal-ordering has been formally defined by Wick [1]. It is sometimes thought of as being no more than the subtraction of ground state expectation values from an operator. However, the normal-ordering prescription is a more sophisticated tool, which we now first work out for bosons.

We denote bosonic creation and annihilation operators collectively by A_k. The key ingredient of a normal-ordering procedure are its contractions C_{kl}, which are real numbers with the property

$$[A_k, A_l] = C_{kl} - C_{lk} \ . \tag{4.5}$$

In practice the contractions will either be expectation values with respect to some reference state $|\Psi_{NO}\rangle$ (usually the ground state of the free theory H_0),

$$C_{kl} \stackrel{\rm def}{=} \langle \Psi_{NO} \,|\, A_k A_l \,|\, \Psi_{NO} \rangle \ , \tag{4.6}$$

or expectation values in some mixed state described by a density matrix ρ,

$$C_{kl} \stackrel{\rm def}{=} {\rm Tr}(\rho \, A_k \, A_l) \ . \tag{4.7}$$

It is easy to verify that (4.5) is always fulfilled if the contractions are defined in one of these two ways since the commutator of two bosonic creation or annihilation operators is a c-number:

$$[a_k, a_l^\dagger] = \delta_{kl} \ , \quad [a_k^\dagger, a_l^\dagger] = [a_k, a_l] = 0 \ . \tag{4.8}$$

For example normal-ordering with respect to the vacuum $|\Omega\rangle$ leads to the following contractions:

[1] The presentation closely follows unpublished notes by F. Wegner.

$$\begin{aligned}
\langle \Omega \,|\, a_k^\dagger a_l \,|\, \Omega \rangle &= 0 \\
\langle \Omega \,|\, a_k a_l^\dagger \,|\, \Omega \rangle &= \delta_{kl} \\
\langle \Omega \,|\, a_k^\dagger a_l^\dagger \,|\, \Omega \rangle &= 0 \\
\langle \Omega \,|\, a_k a_l \,|\, \Omega \rangle &= 0 \; . \qquad (4.9)
\end{aligned}$$

Normal-ordering of a composite operator O is denoted by $: O :$ and is defined by the following three rules due to Wick:

1. Initial step: c-numbers remain unchanged,
$$: 1 := 1 \; . \qquad (4.10)$$
2. Normal-ordering is linear,
$$: \alpha_1 O_1 + \alpha_2 O_2 := \alpha_1 \; : O_1 : + \alpha_2 \; : O_2 : \, , \qquad (4.11)$$
where α_1, α_2 are arbitrary complex numbers.
3. Recurrence relation
$$A_k \; : O := : A_k \, O : + \sum_l C_{kl} \; : \frac{\partial O}{\partial A_l} : \, , \qquad (4.12)$$
where O is considered as a function of the creation and annihilation operators A_l.

Let us solve this recurrence relation explicitly for the first normal-ordering steps with respect to the vacuum:

$$\begin{aligned}
: a_k^\dagger : &= a_k^\dagger \qquad , \quad : a_k := a_k \qquad (4.13) \\
: a_k^\dagger a_l^\dagger : &= a_k^\dagger a_l^\dagger \quad , \quad : a_k a_l := a_k a_l \qquad (4.14) \\
: a_k^\dagger a_l : &= a_k^\dagger a_l \qquad (4.15) \\
: a_k a_l^\dagger : &= a_k a_l^\dagger - \delta_{kl} \; . \qquad (4.16)
\end{aligned}$$

From the recurrence relation we can deduce Wick's first theorem:

$$\begin{aligned}
A_{k_1} A_{k_2} \ldots A_{k_m} = : \left(A_{k_1} + \sum_{l_1} C_{k_1 l_1} \frac{\partial}{\partial A_{l_1}} \right) \left(A_{k_2} + \sum_{l_2} C_{k_2 l_2} \frac{\partial}{\partial A_{l_2}} \right) \ldots \\
\times \ldots \left(A_{k_{m-1}} + \sum_{l_{m-1}} C_{k_{m-1} l_{m-1}} \frac{\partial}{\partial A_{l_{m-1}}} \right) A_{k_m} : \qquad (4.17)
\end{aligned}$$

or

$$\begin{aligned}
: A_{k_1} A_{k_2} \ldots A_{k_m} : = \left(A_{k_1} - \sum_{l_1} C_{k_1 l_1} \frac{\partial}{\partial A_{l_1}} \right) \left(A_{k_2} - \sum_{l_2} C_{k_2 l_2} \frac{\partial}{\partial A_{l_2}} \right) \ldots \\
\times \ldots \left(A_{k_{m-1}} - \sum_{l_{m-1}} C_{k_{m-1} l_{m-1}} \frac{\partial}{\partial A_{l_{m-1}}} \right) A_{k_m} \qquad (4.18)
\end{aligned}$$

For example we find for vacuum normal-ordering

$$\begin{aligned} :a_{k_1}a_{k_2}a^\dagger_{k_3}a^\dagger_{k_4}: = {} & a_{k_1}a_{k_2}a^\dagger_{k_3}a^\dagger_{k_4} \\ & -\delta_{k_1k_3}a_{k_2}a^\dagger_{k_4} - \delta_{k_1k_4}a_{k_2}a^\dagger_{k_3} - \delta_{k_2k_3}a_{k_1}a^\dagger_{k_4} - \delta_{k_2k_4}a_{k_1}a^\dagger_{k_3} \\ & +\delta_{k_1k_3}\delta_{k_2k_4} + \delta_{k_1k_4}\delta_{k_2k_3} \ . \end{aligned} \tag{4.19}$$

On closer inspection this is simply

$$:a_{k_1}a_{k_2}a^\dagger_{k_3}a^\dagger_{k_4}: := a^\dagger_{k_3}a^\dagger_{k_4}a_{k_1}a_{k_2} \ , \tag{4.20}$$

that is all annihilation operators have been moved all the way to the right, and the creation operators all the way to the left. However, this "simple" interpretation of normal-ordering only works with respect to the vacuum (which is what we are often used to from quantum field theory). It cannot, e.g., be generalized to normal-ordering with respect to a finite temperature state defined by a density matrix like in (4.7).

We will frequently need to express the product of two normal-ordered operators as a sum of normal-ordered terms. This is the content of Wick's second theorem:

$$:O_1::O_2:=:\exp\left(\sum_{k,l} C_{kl}\frac{\partial^2}{\partial A_k \partial A'_l}\right) O_1(A)\,O_2(A'):\Big|_{A'=A} \ . \tag{4.21}$$

Here the operators on the right hand side are formally thought to be functions of different sets of creation and annihilation operators A and A' for the purpose of differentiation, and only afterwards identified again. Let us see how this works in a simple example for vacuum normal-ordering:

$$:a^\dagger_{k_3}a_{k_1}::a^\dagger_{k_4}a_{k_2}:=:a^\dagger_{k_3}a_{k_1}a^\dagger_{k_4}a_{k_2}:+\delta_{k_1k_4}\ :a^\dagger_{k_3}a_{k_2}: \ . \tag{4.22}$$

Condition (4.5) leads to the important property that operators within a normal-ordered expression can be commuted. We first exchange two neighboring factors

$$:A_{k_1}\dots A_{k_{i-1}}A_{k_i}A_{k_{i+1}}A_{k_{i+2}}\dots A_{k_m}:=:A_{k_1}\dots A_{k_{i-1}}A_{k_{i+1}}A_{k_i}A_{k_{i+2}}\dots A_{k_m}: \tag{4.23}$$

According to (4.18) this leads to the following commutator on the right hand side:

$$\begin{aligned} \left[\left(A_{k_i}-\sum_{l_i}C_{k_il_i}\frac{\partial}{\partial A_{l_i}}\right) \ , \ \left(A_{k_{i+1}}-\sum_{l_{i+1}}C_{k_{i+1}l_{i+1}}\frac{\partial}{\partial A_{l_{i+1}}}\right)\right] & \\ = [A_{k_i},A_{k_{i+1}}] - C_{k_ik_{i+1}} + C_{k_{i+1}k_i} & \\ = 0 \ . & \end{aligned} \tag{4.24}$$

Therefore the difference (4.23) vanishes, which can easily be extended to the statement that any two operators in a normal-ordered expression $:A_{k_1}A_{k_2}\ldots A_{k_n}:$ can be exchanged. This commutativity property combined with Wick's second theorem (4.21) is often the fastest way to normal-order a complicated composite operator.

We now come to the underlying reason for the usefulness of normal-ordering for organizing flow equation expansion schemes. The following considerations are only applicable if normal-ordering is defined with respect to either the ground state of a Hamiltonian H_0 that is bilinear in creation and annihilation operators, or with respect to its density matrix,

$$\rho = \frac{\mathrm{e}^{-\beta H_0}}{\mathrm{Tr}\,\mathrm{e}^{-\beta H_0}} \ . \tag{4.25}$$

We denote both these expectation values by $\langle O\rangle$. Next we show that the expectation value of a normal-ordered composite operator that contains at least one creation or annihilation operator vanishes. For this purpose we first employ the recurrence relation (4.12),

$$\langle :A_k\,O: \rangle = \langle A_k\ :O: \rangle - \sum_l C_{kl}\,\langle :\frac{\partial O}{\partial A_l}: \rangle \ . \tag{4.26}$$

Now one can easily prove the following rule for a bilinear operator H_0:

$$\langle A_k\,O\rangle = \sum_l \langle A_k\,a_l^\dagger\rangle\,\langle\,[a_l\,,O]\,\rangle - \sum_l \langle A_k\,a_l\,\rangle\,\langle\,[a_l^\dagger,O]\,\rangle \ . \tag{4.27}$$

From the fundamental bosonic commutation relations one derives

$$[a_l^\dagger,O] = -\frac{\partial O}{\partial a_l} \quad , \quad [a_l\,,O] = \frac{\partial O}{\partial a_l^\dagger} \ , \tag{4.28}$$

which allows one to express (4.27) in compact form:

$$\begin{aligned}\langle A_k\,O\rangle &= \sum_l \langle A_k\,A_l\rangle\,\left\langle \frac{\partial O}{A_l}\right\rangle \\ &= \sum_l C_{kl}\,\left\langle \frac{\partial O}{A_l}\right\rangle \ .\end{aligned} \tag{4.29}$$

Combined with (4.26) this proves

$$\langle :A_k\,O: \rangle = 0 \tag{4.30}$$

and therefore the expectation value of a normal-ordered operator always vanishes unless this operator is just a c-number.

We arrive at the following fundamental property: Let $E_n^{(1)}$ and $E_n^{(2)}$ be two composite operators consisting of a total of n creation or annihilation

operators. We think of these operators as n-particle excitations out of the ground state/mixed state. Then for any normal-ordered operator consisting of $2m$ creation or annihilation operators $: O_{2m} :$ we can only have a nonvanishing matrix element with respect to these excited states,

$$\langle E_n^{(1)} \, : O_{2m} : \, E_n^{(2)} \rangle \neq 0 \; , \tag{4.31}$$

if $n \geqq m$.

The proof for this property is straightforward by noticing that a product of two normal-ordered operators with s_1 and s_2 creation or annihilation operators can be written as a sum over normal-ordered operators with $s = |s_1 - s_2|, \ldots, |s_1 + s_2|$ creation or annihilation operators (compare (4.21). Therefore $\langle : O_{s_1} :: O_{s_2} : \rangle$ can be nonzero if and only if $s_1 = s_2$. From this one immediately deduces (4.31). Notice that this property is trivial for normal-ordering with respect to the vacuum if one looks at (4.20).

What does this property (4.31) mean in physical terms? Imagine that we are interested in a one-particle excitation energy, e.g. for a boson with quantum number k. For a normal-ordered Hamiltonian we can write in lowest order of the coupling constant

$$\begin{aligned} E_k^{(1)} &= \langle a_k \, : H : \, a_k^\dagger \rangle \\ &= \langle a_k \, : H_2 : \, a_k^\dagger \rangle \; , \end{aligned} \tag{4.32}$$

where $: H_2 :$ contains only operators consisting of two elementary (i.e., creation or annihilation) operators. Likewise for the interaction energy of two excited particles:

$$\begin{aligned} E_{k_1,k_2}^{(2)} &= \langle a_{k_1} a_{k_2} \, : H : \, a_{k_1}^\dagger a_{k_2}^\dagger \rangle - E_{k_1}^{(1)} - E_{k_2}^{(1)} \\ &= \langle a_{k_1} a_{k_2} \, : H_4 : \, a_{k_1}^\dagger a_{k_2}^\dagger \rangle \; . \end{aligned} \tag{4.33}$$

This means that $: H_2 :$ contains all the information about the one-particle excitations (quasiparticle energies), $: H_4 :$ contains all the information about two-particle interactions (quasiparticle interaction), etc.[2] Without normal-ordering for example the coefficients from H_4 could also contribute to the one-particle energies in (4.32). If we later on truncate the series of higher and higher order interactions in the flow equation scheme by neglecting *normal-ordered* interactions $: H_n :$ with $n \geqq n_{\max}$, we make a "smaller" error than by neglecting not normal-ordered terms since normal-ordered terms only contribute for higher particle excitations from the ground state. Loosely speaking normal-ordered operators have less "content" (nonvanishing matrix elements) than their not normal-ordered counterparts. And if we are forced to use an

[2]The terminology "quasiparticle" as it is used here differs from Landau quasiparticles in Fermi liquid theory A different terminology would be to speak of "flow equation quasiparticle". We will have more to say on this subject in Sect. 4.4.1 on Fermi liquid theory.

approximation, we obviously want to use an approximation that has the smallest possible deviation from the exact result. Normal-ordering will also turn out to be the necessary ingredient to obtain the conventional scaling equations in the IR limit of the flow equation approach.[3]

4.1.2 Fermions

For fermions some of the above expressions need to be modified since commutation relations are replaced by anticommutators. We again collectively denote fermionic creation and annihilation operator by A_k and have instead of (4.5):

$$\{A_k, A_l\} = C_{kl} + C_{lk} \ . \tag{4.34}$$

For deriving Wick's first theorem one now needs to use the rule

$$\frac{\partial}{\partial A_l} A_k = \delta_{kl} - A_k \frac{\partial}{\partial A_l} \ , \tag{4.35}$$

otherwise (4.17) and (4.18) remain unchanged. Let us work out two simple examples:

$$: c^\dagger_{k_3} c_{k_1} : = c^\dagger_{k_3} c_{k_1} - C_{k_3 k_1} \tag{4.36}$$

$$\begin{aligned} : c^\dagger_{k_3} c_{k_1} c^\dagger_{k_4} c_{k_2} : &= c^\dagger_{k_3} c_{k_1} c^\dagger_{k_4} c_{k_2} \\ &\quad - C_{k_4 k_2} c^\dagger_{k_3} c_{k_1} - C_{k_3 k_1} c^\dagger_{k_4} c_{k_2} - C_{k_1 k_4} c^\dagger_{k_3} c_{k_2} - C_{k_3 k_2} c_{k_1} c_{k_4} \\ &\quad + C_{k_3 k_1} C_{k_4 k_2} + C_{k_1 k_4} C_{k_3 k_2} \end{aligned} \tag{4.37}$$

$$\begin{aligned} &= : c^\dagger_{k_3} c_{k_1} : : c^\dagger_{k_4} c_{k_2} : \\ &\quad + C_{k_3 k_2} : c^\dagger_{k_4} c_{k_1} : - C_{k_1 k_4} : c^\dagger_{k_3} c_{k_2} : - C_{k_1 k_4} C_{k_3 k_2} \ . \end{aligned} \tag{4.38}$$

In Wick's second theorem we need to take into account the correct sequence of differentiations, which for fermions leads to

$$: O_1 : : O_2 :=: \exp\left(\sum_{k,l} C_{kl} \frac{\partial^2}{\partial A'_l \partial A_k} \right) O_1(A)\, O_2(A') : \Big|_{A'=A} \ . \tag{4.39}$$

Notice that (4.34) also holds for the exchange of the fields A and A'. This gives us another (faster) way for deriving (4.38):

$$\begin{aligned} : c^\dagger_{k_3} c_{k_1} : : c^\dagger_{k_4} c_{k_2} : &= : c^\dagger_{k_3} c_{k_1} c^\dagger_{k_4} c_{k_2} : \\ &\quad + C_{k_3 k_2} : c_{k_1} c^\dagger_{k_4} : + C_{k_1 k_4} : c^\dagger_{k_3} c_{k_2} : + C_{k_1 k_4} C_{k_3 k_2} \ . \end{aligned} \tag{4.40}$$

[3] Without normal-ordering there is no feedback from higher orders in the coupling constant to lower orders, which leads to worse convergence properties of a not normal-ordered expansion since it cannot describe nonperturbative energy scales.

This expression agrees with (4.38) since the exchange of neighboring fermionic creation or annihilation operators picks up a minus sign. Therefore (4.23) is replaced by

$$:A_{k_1}\dots A_{k_{i-1}}A_{k_i}A_{k_{i+1}}A_{k_{i+2}}\dots A_{k_m}:+:A_{k_1}\dots A_{k_{i-1}}A_{k_{i+1}}A_{k_i}A_{k_{i+2}}\dots A_{k_m}: = 0\ . \tag{4.41}$$

The rules for multiple exchanges etc. can all be easily derived from this rule. Finally the properties (4.30)–(4.33) of expectation values of normal-ordered operators with respect to a Hamiltonian bilinear in fermionic creation and annihilation operators carry over without change.

4.1.3 Important Commutators

We will here briefly sum up some of the most important commutators and normal-ordered expressions that one needs for deriving the Hamiltonian flow for interacting many-particle systems. In practice, all terms will always be normal-ordered, so we will focus on commutators of normal-ordered interaction terms.

Bosons

We consider normal-ordering with respect to the usual diagonal Hamiltonian

$$H_0 = \sum_k \omega_k\, a_k^\dagger a_k \quad \text{with } \omega_k \geqq 0\ . \tag{4.42}$$

Therefore the only nonvanishing contractions are

$$\langle a_{k'}^\dagger a_k\rangle = \delta_{k'k}\, n(k)\ . \tag{4.43}$$

Hence $n(k)$ is the particle-number expectation value at either zero ($n(k)\equiv 0$) or finite temperature. Notice that

$$\langle a_k a_{k'}^\dagger\rangle = \delta_{k'k}\ (n(k)+1) \tag{4.44}$$

due to the bosonic commutation relations.

Here is a list of some important normal-ordered expressions (the notation should be obvious):

$$a_{1'}^\dagger a_1 = :a_{1'}^\dagger a_1: +\delta_{1'1}\, n(1) \tag{4.45}$$

$$a_1 a_{1'}^\dagger = :a_{1'}^\dagger a_1: +\delta_{1'1}\,(n(1)+1) \tag{4.46}$$

$$\begin{aligned} :a_{1'}^\dagger a_1:\,:a_{2'}^\dagger a_2: = {} & :a_{1'}^\dagger a_{2'}^\dagger a_2 a_1: \\ & +\delta_{12'}(n(1)+1)\ :a_{1'}^\dagger a_2: +\delta_{1'2} n(1')\ :a_{2'}^\dagger a_1: \\ & +\delta_{12'}\delta_{1'2}\,(n(1)+1)\ n(1') \end{aligned} \tag{4.47}$$

The first commutators of normal-ordered operators are:

$$[a_1, a_{1'}^\dagger] = \delta_{1'1} \tag{4.48}$$

$$\begin{aligned}[: a_{1'}^\dagger a_1 :, : a_{2'}^\dagger a_2 :] = \delta_{12'} : a_{1'}^\dagger a_2 : - \delta_{1'2} : a_{2'}^\dagger a_1 : \\ + \delta_{12'}\delta_{1'2}\ (n(1') - n(1))\end{aligned} \tag{4.49}$$

$$\begin{aligned}&[: a_{1'}^\dagger a_{2'}^\dagger a_2 a_1 :, : a_{3'}^\dagger a_3 :] = \\ &= \delta_{23'} : a_{1'}^\dagger a_{2'}^\dagger a_3 a_1 : + \delta_{13'} : a_{1'}^\dagger a_{2'}^\dagger a_3 a_2 : \\ &\quad - \delta_{2'3} : a_{1'}^\dagger a_{3'}^\dagger a_2 a_1 : - \delta_{1'3} : a_{2'}^\dagger a_{3'}^\dagger a_2 a_1 : \\ &\quad + \delta_{23'}\delta_{2'3}\,(n(2') - n(2))\ : a_{1'}^\dagger a_1 : + \delta_{23'}\delta_{1'3}\,(n(1') - n(2))\ : a_{2'}^\dagger a_1 : \\ &\quad + \delta_{13'}\delta_{2'3}\,(n(2') - n(1))\ : a_{1'}^\dagger a_2 : + \delta_{13'}\delta_{1'3}\,(n(1') - n(1))\ : a_{2'}^\dagger a_2 :\ .\end{aligned} \tag{4.50}$$

The last expression can be somehow simplified: in flow equation commutators the indices are always summed over with suitably symmetric functions due to the bosonic exchange symmetry. Therefore we will usually be interested in a commutator of the form

$$\sum_{1',2',1,2,3',3} A(1'2',21)\, B(3',3)\, [: a_{1'}^\dagger a_{2'}^\dagger a_2 a_1 :, : a_{3'}^\dagger a_3 :]\ , \tag{4.51}$$

where

$$A(1'2',21) = A(2'1',21) = A(1'2',12) = A(2'1',12)\ . \tag{4.52}$$

This yields a more compact expression than (4.50):

$$\begin{aligned}&\sum A(1'2',21)\, B(3',3)\, [: a_{1'}^\dagger a_{2'}^\dagger a_2 a_1 :, : a_{3'}^\dagger a_3 :] \\ &= \sum \Big(A(1'2',x1)\, B(x,2) + A(1'2',2x)\, B(x,1) \\ &\qquad - A(1'x,21)\, B(2',x) - A(x2',21)\, B(1',x) \Big)\ : a_{1'}^\dagger a_{2'}^\dagger a_2 a_1 : \\ &\quad + 4 \sum A(1'x,y1)\, B(y,x)\ (n(x) - n(y))\ : a_{1'}^\dagger a_1 :\ ,\end{aligned} \tag{4.53}$$

where the sums run over all indices including x and y.

Fermions

The diagonal Hamiltonian that we use subsequently for normal-ordering purposes describes a noninteracting Fermi gas,

$$H_0 = \sum_k (\epsilon_k - \mu)\, c_k^\dagger c_k\ . \tag{4.54}$$

Therefore the only nonvanishing contractions are

$$\langle c^\dagger_{k'} c_k \rangle = \delta_{k'k}\, n(k)\ . \tag{4.55}$$

Here $n(k)$ is the Fermi function at either zero ($n(k) \equiv \Theta(\mu - \epsilon_k)$) or finite temperature. Notice

$$\langle c_k c^\dagger_{k'} \rangle = \delta_{k'k}\ (1 - n(k)) \tag{4.56}$$

due to the fermionic anticommutation relation $\{c_k, c^\dagger_{k'}\} = \delta_{k'k}$.

Here are some important normal-ordered expressions:

$$c^\dagger_{1'} c_1 = :c^\dagger_{1'} c_1: + \delta_{1'1}\, n(1) \tag{4.57}$$

$$c_1 c^\dagger_{1'} = -:c^\dagger_{1'} c_1: + \delta_{1'1}\,(1 - n(1)) \tag{4.58}$$

$$\begin{aligned} :c^\dagger_{1'} c_1 :: c^\dagger_{2'} c_2 : &= :c^\dagger_{1'} c^\dagger_{2'} c_2 c_1: \\ &\quad + \delta_{12'}\ (1 - n(1))\ :c^\dagger_{1'} c_2 : - \delta_{1'2}\, n(1')\ :c^\dagger_{2'} c_1 : \\ &\quad + \delta_{1'2}\delta_{12'}\, n(1')\ (1 - n(1))\ . \end{aligned} \tag{4.59}$$

The first commutators of normal-ordered operators are:

$$\begin{aligned} [:c^\dagger_{1'} c_1 :, :c^\dagger_{2'} c_2 :] &= \delta_{12'}\ :c^\dagger_{1'} c_2 : - \delta_{1'2}\ :c^\dagger_{2'} c_1 : \\ &\quad + \delta_{12'}\delta_{1'2}\ (n(1') - n(1)) \end{aligned} \tag{4.60}$$

$$\begin{aligned} &[:c^\dagger_{1'} c^\dagger_{2'} c_2 c_1 :, :c^\dagger_{3'} c_3 :] = \\ &= \delta_{23'}\ :c^\dagger_{1'} c^\dagger_{2'} c_3 c_1 : - \delta_{13'}\ :c^\dagger_{1'} c^\dagger_{2'} c_3 c_2 : \\ &\quad - \delta_{2'3}\ :c^\dagger_{1'} c^\dagger_{3'} c_2 c_1 : + \delta_{1'3}\ :c^\dagger_{2'} c^\dagger_{3'} c_2 c_1 : \\ &\quad + \delta_{23'}\delta_{2'3}\,(n(2') - n(2))\ :c^\dagger_{1'} c_1 : + \delta_{23'}\delta_{1'3}\,(n(2) - n(1'))\ :c^\dagger_{2'} c_1 : \\ &\quad + \delta_{13'}\delta_{2'3}\,(n(1) - n(2'))\ :c^\dagger_{1'} c_2 : + \delta_{13'}\delta_{1'3}\,(n(1') - n(1))\ :c^\dagger_{2'} c_2 :\ . \end{aligned} \tag{4.61}$$

Similar to the discussion for bosons in the previous chapter we will usually need expressions of the type

$$\sum_{1',2',1,2,3',3} A(1'2',21)\, B(3',3)\, [:c^\dagger_{1'} c^\dagger_{2'} c_2 c_1 :, :c^\dagger_{3'} c_3 :]\ , \tag{4.62}$$

where

$$A(1'2',21) = -A(2'1',21) = A(2'1',12) = -A(1'2',12)\ . \tag{4.63}$$

This yields a more compact expression than (4.61):

$$\begin{aligned} &\sum A(1'2',21)\, B(3',3)\, [:c^\dagger_{1'} c^\dagger_{2'} c_2 c_1 :, :c^\dagger_{3'} c_3 :] \\ &= \sum \Big(A(1'2',x1)\, B(x,2) + A(1'2',2x)\, B(x,1) \\ &\qquad - A(1'x,21)\, B(2',x) - A(x2',21)\, B(1',x) \Big)\ :c^\dagger_{1'} c^\dagger_{2'} c_2 c_1 : \\ &\quad + 4 \sum A(1'x,y1)\, B(y,x)\ (n(x) - n(y))\ :c^\dagger_{1'} c_1 :\ . \end{aligned} \tag{4.64}$$

Notice that (4.49) and (4.53) for bosons are structurally identical with (4.60) and (4.64) for fermions. Therefore the corresponding flow equations for a fermionic and a bosonic system are structurally identical if only the above commutators appear. However, this property cannot be generalized, for example it does not hold anymore for commutators of two-particle interaction terms.

4.1.4 Normal-Ordered Expansions

We next analyze the general structure of a flow-equation expansion for an interacting many-particle system before proceeding with concrete model investigations. A suitable Hamiltonian for bringing out the general structure is, e.g., a system of interacting spinless fermions:

$$H = \sum \epsilon_k \, c_k^\dagger c_k + \lambda \sum g(k_1' k_2', k_2 k_1) \; : c_{k_1'}^\dagger c_{k_2'}^\dagger c_{k_2} c_{k_1} : \; . \tag{4.65}$$

Here λ is an expansion parameter that we assume to be small, $|\lambda| \ll 1$. The diagonal part of H is

$$\begin{aligned} H_0 &= H_{\rm kin} + \lambda \, D_{(4)} \\ &= \sum \epsilon_k \, c_k^\dagger c_k + \lambda \sum g^{(\rm diag)}(k_1' k_2', k_2 k_1) \; : c_{k_1'}^\dagger c_{k_2'}^\dagger c_{k_2} c_{k_1} : \, , \end{aligned} \tag{4.66}$$

where $g^{(\rm diag)}(k_1' k_2', k_2 k_1)$ contains only energy-diagonal scattering processes,

$$\epsilon_{k_1'} + \epsilon_{k_2'} - \epsilon_{k_2} - \epsilon_{k_1} \neq 0 \quad \Rightarrow \quad g^{(\rm diag)}(k_1' k_2', k_2 k_1) = 0 \; . \tag{4.67}$$

The remaining interaction part in $H = H_0 + H_{\rm int}$ is then given by

$$H_{\rm int(4)} = \sum g^{(\rm n-diag)}(k_1' k_2', k_2 k_1) \; : c_{k_1'}^\dagger c_{k_2'}^\dagger c_{k_2} c_{k_1} : \, , \tag{4.68}$$

where $g^{(\rm n-diag)}(k_1' k_2', k_2 k_1)$ contains only non-energy-diagonal scattering matrix elements,

$$\epsilon_{k_1'} + \epsilon_{k_2'} - \epsilon_{k_2} - \epsilon_{k_1} = 0 \quad \Rightarrow \quad g^{(\rm n-diag)}(k_1' k_2', k_2 k_1) = 0 \; . \tag{4.69}$$

Notice that in impurity models terms like $D_{(4)}$ only contribute in $O(1/N)$ (where N is the number of degrees of freedom), as we have seen in Sect. 2.3. Such energy-diagonal scattering processes can therefore be ignored when one works out the perturbative flow equations for impurity models. However, this statement is no longer true in translation-invariant models like Fermi liquids as we will see in Sect. 4.4.1. For this reason we now first work out the flow equation expansion for an impurity model where we can ignore terms like $D_{(4)}$. Afterwards, we discuss the modifications when we cannot ignore such energy-diagonal interaction matrix elements for thermodynamic reasons alone.

Let us derive the flow equation expansion in powers of λ for an impurity model with:

$$H_0 = H_{\rm kin} \tag{4.70}$$

$$H_{\rm int(4)} = \sum g(k_1' k_2', k_2 k_1) \; : c^\dagger_{k_1'} c^\dagger_{k_2'} c_{k_2} c_{k_1} : \; . \tag{4.71}$$

The canonical generator is given by

$$\eta = [H_0, \lambda\, H_{\rm int(4)}] = \lambda\, \eta^{(1)} \; . \tag{4.72}$$

Structurally, the flow equations take the following form with this generator:

$$\begin{aligned} \lambda\, \frac{\partial g(k_1' k_2', k_2 k_1)}{\partial B} &= -(\epsilon_{k_1'} + \epsilon_{k_2'} - \epsilon_{k_1} - \epsilon_{k_2})^2\, \lambda\, g(k_1' k_2', k_2 k_1) \\ &\quad + \lambda^2\, R_g^{(1)} \end{aligned} \tag{4.73}$$

$$\frac{\partial \epsilon_k}{\partial B} = \lambda^2\, R_\epsilon^{(1)} \tag{4.74}$$

$$\frac{\partial E}{\partial B} = \lambda^2\, R_E^{(1)} \tag{4.75}$$

$$\lambda^2\, \frac{\partial u(k_1' k_2' k_3', k_3 k_2 k_1)}{\partial B} = \lambda^2\, R_u^{(1)} \; . \tag{4.76}$$

Here $R_g^{(1)}$ denotes the normal-ordered part of $[\eta^{(1)}, H_{\rm int(4)}]$ that has the structure of the g-interaction term (4.71), etc. The flowing Hamiltonian is given by

$$H(B) = \sum \epsilon_k(B)\, c_k^\dagger c_k + \lambda H_{\rm int(4)}(B) + \lambda^2 H_{\rm int(6)}(B) + E(B) \; . \tag{4.77}$$

Here

$$H_{\rm int(6)} = \sum u(k_1' k_2' k_3', k_3 k_2 k_1) \; : c^\dagger_{k_1'} c^\dagger_{k_2'} c^\dagger_{k_3'} c_{k_3} c_{k_2} c_{k_1} : \tag{4.78}$$

is a newly generated three-particle interaction term and $E(B)$ is a (usually uninteresting) constant.

Let us see how the newly generated interactions modify the flow. In order to eliminate them we extend our generator to take $H_{\rm int(6)}$ into account:

$$\eta = \lambda\, \eta^{(1)} + \lambda^2\, \eta^{(2)} \; , \tag{4.79}$$

where

$$\eta^{(2)} = [H_0, H_{\rm int(6)}] \; . \tag{4.80}$$

We have to evaluate the following new commutators in order λ^3:

$$[\lambda \eta^{(1)}, \lambda^2 H_{\rm int(6)}] \quad \text{and} \quad [\lambda^2 \eta^{(2)}, \lambda H_{\rm int(4)}] \; . \tag{4.81}$$

In the above example this leads to the contribution:

$$
\begin{aligned}
&[\lambda\eta^{(1)}, \lambda^2 H_{\mathrm{int}(6)}] + [\lambda^2\eta^{(2)}, \lambda H_{\mathrm{int}(4)}] \qquad (4.82)\\
&= \lambda^3 \sum (\epsilon_{k_1'} + \epsilon_{k_2'} - \epsilon_{k_1} - \epsilon_{k_2} - \epsilon_{k_3'} - \epsilon_{k_4'} - \epsilon_{k_5'} + \epsilon_{k_3} + \epsilon_{k_4} + \epsilon_{k_5})\\
&\quad \times g(k_1'k_2', k_2k_1)\, u(k_3'k_4'k_5', k_5k_4k_3)\, [: c^\dagger_{k_1'} c^\dagger_{k_2'} c_{k_2} c_{k_1} :, : c^\dagger_{k_3'} c^\dagger_{k_4'} c^\dagger_{k_5'} c_{k_5} c_{k_4} c_{k_3} :]
\end{aligned}
$$

This yields the following new terms in the above set of flow equations:

$$
\begin{aligned}
\lambda \frac{\partial g(k_1'k_2', k_2k_1)}{\partial B} &= -(\epsilon_{k_1'} + \epsilon_{k_2'} - \epsilon_{k_1} - \epsilon_{k_2})^2\, \lambda\, g(k_1'k_2', k_2k_1)\\
&\quad + \lambda^2\, R_g^{(1)} + \lambda^3\, R_g^{(2)} \qquad (4.83)\\
\frac{\partial \epsilon_k}{\partial B} &= \lambda^2\, R_\epsilon^{(1)} + \lambda^3\, R_\epsilon^{(2)} \qquad (4.84)\\
\frac{\partial E}{\partial B} &= \lambda^2\, R_E^{(1)} + \lambda^3\, R_E^{(2)} \qquad (4.85)\\
\lambda^2 \frac{\partial u(k_1'k_2'k_3', k_3k_2k_1)}{\partial B} &= -(\epsilon_{k_1'} + \epsilon_{k_2'} + \epsilon_{k_3'} - \epsilon_{k_1} - \epsilon_{k_2} - \epsilon_{k_3})^2\\
&\quad \times \lambda^2 u(k_1'k_2'k_3', k_3k_2k_1)\\
&\quad + \lambda^2\, R_u^{(1)} + \lambda^3\, R_u^{(2)} \qquad (4.86)\\
\lambda^3 \frac{\partial v(k_1'k_2'k_3'k_4', k_4k_3k_2k_1)}{\partial B} &= \lambda^3\, R_v^{(2)}\ . \qquad (4.87)
\end{aligned}
$$

Here the v-coefficient describes a new four-particle interaction term $H_{\mathrm{int}(8)}$.

Analyzing these equations we can see that the result of the leading order of the flow equation expansion

$$
\frac{\partial H(B)}{\partial B} = \lambda\, [\eta^{(1)}, H_0(B) + \lambda\, H_{\mathrm{int}(4)}(B)] + \lambda^2\, [\eta^{(2)}, H_0(B)] \qquad (4.88)
$$

takes the form

$$
H(B=\infty) = \sum \epsilon_k(B=\infty)\, c_k^\dagger c_k + E(B=\infty) + O(\lambda^3)\ . \qquad (4.89)
$$

Here the flow of the coupling constants is determined by (4.73)–(4.75), in particular the newly generated term (4.76) can be ignored. Notice that H_{int} does not appear explicitly anymore in $H(B=\infty)$ since all interactions vanish everywhere in order λ and λ^2 (except for energetically degenerate points that are thermodynamically irrelevant).

Going one order further in the flow equation expansion we find

$$
H(B=\infty) = \sum \epsilon_k(B=\infty)\, c_k^\dagger c_k + E(B=\infty) + O(\lambda^4)\ , \qquad (4.90)
$$

where the flow of the coupling constants is now determined by (4.83)–(4.86). While this expansion is perturbative in λ for a finite step ΔB, the overall integration over the flow parameter B makes it nonperturbative similar to the conventional scaling approach. We will later see that in a suitable limit

(4.89) reproduces the 1-loop β-function for the running coupling constant g, and (4.90) reproduces the results of a 2-loop calculation. The generalization to higher orders is straightforward, albeit the computational effort increases considerably. Notice that in order to get the 2-loop β-function for g from (4.83), we can ignore the λ^3-terms in the other differential equations (4.84)–(4.86).

After looking at an impurity model, we now investigate the translation-invariant system (4.65) with the split-up (4.66) and (4.68). Here we cannot ignore the energy-diagonal scattering processes $D_{(4)}$ as we could do in the impurity model discussed above. For simplicity we only study the differences in the leading order of the flow equations (4.73)–(4.75).

First of all, the generator (4.72) acquires a term in $O(\lambda^2)$,

$$\eta = [H_0, H_{\mathrm{int}(4)}] = \lambda\, \eta^{(1)} + \lambda^2\, \eta^{(2-\mathrm{part})} \ , \tag{4.91}$$

with

$$\begin{aligned} \eta^{(1)} &= [H_{\mathrm{kin}}, H_{\mathrm{int}(4)}] \\ \eta^{(2-\mathrm{part})} &= [D_{(4)}, H_{\mathrm{int}(4)}] \ . \end{aligned} \tag{4.92}$$

Equations (4.73)–(4.75) are then replaced by

$$\lambda\, \frac{\partial g^{(\mathrm{diag})}(k_1' k_2', k_2 k_1)}{\partial B} = \lambda^2\, R^{(1)}_{g-\mathrm{diag}} \tag{4.93}$$

$$\begin{aligned} \lambda\, \frac{\partial g^{(\mathrm{n-diag})}(k_1' k_2', k_2 k_1)}{\partial B} &= -(\epsilon_{k_1'} + \epsilon_{k_2'} - \epsilon_{k_1} - \epsilon_{k_2})^2\, \lambda\, g^{(\mathrm{n-diag})}(k_1' k_2', k_2 k_1) \\ &\quad + \lambda^2\, R^{(1)}_{g-\mathrm{n-diag}} + \lambda^2\, R^{(2-\mathrm{part})}_{g-\mathrm{n-diag}} \end{aligned} \tag{4.94}$$

$$\frac{\partial \epsilon_k}{\partial B} = \lambda^2\, R^{(1)}_{\epsilon} \tag{4.95}$$

$$\frac{\partial E}{\partial B} = \lambda^2\, R^{(1)}_{E} \tag{4.96}$$

$$\lambda^2\, \frac{\partial u(k_1' k_2' k_3', k_3 k_2 k_1)}{\partial B} = \lambda^2\, R^{(1)}_{u} + \lambda^2\, R^{(2-\mathrm{part})}_{u} \ . \tag{4.97}$$

Notice that there is no contribution from the commutator $[H_{\mathrm{kin}}, \eta^{(2-\mathrm{part})}]$ in (4.93) since normal-ordering of this commutator cannot yield energy-diagonal 2-particle interactions. Likewise the contribution $R^{(2-\mathrm{part})}_{g-\mathrm{n-diag}}$ in (4.94) vanishes linearly with its energy transfer $\Delta E = \epsilon_{k_1'} + \epsilon_{k_2'} - \epsilon_{k_1} - \epsilon_{k_2}$. Its feedback does therefore not affect the leading scaling behavior of the energy-diagonal scattering processes (4.93). The generalization of (4.89) takes the form:

$$\begin{aligned} H(B=\infty) = &\sum \epsilon_k(B=\infty)\, c_k^\dagger c_k + E(B=\infty) \\ &+ \lambda \sum g^{(\mathrm{diag})}(k_1' k_2', k_2 k_1)(B=\infty)\ :c_{k_1'}^\dagger c_{k_2'}^\dagger c_{k_2} c_{k_1}: + O(\lambda^3) \ . \end{aligned} \tag{4.98}$$

We conclude that terms like $D_{(4)}$ do not influence the flow equation results in leading order in the universal low-energy limit. This observation does not hold anymore in higher orders of the flow equation expansion.

4.1.5 Normal-Ordering with Respect to Which State?

In the above discussion we have ignored a subtle point that can be important in higher order calculations. The normal-ordering procedure should be defined with respect to the ground state of the interacting system. This is just the ground state $|\mathrm{GS}\rangle$ of the diagonal Hamiltonian $H(B=\infty)$, which can usually be identified easily. However, in the initial basis for $B=0$ this state will look very different. In order to use a normal-ordering prescription with respect to the same quantum state for all values of B, we need to define normal-ordering with respect to the interacting ground state in the basis for a given value of B,

$$|\mathrm{GS}(B)\rangle \stackrel{\mathrm{def}}{=} U(B)\,U^\dagger(B=\infty)\,|\mathrm{GS}\rangle\ . \tag{4.99}$$

Equation (3.5) is a special case of this relation for $B=0$. For example for fermions the definition of normal-ordering (4.55) then becomes B-dependent,

$$n^{(\mathrm{int})}_{k'k}(B) \stackrel{\mathrm{def}}{=} \langle \mathrm{GS}(B)|c^\dagger_{k'}c_k|\mathrm{GS}(B)\rangle\ . \tag{4.100}$$

In the language of infinitesimal unitary transformations one can rewrite (4.100) as

$$n^{(\mathrm{int})}_{k'k}(B) = \langle \mathrm{GS}|\bar{c}^\dagger_{k'}(B)\bar{c}_k(B)|\mathrm{GS}\rangle\ . \tag{4.101}$$

Here

$$\bar{O}(B) \stackrel{\mathrm{def}}{=} U(B=\infty)\,U^\dagger(B)\,O\,U(B)\,U^\dagger(B=\infty)\ , \tag{4.102}$$

which can be found as the solution of two differential equations: First solve

$$\frac{\mathrm{d}O(B')}{\mathrm{d}B'} = -[\eta(B'),O(B')] \tag{4.103}$$

with the initial condition $O(B'=0)=O$ up to $B'=B$, $O^*_B \stackrel{\mathrm{def}}{=} O(B'=B)$. Then solve

$$\frac{\mathrm{d}O(B')}{\mathrm{d}B'} = [\eta(B'),O(B')] \tag{4.104}$$

with the initial condition $O(B'=0)=O^*_B$. The result of this differential equation for $B'=\infty$ is the operator we are looking for,

$$\bar{O}(B) = O(B'=\infty)\ . \tag{4.105}$$

All the contractions on the right hand side of (4.83)–(4.86) should then be performed with respect to the B-dependent contraction (4.101). The problem with this normal-ordering prescription is that one first needs to know the interacting ground state, i.e. $\eta(B)$ for all values of B in (4.104), before one

can actually define normal-ordering for any finite value of B. A possible way out of this problem is to first run the flow equations from $B = 0$ to $B = \infty$ with the trivial normal-ordering prescription for a noninteracting system, $n^{(\mathrm{int})}_{k'k}(B = \infty)$, and then to define the B-dependent normal-ordering prescription according to (4.101). This allows one to find an improved result for the interacting ground state by running the flow equations again from $B = 0$ to $B = \infty$ with the B-dependent normal-ordering. This procedure can be iterated until convergence is reached.

While (4.101) is in principle important to define the flow equation procedure to higher orders, few calculations have been published that actually make use of such B-dependent normal-ordering. The main reason is that the difference between the "naive" B-independent definition (that we will generically use in the following chapters)

$$n^{(0)}_{k'k} = \langle \mathrm{GS}|c^\dagger_{k'}\, c_k|\mathrm{GS}\rangle \tag{4.106}$$

and $n^{(\mathrm{int})}_{k'k}(B)$ is at least of order λ. Therefore this difference does not affect our results in leading order of the normal-ordered flow equation expansion (4.89) or (4.98). Putting it otherwise: *In leading order of the flow equation expansion we can use contractions that are simply given by noninteracting occupation numbers according to Bose-Einstein (for bosons) or Fermi-Dirac statistics (for fermions).*[4]

One situation where B-dependent normal-ordering can be very important is for systems with phase transitions, where the interacting ground state is very different from the noninteracting ground state. This has been cleverly demonstrated for the phase transition in the Lipkin model using an implementation of (4.100) in [2, 3]. Similar ideas have been applied in the context of symmetry breaking in fermionic systems where normal ordering is adjusted to the flow of H_0 [4].[5] However, more research needs to be done along these lines, which presents a promising future direction for applications of the flow equation method.

4.2 Kondo Model

The Kondo model is of paradigmatic importance in correlated electron physics. It was already introduced in Sect. 2.1.2, where its scaling properties were derived using the conventional "poor man's" scaling approach. In this chapter we use the Kondo model as a pedagogical example for the flow equation approach in an interacting many-particle system, and for an explicit realization of the general ideas outlined in Sect. 4.1.4.

[4] Except possibly for the constant $E(B)$, which, however, does not feed back into the other equations.

[5] Related ideas can also be found in [5, 6].

In the next subsection we will first derive the leading order of the flow equation expansion, which will essentially yield the β-function in 1-loop order. In Sect. 4.2.2 we then extend this calculation to the next order. Since the Kondo model is a strong-coupling model, we can only trust the expansion scheme in the running coupling constant presented here for sufficiently large temperature.[6] This is analyzed in more detail in 4.2.3, followed by the explicit evaluation of dynamical spin correlation functions in 4.2.4 and 4.2.5. The final Sect. 4.2.6 contains a discussion of the pseudogap Kondo model in the flow equation framework, which features a quantum phase transition with nontrivial power laws. Sections. 4.2.4 to 4.2.6 are of particular importance since they demonstrate the evaluation of observables in an interacting many-body system, thereby extending the ideas presented in Chap. 3.

4.2.1 Expansion in 1st Order (1-Loop Results)

The calculations shown here and in the next subsection are largely taken from [8] and presented in a more pedagogical way. We start with the parametrization of the flowing Kondo Hamiltonian,

$$H(B) = H_0 + H_{\text{int}}(B) \ . \tag{4.107}$$

Here H_0 denotes the conduction band of electrons

$$H_0 = \sum_{t,\alpha} \epsilon_t \, c^\dagger_{t\alpha} c_{t\alpha} \ , \tag{4.108}$$

and H_{int} describes the interaction with the spin-1/2 degree of freedom $\boldsymbol{S}$,

$$H_{\text{int}}(B) = \sum_{t',t} J_{t't}(B) \ : \boldsymbol{S} \cdot \boldsymbol{s}_{t't} : \ . \tag{4.109}$$

Here t' and t denote general multi-indices. For the equilibrium Kondo model discussed here they just represent wave vectors, but for the non-equilibrium Kondo model discussed later in Sect. 5.2 more general representations are possible. $\boldsymbol{s}_{t't}$ is an abbreviation for the conduction band electron spin operator,

$$\boldsymbol{s}_{t't} \stackrel{\text{def}}{=} \sum_{\alpha,\beta} c^\dagger_{t'\alpha} \, \frac{\boldsymbol{\sigma}_{\alpha\beta}}{2} \, c_{t\beta} \ , \tag{4.110}$$

where $\boldsymbol{\sigma}$ are the usual Pauli matrices. The normal-ordering prescription in (4.109) is defined with respect to the noninteracting Fermi sea as the ground

[6] In fact, it is also possible to derive a controlled flow equation expansion in the strong-coupling regime of the Kondo model [7]. However, we postpone the discussion of such strong-coupling expansions to Sect. 5.1. Controlled strong-coupling expansion are not always possible and in this section we mainly want to illustrate the generic approach to interacting many-body systems.

state of H_0 where we take the chemical potential to be zero.[7] The initial condition for a constant antiferromagnetic exchange interaction is $J_{t't}(B = 0) \equiv J/N > 0$, where N is the number of band states. Notice that the hermiticity property $J_{t't}(B) = J_{tt'}(B)$ always remains fulfilled during the flow.

Canonical Generator

The canonical generator follows immediately from $[H_0, H_{\rm int}(B)]$,

$$\begin{aligned}\eta^{(1)}(B) &= [H_0, H_{\rm int}(B)] \\ &= \sum_{t',t} \eta^{(1)}_{t't}(B) \; :\boldsymbol{S}\cdot\boldsymbol{s}_{t't}: \end{aligned} \tag{4.111}$$

with

$$\eta^{(1)}_{t't}(B) = (\epsilon_{t'} - \epsilon_t)\, J_{t't}(B) \; . \tag{4.112}$$

The commutator of the canonical generator with H_0 then takes the expected form:

$$[\eta^{(1)}(B), H_0] = -\sum_{t',t} (\epsilon_{t'} - \epsilon_t)^2 \, J_{t't}(B) \; :\boldsymbol{S}\cdot\boldsymbol{s}_{t't}: \; . \tag{4.113}$$

Commutator $[\eta, H_{\rm int}]$

The evaluation of the commutator of the generator with the interaction part of the Hamiltonian, and the subsequent normal-ordering of the resulting terms plays the key role in the flow equation solution of an interacting many-body system (compare Sect. 4.1.4). In leading order of the flow equation analysis of the Kondo model we have to evaluate

$$\begin{aligned} C^{(1)} &= [\eta^{(1)}(B), H_{\rm int}(B)] \\ &= [\sum_{t',t} \eta^{(1)}_{t't}(B) \; :\boldsymbol{S}\cdot\boldsymbol{s}_{t't}:, \sum_{u',u} J_{u'u}(B) \; :\boldsymbol{S}\cdot\boldsymbol{s}_{u'u}:] \; . \end{aligned} \tag{4.114}$$

Therefore we have to work out the following commutator:

$$B^{(1)} = [:\boldsymbol{S}\cdot\boldsymbol{s}_{t't}:, :\boldsymbol{S}\cdot\boldsymbol{s}_{u'u}:] \; . \tag{4.115}$$

Let us do this in full detail. We use the following fundamental property of the spin-1/2 algebra,

$$S^i \, S^j = \frac{1}{4}\,\delta_{ij} + \frac{\rm i}{2} \sum_k \epsilon_{ijk}\, S^k \; , \tag{4.116}$$

[7] One can in fact omit normal-ordering $: \ldots :$ in (4.109) due to the properties of the Pauli matrices and the absence of a magnetic field acting on the conduction band electrons.

and insert it into the above commutator:

$$
\begin{aligned}
B^{(1)} = \frac{1}{4}\sum_{i,j}\Big(& S^iS^j \;:c^\dagger_{t'\alpha}\sigma^i_{\alpha\beta}c_{t\beta}::c^\dagger_{u'\mu}\sigma^j_{\mu\nu}c_{u\nu}: \\
& -S^jS^i \;:c^\dagger_{u'\mu}\sigma^j_{\mu\nu}c_{u\nu}::c^\dagger_{t'\alpha}\sigma^i_{\alpha\beta}c_{t\beta}:\Big) \\
= \frac{\mathrm{i}}{8}\sum_{i,j,k}\epsilon_{ijk}\sigma^i_{\alpha\beta}\sigma^j_{\mu\nu}S^k & \Big(:c^\dagger_{t'\alpha}c_{t\beta}::c^\dagger_{u'\mu}c_{u\nu}:+:c^\dagger_{u'\mu}c_{u\nu}::c^\dagger_{t'\alpha}c_{t\beta}:\Big) \\
+\frac{1}{16}\sum_i(\sigma^i_{\alpha\beta}\sigma^i_{\mu\nu}) & \,[:c^\dagger_{t'\alpha}c_{t\beta}:,:c^\dagger_{u'\mu}c_{u\nu}:] \\
= \frac{\mathrm{i}}{8}\sum_{i,j,k}\epsilon_{ijk}\sigma^i_{\alpha\beta}\sigma^j_{\mu\nu}S^k & \Big(:c^\dagger_{t'\alpha}c_{t\beta}::c^\dagger_{u'\mu}c_{u\nu}:+:c^\dagger_{u'\mu}c_{u\nu}::c^\dagger_{t'\alpha}c_{t\beta}:\Big) \\
+\frac{3}{16}\sum_\alpha & \Big(\delta_{tu'}\;:c^\dagger_{t'\alpha}c_{u\alpha}:-\delta_{t'u}\;:c^\dagger_{u'\alpha}c_{t\alpha}:\Big) \\
+\frac{3}{8}\,\delta_{tu'}\,\delta_{t'u} & \,(n(t')-n(t))\;. \qquad (4.117)
\end{aligned}
$$

The last term follows from using (4.60). The additional factor 2 is due to the sum over the spin index α since normal-ordering is independent of α,

$$
n(t) = \langle \mathrm{GS}|c^\dagger_{t\uparrow}c_{t\uparrow}|\mathrm{GS}\rangle = \langle \mathrm{GS}|c^\dagger_{t\downarrow}c_{t\downarrow}|\mathrm{GS}\rangle\;. \qquad (4.118)
$$

Next we need to normal-order the four fermion terms in (4.117) using (4.59). The result is straightforward using the standard identities for Pauli matrices and we find:

$$
\begin{aligned}
B^{(1)} = \mathrm{i}\,:\boldsymbol{S}\cdot(\boldsymbol{s}_{t't}\times\boldsymbol{s}_{u'u}): & \qquad (4.119)\\
+:\boldsymbol{S}\cdot\boldsymbol{s}_{t'u}:\,\delta_{tu'}(n(t)-1/2) & -:\boldsymbol{S}\cdot\boldsymbol{s}_{u't}:\,\delta_{t'u}(n(t')-1/2) \\
+\frac{3}{16}\sum_\alpha & \Big(\delta_{tu'}\;:c^\dagger_{t'\alpha}c_{u\alpha}:-\delta_{t'u}\;:c^\dagger_{u'\alpha}c_{t\alpha}:\Big) \\
+\frac{3}{8}\,\delta_{tu'}\delta_{t'u} & \,(n(t')-n(t))\;.
\end{aligned}
$$

Using this it is easy to work out (4.114):

$$
\begin{aligned}
C^{(1)} = \mathrm{i}\sum_{t',t,u,u'}(\epsilon_{t'}-\epsilon_t)J_{t't}J_{u'u}\;:\boldsymbol{S}\cdot(\boldsymbol{s}_{t't}\times\boldsymbol{s}_{u'u}): & \qquad (4.120)\\
+\sum_{t',t,v}(\epsilon_{t'}+\epsilon_t-2\epsilon_v)J_{t'v}J_{vt}\,(n(v)-1/2)\;:\boldsymbol{S}\cdot\boldsymbol{s}_{t't}: & \\
+\frac{3}{16}\sum_{t',t,v,\alpha}(\epsilon_{t'}+\epsilon_t-2\epsilon_v)J_{t'v}J_{vt}\;:c^\dagger_{t'\alpha}c_{t\alpha}: & \\
+2\times\frac{3}{16}\sum_{t,v}(2\epsilon_t-2\epsilon_v)J_{tv}J_{vt}\,n(t)\;. &
\end{aligned}
$$

Flow Equations

As we have discussed in Sect. 4.1.4, in first order of the flow equation expansion we only need to identify the terms that have the structure of the original interaction term in (4.120). The flow equation for the coupling constants $J_{t't}(B)$ in the Kondo Hamiltonian (4.107) is therefore determined by (4.113) and the second line of (4.120):

$$\begin{aligned}\frac{\mathrm{d}J_{t't}}{\mathrm{d}B} &= -(\epsilon_{t'}-\epsilon_t)^2 J_{t't} \\ &\quad + \sum_v (\epsilon_{t'}+\epsilon_t-2\epsilon_v) J_{t'v} J_{vt}\,(n(v)-1/2) \\ &\quad + O(J^3)\ .\end{aligned} \tag{4.121}$$

Now the solution methods that have been introduced in Sect. 2.3.2 can be employed to tackle this system of coupled differential equations.. In the sequel we will mainly be interested in the behavior in the vicinity of the Fermi surface. Therefore the natural parametrization is the infrared parametrization from Sect. 2.3.2,

$$J_{t't}(B) = \frac{J_{\mathrm{IR}}(B)}{N}\,\mathrm{e}^{-B(\epsilon_{t'}-\epsilon_t)^2}\ . \tag{4.122}$$

Here the flow of $J_{\mathrm{IR}}(B)$ is determined by the flow of $J_{00}(B)$ in (4.121) ($t=0$ corresponds to the Fermi level). This leads to

$$\begin{aligned}\frac{\mathrm{d}J_{\mathrm{IR}}}{\mathrm{d}B} &= -2J_{\mathrm{IR}}^2\,\frac{1}{N}\sum_v \epsilon_v\,\mathrm{e}^{-2B\epsilon_v^2}\,(n(\epsilon_v)-1/2) \\ &= -2J_{\mathrm{IR}}^2\int \mathrm{d}\epsilon\,\rho(\epsilon)\,\epsilon\ \ \mathrm{e}^{-2B\epsilon^2}\,(n(\epsilon)-1/2)\ .\end{aligned} \tag{4.123}$$

We assume a constant density of states, $\rho(\epsilon) \equiv \rho_{\epsilon_F}$, conduction band width $2D$ ($\epsilon \in [-D, D]$) and zero temperature. The electron occupation number with respect to the noninteracting Fermi sea is then simply:

$$n(\epsilon) = \begin{cases} 0 & \text{for } \epsilon > 0 \\ 1 & \text{for } \epsilon < 0\ . \end{cases} \tag{4.124}$$

The flow equation for the dimensionless coupling constant $g \stackrel{\mathrm{def}}{=} \rho_{\epsilon_F} J$ takes the following form:

$$\begin{aligned}\frac{\mathrm{d}g}{\mathrm{d}B} &= g^2 \int_{-D}^{D} \mathrm{d}\epsilon\,|\epsilon|\,\mathrm{e}^{-2B\epsilon^2} \\ &= \frac{g^2}{2B}\left(1-\mathrm{e}^{-2B\,D^2}\right)\ .\end{aligned} \tag{4.125}$$

The flow is negligible for $B \lesssim D^{-2}$ as should be expected. Therefore we can replace this differential equation by the simpler form

$$\frac{\mathrm{d}g}{\mathrm{d}B} = \frac{g^2}{2B} \tag{4.126}$$

with the initial condition now posed at $B = D^{-2}$:

$$g(B = D^{-2}) = g_0 = \rho_{\epsilon_F} J \ . \tag{4.127}$$

Here J is the bare coupling constant of the original Kondo Hamiltonian (2.40). Equation (4.126) can be rewritten in terms of the flow parameter $\Lambda_{\mathrm{feq}} = B^{-1/2}$:

$$\frac{\mathrm{d}g}{\mathrm{d}\ln \Lambda_{\mathrm{feq}}} = -g^2 \ . \tag{4.128}$$

This agrees with the conventional β-function (2.47)

$$\frac{\mathrm{d}g}{\mathrm{d}\ln \Lambda_{\mathrm{RG}}} = -\beta(g) = -g^2 + O(g^3) \tag{4.129}$$

up to higher order terms with the identification $\Lambda_{\mathrm{feq}} = \Lambda_{\mathrm{RG}}$. In the next section we also derive the term in order g^3 in (4.128).

A final comment regarding the relation between the full system of differential equations (4.121) and the infrared parametrization (4.122). The analysis of Sect. 2.3.2 for the potential scattering model can be carried through in the same way, especially if one is interested in the coupling constant at higher energies. We will return to this point later when we discuss dynamical correlation functions. However, if one is only interested in the behavior at the Fermi level, the infrared parametrization becomes asymptotically correct by comparison with the full numerical solution.

4.2.2 Expansion in 2nd Order (2-Loop Results)

As we have seen in Sect. 4.1.4 we need to take the newly generated terms in (4.120) into account to go to the next order in the flow equation expansion. Let us first look at the term in the third line of (4.120). This contributes a new potential scattering term

$$\sum_{t',t,\alpha} V_{t't}(B) \ : c^\dagger_{t'\alpha} c_{t\alpha} : \tag{4.130}$$

in the flowing Hamiltonian $H(B)$:

$$\frac{\mathrm{d}V_{t't}}{\mathrm{d}B} = \frac{3}{16} \sum_v (\epsilon_{t'} + \epsilon_t - 2\epsilon_v) J_{t'v} J_{vt} \ . \tag{4.131}$$

Now we plug in the infrared parametrization (4.122) and find

$$\frac{\mathrm{d}V_{t't}}{\mathrm{d}B} = \frac{3}{16}\,\frac{J_{\mathrm{IR}}^2}{N^2}\sum_v(\epsilon_{t'}+\epsilon_t-2\epsilon_v)\,\mathrm{e}^{-B((\epsilon_{t'}-\epsilon_v)^2+(\epsilon_v-\epsilon_t)^2)}$$
$$= 0 \tag{4.132}$$

by explicitly performing the v-summation assuming a constant density of states. We neglect band edge effects by taking the universal scaling limit $|\epsilon_{t'}|, |\epsilon_t| \ll D$. Therefore no potential scattering term is generated in order J^2, and likewise also the constant contribution in the fourth line of (4.120) vanishes.[8]

K-Term

The only newly generated term from the leading order of the flow equation expansion is therefore given by the first line of (4.120). As discussed in Sect. 4.1.4 we take this into account by allowing this new term in the interaction Hamiltonian (4.109):

$$H_{\mathrm{int}}(B) = \sum_{t',t} J_{t't}(B)\ :\boldsymbol{S}\cdot\boldsymbol{s}_{t't}: \tag{4.133}$$
$$+\mathrm{i}\sum_{t',t,u',u} K_{t't,u'u}(B)\ :\boldsymbol{S}\cdot(\boldsymbol{s}_{t't}\times\boldsymbol{s}_{u'u}):\ .$$

Hermiticity requires $K_{t't,u'u}(B) = -K_{tt',uu'}(B)$ and the initial condition is $K_{t't,u'u}(B=0) \equiv 0$. According to (4.80) our generator picks up a new term $\eta^{(2)}$:

$$\eta = \sum_{t',t}\eta^{(1)}_{t't}\ :\boldsymbol{S}\cdot\boldsymbol{s}_{t't}: + \mathrm{i}\sum_{t',t,u',u}\eta^{(2)}_{t't,u'u}\ :\boldsymbol{S}\cdot(\boldsymbol{s}_{t't}\times\boldsymbol{s}_{u'u}):\,, \tag{4.134}$$

where

$$\eta^{(1)}_{t't} = (\epsilon_{t'}-\epsilon_t)\,J_{t't}$$
$$\eta^{(2)}_{t't,u'u} = (\epsilon_{t'}+\epsilon_{u'}-\epsilon_t-\epsilon_u)\,K_{t't,u'u}\ . \tag{4.135}$$

We can now combine the source term for the K-interaction in the first line of (4.120) with the usual linear term generated by $[\eta^{(2)}, H_0]$. We find the flow equation:

$$\frac{\mathrm{d}K_{t't,u'u}}{\mathrm{d}B} = -(\epsilon_{t'}+\epsilon_{u'}-\epsilon_t-\epsilon_u)^2\,K_{t't,u'u} \tag{4.136}$$
$$+(\epsilon_{t'}-\epsilon_t)J_{t't}J_{u'u}\ ,$$

which implies that the K-term is generated in $O(J^2)$.

[8] By comparison with the Bethe ansatz solution one can deduce that the potential scattering term is in fact only generated in order J^4.

Commutator $[\eta, H_{\rm int}]$

Next we need to identify the new terms in $O(J^3)$ in the commutator $[\eta, H_{\rm int}]$. There are two contributions

$$C_a^{(2)} = \left[\sum_{u',u} \eta^{(1)}_{u'u} \, : \boldsymbol{S} \cdot \boldsymbol{s}_{u'u} :, \mathrm{i} \sum_{v',v,w',w} K_{v'v,w'w} \, : \boldsymbol{S} \cdot (\boldsymbol{s}_{v'v} \times \boldsymbol{s}_{w'w}) : \right] \tag{4.137}$$

and

$$C_b^{(2)} = \left[\mathrm{i} \sum_{v',v,w',w} \eta^{(2)}_{v'v,w'w} \, : \boldsymbol{S} \cdot (\boldsymbol{s}_{v'v} \times \boldsymbol{s}_{w'w}) :, \sum_{u',u} J_{u'u} \, : \boldsymbol{S} \cdot \boldsymbol{s}_{u'u} : \right] . \tag{4.138}$$

These can be combined into

$$\begin{aligned} C^{(2)} = & \sum (\epsilon_{u'} - \epsilon_u - \epsilon_{v'} + \epsilon_v - \epsilon_{w'} + \epsilon_w) \, J_{u'u} K_{v'v,w'w} \\ & \times \mathrm{i} \, [: \boldsymbol{S} \cdot \boldsymbol{s}_{u'u} :, : \boldsymbol{S} \cdot (\boldsymbol{s}_{v'v} \times \boldsymbol{s}_{w'w}) :] \, . \end{aligned} \tag{4.139}$$

The basic commutator that we need to work out is:

$$B^{(2)} = [: \boldsymbol{S} \cdot \boldsymbol{s}_{u'u} :, : \boldsymbol{S} \cdot (\boldsymbol{s}_{v'v} \times \boldsymbol{s}_{w'w}) :] \, . \tag{4.140}$$

The evaluation is straightforward but somehow lengthy (for details see [8]):

$$\begin{aligned} B^{(2)} = & \frac{i}{2} \, \delta_{w'u} \delta_{wu'} \left(n(w')(1 - n(w)) + n(w)(1 - n(w')) \right) \, : \boldsymbol{S} \cdot \boldsymbol{s}_{v'v} : \\ & - \frac{i}{2} \, \delta_{v'u} \delta_{vu'} \left(n(v')(1 - n(v)) + n(v)(1 - n(v')) \right) \, : \boldsymbol{S} \cdot \boldsymbol{s}_{w'w} : \\ & + \text{normal} - \text{ordered terms with different structure} \, . \end{aligned} \tag{4.141}$$

With the same reasoning as above, we can ignore the other normal-ordered terms in this expression. Interaction terms that are not contained in (4.133) do not play a role in this order of the flow equation expansion. Notice that $B^{(2)}$ does also contain a contribution to the K-term. However, this contribution is necessarily $O(J^3)$ in (4.136). Therefore the feedback of this contribution into the flow equation for J is only of order J^4, which is one order further than our current calculation allows anyway.

Putting everything together we find:

$$\begin{aligned} C^{(2)} = & \frac{1}{2} \sum (2\epsilon_u - 2\epsilon_{u'} + \epsilon_t - \epsilon_{t'}) \, J_{u'u} (K_{u'u,t't} - K_{t't,u'u}) \\ & \times \big(n(u') \, (1 - n(u)) + n(u) \, (1 - n(u')) \big) \\ & \times : \boldsymbol{S} \cdot \boldsymbol{s}_{t't} : \\ & + \text{normal} - \text{ordered terms with different structure} \, . \end{aligned} \tag{4.142}$$

Flow Equations

With the new contribution from (4.142) we can now write down the full set of flow equations:

$$\begin{aligned}\frac{\mathrm{d}J_{t't}}{\mathrm{d}B} &= -(\epsilon_{t'}-\epsilon_t)^2 J_{t't} \\ &\quad + \sum_v (\epsilon_{t'}+\epsilon_t-2\epsilon_v) J_{t'v} J_{vt}\,(n(v)-1/2) \\ &\quad + \frac{1}{2}\sum_{u',u} (2\epsilon_u - 2\epsilon_{u'} + \epsilon_t - \epsilon_{t'})\, J_{u'u}(K_{u'u,t't} - K_{t't,u'u}) \\ &\qquad \times \big(n(u')\,(1-n(u)) + n(u)\,(1-n(u'))\big) \\ &\quad + O(J^4)\end{aligned} \tag{4.143}$$

$$\begin{aligned}\frac{\mathrm{d}K_{t't,u'u}}{\mathrm{d}B} &= -(\epsilon_{t'}+\epsilon_{u'}-\epsilon_t-\epsilon_u)^2\, K_{t't,u'u} \\ &\quad + (\epsilon_{t'}-\epsilon_t) J_{t't} J_{u'u} \\ &\quad + O(J^3)\;.\end{aligned} \tag{4.144}$$

This system of differential equations contains the whole flow behavior of the Kondo Hamiltonian up to $O(J^4)$ in (4.143) and up to $O(J^3)$ in (4.144). It will be the basis for discussing the very interesting and nontrivial scaling behavior of the non-equilibrium Kondo model later in Sect. 5.2. For now we will, however, restrict ourselves to the equilibrium case with a constant density of states. Notice that the hermiticity conditions for the running coupling constants in the flowing Hamiltonian always remain fulfilled in the system of equations (4.143) and (4.144).[9]

IR-Parametrization

We use the infrared parametrization (4.122) and find the following flow equation for the dimensionless coupling constant:

$$\begin{aligned}\frac{\mathrm{d}g}{\mathrm{d}B} &= -2g^2 \int_{-D}^{D} \mathrm{d}\epsilon\, \epsilon\, \mathrm{e}^{-2B\epsilon^2}\,(n(\epsilon)-1/2) \\ &\quad + \int_{-D}^{D} \mathrm{d}\epsilon\, \mathrm{d}\epsilon'\,(\epsilon-\epsilon')\, g\, \mathrm{e}^{-B(\epsilon'-\epsilon)^2}\,(K_{\epsilon'\epsilon,00} - K_{00,\epsilon'\epsilon}) \\ &\qquad \times \big(n(\epsilon')(1-n(\epsilon)) + n(\epsilon)(1-n(\epsilon'))\big)\;.\end{aligned} \tag{4.145}$$

We first need to determine the flow of K from (4.144) in order to solve this differential equation:

[9] It is very worthwhile to verify this as a consistency check for every flow equation calculation.

$$K_{00,\epsilon'\epsilon}(B) \equiv 0 \tag{4.146}$$

$$\frac{\mathrm{d}K_{\epsilon'\epsilon,00}}{\mathrm{d}B} = -(\epsilon'-\epsilon)^2\, K_{\epsilon'\epsilon,00} + g^2\, \mathrm{e}^{-B(\epsilon'-\epsilon\ )^2}\, (\epsilon'-\epsilon)\ . \tag{4.147}$$

Equation (4.147) can be solved easily,

$$K_{\epsilon'\epsilon,00}(B) = (\epsilon'-\epsilon)\, \mathrm{e}^{-B(\epsilon'-\epsilon)^2} \int_0^B \mathrm{d}B'\, g^2(B')\ . \tag{4.148}$$

Since the running coupling constant $g(B')$ grows logarithmically (i.e., very slowly), one can replace the integral on the right hand side of this equation by the value on the scale B (up to higher order corrections that do not contribute in this order of the calculation anymore):

$$K_{\epsilon'\epsilon,00}(B) = (\epsilon'-\epsilon)\, \mathrm{e}^{-B(\epsilon'-\epsilon)^2}\, B\, (g^2(B) + O(g^3))\ . \tag{4.149}$$

We now have a closed differential equation for the dimensionless coupling constant:

$$\begin{aligned}\frac{\mathrm{d}g}{\mathrm{d}B} = &-2g^2 \int_{-D}^{D} \mathrm{d}\epsilon\, \epsilon\, \mathrm{e}^{-2B\epsilon^2}\, (n(\epsilon) - 1/2) \\ &-2g^3\, B \int_{-D}^{D} \mathrm{d}\epsilon\, \mathrm{d}\epsilon'\, (\epsilon'-\epsilon)^2\, \mathrm{e}^{-2B(\epsilon'-\epsilon)^2}\, n(\epsilon')(1-n(\epsilon))\ .\end{aligned} \tag{4.150}$$

Zero Temperature

Let us analyze (4.150) for zero temperature (4.124). As before we extend the energy integrations to $\pm\infty$, but pose the initial condition at the scale $B = D^{-2}$. Then the integrals in the second line of (4.150) can be done in closed form,

$$\int_{-\infty}^{\infty} \mathrm{d}\epsilon\, \mathrm{d}\epsilon'\, (\epsilon'-\epsilon)^2\, \mathrm{e}^{-2B(\epsilon'-\epsilon)^2}\, n(\epsilon')(1-n(\epsilon)) \tag{4.151}$$

$$= \int_0^{\infty} \mathrm{d}\epsilon \int_{-\infty}^{0} \mathrm{d}\epsilon' (\epsilon'-\epsilon)^2\, \mathrm{e}^{-2B(\epsilon'-\epsilon)^2}$$

$$= \frac{1}{8B^2}\ . \tag{4.152}$$

This yields

$$\frac{\mathrm{d}g}{\mathrm{d}B} = \frac{g^2}{2B} - \frac{g^3}{4B} + \frac{O(g^4)}{B}\ . \tag{4.153}$$

and with the identification $\Lambda_{\mathrm{feq}} = B^{-1/2}$:

$$\frac{\mathrm{d}g}{\mathrm{d}\ln \Lambda_{\mathrm{feq}}} = -g^2 + \frac{1}{2}\, g^3 + O(g^4) \ . \tag{4.154}$$

This is the correct β-function of the Kondo model to 2-loop order.

This result shows that it is possible to extend flow equation calculations beyond the leading order. A careful reader might wonder about the effect of the B-independent normal-ordering prescription that we have implicitly used here. In Sect. 4.1.5 we had argued that beyond leading order it is generally necessary to use $n^{(\mathrm{int})}_{k'k}(B)$ defined in (4.101). However, it is easy to verify that

$$\bar{c}_{k\alpha}(B) = c_{k\alpha} + O(J) \times \text{ composite operator containing one spin operator } \boldsymbol{S} \ . \tag{4.155}$$

Since $\langle \mathrm{GS}|\boldsymbol{S}|\mathrm{GS}\rangle = 0$ without an external magnetic field, the expectation value $n^{(\mathrm{int})}_{k'k}(B)$ can only differ from the noninteracting value in order J^2,

$$n^{(\mathrm{int})}_{k'k}(B) - \langle \mathrm{GS}|c^\dagger_{k'\alpha} c_{k\alpha}|\mathrm{GS}\rangle \propto O(J^2) \ . \tag{4.156}$$

If we plug $n^{(\mathrm{int})}_{k'k}(B)$ into the second line of (4.143), the difference from the noninteracting normal-ordering prescription is effectively of order $O(J^4)$ in the differential equations. It is therefore negligible in the present order of the expansion.

4.2.3 Nonzero Temperature

The β-function of the Kondo model shows strong-coupling behavior. The solution of (4.153) takes the following form (plus subleading corrections):

$$g(\Lambda_{\mathrm{feq}}) = \frac{1}{\ln(\Lambda_{\mathrm{feq}}/T_{\mathrm{K}})} \ . \tag{4.157}$$

The Kondo temperature is given by

$$T_{\mathrm{K}} = D\, \sqrt{g_0}\, \mathrm{e}^{-1/g_0} \ , \tag{4.158}$$

where g_0 is the original (bare) coupling constant in the Kondo Hamiltonian. Since we are effectively performing an expansion in the running coupling constant $g(\Lambda_{\mathrm{feq}})$, this means that our expansion parameter becomes large and therefore our results unreliable once the scaling parameter Λ_{feq} is of order the Kondo temperature. One possibility to retain a controlled expansion in a small parameter is to go to nonzero temperature $T \gg T_{\mathrm{K}}$, where $g(\Lambda_{\mathrm{feq}})$ always remains small as we will see below.

We go back to (4.150) and insert the fermion occupation numbers at nonzero temperature,

$$n(\epsilon) = \frac{1}{\mathrm{e}^{\epsilon/T} + 1} \ . \tag{4.159}$$

The leading behavior of the integrations remains unchanged for $B \ll T^{-2}$ and therefore the scaling equation (4.154),

$$\frac{\mathrm{d}g}{\mathrm{d}\Lambda_{\mathrm{feq}}} = -\frac{g^2}{\Lambda_{\mathrm{feq}}} + \frac{1}{2}\,\frac{g^3}{\Lambda_{\mathrm{feq}}}\ , \tag{4.160}$$

remains unchanged for $\Lambda_{\mathrm{feq}} \gg T$ as expected.

For $B \gg T^{-2}$ the leading behavior of the integrals in (4.150) is given by:

$$\begin{aligned}
\frac{\mathrm{d}g}{\mathrm{d}B} &= g^2 \int_{-\infty}^{\infty} \mathrm{d}\epsilon\, \epsilon\, \mathrm{e}^{-2B\epsilon^2}\, \tanh(\epsilon/2T) \\
&\quad -2g^3\, B \int_{-\infty}^{\infty} \mathrm{d}\epsilon\, \mathrm{d}\epsilon'\, (\epsilon'-\epsilon)^2\, \mathrm{e}^{-2B(\epsilon'-\epsilon)^2}\, n(\epsilon')(1-n(\epsilon))\ . \\
&= \frac{g^2}{2T} \int_{-\infty}^{\infty} \mathrm{d}\epsilon\, \epsilon^2\, \mathrm{e}^{-2B\epsilon^2} \\
&\quad -2g^3\, B \int_{-\infty}^{\infty} \mathrm{d}\epsilon\, n(\epsilon)(1-n(\epsilon)) \int_{-\infty}^{\infty} \mathrm{d}\epsilon'\, \epsilon'^2\, \mathrm{e}^{-2B\epsilon'^2} \\
&= \frac{\sqrt{2\pi}}{16}\, g^2\, \frac{1}{T\, B^{3/2}} - \frac{\sqrt{2\pi}}{4}\, g^3\, \frac{T}{B^{1/2}}
\end{aligned} \tag{4.161}$$

Equivalently ($\Lambda_{\mathrm{feq}} \ll T$):

$$\frac{\mathrm{d}g}{\mathrm{d}\Lambda_{\mathrm{feq}}} = -\frac{\sqrt{2\pi}}{8}\, g^2\, \frac{1}{T} + \frac{\sqrt{2\pi}}{2}\, g^3\, \frac{T}{\Lambda_{\mathrm{feq}}^2}\ . \tag{4.162}$$

At this point it is worthwhile to pause a moment and to remember that one stops the scaling flow once $\Lambda_{\mathrm{RG}} \approx T$ in the conventional scaling analysis. Then all excitation energies up to approximately the temperature scale contribute to the physical properties. However, the flow equation expansion can be viewed as a diagonalization procedure. Therefore there is no reason to stop the flow at the scale $\Lambda_{\mathrm{feq}} \approx T$. In fact, we do not want to stop there in order to be able to calculate dynamical correlation functions also for very small frequencies.

Due to this conceptual difference (4.162) is structurally different from the scaling equations that we are used to from conventional scaling analysis. First of all, it is worthwhile to verify that all dimensions are correct: Since temperature has the dimension of energy, not only the familiar $1/\Lambda_{\mathrm{feq}}$-behavior from (4.160) occurs on the right hand side of (4.162).

We can argue that we can integrate (4.160) down to $\Lambda_{\mathrm{feq}} = T$, and then use

$$g_* \stackrel{\mathrm{def}}{=} \frac{1}{\ln(T/T_{\mathrm{K}})} \tag{4.163}$$

as the initial condition of (4.162) at $\Lambda_{\mathrm{feq}} = T$, $g(\Lambda_{\mathrm{feq}} = T) = g_*$. If it were only for the second order term in (4.162), the scaling flow of the coupling constant would then effectively stop below the temperature scale.[10] This agrees with the philosophy of the conventional scaling approach. However, the term in

[10] To be precise: there would only be a small additional shift of $O(g_*^2)$

third order of the coupling constant in (4.162) dominates the scaling equation for $\Lambda_{\rm feq} \ll T$ due to its more infrared divergent $1/\Lambda_{\rm feq}^2$-behavior. One finds the following solution,

$$g(\Lambda_{\rm feq}) = \frac{g_*}{\sqrt{1+\Gamma_{\rm rel}/\Lambda_{\rm feq}}}\,(1+O(g_*))\ , \tag{4.164}$$

with

$$\Gamma_{\rm rel} = \sqrt{2\pi}\,g_*^2\,T\ . \tag{4.165}$$

The flow of the coupling constant therefore crosses over to a universal decay for scaling parameters smaller than the energy scale set by $\Gamma_{\rm rel}$:

$$g(\Lambda_{\rm feq}) = (2\pi)^{-1/4}\sqrt{\frac{\Lambda_{\rm feq}}{T}}\quad \text{for } \Lambda_{\rm feq} \ll \Gamma_{\rm rel}\ . \tag{4.166}$$

Going back to the discussion of the resonant level model in Sect. 3.3.2, we will remember that there an algebraic decay set in once the scaling parameter was of order the hybridization strength (3.85). The onset of the algebraic decay signaled the width of the peak in the impurity density of states around ϵ_d. We will see in the next chapter that a similar interpretation holds in the Kondo model: $\Gamma_{\rm rel}$ determines the width of the zero frequency peak in the spin-spin correlation function. In physical terms this means that $\Gamma_{\rm rel}$ is the *spin relaxation rate*. The way in which decoherence like finite temperature spin relaxation enters into the scaling equation (4.162) is the first "real" difference between flow equations and the conventional scaling approach up to this point in this book. These decoherence terms in the flow equation formalism will later play a major role in understanding the scaling behavior of the non-equilibrium Kondo model in Sect. 5.2.

Putting everything together, we have shown that the flow equation expansion is reliable as long as the running coupling remains small during the entire flow, $g_* \ll 1$ for all $\Lambda_{\rm feq}$. This is achieved for sufficiently high temperature $T \gg T_{\rm K}$.

Before proceeding with the evaluation of correlation functions, a short comment on the question why our diagonalization procedure depends on temperature in the first place. For an exact diagonalization of the Hamiltonian this should of course not be the case, and in fact it was never the case in our solutions of quadratic Hamiltonians in Sects. 2.3 and 3.3. However, for an interacting Hamiltonian like the Kondo model we are effectively trying to find a diagonal Hamiltonian that comes as close as possible to describing the dynamics for a *given* nonzero temperature. Hence this "effective" diagonal Hamiltonian for a given temperature will in general depend on temperature.[11]

[11] Technically the way in which temperature enters into the flow equations is through the normal-ordering procedure.

4.2.4 Transformation of the Spin Operator

After finding the approximate flow equation diagonalization of the Kondo Hamiltonian, we now want to make use of this to evaluate dynamical correlation functions. Different from the examples in Chap. 3, additional approximations in the transformation of the observable are necessary in a generic interacting many-body system. Since the spin-spin correlation functions in the Kondo model are of particular interest, we will use them as a pedagogical example to introduce the reader to this very important topic.

Flow Equation

First we need to solve the flow equation (3.8) for the observable S^a, $a = x, y, z$,

$$\frac{\mathrm{d}S^a(B)}{\mathrm{d}B} = [\eta(B), S^a(B)] \; . \tag{4.167}$$

Similar to the expansion of the Hamiltonian in terms of a small parameter (4.77), we expand the operator $S^a(B)$ in terms of the running coupling constant of the Kondo model. The leading terms are then given by the commutator with $\eta^{(1)}$ from (4.111): Since the initial condition is $S^a(B=0) = S^a$, we first need to evaluate:

$$\begin{aligned}
[\eta^{(1)}(B), S^a] &= \sum_{t',t} \sum_i (\epsilon_{t'} - \epsilon_t)\, J_{t't}\, [S^i, S^a]\; :s^i_{t't}: \\
&= \mathrm{i} \sum_{t',t} (\epsilon_{t'} - \epsilon_t)\, J_{t't}\; :(\boldsymbol{S} \times \boldsymbol{s}_{t't})^a: \; .
\end{aligned} \tag{4.168}$$

This suggests the following ansatz for the flowing observable,

$$S^a(B) = h(B)\, S^a + \mathrm{i} \sum_{u'u} \gamma_{u'u}(B)\; :(\boldsymbol{S} \times \boldsymbol{s}_{u'u})^a: \; . \tag{4.169}$$

In order to solve (4.167) we also need the commutator

$$\begin{aligned}
[:\boldsymbol{S}\cdot\boldsymbol{s}_{t't}:, :(\boldsymbol{S}\times\boldsymbol{s}_{u'u})^a:] &= +\mathrm{i}\; :s^a_{u'u}\,(\boldsymbol{S}\cdot\boldsymbol{s}_{t't}): - \mathrm{i}\, S^a :\boldsymbol{s}_{t't}\cdot\boldsymbol{s}_{u'u}: \\
&+\frac{\mathrm{i}}{4}\,\delta_{tu'} :s^a_{t'u}: + \frac{\mathrm{i}}{4}\,\delta_{t'u}\; :s^a_{u't}: \\
&-\frac{\mathrm{i}}{2} S^a \Big(\frac{1}{2}\,\delta_{tu'}(1-2n(t)) \sum_\alpha :c^\dagger_{t'\alpha} c_{u\alpha}: + \frac{1}{2}\,\delta_{t'u}(1-2n(t')) \sum_\alpha :c^\dagger_{u'\alpha} c_{t\alpha}: \\
&\qquad +2\delta_{tu'}\delta_{t'u}\,(1-n(t))n(t') \Big) \\
&-\frac{1}{4}\,\delta_{tu'}(1-2n(t))\; :(\boldsymbol{S}\times\boldsymbol{s}_{t'u})^a: + \frac{1}{4}\,\delta_{t'u}(1-2n(t'))\; :(\boldsymbol{S}\times\boldsymbol{s}_{tu'})^a:
\end{aligned} \tag{4.170}$$

after some straightforward algebra. This shows a number of new terms not contained in the ansatz (4.169). However, all these terms will initially only

be generated in $O(J^2)$, therefore we restrict the calculation to terms of the structure (4.169) and neglect all other terms. We obtain the following set of differential equations after identifying the coefficients from (4.169), (4.168) and (4.170):

$$\frac{\mathrm{d}h}{\mathrm{d}B} = \sum_{t',t} (\epsilon_{t'} - \epsilon_t)\, J_{t't}\, \gamma_{tt'}\, n(t')\, (1 - n(t)) \tag{4.171}$$

$$\begin{aligned} \frac{\mathrm{d}\gamma_{t't}}{\mathrm{d}B} &= h\, (\epsilon_{t'} - \epsilon_t)\, J_{t't} \\ &\quad -\frac{1}{4} \sum_u \Big((\epsilon_{t'} - \epsilon_u)\, J_{t'u}\, \gamma_{ut} + (\epsilon_t - \epsilon_u)\, J_{ut}\, \gamma_{t'u} \Big)\, (1 - 2n(u)) \ . \end{aligned} \tag{4.172}$$

Sum Rules

We remember from the examples in Chap. 3 that commutation or anticommutation relations of operators resulting in c-numbers should remain exactly fulfilled under the unitary flow, for example (3.75). In the present example this would imply

$$\big(S^a(B)\big)^2 = \frac{1}{4} \quad \forall B \ . \tag{4.173}$$

Since we are using a normal-ordering prescription for truncating the flow equations for the flowing observable, this is clearly a too ambitious requirement. We can only expect (4.173) to hold with respect to the state used for the normal-ordering prescription,

$$\langle \big(S^a(B)\big)^2 \rangle = \frac{1}{4} \quad \forall B \ . \tag{4.174}$$

Here the expectation value is taken either with respect to the ground state of H_0 or the respective finite temperature density matrix.

Let us work this out explicitly for (4.169):

$$\langle \big(S^a(B)\big)^2 \rangle = \frac{1}{4}\, h^2(B) - \frac{1}{4} \sum_{t,t'} \gamma_{t't}(B) \gamma_{tt'}(B)\, n(t')\, (1 - n(t)) \ . \tag{4.175}$$

Initially for $B = 0$ the condition is of course fulfilled and we differentiate with respect to B,

$$\begin{aligned} \frac{\mathrm{d}}{\mathrm{d}B} \langle \big(S^a(B)\big)^2 \rangle &= \frac{1}{2} \left(\frac{\mathrm{d}h(B)}{\mathrm{d}B} h(B) - \sum_{t,t'} \frac{\gamma_{t't}(B)}{dB} \gamma_{tt'}(B)\, n(t')\, (1 - n(t)) \right) \\ &= \frac{1}{8} \sum_{t,t',u} \Big((\epsilon_{t'} - \epsilon_u)\, J_{t'u}\, \gamma_{ut} + (\epsilon_t - \epsilon_u)\, J_{ut}\, \gamma_{t'u} \Big)\, \gamma_{tt'} \\ &\qquad \times (1 - 2n(u))\, n(t')\, (1 - n(t)) \ . \end{aligned} \tag{4.176}$$

Notice that the terms coming from (4.171) and the first line of (4.172) cancel exactly.

However, the remaining term (4.176) is generally nonzero and amounts to a violation of the property (4.174). This is a rather general observation in flow equation expansions for interacting many-body systems:[12] Working within a given set of operators like in (4.169) and taking all flow equations into account except for the ones generating additional terms is no guarantee for fulfilling a condition like (4.174). In fact, one can verify that only with the additional property

$$\langle [\eta(B), \big(S^a(B)\big)^2] \rangle = 0 \tag{4.177}$$

can one expect

$$\frac{\mathrm{d}}{\mathrm{d}B} \langle \big(S^a(B)\big)^2 \rangle = 0 \tag{4.178}$$

to hold *exactly*. Still the violation of (4.178) will become smaller if one takes more terms into account in the ansatz (4.169) since these new terms are generated in higher orders of the expansion parameter (as long as the expansion parameter itself remains sufficiently small during the flow). For our purposes here we will restrict ourselves to the ansatz (4.169), therefore we can consistently neglect the effect of $\eta^{(2)}$ since it only produces higher order terms.

Summing up, violations of sum rules like (4.178) are often encountered in flow equation expansions. Notice that the size of the violation gives some measure for the reliability of the ansatz for the flowing observable. In the next section we will see in detail that e.g. for the Kondo model the additional terms (4.176) lead to very small effects. Sometimes one can also show that additional higher order terms cannot contribute to the dominant long-time behavior in correlation functions and are asymptotically irrelevant. We will return to this point in Sect. 4.3 for the spin–boson model.

Approximate Solution

We now deduce an approximate analytical solution of the system of differential equations (4.171) and (4.172) along the same lines as in the discussion of the resonant level model in Sect. 3.3.2. Later we will verify the accuracy of our approximations with a full numerical solution in order to obtain quantitative results. Still the analytical solution derived here is very valuable because it gives us analytical insights into the qualitative behavior.

First we notice that $\gamma_{s's}(B)$ is generated in order J, therefore the second term on the right hand side of (4.172) can initially be neglected since it only contributes in $O(J^2)$. Next (similar to Sect. 3.3.2) we take $h(B)$ as unchanged and find

[12] In other interacting fermion systems one e.g. often encounters conditions like $\{c^\dagger_{k'}(B), c_k(B)\} = \delta_{k'k}\ \forall B$.

$$\gamma_{s's}(B) = \frac{J_{\rm IR}(B=\epsilon_{\overline{s's}}^{-2})}{\epsilon_{s'}-\epsilon_s}\left(1-\mathrm{e}^{-B(\epsilon_{s'}-\epsilon_s)^2}\right) . \tag{4.179}$$

Notice that the coupling constant can be taken at the average energy (2.106), $\epsilon_{\overline{s's}} = (\epsilon_{s'}+\epsilon_s)/2$ to leading order. Of course, we need to verify up to what point the approximation $h(B) \approx 1$ can still be used. We put the approximate solution (4.179) into (4.171) and find:

$$\frac{\mathrm{d}h}{\mathrm{d}B} = -J^2 \sum_{s,s'} \mathrm{e}^{-B(\epsilon_{s'}-\epsilon_s)^2}\left(1-\mathrm{e}^{-B(\epsilon_{s'}-\epsilon_s)^2}\right) n(\epsilon_s)\,(1-n(\epsilon_{s'})) . \tag{4.180}$$

As long as $B \ll T^{-2}$ the integrations yield a simple result,

$$\frac{\mathrm{d}h}{\mathrm{d}B} = -\frac{g^2}{4B} . \tag{4.181}$$

This implies that $h(B)$ deviates only very slowly from 1 with

$$1-h(B=T^{-2}) = 2g^2(B=T^{-2})\,\ln(D/T) , \tag{4.182}$$

which is in leading order negligible for $T \gg T_{\rm K}$. Let us analyze what happens once $B \gg T^{-2}$. Then the integrations in (4.180) give

$$\frac{\mathrm{d}h}{\mathrm{d}B} = -g^2\,T\,B^{-1/2} . \tag{4.183}$$

One concludes that $h(B)$ starts to deviate noticeably from its initial value once $g^2(B)\,T\,B^{1/2} \sim 1$. This is equivalent to $\Lambda_{\rm feq} \sim \Gamma_{\rm rel}$, where $\Gamma_{\rm rel}$ is the spin relaxation rate introduced in (4.165):

$$\Gamma_{\rm rel} = \sqrt{2\pi}\,g^2(\Lambda_{\rm feq}=T)\,T . \tag{4.184}$$

This implies

$$\rho\,\gamma_{s's}(B=\infty) = \frac{g(B=\epsilon_{\overline{s's}}^{-2})}{\epsilon_{s'}-\epsilon_s} \tag{4.185}$$

for energy differences $|\epsilon_{s'}-\epsilon_s| \gtrsim \Gamma_{\rm rel}$. Due to the decay of $h(B)$ these coefficients remain approximately constant for energy differences $|\epsilon_{s'}-\epsilon_s| \lesssim \Gamma_{\rm rel}$ (compare the discussion in Sect. 3.3.2):[13]

$$\begin{aligned}\rho\,\gamma_{s's}(B=\infty) &\sim \frac{g_*}{\Gamma_{\rm rel}\,\mathrm{sgn}(\epsilon_{s'}-\epsilon_s)} \\ &\sim \frac{\mathrm{sgn}(\epsilon_{s'}-\epsilon_s)}{g_*\,T} .\end{aligned} \tag{4.186}$$

[13] Here it becomes important that the *decoherence term* in the flow equation (4.162) drives the coupling constant to zero for $\Lambda_{\rm feq} \to 0$ as one can verify from the numerical solution.

Asymptotically one finds $h(B=\infty)=0$, that is the observable becomes completely entangled with environmental degrees of freedom. In the next section we will explore what (4.185) and (4.186) imply for spin-spin correlation functions.

4.2.5 Spin Correlation Function and Dynamical Susceptibility

We are interested in the symmetrized spin-spin correlation function,

$$C(t)=\frac{1}{2}\left\langle\{S^z(0),S^z(t)\}\right\rangle\ . \tag{4.187}$$

We use (3.38) and express the Fourier transform in terms of the coefficients $\gamma_{s's}(B)$ for $B=\infty$:

$$\begin{aligned} C(\omega)=-\frac{\pi}{\tilde{Z}(\beta)}\sum_n \mathrm{e}^{-\beta E_n}\sum_{t,t'}\sum_{u,u'}\gamma_{t't}(B=\infty)\gamma_{u'u}(B=\infty) \\ \times\langle n|:(\boldsymbol{S}\times\boldsymbol{s}_{t't})^z::(\boldsymbol{S}\times\boldsymbol{s}_{u'u})^z:|n\rangle \\ \times\Big(\delta(\omega-\epsilon_{u'}+\epsilon_u)+\delta(\omega+\epsilon_{u'}-\epsilon_u)\Big)\ . \end{aligned} \tag{4.188}$$

Now

$$\begin{aligned} &\langle n|:(\boldsymbol{S}\times\boldsymbol{s}_{t't})^z::(\boldsymbol{S}\times\boldsymbol{s}_{u'u})^z:|n\rangle \\ &=\sum_{i,j,k,l}\epsilon_{zij}\epsilon_{zkl}\,\langle n|S^iS^k|n\rangle\,\langle n|:s^j_{t't}::s^l_{u'u}:|n\rangle \end{aligned} \tag{4.189}$$

and the only contributions come from $i=k$ (since $\langle n|S^{x,y,z}|n\rangle=0$). One easily shows

$$\begin{aligned} \langle n|:(\boldsymbol{S}\times\boldsymbol{s}_{t't})^z::(\boldsymbol{S}\times\boldsymbol{s}_{u'u})^z:|n\rangle&=\frac{1}{6}\,\langle n|:\boldsymbol{s}_{t't}:\cdot:\boldsymbol{s}_{u'u}:|n\rangle \\ &=\frac{1}{6}\,\langle n|:\boldsymbol{s}_{uu'}:\cdot:\boldsymbol{s}_{u'u}:|n\rangle \end{aligned} \tag{4.190}$$

since only matrix elements with $t'=u$, $t=u'$ can be nonvanishing. Plugging this back into (4.188) yields:

$$\begin{aligned} C(\omega)&=\pi\sum_{u,u'}\gamma^2_{u'u}(B=\infty)\,\frac{1}{6}\times\frac{3}{2}\,n(u)\,(1-n(u')) \\ &\qquad\times\Big(\delta(\omega-\epsilon_{u'}+\epsilon_u)+\delta(\omega+\epsilon_{u'}-\epsilon_u)\Big) \qquad (4.191) \\ &=\frac{\pi}{4}\sum_u\gamma^2_{\epsilon_u+\omega,\epsilon_u}(B=\infty) \\ &\qquad\times\big(n(\epsilon_u)\,(1-n(\epsilon_u+\omega))+n(\epsilon_u+\omega)\,(1-n(\epsilon_u))\big). \qquad (4.192) \end{aligned}$$

We distinguish three cases:

1. $|\omega| \lesssim \Gamma_{\rm rel}$: Then according to (4.186)

$$C(\omega) \sim \frac{1}{g_*^2 T^2} \sum_u \big(n(\epsilon_u) \left(1 - n(\epsilon_u + \omega)\right) + n(\epsilon_u + \omega) \left(1 - n(\epsilon_u)\right) \big) \\ \propto \frac{1}{\Gamma_{\rm rel}} \ , \tag{4.193}$$

since the summation over u yields a factor proportional to temperature. Hence for small frequencies the spin-spin correlation function is proportional to the inverse of the spin relaxation rate $\Gamma_{\rm rel}$ as expected.

2. $\Gamma_{\rm rel} \lesssim |\omega| \lesssim T$: Likewise according to (4.185)

$$C(\omega) \sim \frac{g_*^2}{\omega^2} \sum_u \big(n(\epsilon_u) \left(1 - n(\epsilon_u + \omega)\right) + n(\epsilon_u + \omega) \left(1 - n(\epsilon_u)\right) \big) \\ \propto \frac{\Gamma_{\rm rel}}{\omega^2} \ , \tag{4.194}$$

since again the summation over u yields a factor proportional to T.

3. $T \lesssim |\omega|$: For such large frequencies

$$C(\omega) \sim \frac{g^2(\Lambda_{\rm feq} = |\omega|)}{\omega^2} \sum_u \big(n(\epsilon_u)(1 - n(\epsilon_u + \omega)) + n(\epsilon_u + \omega)(1 - n(\epsilon_u)) \big) \\ \propto \frac{g^2(\Lambda_{\rm feq} = |\omega|)}{\omega} \ , \tag{4.195}$$

since here the summation over u yields a factor proportional to ω. The coupling constant has to be evaluated at the flow parameter scale corresponding to ω.

The dynamical quantity most frequently discussed in the literature is not the symmetrized spin correlation function, but the imaginary part of the dynamical spin susceptibility $\chi''(\omega)$. Using the fluctuation–dissipation theorem (3.40),

$$\chi''(\omega) = \tanh\left(\frac{\omega}{2T}\right) \, C(\omega) \ , \tag{4.196}$$

it is easy to deduce its behavior from our results for the spin correlation function:

1. $|\omega| \lesssim \Gamma_{\rm rel}$: At small frequencies the dynamical spin susceptibility is linear in ω:

$$\chi''(\omega) \propto \frac{\omega}{\Gamma_{\rm rel}\, T} \ . \tag{4.197}$$

2. $\Gamma_{\rm rel} \lesssim |\omega|$: Both (4.194) and (4.195) lead to the same behavior for the dynamical spin susceptibility:

$$\chi''(\omega) \propto \frac{g^2(\Lambda_{\rm feq} = |\omega|)}{\omega} \ . \tag{4.198}$$

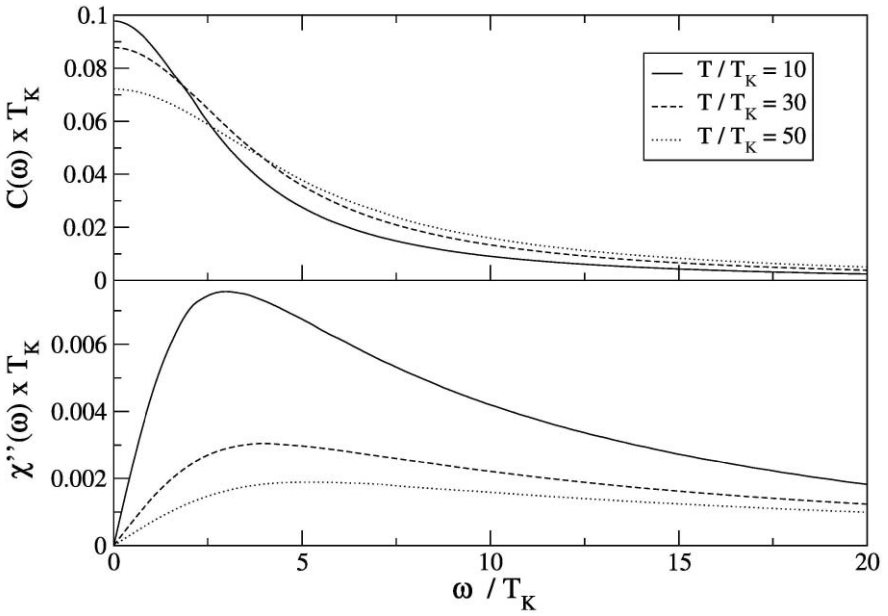

Fig. 4.1. Universal curves for the spin-spin correlation function $C(\omega)$ and the imaginary part of the dynamical spin susceptibility $\chi''(\omega)$ obtained from the full numerical solution of (4.171) and (4.172) for various temperatures. The fluctuation–dissipation theorem (3.40) is exactly fulfilled for these curves

Typical curves are shown in Fig. (4.1). Notice that the symmetric spin-spin correlation function shows the expected zero frequency decoherence peak with width $\Gamma_{\rm rel}$. The dynamical spin susceptibility has its maximum for $\omega \approx \Gamma_{\rm rel}$ with

$$\chi''(\omega = \Gamma_{\rm rel}) \propto \frac{1}{T} \; . \tag{4.199}$$

Since the curves in Fig. (4.1) are obtained from the solution of (4.171) and (4.172), the sum rule

$$\int_0^\infty {\rm d}\omega \, C(\omega) = \frac{\pi}{4} \tag{4.200}$$

will generally be violated due to the remaining nonzero terms in (4.176). This violation was due to the second line of (4.172), which should be a small term for small running coupling constants. We can see this explicitly in Fig. 4.2 where we compare the full solution of (4.171) and (4.172) with the approximate solution where the second line of (4.172) is omitted (and therefore the sum rule exactly fulfilled). The agreement between the curves is excellent. The inset of Fig. 4.2 shows the violation of the sum rule that becomes smaller for larger temperature and therefore smaller coupling constants.

Via a Kramers-Kronig relation one can also obtain the static susceptibility,

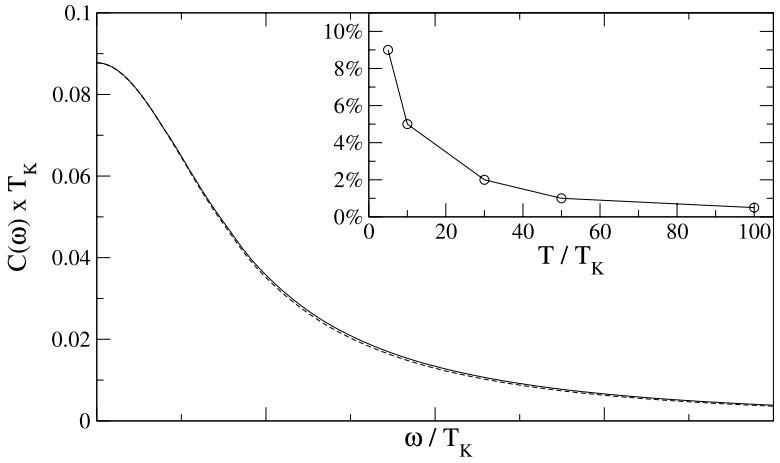

Fig. 4.2. The spin-spin correlation function $C(\omega)$ obtained from the full numerical solution of (4.171) and (4.172) (full line) versus the numerical solution where the second line of (4.172) is omitted (dashed line) for $T/T_{\rm K} = 30$. The inset shows the violation of the sum rule (4.200) from the full solution of (4.171) and (4.172), see text

$$\chi_0 = \frac{2}{\pi} \int_0^\infty {\rm d}\omega \, \frac{\chi''(\omega)}{\omega} \; . \tag{4.201}$$

From the above results for $\chi''(\omega)$ it is easy to see that

$$\chi_0(T) \propto \frac{1}{T} \; . \tag{4.202}$$

In fact one can verify (see Fig. 4.3):

$$T\,\chi_0(T) = \frac{1}{4}\,(1 - g_*) = \frac{1}{4}\,\left(1 - \frac{1}{\ln(T/T_{\rm K})}\right) \tag{4.203}$$

for $T/T_{\rm K} \gg 1$, which shows the correct crossover to a free spin-1/2 at high temperature [9].

4.2.6 Pseudogap Kondo Model

In this chapter we discuss the pseudogap Kondo model [10], that is the Kondo model with a nontrivial density of states

$$\rho(\epsilon) = \rho_0\,|\epsilon|^r \tag{4.204}$$

with $r > 0$. Such models have been widely discussed in the literature to describe magnetic impurities in hosts with a pseudogap density of states [11]. From our point of view, we are interested in this model since it allows us to understand:

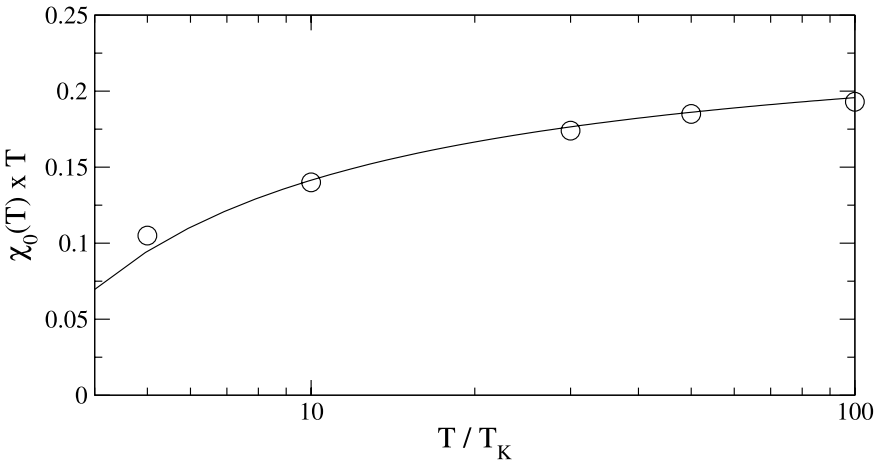

Fig. 4.3. Effective magnetic moment squared $T\,\chi_0(T)$ from (4.203) as a function of temperature. The circles denote data points obtained using the flow equation solution and the full line is the analytical result (4.203) describing the leading logarithmic correction. The data in Fig. 4.1 need to be calculated to very large frequencies in order to see the reduction of the effective magnetic moment when lowering temperature

- how quantum phase transitions emerge within the flow equation framework
- how nontrivial power laws in correlation functions can be generated through the nonperturbative structure of the transformation of observables in the flow equation method.

Let us first study the scaling behavior of the coupling constant in the infrared limit at zero temperature. Equation (4.123) takes the following form

$$\frac{\mathrm{d}J_{\mathrm{IR}}}{\mathrm{d}B} = -2J_{\mathrm{IR}}^2\,\rho_0 \int \mathrm{d}\epsilon\,|\epsilon|^r\,\epsilon\,\mathrm{e}^{-2B\epsilon^2}\,(n(\epsilon)-1/2)\;nn \tag{4.205}$$

$$= 2J_{\mathrm{IR}}^2\,\rho_0\,\frac{\Gamma(1+r/2)}{(2B)^{1+r/2}}\;. \tag{4.206}$$

This differential equation allows the following solution with a scaling structure,

$$J_{\mathrm{IR}}(B) = J_c\,B^{r/2}\;, \tag{4.207}$$

with a specific *critical* coupling

$$\rho_0 J_c = g_c = \frac{r}{2^{r/2}\,\Gamma(1+r/2)} = r + O(r^2)\;. \tag{4.208}$$

The expansion parameter of the flow equation approach (and conventional scaling approaches) is given by the dimensionless parameter

$$g(B) \stackrel{\text{def}}{=} \rho(\epsilon = B^{-1/2})\, J_{\text{IR}}(B) \ . \tag{4.209}$$

Here the density of states is evaluated at the energy scale corresponding to the flow parameter. For the critical coupling (4.207) $g(B)$ becomes B-independent,

$$g(B) \equiv g_c = \rho_0\, J_c \ . \tag{4.210}$$

For $J(B = D^{-2}) < J_c\, D^{-r}$ the expansion parameter flows to zero, and it diverges for $J(B = D^{-2}) > J_c\, D^{-r}$. The critical coupling therefore describes a quantum phase transition between a weak-coupling and a strong-coupling phase. Notice that we can reliably describe both the weak-coupling phase and the quantum phase transition for small r at zero temperature according to (4.210).[14]

In the sequel we are interested in analytical results at the quantum phase transition for small parameters r.[15] The quantity that we want to study is the dynamical spin susceptibility, in particular its scaling behavior at the quantum phase transition. We will see that this is linked to the behavior of $h(B)$ in the flow equation framework.

Similar to the previous discussion for the conventional Kondo model we can formally solve (4.172):

$$\gamma_{t't}(B) = (\epsilon_{t'} - \epsilon_t)\, J_c \int_0^B \mathrm{d}B'\, (B')^{r/2}\, h(B')\, \mathrm{e}^{-B'(\epsilon_{t'}-\epsilon_t)^2} \ . \tag{4.211}$$

Inserting this into the differential equation (4.171) for $h(B)$ yields:

$$\begin{aligned}
\frac{\mathrm{d}h}{\mathrm{d}B} &= -J_c^2 \int_0^\infty \mathrm{d}\epsilon'\, \rho(\epsilon') \int_{-\infty}^0 \mathrm{d}\epsilon\, \rho(\epsilon)\, B^{r/2}\, (\epsilon' - \epsilon)^2\, \mathrm{e}^{-B(\epsilon'-\epsilon)^2} \\
&\qquad \times \int_0^B \mathrm{d}B'\, (B')^{r/2}\, h(B')\, \mathrm{e}^{-B'(\epsilon'-\epsilon)^2} \\
&= -J_c^2 \int_0^\infty \mathrm{d}\epsilon'\, \rho(\epsilon') \int_{-\infty}^0 \mathrm{d}\epsilon\, \rho(\epsilon)\, B^{r/2}\, \mathrm{e}^{-B(\epsilon'-\epsilon)^2} \\
&\qquad \times \frac{\partial}{\partial B} \int_0^B \mathrm{d}B'\, (B')^{r/2}\, h(B')\, \mathrm{e}^{-B'(\epsilon'-\epsilon)^2} \\
&\qquad + J_c^2 \times O(r) \ .
\end{aligned} \tag{4.212}$$

Here we have used partial integration over B. The terms $J_c^2 \times O(r) \propto r^3$ can be neglected in leading order of the calculation as we will see below. The

[14] In order to have a controlled expansion in the strong-coupling phase we would again need nonzero temperature similar to the discussion of the conventional Kondo model in the previous section.

[15] Notice that we can safely neglect higher order terms in (4.206) in this regime since they only produce corrections in $O(r^2)$.

integrations over ϵ' and ϵ can now be done in closed form[16] and we find a simple differential equation for $h(B)$:

$$\frac{\mathrm{d}h}{\mathrm{d}B} = -g_c^2\, h(B)\, \frac{1}{4B} \ . \tag{4.213}$$

Its solution is

$$h(B) \propto B^{-g_c^2/4} \ , \tag{4.214}$$

and inserting this back into (4.211) results in

$$\gamma_{t't}(B=\infty) = \frac{\mathrm{sgn}(\epsilon_{t'} - \epsilon_t)}{|\epsilon_{t'} - \epsilon_t|^{1+r-g_c^2/2}} \ . \tag{4.215}$$

The low-frequency behavior of the spin-spin correlation function is then according to (4.192):

$$\begin{aligned} C(\omega) &\propto \frac{1}{|\omega|^{2+2r-g_c^2}} \int_0^\infty \mathrm{d}\epsilon' \int_{-\infty}^0 \mathrm{d}\epsilon\, \rho(\epsilon)\, \rho(\epsilon')\, \delta(|\omega| - \epsilon' + \epsilon) \\ &\propto \frac{1}{|\omega|^{1-g_c^2}} \ . \end{aligned} \tag{4.216}$$

Respectively, the imaginary part of the dynamical spin susceptibility at the quantum phase transition is given by

$$\chi''(\omega) \propto \frac{\mathrm{sgn}(\omega)}{|\omega|^{1-g_c^2}} \ . \tag{4.217}$$

The flow equation calculation therefore reproduces the correct result [12] for the anomalous dimension η_χ defined as $\chi''(\omega) \propto |\omega|^{-1+\eta_\chi}$,

$$\eta_\chi = r^2 + O(r^3) \ . \tag{4.218}$$

Notice that this is a rather nontrivial result from the point of view of the perturbative renormalization group. Using the flow equation method we have in fact been able to explicitly extract a nontrivial power-law. We did not have to resort to the usual reasoning of summing up leading logarithms under a scaling assumption for the dynamical behavior.

The deeper reason for this observation is the highly nontrivial and nonperturbative structure of the differential equations (4.171) and (4.172) governing the transformation of the observable. In a way this is also responsible for our difficulties in finding a good analytical solution for the transformation of observables in a simple model like the resonant level model in Sect. 3.3.2. The systems of differential equations are essentially the same and govern very different behavior from local Fermi liquids to nontrivial power laws. Our difficulties in finding a good analytical solution are probably related to the wealth of different phenomena that can be described by these differential equations.

[16] We can set $r = 0$ in the integral to leading order of the calculation.

This concludes our discussion of the Kondo model as a pedagogical introduction to "real" applications of the flow equation machinery in interacting many-body systems. We will return to the Kondo model later in Sect. 5.2 when we discuss its behavior in non-equilibrium.

4.3 Spin–Boson Model

The spin–boson model is of paradigmatic importance for understanding dissipative quantum systems. It has also played an important role in the development of the flow equation method. While there are many similarities to the Kondo model discussed above, the spin–boson model also highlights some new aspects in applications of the flow equation technique. We discuss its flow equation solution in this chapter, though in a somehow more abbreviated manner than the discussion of the Kondo model above.

4.3.1 Flow of the Hamiltonian

The spin–boson model is defined by the Hamiltonian:

$$H = -\frac{\Delta}{2}\,\sigma_x + \frac{1}{2}\,\sigma_z \sum_k \lambda_k\,(a_k + a_k^\dagger) + \sum_k \omega_k\, a_k^\dagger a_k\ . \tag{4.219}$$

It describes a two-level system defined by Pauli matrices coupled to a thermodynamically large bath consisting of harmonic oscillators with bosonic creation and annihilation operators $a_k^\dagger$, a_k. Δ is the tunneling matrix element of the two-level system and the matrix elements λ_k describe the coupling to the bath degrees of freedom. One can verify that the two-level dynamics is completely determined by the spectral function $J(\omega)$,

$$J(\omega) \stackrel{\text{def}}{=} \sum_k \lambda_k^2\,\delta(\omega - \omega_k)\ . \tag{4.220}$$

For reviews of the many applications of the spin–boson model one can consult [13, 14]. Notice that in particular for an Ohmic bath, $J(\omega) = 2\alpha\omega$, the spin–boson model can be mapped to a Kondo model and vice versa via bosonization and refermionization techniques.

Flow Equations

Let us set up the flow equations for the Hamiltonian (4.219). Our presentation follows [15, 16], which can be consulted for more details. Clearly, the interaction term that we want to eliminate in (4.219) is the coupling of system and bath,

$$H_{\rm int} = \frac{1}{2}\,\sigma_z \sum_k \lambda_k\,(a_k + a_k^\dagger)\ . \tag{4.221}$$

The canonical generator takes the following structure

$$\eta = i\,\sigma_y \sum_k \eta_k^{(y)}\,(a_k + a_k^\dagger) + \sigma_z \sum_k \eta_k^{(z)}\,(a_k - a_k^\dagger) \tag{4.222}$$

with

$$\eta_k^{(y)} = \frac{\lambda_k}{2}\,\Delta\ , \quad \eta_k^{(z)} = -\frac{\lambda_k}{2}\,\omega_k\ . \tag{4.223}$$

If we work out the commutator $[\eta, H_0]$, we see that a new coupling of system and bath is generated with the structure:

$$i\,\sigma_y \sum_k \mu_k\,(a_k - a_k^\dagger)\ . \tag{4.224}$$

The coefficients μ_k are generated in linear order of the small parameters λ_k. Along the lines of the discussion in Sect. 4.1.4 we therefore need to take these new terms into account *even in lowest order* of the flow equation expansion.

However, we can take a different route that remains faithful to the general principles of the flow equation approach by using a different generator than the canonical one. We keep the general structure (4.222) of the canonical generator, but allow a more general parametrization of its coefficients:

$$\eta_k^{(y)} = \frac{\lambda_k}{2}\,\Delta\,f_k^{(y)}\ , \quad \eta_k^{(z)} = -\frac{\lambda_k}{2}\,\omega_k\,f_k^{(z)}\ . \tag{4.225}$$

Here $f_k^{(y)}$ and $f_k^{(z)}$ are suitable dimensionless coefficients. We then obtain the following commutator:

$$\begin{aligned}[\eta, H_0] = {}& \sigma_z \sum_k (\omega_k\,\eta_k^{(z)} - \Delta\,\eta_k^{(y)})\,(a_k + a_k^\dagger) \\ & + i\sigma_y \sum_k (\omega_k\,\eta_k^{(y)} - \Delta\,\eta_k^{(z)})\,(a_k - a_k^\dagger)\ .\end{aligned} \tag{4.226}$$

The second term on the right hand side vanishes if we choose $f_k^{(y)} = -f_k^{(z)}$, while the flow equation for λ_k determined from $[\eta, H_0]$ takes the following form:

$$\frac{{\rm d}\lambda_k}{{\rm d}B} = -\lambda_k\,(\omega_k^2 - \Delta^2)\,f_k^{(z)}\ . \tag{4.227}$$

We want to achieve the usual energy scale separation with respect to energy differences:

$$\frac{{\rm d}\lambda_k}{{\rm d}B} = -(\omega_k - \Delta)^2\,\lambda_k\ . \tag{4.228}$$

This dictates the structure of $f_k^{(z)}$:

$$f_k^{(z)} = \frac{\omega_k - \Delta}{\omega_k + \Delta} \tag{4.229}$$

$$\Rightarrow \quad \eta_k^{(y)} = -\frac{\lambda_k}{2}\,\Delta\,\frac{\omega_k - \Delta}{\omega_k + \Delta}\;, \quad \eta_k^{(z)} = -\frac{\lambda_k}{2}\,\omega_k\,\frac{\omega_k - \Delta}{\omega_k + \Delta}\;. \tag{4.230}$$

Notice that we could modify our generator such that the structure of the system of flow equations simplified considerably, while remaining faithful to the underlying principle of energy scale separation. In particular, the matrix elements in our new generator vanish linearly for energy-diagonal scattering processes $|\omega_k - \Delta| \to 0$ as required in our discussion in Sect. 2.2.4. For an in depth discussion regarding the choice of the flow equation generator the reader can consult [17], where the Rabi model is analyzed both with the canonical and the form-invariant generator.

Next we need to work out the commutator with the interaction part of the Hamiltonian. Using normal-ordering with respect to the bosonic vacuum or the finite temperature free density matrix one finds:

$$\begin{aligned}[\eta, H_{\rm int}] = &-\sigma_x \sum_k \eta_k^{(y)}\,\lambda_k\,(2n(k)+1) \\ &-\frac{1}{2}\,\sigma_x \sum_{k,l} (\eta_k^{(y)}\,\lambda_l + \eta_l^{(y)}\,\lambda_k)\;:(a_k + a_k^\dagger)(a_l + a_l^\dagger):\\ &+\sum_k \eta_k^{(z)}\,\lambda_k\;. \end{aligned} \tag{4.231}$$

In leading order we can neglect the feedback of the newly generated interaction in the second line of the above equation. We find the following system of differential equations by comparing coefficients:

$$\frac{\mathrm{d}\Delta(B)}{\mathrm{d}B} = -\Delta(B)\int \mathrm{d}\omega\, J(\omega, B)\,\frac{\omega - \Delta(B)}{\omega + \Delta(B)}\,\coth(\beta\omega/2) \tag{4.232}$$

$$\frac{\partial \lambda_k(B)}{\partial B} = -\left(\omega_k - \Delta(B)\right)^2\,\lambda_k(B)\;. \tag{4.233}$$

Equivalently, one can write instead of (4.233):

$$\frac{\partial J(\omega, B)}{\partial B} = -2\left(\omega - \Delta(B)\right)^2\,J(\omega, B)\;. \tag{4.234}$$

Here we have introduced the flowing spectral function

$$J(\omega, B) \stackrel{\rm def}{=} \sum_k \lambda_k^2(B)\,\delta(\omega - \omega_k)\;. \tag{4.235}$$

The final Hamiltonian has the following structure in this order of the calculation:

$$H(B=\infty) = -\frac{\Delta(B=\infty)}{2}\,\sigma_x + \sum_k \omega_k\, a_k^\dagger a_k \tag{4.236}$$
$$-\frac{1}{2}\,\sigma_x \sum_{k,l} \omega_{kl}(B=\infty)\; :(a_k + a_k^\dagger)(a_l + a_l^\dagger): + E(B=\infty)\;.$$

The newly generated terms are produced by differential equations deduced from the second and third line of (4.231):

$$\frac{\mathrm{d}\omega_{kl}(B)}{\mathrm{d}B} = -\frac{\lambda_k(B)\lambda_q(B)}{2}\,\Delta(B)\,\left(\frac{\omega_k - \Delta(B)}{\omega_k + \Delta(B)} + \frac{\omega_q - \Delta(B)}{\omega_q + \Delta(B)}\right) \tag{4.237}$$

$$\frac{\mathrm{d}E(B)}{\mathrm{d}B} = -\frac{1}{2}\int \mathrm{d}\omega\, J(\omega, B)\,\omega\,\frac{\omega - \Delta(B)}{\omega + \Delta(B)}\;. \tag{4.238}$$

In (4.236) we have therefore eliminated the interaction of system and bath in linear order of the small matrix elements λ_k.

Renormalized Tunneling Matrix Element

The solution of the flow equations (4.232) and (4.234) is of major importance for our analysis. We will restrict ourselves to the zero temperature case, though the generalization to nonzero temperature is straightforward. For $T = 0$ we can rewrite (4.232) as:

$$\frac{\mathrm{d}\ln\Delta(B)}{\mathrm{d}B} = \frac{1}{2}\int \mathrm{d}\omega\,\frac{\partial J(\omega, B)}{\partial B}\,\frac{1}{\omega^2 - \Delta^2(B)}\;. \tag{4.239}$$

Fast modes renormalize the tunneling matrix element to smaller values, while slow modes try to shift the tunneling matrix element to larger values. This is essentially an effect of level repulsion.

Eventually, the flowing spectral function only has nonzero matrix elements around $\omega = \Delta(B = \infty)$, see Fig. 4.4. The numerical solution of (4.239) is straightforward for any spectral function that one might be interested in. However, important insights can also be gained analytically for spectral functions that are of particular importance in many applications:

– Super-Ohmic bath:

$$J(\omega) = K^{1-s}\omega^s\,\Theta(\omega_c - \omega) \quad \text{with } s > 1\;, \tag{4.240}$$

where is K is a parameter with dimension energy.

– Ohmic bath:

$$J(\omega) = 2\alpha\omega\,\Theta(\omega_c - \omega)\;, \tag{4.241}$$

where α is a dimensionless parameter measuring the strength of dissipation.

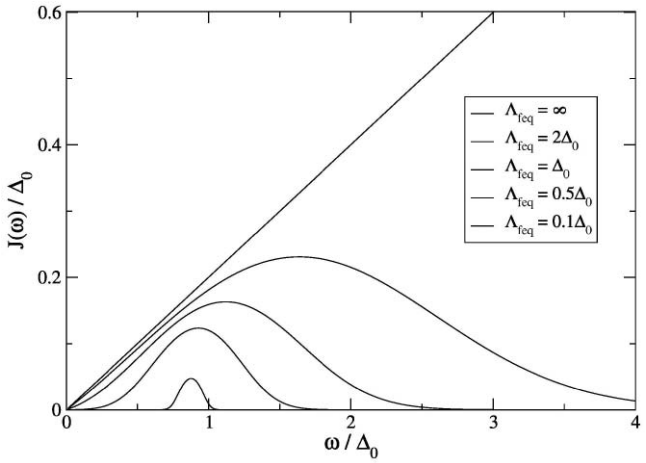

Fig. 4.4. The behavior of the spectral function $J(\omega, B)$ during the flow equation procedure (here for an Ohmic bath with $\alpha = 0.1$). The flow is generated by (4.260) and already incorporates the higher-order terms responsible for the algebraic decay of $J(\omega = \Delta_r, B)$

In both cases ω_c is a high-frequency cutoff, $\omega_c \gg \Delta$. Except for the final phase of the flow when $B^{-1/2} \lesssim \Delta(B = \infty)$, large frequencies $\omega \gg \Delta(B)$ dominate the integral in (4.239) and we can reformulate it as a self-consistency problem:

$$\frac{\mathrm{d} \ln \Delta(B)}{\mathrm{d}B} = \frac{1}{2} \int \mathrm{d}\omega \, \frac{\partial J(\omega, B)}{\partial B} \, \frac{1}{\omega^2 - \Delta^2(B = \infty)}$$

$$\Rightarrow \quad \ln \left(\frac{\Delta(B = \infty)}{\Delta(B = 0)} \right) = -\frac{1}{2} \int \mathrm{d}\omega \, \frac{J(\omega, B = 0)}{\omega^2 - \Delta^2(B = \infty)} \; . \tag{4.242}$$

Denoting $\Delta_r = \Delta(B = \infty)$ and $\Delta_0 = \Delta(B = 0)$, this gives the following solutions for the super-Ohmic bath:

$$\Delta_r \propto \Delta_0 \, \exp \left(-\frac{1}{2(s-1)} \left(\frac{\omega_c}{K} \right)^{s-1} \right) \tag{4.243}$$

and the Ohmic bath:

$$\Delta_r \propto \Delta_0 \left(\frac{\Delta_0}{\omega_c} \right)^{\alpha/(1-\alpha)} \; . \tag{4.244}$$

In both cases the proportionality constant is of order 1. Notice the strong nonperturbative renormalization effects (also known from other approaches [13]) that render naive perturbation theory in the small matrix elements λ_k useless. Also notice the quantum phase transition that occurs in the Ohmic case for $\alpha = 1$, when the renormalized tunneling matrix elements becomes

zero. This is a Kosterlitz–Thouless transition where the tunneling particle becomes localized in one state [13].

A final note regarding the comparison with the conventional scaling approach. There the term $\Delta^2(B)$ in the denominator on the right hand side of (4.239) is absent [13]. This leads to the mistaken interpretation that all modes contribute to a downward renormalization of the tunneling matrix element, which then necessitates some gesticulations in order to obtain the correct result (4.244).

4.3.2 Low-Energy Observables

We have previously encountered various impurity models where the flow equations have generated a flow of the single particle energy levels in order $1/N$ that could be neglected for solving the differential equations, compare e.g. (3.70). However, if one is interested in the impurity contribution to the specific heat, these $O(1/N)$-terms add up and give a finite contribution. We will use the example of the spin–boson model to show this explicitly.

Impurity Specific Heat

The impurity contribution to the specific heat $c_{\mathrm{imp}}(T)$ is defined as the difference of two thermodynamically large quantities, namely the specific heat of system plus bath minus the specific heat of only the bosonic bath. In the ground state of (4.236) we certainly have $\langle \sigma_x \rangle = 1$ (since $\Delta_r > 0$) and therefore the single particle energy levels are shifted to

$$E_k = \omega_k - \omega_{kk}(B = \infty) \; . \tag{4.245}$$

For small energies $\omega_k \ll \Delta_r$ this is easily worked out from the solution of (4.237):

$$E_k = \omega_k - \frac{\lambda_k^2(B=0)}{2\Delta_r} \; . \tag{4.246}$$

Then[17]

$$\begin{aligned} c_{\mathrm{imp}}(T) &= \frac{\partial}{\partial T} \left(\sum_k \frac{E_k}{\mathrm{e}^{E_k/T} - 1} - \sum_k \frac{\omega_k}{\mathrm{e}^{\omega_k/T} - 1} \right) \\ &= \frac{\partial}{\partial T} \left(\sum_k (E_k - \omega_k) \left. \frac{\partial}{\partial \omega} \right|_{\omega=\omega_k} \frac{\omega}{\mathrm{e}^{\omega/T} - 1} \right) \\ &= -\frac{1}{2\Delta_r} \frac{\partial}{\partial T} \left(\int \mathrm{d}\omega \, J(\omega) \left. \frac{\partial}{\partial \omega} \right|_{\omega=\omega_k} \frac{\omega}{\mathrm{e}^{\omega/T} - 1} \right) \\ &= \frac{J(T)}{\Delta_r} \frac{s}{2} \, \Gamma(s+2) \, \xi(s+1) \end{aligned} \tag{4.247}$$

[17] Notice that $E(B = \infty)$ in (4.236) is independent of temperature and therefore does not contribute to $c_{\mathrm{imp}}(T)$.

for low temperatures $T/\Delta_r \to 0$. We see that the impurity contribution to the specific heat depends on the renormalized parameter Δ_r. It has a power-law behavior determined by the spectral function, $c_{\rm imp}(T) \propto T^s$.

Dynamical Spin Susceptibility

Next we are interested in the spin dynamics. For example, we want to calculate the following spin-spin correlation function:

$$C_{zz}^{(\rm sym)}(t) \stackrel{\rm def}{=} \frac{1}{2} \langle {\rm GS}|\{\sigma_z(0), \sigma_z(t)\}|{\rm GS}\rangle \ . \tag{4.248}$$

As usual we need to study the transformation of the observable σ_z,

$$\frac{{\rm d}\sigma_z(B)}{{\rm d}B} = [\eta(B), \sigma_z(B)] \ . \tag{4.249}$$

We make the following ansatz and neglect higher order terms:

$$\sigma_z(B) = h(B)\, \sigma_z + \sigma_x \sum_k \chi_k(B)\, (a_k + a_k^\dagger) \ . \tag{4.250}$$

The system of differential equations then takes the following form:

$$\frac{{\rm d}h}{{\rm d}B} = -\Delta \sum_k \lambda_k\, \chi_k\, \frac{\omega_k - \Delta}{\omega_k + \Delta}\, \coth(\beta\omega_k/2) \tag{4.251}$$

$$\frac{{\rm d}\chi_k}{{\rm d}B} = \Delta\, h\, \lambda_k\, \frac{\omega_k - \Delta}{\omega_k + \Delta} \ . \tag{4.252}$$

It is easy to verify that under this transformation

$$\langle (\sigma_z(B))^2 \rangle = 1 \tag{4.253}$$

remains fulfilled with respect to the ground state or the finite temperature free density matrix. As by now seen numerous times, the observable "decays" completely into a different form where it is entangled with environment degrees of freedom, $h(B) \stackrel{B\to\infty}{\longrightarrow} 0$. This is true when

- Δ_r lies in the support of $J(\omega)$
- and $\Delta_r \neq 0$, that is we are not in the localized phase of the Ohmic spin–boson model.

These observations are indicative of decoherence in the flow equation framework. Conventionally, decoherence is associated with a growing entanglement of system and environment as a function of time. In the flow equation framework the Hamiltonian is diagonalized and no exchange of energy between system and bath is possible for $B = \infty$. However, now the observable becomes entangled with environment degrees of freedom.[18]

[18] These observations were in fact first made in the flow equation analysis of the spin–boson model in [15].

The above system of flow equations is quite sufficient if one is interested in the dynamics away from the resonance. For example for the zero temperature long-time limit $|\omega| \ll \Delta_r$ one finds:

$$\chi_k(B=\infty) = -\frac{\lambda_k(B=0)}{\Delta_r} \qquad (|\omega_k| \ll \Delta_r) \tag{4.254}$$

$$\Rightarrow \quad \chi''_{zz}(\omega) = \mathrm{sgn}(\omega)\, C^{(\mathrm{sym})}_{zz}(\omega) = \pi\, \frac{J(\omega)}{\Delta_r^2}\ . \tag{4.255}$$

This is equivalent to a t^{-s-1}-algebraic decay of the spin-spin correlation function. This is the correct power law behavior, which can be quite difficult to obtain with other analytical methods (compare [13]). It should also be mentioned that higher order terms in the expansion of the flowing observable (4.250) do not contribute to or modify this long-time behavior. It is easy to verify that due to zero temperature phase space arguments terms with more bosonic creation or annihilation operators lead to contributions with additional powers of ω in (4.255).

4.3.3 Resonant Behavior

We need to be more careful when studying the dynamics in the vicinity of the resonance, $\omega \approx \Delta_r$. We focus on the zero temperature case. Remember that the unitary transformations generated a new term with the structure

$$-\frac{1}{2}\,\sigma_x \sum_{k,l} \omega_{kl}(B)\ :(a_k + a_k^\dagger)(a_l\ + a_l^\dagger):\tag{4.256}$$

in the flowing Hamiltonian. The matrix elements ω_{kl} were determined by the differential equation (4.237). It is easy to verify that these matrix elements do not remain small close to the resonance, and therefore we cannot ignore them if we want to describe the resonance peak in $\chi''_{zz}(\omega)$ or $C^{(\mathrm{sym})}_{zz}(\omega)$.

Canonical Approach

To deal with this problem in the canonical approach, we should go one order further in the flow equation expansion. The flowing Hamiltonian then takes the structure:

$$\begin{aligned} H(B) = &-\frac{\Delta(B)}{2}\,\sigma_x + \frac{1}{2}\,\sigma_z \sum_k \lambda_k(B)\,(a_k + a_k^\dagger) + \sum_k \omega_k\, a_k^\dagger a_k \\ &+\sigma_x \sum_{k,l} \Big(t_{kl}(B)\,(a_k^\dagger a_l^\dagger + a_k a_l\,) + 2 s_{kl}(B)\, a_k^\dagger a_l \Big)\ . \end{aligned} \tag{4.257}$$

The generator acquires a new part:

$$\eta^{(2)} = \sigma_x \sum_{k,l} \Big((\omega_k + \omega_l)\, t_{kl} (a_k^\dagger a_l^\dagger - a_k a_l) + 2(\omega_k - \omega_l)\, s_{kl}\, a_k^\dagger a_l \Big) \ . \quad (4.258)$$

One finds the following flow equations for the new coefficients:

$$\begin{aligned} \frac{\mathrm{d}t_{kl}}{\mathrm{d}B} &= -(\omega_k + \omega_l)^2\, t_{kl} + \frac{\Delta}{4}\, \lambda_k \lambda_l \left(\frac{\omega_k - \Delta}{\omega_k + \Delta} + \frac{\omega_l - \Delta}{\omega_l + \Delta} \right) \\ \frac{\mathrm{d}s_{kl}}{\mathrm{d}B} &= -(\omega_k - \omega_l)^2\, s_{kl} + \frac{\Delta}{4}\, \lambda_k \lambda_l \left(\frac{\omega_k - \Delta}{\omega_k + \Delta} + \frac{\omega_l - \Delta}{\omega_l + \Delta} \right) \ . \end{aligned} \quad (4.259)$$

We need to discuss the feedback of these new terms on the coefficients already present in the Hamiltonian. The only modification arises from the commutator of $\eta^{(y)}$ from (4.222) with the second line in (4.257). It gives

$$\frac{\mathrm{d}\lambda_k}{\mathrm{d}B} = -(\omega_k - \Delta)^2\, \lambda_k - 2\Delta \sum_p \lambda_p\, \frac{\omega_p - \Delta}{\omega_p + \Delta}\, (t_{pk} + s_{pk}) \ , \quad (4.260)$$

which replaces (4.233). It is easy to verify that this yields a differential equation of the same kind that we have seen for the resonant level model (3.84) or the Kondo model (4.162):

$$\frac{\mathrm{d}\lambda_{\Delta_r}}{\mathrm{d}B} = -c\, \lambda_{\Delta_r}^3\, \rho(\omega = \Delta_r)\, B^{-1/2} \ , \quad (4.261)$$

where c is a positive constant of order 1. Similar to the discussion for the resonant level model or the Kondo model, this means that an algebraic $B^{-1/4}$-decay of $\lambda_{\Delta_r}(B)$ sets in once $B^{-1/2} = \Lambda_{\mathrm{feq}} \approx J(\omega = \Delta_r)$. It is easy to verify that on the same energy scale $h(B)$ from (4.251) starts to deviate noticeably from its initial value $h(B = 0) = 1$. For a more in depth discussion of the asymptotic behavior of the flow equations the reader can consult [18].

We can conclude that the width of the resonance peak in the dynamical spin function is given by $J(\omega = \Delta_r)$. This is the correct zero temperature result also known from other approaches [13]. However, the full line shape of $C_{zz}^{(\mathrm{sym})}(\omega)$ in the vicinity of $\omega \approx \Delta_r$ is not very accurately described by the above system of flow equations, in fact only the width comes out reliably. This is different from the situation in the finite temperature Kondo model where this order of the flow equation expansion was already sufficient. The deeper reason for this lies in the nontrivial flow behavior of $\Delta(B)$, which has no analogue in the SU(2)-symmetric Kondo model. If one wants to obtain the line shape of the correlation functions in the spin–boson model accurately even close to the resonance, one actually needs to take all interaction terms into account that contain up to two bosonic bath operators, including their mutual feedback.[19] The same holds for the transformation of the observable $\sigma_z(B)$.[20]

[19] This observation appears to hold generally, not only in the spin–boson model.

[20] This is reminiscent of the observations for the resonant level model in Sect. 3.3.2.

While one can certainly follow the above route with very accurate results, the resulting systems of differential equations are rather lengthy and cumbersome. In the next subsection we will therefore present an alternative approach that is "less canonical" but considerably shorter, and in fact produces essentially the same quantitative results.

Ground State Approximation

The basis for this approximation is the observation that σ_x has a nonvanishing ground state expectation value, $\langle\sigma_x\rangle = 1$, with respect to $H(B=\infty)$ at zero temperature. It is therefore a plausible idea to split up σ_x into its expectation value and a fluctuating part,

$$\sigma_x = \langle\sigma_x\rangle + *\sigma_x* \ . \tag{4.262}$$

This defines the operation $* \ *$, which amounts to subtracting the ground state expectation value. It can be thought of as a simplistic normal-ordering prescription. We now neglect the fluctuating $*\sigma_x*$-part in (4.256) and take only the expectation value into account in the new term generated by the unitary transformations:

$$-\frac{1}{2}\sum_{k,l}\omega_{kl}(B)\ :(a_k + a_k^\dagger)(a_l + a_l^\dagger):\ . \tag{4.263}$$

This is simply a potential scattering term. We next use the observation that we can prevent this term from appearing at all if we introduce the additional part of the generator

$$\eta^{(2)} = \sum_{k,l}\eta_{kl}(B)\ :(a_k + a_k^\dagger)(a_l - a_l^\dagger):\tag{4.264}$$

with

$$\eta_{kl} = \frac{\lambda_k\lambda_l\,\Delta\,\omega_l}{2(\omega_k^2-\omega_l^2)}\left(\frac{\omega_k-\Delta}{\omega_k+\Delta}+\frac{\omega_l-\Delta}{\omega_l+\Delta}\right)\ . \tag{4.265}$$

The flowing Hamiltonian then remains form invariant:

$$H(B) = -\frac{\Delta(B)}{2}\,\sigma_x + \frac{1}{2}\,\sigma_z\sum_k\lambda_k(B)\,(a_k+a_k^\dagger) + \sum_k\omega_k\,a_k^\dagger a_k\ . \tag{4.266}$$

The only change is a new differential equation for λ_k which replaces (4.233):

$$\frac{\mathrm{d}\lambda_k}{\mathrm{d}B} = -(\omega_k-\Delta)^2\,\lambda_k + \Delta\,\lambda_k\sum_p\frac{\lambda_p^2\,\omega_p}{\omega_k^2-\omega_p^2}\left(\frac{\omega_k-\Delta}{\omega_k+\Delta}+\frac{\omega_p-\Delta}{\omega_p+\Delta}\right)\ . \tag{4.267}$$

Also the flow equations governing the transformation of the observable $\sigma_z(B)$ from (4.250) change:

$$\frac{\mathrm{d}h}{\mathrm{d}B} = -\Delta \sum_k \lambda_k \chi_k \frac{\omega_k - \Delta}{\omega_k + \Delta} \tag{4.268}$$

$$\frac{\mathrm{d}\chi_k}{\mathrm{d}B} = \Delta h \lambda_k \frac{\omega_k - \Delta}{\omega_k + \Delta} + \Delta \lambda_k \sum_p \frac{\chi_p \lambda_p \omega_p}{\omega_k^2 - \omega_p^2} \left(\frac{\omega_k - \Delta}{\omega_k + \Delta} + \frac{\omega_p - \Delta}{\omega_p + \Delta} \right) \tag{4.269}$$

Notice that the sum rule (4.253) is no longer exactly fulfilled. However, the violation turns out to be very small in all the cases discussed below with errors not larger than a few percent.

Several correlation functions obtained for an Ohmic bath via the equations (4.232), (4.267), (4.268) and (4.269) are shown in Fig. 4.5. One of the very useful features of the flow equation approach is that it is not limited to power-law spectral functions like (4.240) and (4.241), but that one can use an arbitrary spectral density $J(\omega)$. This property has been used in the context of quantum computing in [19] for evaluating a number of nontrivial correlation functions based on the above system of differential equations.

However, it should also be mentioned that limitations of our approach show up in the Ohmic case for stronger dissipation $\alpha \gtrsim 0.1$: The analysis of higher orders in the flow equation expansion reveals strong-coupling behavior [15] and a different approach is needed.[21] On the other hand, for a super-Ohmic bath the flow equation expansion shown above has generally proven to be very reliable for all coupling strengths.

At this point, it is appropriate to have a critical look at the "ground state approximation" used here instead of the full canonical approach. The latter gives essentially the same results, but with a more complicated system of differential equations. Two issues require justification:

1. $\eta^{(2)}$ introduced in (4.264) contains an energy denominator that violates the idea of energy scale separation in the flow equation approach. This was the price that we had to pay in order to keep the Hamiltonian $H(B)$ form invariant. However, $\eta^{(2)}$ has the structure of a potential scattering term and its commutators can be evaluated exactly without any approximations. Therefore we cannot generate energy denominator problems in higher orders of the expansion, and the energy denominator in (4.265) is unproblematic.
2. In what sense is the approximation to neglect the fluctuating part $*\sigma_x*$ controlled? A detailed analysis shows that this approximation becomes asymptotically exact in the limit when the flowing spectral function $J(\omega, B)$ couples only modes in the vicinity of the resonance, that is in the late stages of the flow in Fig. 4.4. This motivates our approximation to take only the expectation value $\langle \sigma_x \rangle$ into account since only the

[21] This strong-coupling behavior is related to the strong-coupling physics of the zero temperature Kondo model and a different kind of expansion is needed, compare Sect. 5.1.

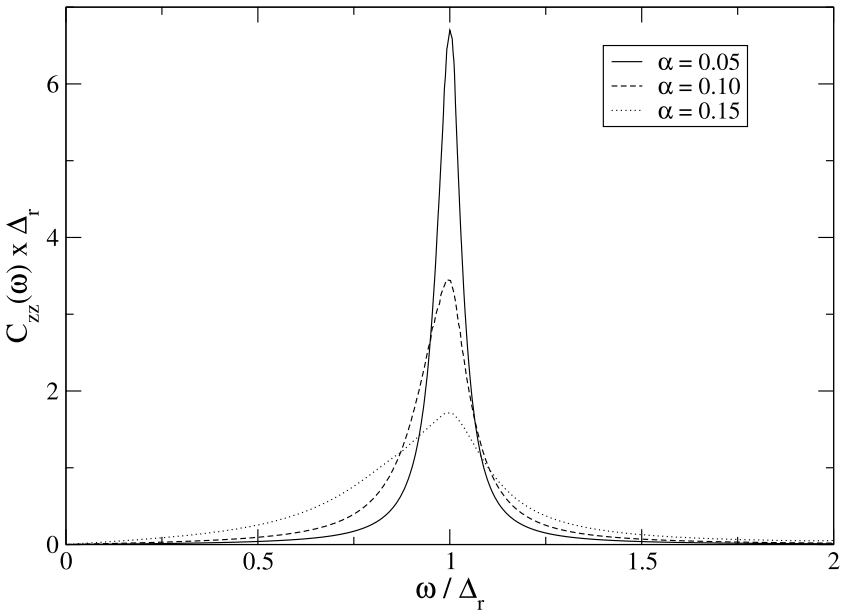

Fig. 4.5. Spin-spin correlation functions for the spin–boson model with an Ohmic bath (4.241) for various dissipation strengths α at zero temperature. For details of the flow equation calculation see the text

matrix elements ω_{kl} close to the resonance become large anyway. The deeper reason for this observation is the fact that the spin–boson model for $\Lambda_{\rm feq} \gg \Delta_r$ becomes equivalent to a dissipative harmonic oscillator, which can be solved exactly. More information regarding this issue can be found in the literature [15].

Summing up, we have seen that it was straightforward to obtain the low-energy behavior of observables plus the renormalized resonance frequency and its decay rate (= the peak width in the correlation function). Extra work was needed if one wants additional quantitative information regarding the line shape close to the resonance.

4.4 Interacting Fermions in $d > 1$ Dimensions

In the previous sections we have used the flow equation method to study various impurity models like the Kondo model or the spin–boson model. In this section, we look at another important class of interacting many-body systems: those with a translation-invariant interaction like interacting electrons on a lattice. In fact, Wegner's initial publication [20] on flow equations dealt with such a system in $d = 1$ dimension, namely a Luttinger liquid. In

this section, we give a brief overview over $d > 1$ dimensional applications of flow equations.. In particular, we will see that Landau's Fermi liquid theory emerges as the natural result of the flow equation approach and can thereby be justified in a new microscopic way.

4.4.1 Flow Equations and Fermi Liquid Theory

The starting point is a d dimensional electron system with a two-particle interaction described by the Hamiltonian:

$$H = \sum_{\boldsymbol{k},\alpha} \epsilon_k^0 \ : c_{\boldsymbol{k}\alpha}^\dagger c_{\boldsymbol{k}\alpha} : \tag{4.270}$$
$$+\frac{1}{2\Omega} \sum_{\boldsymbol{k}_1',\boldsymbol{k}_2',\boldsymbol{k}_1,\boldsymbol{k}_2} \sum_{\alpha_1,\alpha_2} V_{\alpha_1\alpha_2}(\boldsymbol{k}_1',\boldsymbol{k}_2';\boldsymbol{k}_1,\boldsymbol{k}_2) \ : c_{\boldsymbol{k}_1'\alpha_1}^\dagger c_{\boldsymbol{k}_1\alpha_1} c_{\boldsymbol{k}_2'\alpha_2}^\dagger c_{\boldsymbol{k}_2\alpha_2} : \ .$$

Here Ω denotes the system size, the Fermi energy is set to zero ($\epsilon_F = 0$) and translation invariance implies that only the interaction matrix elements with

$$\boldsymbol{k}_1' + \boldsymbol{k}_2' = \boldsymbol{k}_1 + \boldsymbol{k}_2 \tag{4.271}$$

are nonzero. We now diagonalize (4.270) by using the canonical generator $\eta = [H, H_{\rm int}]$, where $H_{\rm int}$ contains all the interaction matrix elements in (4.270) that do not conserve the energy, $\epsilon_{\boldsymbol{k}_1'} + \epsilon_{\boldsymbol{k}_2'} \neq \epsilon_{\boldsymbol{k}_1} + \epsilon_{\boldsymbol{k}_2}$. This means that our diagonalized Hamiltonian $\tilde{H}$ only contains energy-diagonal matrix elements

$$\epsilon_{\boldsymbol{k}_1'} + \epsilon_{\boldsymbol{k}_2'} = \epsilon_{\boldsymbol{k}_1} + \epsilon_{\boldsymbol{k}_2} \ . \tag{4.272}$$

For a general model in $d > 1$ dimensions the combination of (4.271) and (4.272) implies the following form for $\tilde{H}$:

$$\tilde{H} = \sum_{\boldsymbol{k},\alpha} \epsilon_k \ : c_{\boldsymbol{k}\alpha}^\dagger c_{\boldsymbol{k}\alpha} : \tag{4.273}$$
$$+\frac{1}{2\Omega} \sum_{\boldsymbol{k},\boldsymbol{p}} \sum_{\alpha,\beta} V_H(\boldsymbol{k},\boldsymbol{p}) \ : c_{\boldsymbol{k}\alpha}^\dagger c_{\boldsymbol{k}\alpha} c_{\boldsymbol{p}\beta}^\dagger c_{\boldsymbol{p}\beta} :$$
$$+\frac{1}{2\Omega} \sum_{\boldsymbol{k},\boldsymbol{p}} \sum_{\alpha,\beta} V_F(\boldsymbol{k},\boldsymbol{p}) \ : c_{\boldsymbol{k}\alpha}^\dagger c_{\boldsymbol{p}\alpha} c_{\boldsymbol{p}\beta}^\dagger c_{\boldsymbol{k}\beta} :$$

plus normal-ordered 3-particle interactions and higher order interaction terms. Notice that (4.271) and (4.272) are equivalent in one-dimensional systems with a linear dispersion relation. Therefore the above form (4.273) of the diagonal Hamiltonian is too restrictive in $d = 1$. This leads to unpleasant divergences in the running coupling constants if one still tries to implement the above diagonalization route in one-dimensional systems. In this case a more appropriate route is to reach a form of the Hamiltonian that conserves

the number of quasiparticles. For a discussion of these points the reader is referred to [20, 21]. Alternatively, one can combine flow equations with bosonization [22].

Let us return to $d > 1$ dimensional interacting electron systems. The energy-diagonal Hamiltonian (4.273) is closely related to Landau's Fermi liquid theory (for a good review see, e.g., [23, 24]). Landau assumed a one to one correspondence between noninteracting electrons and *quasiparticles* with the same quantum numbers upon adiabatically turning on the interaction. At low temperature and close to the Fermi surface, these quasiparticles are long-lived excitations and Landau assumed that the energy of the system can be expressed as

$$E = E_0 + \sum_{\boldsymbol{k},\alpha} \epsilon_k \, \delta n_{\boldsymbol{k}\alpha} + \frac{1}{2\Omega} \sum_{\boldsymbol{k},\alpha,\boldsymbol{p},\beta} f(\boldsymbol{k}\alpha, \boldsymbol{p}\beta) \, \delta n_{\boldsymbol{k}\alpha} \delta n_{\boldsymbol{p}\beta} \; . \tag{4.274}$$

Here $\delta n_{\boldsymbol{k}\alpha}$ denotes the change in the number of quasiparticles with quantum numbers momentum $\boldsymbol{k}$ and spin α from the ground state distribution, i.e. the number of quasiparticles added above the Fermi level or removed from below the Fermi level. Adding or removing a quasiparticle changes the total energy by

$$\begin{aligned} E_{\boldsymbol{k}\alpha} &= \frac{\mathrm{d}E}{\mathrm{d}\delta n_{\boldsymbol{k}\alpha}} \\ &= \epsilon_k + \frac{1}{\Omega} \sum_{\boldsymbol{p},\beta} f(\boldsymbol{k}\alpha, \boldsymbol{p}\beta) \, \delta n_{\boldsymbol{p}\beta} \; . \end{aligned} \tag{4.275}$$

This identifies ϵ_k as the single-particle energy for adding or removing this quasiparticle, while the coefficients $f(\boldsymbol{k}\alpha, \boldsymbol{p}\beta)$ describe the interaction between quasiparticles.

It is easy to verify that Landau's expression (4.274) follows from the energy-diagonal Hamiltonian (4.273) with the following mapping of coefficients:

$$f(\boldsymbol{k}\alpha, \boldsymbol{p}\beta) = V_H(\boldsymbol{k}, \boldsymbol{p}) - \frac{1 + \alpha\beta}{2} \, V_F(\boldsymbol{k}, \boldsymbol{p}) \; . \tag{4.276}$$

Notice that the flow to the energy-diagonal Hamiltonian also leads to a flow of the single-particle energies: in general one finds $\epsilon_k \neq \epsilon_k^0$. Different from impurity models, this shift is not negligible since the interaction is translation-invariant. This results in a different density of states for the Hamiltonian $\tilde{H}$, which will show up in thermodynamic observables like the specific heat. In the language of Fermi liquid theory, the flow of the single-particle energies $\epsilon_k(B)$ amounts to a nontrivial ratio $m^*/m \neq 1$ and a Sommerfeld coefficient different from its noninteracting value.

Landau's Fermi liquid picture therefore appears as the natural structure of a theory describing interacting electrons resulting from the application of

the flow equation method with the canonical generator. The connection between the physical fermions and the quasiparticles follows from the unitary transformation of the fermion creation and annihilation operators. The general structure of this transformation for a translation-invariant spin-SU(2)-symmetric interaction is

$$\begin{aligned}\tilde{c}_{\boldsymbol{k}\alpha} &= c_{\boldsymbol{k}\alpha}(B=\infty) \\ &= h_{\boldsymbol{k}}(B=\infty)\, c_{\boldsymbol{k}\alpha} + \frac{1}{\Omega}\sum_{\boldsymbol{k}_1,\boldsymbol{k}_2} \gamma^{(s:\boldsymbol{k})}_{\boldsymbol{k}_1\boldsymbol{k}_2}(B=\infty) : c^\dagger_{\boldsymbol{k}_1+\boldsymbol{k}_2-\boldsymbol{k},\alpha} c_{\boldsymbol{k}_1\alpha} c_{\boldsymbol{k}_2\alpha} : \\ &\quad + \frac{1}{\Omega}\sum_{\boldsymbol{k}_1,\boldsymbol{k}_2} \gamma^{(a:\boldsymbol{k})}_{\boldsymbol{k}_1\boldsymbol{k}_2}(B=\infty) : c^\dagger_{\boldsymbol{k}_1+\boldsymbol{k}_2-\boldsymbol{k},-\alpha} c_{\boldsymbol{k}_1-\alpha} c_{\boldsymbol{k}_2\alpha} :\end{aligned} \tag{4.277}$$

plus higher normal-ordered terms. Given this structure, it is easy to verify that the discontinuity of the electron occupation number in the interacting system is determined by

$$\left(\lim_{\boldsymbol{k}\to\boldsymbol{k}_F^-} - \lim_{\boldsymbol{k}\to\boldsymbol{k}_F^+}\right) \langle c^\dagger_{\boldsymbol{k}\alpha} c_{\boldsymbol{k}\alpha}\rangle = h^2_{\boldsymbol{k}_F}(B=\infty)\ . \tag{4.278}$$

Here the notation means that we approach the same point at the Fermi surface from inside ($\boldsymbol{k}_F^-$) and outside ($\boldsymbol{k}_F^+$). The terms with more creation and annihilation operators in (4.277) only lead to continuous contributions in this limiting process (due to phase space arguments) which vanish if the difference is taken in (4.278).[22] Equation (4.278) allows us to identify

$$Z_{\boldsymbol{k}_F} = h^2_{\boldsymbol{k}_F}(B=\infty)\ , \tag{4.279}$$

where $Z_{\boldsymbol{k}_F}$ is just the usual Z-factor of Fermi liquid theory.

Let us illustrate these observations with an example, namely the Hubbard model:

$$H = \sum_{\boldsymbol{k},\alpha} \epsilon_k\ : c^\dagger_{\boldsymbol{k}\alpha} c_{\boldsymbol{k}\alpha} : + \frac{U}{\Omega} \sum_{\boldsymbol{k}_1',\boldsymbol{k}_2',\boldsymbol{k}_1,\boldsymbol{k}_2} \delta_{\boldsymbol{k}_1'+\boldsymbol{k}_2',\boldsymbol{k}_1+\boldsymbol{k}_2}\ : c^\dagger_{\boldsymbol{k}_1'\uparrow} c_{\boldsymbol{k}_1\uparrow} c^\dagger_{\boldsymbol{k}_2'\downarrow} c_{\boldsymbol{k}_2\downarrow} :\ . \tag{4.280}$$

During the flow, we have a more general structure:

$$\begin{aligned}H(B) &= \sum_{\boldsymbol{k},\alpha} \epsilon_k(B)\ : c^\dagger_{\boldsymbol{k}\alpha} c_{\boldsymbol{k}\alpha} : \\ &\quad + \frac{1}{\Omega} \sum_{\boldsymbol{k}_1',\boldsymbol{k}_2',\boldsymbol{k}_1,\boldsymbol{k}_2} V^{(a)}_{\boldsymbol{k}_1',\boldsymbol{k}_2';\boldsymbol{k}_1,\boldsymbol{k}_2}(B)\ : c^\dagger_{\boldsymbol{k}_1'\uparrow} c_{\boldsymbol{k}_1\uparrow} c^\dagger_{\boldsymbol{k}_2'\downarrow} c_{\boldsymbol{k}_2\downarrow} : \\ &\quad + \frac{1}{\Omega} \sum_{\boldsymbol{k}_1',\boldsymbol{k}_2',\boldsymbol{k}_1,\boldsymbol{k}_2} \sum_\alpha V^{(s)}_{\boldsymbol{k}_1',\boldsymbol{k}_2';\boldsymbol{k}_1,\boldsymbol{k}_2}(B)\ : c^\dagger_{\boldsymbol{k}_1'\alpha} c_{\boldsymbol{k}_1\alpha} c^\dagger_{\boldsymbol{k}_2'\alpha} c_{\boldsymbol{k}_2\alpha} :\end{aligned} \tag{4.281}$$

[22] The coefficients $\gamma^{(a:\boldsymbol{k})}_{\boldsymbol{k}_1\boldsymbol{k}_2}(B=\infty)$ are well-behaved for non-singular interactions.

plus higher-order normal-ordered interaction terms. Initially

$$V^{(a)}_{\boldsymbol{k}'_1,\boldsymbol{k}'_2;\boldsymbol{k}_1,\boldsymbol{k}_2}(B=0) = U\,\delta_{\boldsymbol{k}'_1+\boldsymbol{k}'_2,\boldsymbol{k}_1+\boldsymbol{k}_2} \tag{4.282}$$
$$V^{(s)}_{\boldsymbol{k}'_1,\boldsymbol{k}'_2;\boldsymbol{k}_1,\boldsymbol{k}_2}(B=0) = 0\ .$$

The canonical generator has the following structure:

$$\begin{aligned}\eta(B) = \frac{1}{\Omega}\sum_{\boldsymbol{k}'_1,\boldsymbol{k}'_2,\boldsymbol{k}_1,\boldsymbol{k}_2} &(\epsilon_{\boldsymbol{k}'_1}+\epsilon_{\boldsymbol{k}'_2}-\epsilon_{\boldsymbol{k}_1}-\epsilon_{\boldsymbol{k}_2})\,V^{(a)}_{\boldsymbol{k}'_1,\boldsymbol{k}'_2;\boldsymbol{k}_1,\boldsymbol{k}_2}(B)\\ &\times\ :c^\dagger_{\boldsymbol{k}'_1\uparrow}c_{\boldsymbol{k}_1\uparrow}c^\dagger_{\boldsymbol{k}'_2\downarrow}c_{\boldsymbol{k}_2\downarrow}: \\ +\frac{1}{\Omega}\sum_{\boldsymbol{k}'_1,\boldsymbol{k}'_2,\boldsymbol{k}_1,\boldsymbol{k}_2}\sum_{\alpha} &(\epsilon_{\boldsymbol{k}'_1}+\epsilon_{\boldsymbol{k}'_2}-\epsilon_{\boldsymbol{k}_1}-\epsilon_{\boldsymbol{k}_2})\,V^{(s)}_{\boldsymbol{k}'_1,\boldsymbol{k}'_2;\boldsymbol{k}_1,\boldsymbol{k}_2}(B)\\ &\times\ :c^\dagger_{\boldsymbol{k}'_1\alpha}c_{\boldsymbol{k}_1\alpha}c^\dagger_{\boldsymbol{k}'_2\alpha}c_{\boldsymbol{k}_2\alpha}:\ ,\end{aligned} \tag{4.283}$$

where we have ignored all higher order terms since we will focus on the leading-order results. The resulting flow equations can be worked out easily using the results from Sect. 4.1:

$$\begin{aligned}\frac{\mathrm{d}V^{(a)}_{\boldsymbol{k}'_1,\boldsymbol{k}'_2;\boldsymbol{k}_1,\boldsymbol{k}_2}}{\mathrm{d}B} &= -(\epsilon_{\boldsymbol{k}'_1}+\epsilon_{\boldsymbol{k}'_2}-\epsilon_{\boldsymbol{k}_1}-\epsilon_{\boldsymbol{k}_2})^2\,V^{(a)}_{\boldsymbol{k}'_1,\boldsymbol{k}'_2;\boldsymbol{k}_1,\boldsymbol{k}_2}\\ &\quad+\frac{1}{\Omega}\sum_{\boldsymbol{q}_1,\boldsymbol{q}_2}(\epsilon_{\boldsymbol{k}'_1}+\epsilon_{\boldsymbol{k}'_2}+\epsilon_{\boldsymbol{k}_1}+\epsilon_{\boldsymbol{k}_2}-2(\epsilon_{\boldsymbol{q}_1}+\epsilon_{\boldsymbol{q}_2}))\\ &\qquad\times V^{(a)}_{\boldsymbol{k}'_1,\boldsymbol{k}'_2;\boldsymbol{q}_1,\boldsymbol{q}_2}\,V^{(a)}_{\boldsymbol{q}_1,\boldsymbol{q}_2;\boldsymbol{k}_1,\boldsymbol{k}_2}\,(1-n(\boldsymbol{q}_1)-n(\boldsymbol{q}_2))\\ &\quad+\frac{1}{\Omega}\sum_{\boldsymbol{q}_1,\boldsymbol{q}_2}(\epsilon_{\boldsymbol{k}'_1}-\epsilon_{\boldsymbol{k}'_2}+\epsilon_{\boldsymbol{k}_1}-\epsilon_{\boldsymbol{k}_2}-2(\epsilon_{\boldsymbol{q}_1}-\epsilon_{\boldsymbol{q}_2}))\\ &\qquad\times V^{(a)}_{\boldsymbol{k}'_1,\boldsymbol{q}_2;\boldsymbol{q}_1,\boldsymbol{k}_2}\,V^{(a)}_{\boldsymbol{q}_1,\boldsymbol{k}'_2;\boldsymbol{k}_1,\boldsymbol{q}_2}\,(n(\boldsymbol{q}_1)-n(\boldsymbol{q}_2))\end{aligned} \tag{4.284}$$

$$\begin{aligned}\frac{\mathrm{d}V^{(s)}_{\boldsymbol{k}'_1,\boldsymbol{k}'_2;\boldsymbol{k}_1,\boldsymbol{k}_2}}{\mathrm{d}B} &= -(\epsilon_{\boldsymbol{k}'_1}+\epsilon_{\boldsymbol{k}'_2}-\epsilon_{\boldsymbol{k}_1}-\epsilon_{\boldsymbol{k}_2})^2\,V^{(s)}_{\boldsymbol{k}'_1,\boldsymbol{k}'_2;\boldsymbol{k}_1,\boldsymbol{k}_2}\\ &\quad+\frac{1}{2\Omega}\sum_{\boldsymbol{q}_1,\boldsymbol{q}_2}(\epsilon_{\boldsymbol{k}'_1}-\epsilon_{\boldsymbol{k}'_2}-\epsilon_{\boldsymbol{k}_1}+\epsilon_{\boldsymbol{k}_2}+2(\epsilon_{\boldsymbol{q}_1}-\epsilon_{\boldsymbol{q}_2}))\\ &\qquad\times V^{(a)}_{\boldsymbol{k}'_1,\boldsymbol{q}_1;\boldsymbol{k}_1,\boldsymbol{q}_2}\,V^{(a)}_{\boldsymbol{k}'_2,\boldsymbol{q}_2;\boldsymbol{k}_2,\boldsymbol{q}_1}\,(n(\boldsymbol{q}_1)-n(\boldsymbol{q}_2))\end{aligned} \tag{4.285}$$

plus terms in $O(U^3)$. Integrating (4.284) and (4.285) in leading order in an expansion in U results in a Hamiltonian of the form (4.273) with only energy-diagonal interactions with the coefficients:[23]

[23] Compare also the identical results obtained in [25] within a somehow different framework.

$$V_F(\boldsymbol{k},\boldsymbol{p}) = U - \frac{U^2}{\Omega}\sum_{\boldsymbol{q}_1,\boldsymbol{q}_2}\frac{1-n(\boldsymbol{q}_1)-n(\boldsymbol{q}_2)}{\epsilon_{\boldsymbol{q}_1}+\epsilon_{\boldsymbol{q}_2}-\epsilon_{\boldsymbol{k}}-\epsilon_{\boldsymbol{p}}}\,\delta_{\boldsymbol{q}_1+\boldsymbol{q}_2,\boldsymbol{k}+\boldsymbol{p}} + O(U^3) \tag{4.286}$$

$$V_H(\boldsymbol{k},\boldsymbol{p}) = V_F(\boldsymbol{k},\boldsymbol{p}) - \frac{U^2}{\Omega}\sum_{\boldsymbol{q}_1,\boldsymbol{q}_2}\frac{n(\boldsymbol{q}_1)-n(\boldsymbol{q}_2)}{\epsilon_{\boldsymbol{q}_1}-\epsilon_{\boldsymbol{q}_2}+\epsilon_{\boldsymbol{k}}-\epsilon_{\boldsymbol{p}}}\,\delta_{\boldsymbol{q}_1+\boldsymbol{q}_2,\boldsymbol{k}+\boldsymbol{p}} + O(U^3)\ . \tag{4.287}$$

Likewise one can work out the flow of the single-particle energies $\epsilon_k(B)$, which gives rise to an increased density of states at the Fermi surface implying a ratio $m^*/m > 1$.

Next we analyze the transformation of the fermion operators under this unitary flow. In the notation of (4.277) one finds (again in leading order):

$$\frac{\mathrm{d}h_{\boldsymbol{k}}(B)}{\mathrm{d}B} = \frac{U}{\Omega^2}\sum_{\boldsymbol{p}_1,\boldsymbol{p}_2}\left(\epsilon_{\boldsymbol{p}_1}+\epsilon_{\boldsymbol{p}_2}-\epsilon_{\boldsymbol{k}}-\epsilon_{\boldsymbol{p}_1+\boldsymbol{p}_2-\boldsymbol{k}}\right)\mathrm{e}^{-B\left(\epsilon_{\boldsymbol{p}_1}+\epsilon_{\boldsymbol{p}_2}-\epsilon_{\boldsymbol{k}}-\epsilon_{\boldsymbol{p}_1+\boldsymbol{p}_2-\boldsymbol{k}}\right)^2} \times\gamma^{(a:\boldsymbol{k})}_{\boldsymbol{p}_1\boldsymbol{p}_2}(B) \times\Big[n(\boldsymbol{p}_1+\boldsymbol{p}_2-\boldsymbol{k})(1-n(\boldsymbol{p}_2))+n(\boldsymbol{p}_1)(n(\boldsymbol{p}_2)-n(\boldsymbol{p}_1+\boldsymbol{p}_2-\boldsymbol{k}))\Big] \tag{4.288}$$

$$\frac{\mathrm{d}\gamma^{(a:\boldsymbol{k})}_{\boldsymbol{k}_1\boldsymbol{k}_2}(B)}{\mathrm{d}B} = h_{\boldsymbol{k}}(B)\,U\left(\epsilon_{\boldsymbol{k}}+\epsilon_{\boldsymbol{k}_1+\boldsymbol{k}_2-\boldsymbol{k}}-\epsilon_{\boldsymbol{k}_1}-\epsilon_{\boldsymbol{k}_2}\right)\mathrm{e}^{-B\left(\epsilon_{\boldsymbol{k}}+\epsilon_{\boldsymbol{k}_1+\boldsymbol{k}_2-\boldsymbol{k}}-\epsilon_{\boldsymbol{k}_1}-\epsilon_{\boldsymbol{k}_2}\right)^2} \tag{4.289}$$

The differential equation for $\gamma^{(s:\boldsymbol{k})}_{\boldsymbol{k}_1\boldsymbol{k}_2}(B)$ can be ignored in this order of the calculation since it is only generated in order U^2. We next analyze the large-B behavior of (4.288) and (4.289). Let us assume a nonzero limit $h_{\boldsymbol{k}}(B=\infty) > 0$. Then we can (approximately) integrate (4.289) and find

$$\gamma^{(a:\boldsymbol{k})}_{\boldsymbol{k}_1\boldsymbol{k}_2}(B) \propto \frac{U}{\epsilon_{\boldsymbol{k}}+\epsilon_{\boldsymbol{k}_1+\boldsymbol{k}_2-\boldsymbol{k}}-\epsilon_{\boldsymbol{k}_1}-\epsilon_{\boldsymbol{k}_2}}\left(1-\mathrm{e}^{-B\left(\epsilon_{\boldsymbol{k}}+\epsilon_{\boldsymbol{k}_1+\boldsymbol{k}_2-\boldsymbol{k}}-\epsilon_{\boldsymbol{k}_1}-\epsilon_{\boldsymbol{k}_2}\right)^2}\right) \tag{4.290}$$

with a nonzero positive proportionality factor. Plugging this into the differential equation for $h_{\boldsymbol{k}}(B)$ yields

$$1-h_{\boldsymbol{k}}(B=\infty) \propto -\frac{U^2}{\Omega^2}\sum_{\boldsymbol{p}_1,\boldsymbol{p}_2}\frac{1}{\left(\epsilon_{\boldsymbol{p}_1}+\epsilon_{\boldsymbol{p}_2}-\epsilon_{\boldsymbol{k}}-\epsilon_{\boldsymbol{p}_1+\boldsymbol{p}_2-\boldsymbol{k}}\right)^2} \times\Big[n(\boldsymbol{p}_1+\boldsymbol{p}_2-\boldsymbol{k})(1-n(\boldsymbol{p}_2))+n(\boldsymbol{p}_1)(n(\boldsymbol{p}_2)-n(\boldsymbol{p}_1+\boldsymbol{p}_2-\boldsymbol{k}))\Big]\ , \tag{4.291}$$

again with a nonzero positive proportionality factor. This is only consistent with our initial assumption $h_{\boldsymbol{k}}(B=\infty) > 0$ when the summation over $\boldsymbol{p}_1, \boldsymbol{p}_2$ gives a finite result. However, the energy denominator in (4.291) makes the sums diverge in many circumstances:

– At nonzero temperature the summations always lead to a divergent result. For example we set $\boldsymbol{p}_2 = \boldsymbol{k}$ and find

$$\Big[n(\boldsymbol{p}_1 + \boldsymbol{p}_2 - \boldsymbol{k})(1 - n(\boldsymbol{p}_2)) + n(\boldsymbol{p}_1)(n(\boldsymbol{p}_2) - n(\boldsymbol{p}_1 + \boldsymbol{p}_2 - \boldsymbol{k}))\Big]_{\boldsymbol{p}_2 = \boldsymbol{k}}$$
$$= n(\boldsymbol{p}_1)(1 - n(\boldsymbol{p}_1)) > 0 \ , \tag{4.292}$$

which implies that the double pole in (4.291) has a nonvanishing positive coefficient for $T > 0$.

– At zero temperature one can easily verify that the combination of occupation numbers in the square brackets in (4.291) is only nonzero for

$$n(\boldsymbol{p}_1) > 0, \quad n(\boldsymbol{p}_2) > 0 \quad \text{and} \quad n(\boldsymbol{p}_1 + \boldsymbol{p}_2 - \boldsymbol{k}) < 0 \tag{4.293}$$

or

$$n(\boldsymbol{p}_1) < 0, \quad n(\boldsymbol{p}_2) < 0 \quad \text{and} \quad n(\boldsymbol{p}_1 + \boldsymbol{p}_2 - \boldsymbol{k}) > 0 \ . \tag{4.294}$$

Therefore we can rewrite (4.291) in the following way:

$$1 - h_{\boldsymbol{k}}(B = \infty) \propto -U^2 \Bigg(\int_{\epsilon_F}^{\infty} \mathrm{d}\epsilon_{\boldsymbol{p}_1} \, \mathrm{d}\epsilon_{\boldsymbol{p}_2} \, \Theta(\epsilon_F - \epsilon_{\boldsymbol{p}_1 + \boldsymbol{p}_2 - \boldsymbol{k}}) \tag{4.295}$$
$$+ \int_{-\infty}^{\epsilon_F} \mathrm{d}\epsilon_{\boldsymbol{p}_1} \, \mathrm{d}\epsilon_{\boldsymbol{p}_2} \, \Theta(\epsilon_{\boldsymbol{p}_1 + \boldsymbol{p}_2 - \boldsymbol{k}} - \epsilon_F) \Bigg)$$
$$\times \rho(\epsilon_{\boldsymbol{p}_1}) \, \rho(\epsilon_{\boldsymbol{p}_2}) \, \frac{1}{(\epsilon_{\boldsymbol{p}_1} + \epsilon_{\boldsymbol{p}_2} - \epsilon_{\boldsymbol{k}} - \epsilon_{\boldsymbol{p}_1 + \boldsymbol{p}_2 - \boldsymbol{k}})^2}$$

For a given value of the total energy $E = \epsilon_{\boldsymbol{p}_1} + \epsilon_{\boldsymbol{p}_2} - \epsilon_{\boldsymbol{p}_1 + \boldsymbol{p}_2 - \boldsymbol{k}}$ these integrals over $\epsilon_{\boldsymbol{p}_1}, \epsilon_{\boldsymbol{p}_2}$ are of the typical structure that also appears in the evaluation of the imaginary part of the electron self-energy. Phase space arguments lead to the well-known factor $(E - \epsilon_F)^2$, which vanishes quadratically as one approaches the Fermi surface. We end up with

$$1 - h_{\boldsymbol{k}}(B = \infty) \propto -U^2 \int \mathrm{d}E \, \rho(E) \, \frac{(E - \epsilon_F)^2}{(E - \epsilon_{\boldsymbol{k}})^2} \ , \tag{4.296}$$

which can only be finite for $\epsilon_{\boldsymbol{k}} = \epsilon_F$.

From the above calculations we conclude that $h_{\boldsymbol{k}}(B = \infty) > 0$ is only possible for zero temperature and at the Fermi surface $\epsilon_{\boldsymbol{k}} = \epsilon_F$. Otherwise necessarily $h_{\boldsymbol{k}}(B = \infty) = 0$ and the structure of the perturbative solution (4.290) has to be modified close to the resonance, that is for $\epsilon_{\boldsymbol{k}} \approx \epsilon_{\boldsymbol{k}_1} + \epsilon_{\boldsymbol{k}_2} - \epsilon_{\boldsymbol{k}_1 + \boldsymbol{k}_2 - \boldsymbol{k}}$.

While we have derived these results in a specific model, our observations hold quite generally for interacting electron systems in $d > 1$ dimensions. We can draw the following conclusions:

- Only for zero temperature and directly at the Fermi surface can a fraction of the physical fermion creation and annihilation operators survive the flow in (4.277). The square of this fraction can be identified with the Z-factor of Landau's Fermi liquid theory, see (4.279).
- Such a nonvanishing term $h_{\boldsymbol{k}}(B=\infty)\, c_{\boldsymbol{k}\alpha}$ in (4.277) has a coherent time evolution under the energy-diagonal Hamiltonian $\tilde{H}$. In the language of many-body theory this amounts to a quasiparticle pole in the Green's function of the physical electrons. The contributions from $\gamma^{(a:\boldsymbol{k})}_{\boldsymbol{k}_1\boldsymbol{k}_2}(B=\infty)$ and $\gamma^{(s:\boldsymbol{k})}_{\boldsymbol{k}_1\boldsymbol{k}_2}(B=\infty)$ lead to a decoherent background of finite width.
- While the structure of the transformed operator $\tilde{c}_{\boldsymbol{k}\alpha}$ changes discontinuously away from the Fermi surface, this discontinuity is not visible in physical Green's functions. Close to the Fermi surface, the coefficients $\gamma^{(a:\boldsymbol{k})}_{\boldsymbol{k}_1\boldsymbol{k}_2}(B=\infty)$ and $\gamma^{(s:\boldsymbol{k})}_{\boldsymbol{k}_1\boldsymbol{k}_2}(B=\infty)$ become more and more dominated by nearly energy-diagonal contributions, $\epsilon_{\boldsymbol{k}_1}+\epsilon_{\boldsymbol{k}_2}-\epsilon_{\boldsymbol{k}_1+\boldsymbol{k}_2-\boldsymbol{k}}\approx\epsilon_{\boldsymbol{k}}$. Therefore these contributions have a "nearly" coherent time evolution, which merges into the well-defined quasiparticles at the Fermi surface.
- In this way, one can trace the quasiparticles from the Fermi surface to Landau's picture of quasiparticles with a finite lifetime even away from the Fermi surface. This just amounts to following how the $h_{\boldsymbol{k}_F}(B=\infty)\, c_{\boldsymbol{k}\alpha}$ contribution decays into a nearly energy-diagonal operator product. Notice that the background of particle-hole excitations already present in the solution of (4.277) at the Fermi surface does not change very much as one goes away from the Fermi surface, and is not considered part of Landau's quasiparticle.
- If additional fields are coupled to a physical fermion in the vicinity of the Fermi surface, then at low energies only the $\sqrt{Z_{\boldsymbol{k}_F}}=h_{\boldsymbol{k}_F}(B=\infty)$ fraction of this coupling acts as the coupling to a fermionic excitation: One thinks of Landau's quasiparticles as the "dressed" physical electrons.

Summing up, from the flow equation point of view the effective Hamiltonian (4.273) of the Landau type is not restricted to the vicinity of the Fermi surface. However, only close to the Fermi surface can the single-particle excitations of (4.273) be directly related in a one to one correspondence with the original fermions. One needs to distinguish carefully between

- the flow equation quasiparticles: these are well-defined single-particle excitations of $\tilde{H}$, which are away from the Fermi surface, however, *not* in one to one correspondence with the physical fermions.
- Landau's quasiparticles: these have an incoherent time-evolution under $\tilde{H}$ away from the Fermi surface (meaning a *finite lifetime*), but are in one to one correspondence with the physical fermions even away (though not too far away) from the Fermi surface. In the flow equation picture they emerge from the evolution of the $h_{\boldsymbol{k}_F}(B=\infty)\, c_{\boldsymbol{k}\alpha}$-part into the nearly energy-diagonal ($\epsilon_{\boldsymbol{k}_1}+\epsilon_{\boldsymbol{k}_2}-\epsilon_{\boldsymbol{k}_1+\boldsymbol{k}_2-\boldsymbol{k}}\approx\epsilon_{\boldsymbol{k}}$) part of the operator products

$: c^\dagger_{\boldsymbol{k}_1+\boldsymbol{k}_2-\boldsymbol{k}} c_{\boldsymbol{k}_1} c_{\boldsymbol{k}_2} :$ in the solution of (4.277) as one goes away from the Fermi surface.[24]

4.4.2 Flow Equations and Molecular-Field Type Hamiltonians

In the previous section we have derived the Hamiltonian (4.273) from a model lattice Hamiltonian. Notice that $\tilde{H}$ contains only biquadratic terms like $c^\dagger_{\boldsymbol{k}\alpha} c_{\boldsymbol{k}\alpha}$, which means that $\tilde{H}$ is of molecular-field type and does not lead to any fluctuations around the molecular-field behavior. Putting it otherwise, the Hartree–Fock approximation becomes *exact* when applied to (4.273). One way of looking at the analysis in the previous chapter is therefore to see it as the derivation of an effective Hamiltonian,[25] which in turn can now be solved exactly using the molecular-field approximation.

This route has been pursued by Wegner and coworkers in a series of papers [25, 26, 27, 28]. We follow their calculation in [25] and introduce the expectation values:

$$\langle \mathrm{GS}_{\mathrm{int}} | c^\dagger_{\boldsymbol{k}\alpha} c_{\boldsymbol{k}\beta} | \mathrm{GS}_{\mathrm{int}} \rangle = \delta_{\alpha\beta} \left(n^0(\boldsymbol{k}) + \nu^s(\boldsymbol{k}) \right) + \sum_i \sigma^i_{\alpha\beta} \, \nu^a_i(\boldsymbol{k}) \; . \tag{4.297}$$

Here $|\mathrm{GS}_{\mathrm{int}}\rangle$ is the ground state of the interacting system that we want to determine, and $n^0(\boldsymbol{k})$ is the occupation number in the noninteracting system. The coefficients $\nu^s(\boldsymbol{k})$ and $\nu^a_i(\boldsymbol{k})$ therefore describe a deviation from the symmetric state: the symmetric state is unstable if one can find nonzero coefficients with a lower free energy than the symmetric state. Due to the biquadratic nature of $\tilde{H}$, it is easy to work out the energy

$$\begin{aligned} E_{HF} = & \frac{1}{\Omega} \sum_{\boldsymbol{k},\boldsymbol{q}} (2V_H(\boldsymbol{k},\boldsymbol{q}) - V_F(\boldsymbol{k},\boldsymbol{q})) \, \nu^s(\boldsymbol{k}) \, \nu^s(\boldsymbol{q}) \\ & - \frac{1}{\Omega} \sum_{\boldsymbol{k},\boldsymbol{q}} \sum_i V_F(\boldsymbol{k},\boldsymbol{q}) \, \nu^a_i(\boldsymbol{k}) \, \nu^a_i(\boldsymbol{q}) \end{aligned} \tag{4.298}$$

and entropy

$$\begin{aligned} S_{HF} = & - \sum_{\boldsymbol{k}} \left(1 + \mathrm{e}^{\beta(\epsilon_{\boldsymbol{k}} - \epsilon_F)} \right) \left(1 + \mathrm{e}^{-\beta(\epsilon_{\boldsymbol{k}} - \epsilon_F)} \right) \\ & \times \left(\nu^s(\boldsymbol{k}) \, \nu^s(\boldsymbol{k}) + \sum_i \nu^a_i(\boldsymbol{k}) \, \nu^a_i(\boldsymbol{k}) \right) \; . \end{aligned} \tag{4.299}$$

[24] And, of course, higher order contributions with more particle-hole pairs.

[25] Another interesting point worth studying in more detail would be the derivation of Landau parameters beyond the Hartree–Fock approximation. This is an interesting point because the calculation of Landau parameters from a microscopic model is difficult.

Therefore the free energy

$$F = E - T\,S \tag{4.300}$$

is a quadratic form in $\nu^s(\boldsymbol{k})$ and $\nu_i^a(\boldsymbol{k})$, of which one needs to find the minimum. For details of these calculations the reader is referred to [25].

Typical instabilities that can occur in this system are ferromagnetism and Pomeranchuk-instabilities. This exhibits one interesting feature of this approach: these instabilities occur for a Hamiltonian with finite effective interactions.[26] The observation that effective interactions in the flow equation scheme remain finite could be useful for making statements about the convergence of the flow equation approach – this topic seems worthwhile exploring in more detail.

At this point it also becomes apparent that the scheme presented in the previous section will be too restrictive in certain situations. Where do other instabilities like antiferromagnetism or superconductivity show up? In fact, closer inspection (here: a nonperturbative analysis of the flow equations) reveals that one has diverging coupling constants on the road to (4.273) if such instabilities are present in a given model Hamiltonian. In order to avoid these divergences, Wegner and coworkers developed a generalization of the ideas leading to (4.273). They showed how one can choose a generator η such that the final Hamiltonian for $B = \infty$ consists of a given set of biquadratic terms. The key step is to introduce a continuously varying "elimination" factor r that indicates whether an interaction should be eliminated ($r \neq 0$) or kept for $B \to \infty$ ($r = 0$). The generator is constructed as usual as a commutator

$$\eta(B) = [H(B), H_{\rm int}^r(B)]\ , \tag{4.301}$$

where $H_{\rm int}^r(B)$ is obtained from the interaction part of the Hamiltonian (4.270):

$$H_{\rm int}^r = \frac{1}{2\Omega} \sum_{\boldsymbol{k}_1',\boldsymbol{k}_2',\boldsymbol{k}_1,\boldsymbol{k}_2} \sum_{\alpha_1,\alpha_2} r(\boldsymbol{k}_1',\boldsymbol{k}_2';\boldsymbol{k}_1,\boldsymbol{k}_2)\, V_{\alpha_1\alpha_2}(\boldsymbol{k}_1',\boldsymbol{k}_2';\boldsymbol{k}_1,\boldsymbol{k}_2) \times :c_{\boldsymbol{k}_1'\alpha_1}^\dagger c_{\boldsymbol{k}_1\alpha_1} c_{\boldsymbol{k}_2'\alpha_2}^\dagger c_{\boldsymbol{k}_2\alpha_2}: \ . \tag{4.302}$$

Notice that η from (4.301) leads to flow equations that respect energy scale separation.

For the explicit case of the two-dimensional Hubbard model (4.280) with nearest neighbor hopping on a square lattice one has the dispersion relation

$$\epsilon_{k} = -2t\,(\cos k_x + \cos k_y)\ , \tag{4.303}$$

where t is the hopping matrix element. At half-filling the Fermi surface is nested, $\epsilon_{\boldsymbol{k}} = -\epsilon_{\boldsymbol{k}+\boldsymbol{Q}}$, with $\boldsymbol{Q} = (\pi,\pi)$, and one expects antiferromagnetic

[26] In other renormalization group inspired approaches to interacting electron systems [29, 32] one deals with truncated and partially integrated interactions, which show divergences at such phase transitions.

instabilities. The two-dimensional Hubbard model is also a candidate for superconductivity. Wegner and coworkers have therefore chosen the elimination factor $r(\boldsymbol{k}_1', \boldsymbol{k}_2'; \boldsymbol{k}_1, \boldsymbol{k}_2)$ such that it vanishes for products of biquadratic terms $c^\dagger_{\boldsymbol{p}_1'\alpha_1} c_{\boldsymbol{p}_1\alpha_2}$, $c^\dagger_{\boldsymbol{p}_1'\alpha_1} c^\dagger_{\boldsymbol{p}_2'\alpha_2}$ and $c_{\boldsymbol{p}_1\alpha_1} c_{\boldsymbol{p}_2\alpha_2}$ with total momenta 0 or $\boldsymbol{Q}$ [25, 28]. The final Hamiltonian $\tilde{H}$ for $B \to \infty$ is then of molecular-field type with the following interactions:

$$V_H(\boldsymbol{k}, \boldsymbol{q}) = V(\boldsymbol{k}, \boldsymbol{q}; \boldsymbol{k}, \boldsymbol{q}) \tag{4.304}$$

$$V_F(\boldsymbol{k}, \boldsymbol{q}) = V(\boldsymbol{k}, \boldsymbol{q}; \boldsymbol{q}, \boldsymbol{k}) \tag{4.305}$$

$$V_A(\boldsymbol{k}, \boldsymbol{q}) = V(\boldsymbol{k}, \boldsymbol{q} + \boldsymbol{Q}; \boldsymbol{q}, \boldsymbol{k} + \boldsymbol{Q}) \tag{4.306}$$

$$V_B(\boldsymbol{k}, \boldsymbol{q}) = V(\boldsymbol{k}, -\boldsymbol{k}; \boldsymbol{q}, -\boldsymbol{q}) \tag{4.307}$$

$$V_C(\boldsymbol{k}, \boldsymbol{q}) = V(\boldsymbol{k}, \boldsymbol{q} + \boldsymbol{Q}; \boldsymbol{k} + \boldsymbol{Q}, \boldsymbol{q}) \tag{4.308}$$

$$V_Y(\boldsymbol{k}, \boldsymbol{q}) = V(\boldsymbol{k}, \boldsymbol{Q} - \boldsymbol{k}; \boldsymbol{q}, \boldsymbol{Q} - \boldsymbol{q}) \ . \tag{4.309}$$

$V_H(\boldsymbol{k}, \boldsymbol{q})$ and $V_F(\boldsymbol{k}, \boldsymbol{q})$ correspond to the Landau parameters already discussed in the previous section. $V_A(\boldsymbol{k}, \boldsymbol{q})$ allows for antiferromagnetic instabilities and $V_B(\boldsymbol{k}, \boldsymbol{q})$ for superconducting instabilities. $V_C(\boldsymbol{k}, \boldsymbol{q})$ and $V_Y(\boldsymbol{k}, \boldsymbol{q})$ can lead to more complicated forms of symmetry breaking involving e.g. a staggered structure of the superconducting condensate. The specific form of r cancels out in the calculation of these effective interactions to second order in U. In particular, the Hartree–Fock type interactions $V_H(\boldsymbol{k}, \boldsymbol{q})$ and $V_F(\boldsymbol{k}, \boldsymbol{q})$ have exactly the same form (4.286) and (4.287) as derived previously.

Wegner and coworkers have thereby established a mapping from an interacting electron system to an effective molecular-field type Hamiltonian that is more general than Fermi liquid theory (4.273). In a similar manner to the analysis leading to (4.298) and (4.299), one can now analyze this effective Hamiltonian with interactions (4.304)–(4.309) in molecular-field theory and derive a phase diagram with various kinds of symmetry breaking. Results from this analysis for the two-dimensional Hubbard model [28] are shown in Fig. 4.6, which compare favorably with other approaches [32, 33]. It seems very worthwhile to explore this route in more detail. One of the important questions to address in this context is up to which values of the expansion parameter U/t one can trust the results quantitatively or qualitatively, resp. Wegner and Körding have also shown that the stability of such expansions can be improved by normal ordering with respect to the interacting (possibly symmetry–broken) ground state [4], which should be explored further.

4.5 Other Applications

In this section we want to outline other applications of the flow equation method that are somehow different in spirit from the previous examples, but that have proven useful in their own right. First we study a system with electron–phonon interaction, where the flow equation method is used to derive

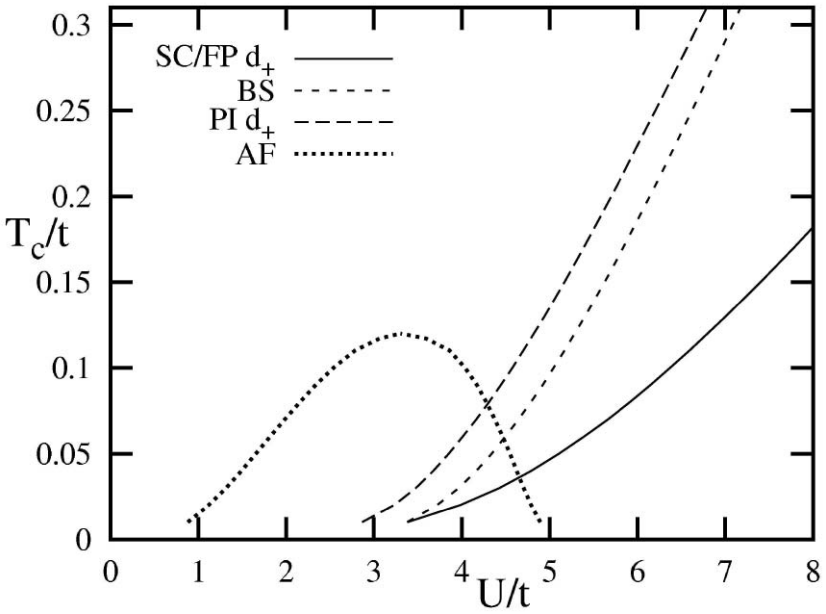

Fig. 4.6. Phase diagram of the two-dimensional Hubbard model (4.280) on a square lattice at half-filling and zero temperature as obtained by the flow equation method (4.304)–(4.309). AF denotes an antiferromagnetic phase, PI a Pomeranchuk instability, BS band splitting, FP a flux phase and SC a d-wave superconducting phase [figure from [28] with friendly permission]

an effective (attractive) electron–electron interaction. This effective electron–electron attraction turns out to be different from the classic result by Fröhlich [34] because the flow equation result also describes retardation effects which are absent in the Fröhlich result. In Sect. 4.5.2 we then use the flow equation method to systematically generate block-diagonal Hamiltonians: this idea has been initiated by Mielke [35] and was then developed further by Uhrig and coworkers in a series of papers.

This is also a good opportunity to mention another "indirect" application of flow equations, namely photorefractive two-beam coupling. It was shown by Anderson et al. [36] that this problem can be cast into a double commutator structure where the density operator of the optical field takes the role of the Hamiltonian. For more details the reader should consult the original literature.

4.5.1 Construction of Effective Hamiltonians: The Fröhlich Transformation Re-examined

Electron–phonon interactions are responsible for conventional superconductivity. The well-known key observation is the fact that electron–phonon

interactions can lead to an attractive electron–electron interaction, which in turn can then generate a pairing instability. The step from the electron–phonon interaction to the attractive electron–electron interaction is conventionally done with the Fröhlich transformation [34]. One starts with the Hamiltonian

$$H = H_0 + H_{\mathrm{e-ph}} \tag{4.310}$$

$$H_0 = \sum_{\boldsymbol{k},\alpha} \epsilon_{\boldsymbol{k}} \, : c^\dagger_{\boldsymbol{k}\alpha} c_{\boldsymbol{k}\alpha} : + \sum_{\boldsymbol{q}} \omega_{\boldsymbol{q}} \, : a^\dagger_{\boldsymbol{q}} a_{\boldsymbol{q}} : \tag{4.311}$$

$$H_{\mathrm{e-ph}} = \frac{1}{\sqrt{\Omega}} \sum_{\boldsymbol{k},\boldsymbol{q},\alpha} M_{\boldsymbol{q}} \, : \left(c^\dagger_{\boldsymbol{k}+\boldsymbol{q},\alpha} c_{\boldsymbol{k}\alpha} a_{\boldsymbol{q}} + c^\dagger_{\boldsymbol{k}\alpha} c_{\boldsymbol{k}+\boldsymbol{q},\alpha} a^\dagger_{\boldsymbol{q}} \right) : , \tag{4.312}$$

Here $a^\dagger_{\boldsymbol{q}}$, $a_{\boldsymbol{q}}$ are the bosonic creation and annihilation operators for the phonons and the parameters $M_{\boldsymbol{q}}$ describe their interaction with the electrons. We assume time-reversal invariance $\epsilon_{\boldsymbol{k}} = \epsilon_{-\boldsymbol{k}}$ and $\omega_{\boldsymbol{q}} = \omega_{-\boldsymbol{q}}$. Fröhlich performs a unitary transformation

$$H^{(\mathrm{Fr})}_{\mathrm{eff}} = \mathrm{e}^{S^{(\mathrm{Fr})}} \, H \, \mathrm{e}^{-S^{(\mathrm{Fr})}} \ , \tag{4.313}$$

where the generator $S^{(\mathrm{Fr})} = -\left(S^{(\mathrm{Fr})}\right)^\dagger$ is determined from the condition that $H^{(\mathrm{Fr})}_{\mathrm{eff}}$ should only contain phonon-number conserving terms in order M. This yields the condition

$$H_{\mathrm{e-ph}} - [H_0, S^{(\mathrm{Fr})}] = 0 \ , \tag{4.314}$$

which is solved by

$$S^{(\mathrm{Fr})} = \frac{1}{\sqrt{\Omega}} \sum_{\boldsymbol{k},\boldsymbol{q},\alpha} \frac{M_{\boldsymbol{q}}}{\epsilon_{\boldsymbol{k}+\boldsymbol{q}} - \epsilon_{\boldsymbol{k}} - \omega_{\boldsymbol{q}}} \, : \left(c^\dagger_{\boldsymbol{k}+\boldsymbol{q},\alpha} c_{\boldsymbol{k}\alpha} a_{\boldsymbol{q}} - c^\dagger_{\boldsymbol{k}\alpha} c_{\boldsymbol{k}+\boldsymbol{q},\alpha} a^\dagger_{\boldsymbol{q}} \right) : \ . \tag{4.315}$$

It is straightforward to derive

$$H^{(\mathrm{Fr})}_{\mathrm{eff}} = H_0 + \frac{1}{\Omega} \sum_{\boldsymbol{k}_1,\boldsymbol{k}_2,\boldsymbol{q},\alpha,\beta} V^{(\mathrm{Fr})}_{\boldsymbol{k}_1,\boldsymbol{k}_2,\boldsymbol{q}} \, : c^\dagger_{\boldsymbol{k}_1+\boldsymbol{q},\alpha} c^\dagger_{\boldsymbol{k}_2-\boldsymbol{q},\beta} c_{\boldsymbol{k}_2\beta} c_{\boldsymbol{k}_1\alpha} : + O(M^3) \tag{4.316}$$

with the effective electron–electron interaction

$$V^{(\mathrm{Fr})}_{\boldsymbol{k}_1,\boldsymbol{k}_2,\boldsymbol{q}} = \frac{M_{\boldsymbol{q}}^2}{2} \left[\frac{\omega_{\boldsymbol{q}}}{(\epsilon_{\boldsymbol{k}_2-\boldsymbol{q}} - \epsilon_{\boldsymbol{k}_2})^2 - \omega_{\boldsymbol{q}}^2} + \frac{\omega_{\boldsymbol{q}}}{(\epsilon_{\boldsymbol{k}_1+\boldsymbol{q}} - \epsilon_{\boldsymbol{k}_1})^2 - \omega_{\boldsymbol{q}}^2} \right] \ . \tag{4.317}$$

Alternatively, let us apply the flow equation method. In the context of the electron–phonon problem this was first done by Lenz and Wegner [37]. The generator η is chosen as

$$\eta(B) = [H_0(B), H_{\mathrm{e-ph}}(B)] \ , \tag{4.318}$$

so we try to eliminate the electron–phonon interaction. It is straightforward to derive the flow equation for the effective electron–electron interaction:

$$\frac{\mathrm{d}V^{(\mathrm{feq})}_{\boldsymbol{k}_1,\boldsymbol{k}_2,\boldsymbol{q}}(B)}{\mathrm{d}B} = M_{\boldsymbol{q}}^2 \Big[(\epsilon_{\boldsymbol{k}_2} - \epsilon_{\boldsymbol{k}_2-\boldsymbol{q}} - \omega_{\boldsymbol{q}})\, \mathrm{e}^{-B[(\epsilon_{\boldsymbol{k}_2}-\epsilon_{\boldsymbol{k}_2-\boldsymbol{q}}-\omega_{\boldsymbol{q}})^2+(\epsilon_{\boldsymbol{k}_1+\boldsymbol{q}}-\epsilon_{\boldsymbol{k}_1}-\omega_{\boldsymbol{q}})^2]} + (\epsilon_{\boldsymbol{k}_2-\boldsymbol{q}} - \epsilon_{\boldsymbol{k}_2} - \omega_{\boldsymbol{q}})\, \mathrm{e}^{-B[(\epsilon_{\boldsymbol{k}_2-\boldsymbol{q}}-\epsilon_{\boldsymbol{k}_2}-\omega_{\boldsymbol{q}})^2+(\epsilon_{\boldsymbol{k}_1}-\epsilon_{\boldsymbol{k}_1+\boldsymbol{q}}-\omega_{\boldsymbol{q}})^2]} \Big] \tag{4.319}$$

Integration over B gives (after symmetrization):

$$V^{(\mathrm{feq})}_{\boldsymbol{k}_1,\boldsymbol{k}_2,\boldsymbol{q}}(B=\infty) = \frac{M_{\boldsymbol{q}}^2}{2} \left[\frac{\epsilon_{\boldsymbol{k}_1+\boldsymbol{q}} - \epsilon_{\boldsymbol{k}_1} - \epsilon_{\boldsymbol{k}_2-\boldsymbol{q}} + \epsilon_{\boldsymbol{k}_2} - 2\omega_{\boldsymbol{q}}}{(\epsilon_{\boldsymbol{k}_2-\boldsymbol{q}} - \epsilon_{\boldsymbol{k}_2} + \omega_{\boldsymbol{q}})^2 + (\epsilon_{\boldsymbol{k}_1+\boldsymbol{q}} - \epsilon_{\boldsymbol{k}_1} - \omega_{\boldsymbol{q}})^2} + \frac{\epsilon_{\boldsymbol{k}_2-\boldsymbol{q}} - \epsilon_{\boldsymbol{k}_2} - \epsilon_{\boldsymbol{k}_1+\boldsymbol{q}} + \epsilon_{\boldsymbol{k}_1} - 2\omega_{\boldsymbol{q}}}{(\epsilon_{\boldsymbol{k}_2-\boldsymbol{q}} - \epsilon_{\boldsymbol{k}_2} - \omega_{\boldsymbol{q}})^2 + (\epsilon_{\boldsymbol{k}_1+\boldsymbol{q}} - \epsilon_{\boldsymbol{k}_1} + \omega_{\boldsymbol{q}})^2} \right] . \tag{4.320}$$

Remarkably, the flow equation result for the effective Hamiltonian

$$H^{(\mathrm{feq})}_{\mathrm{eff}} = H_0 + \frac{1}{\Omega} \sum_{\boldsymbol{k}_1,\boldsymbol{k}_2,\boldsymbol{q},\alpha,\beta} V^{(\mathrm{feq})}_{\boldsymbol{k}_1,\boldsymbol{k}_2,\boldsymbol{q}}(B=\infty)\ {:}\, c^\dagger_{\boldsymbol{k}_1+\boldsymbol{q},\alpha} c^\dagger_{\boldsymbol{k}_2-\boldsymbol{q},\beta} c_{\boldsymbol{k}_2\beta} c_{\boldsymbol{k}_1\alpha} \,{:} + O(M^3) \tag{4.321}$$

differs from the Fröhlich result in $O(M^2)$ although both calculations are correct to $O(M^3)$. Why is this the case? The simple reason is that the condition (4.314) does not uniquely determine a unitary transformation. Any interaction term in $O(M^2)$ that conserves the number of phonons can be added to $S^{(\mathrm{Fr})}$. Putting it otherwise: the effective Hamiltonians differ by a unitary transformation with an electron–electron interaction term in $O(M^2)$. Such a unitary transformation cannot change energy-diagonal scattering processes in leading order, and in fact the two results (4.317) and (4.320) for the effective interaction agree when $\epsilon_{\boldsymbol{k}_1+\boldsymbol{q}} + \epsilon_{\boldsymbol{k}_2-\boldsymbol{q}} = \epsilon_{\boldsymbol{k}_1} + \epsilon_{\boldsymbol{k}_2}$.

However, differences occur for the processes with $\boldsymbol{k}_1 = -\boldsymbol{k}_2$ which are important for superconductivity:

$$V^{(\mathrm{Fr})}_{\boldsymbol{k},-\boldsymbol{k},\boldsymbol{q}} = -\frac{\omega_{\boldsymbol{q}}\, M_{\boldsymbol{q}}^2}{\omega_{\boldsymbol{q}}^2 - (\epsilon_{\boldsymbol{k}+\boldsymbol{q}} - \epsilon_{\boldsymbol{k}})^2} \tag{4.322}$$

$$V^{(\mathrm{feq})}_{\boldsymbol{k},-\boldsymbol{k},\boldsymbol{q}} = -\frac{\omega_{\boldsymbol{q}}\, M_{\boldsymbol{q}}^2}{\omega_{\boldsymbol{q}}^2 + (\epsilon_{\boldsymbol{k}+\boldsymbol{q}} - \epsilon_{\boldsymbol{k}})^2} \,. \tag{4.323}$$

This is depicted in Fig. 4.7. Notice that the flow equation result is attractive for all momenta and does not contain divergences. This observation that the

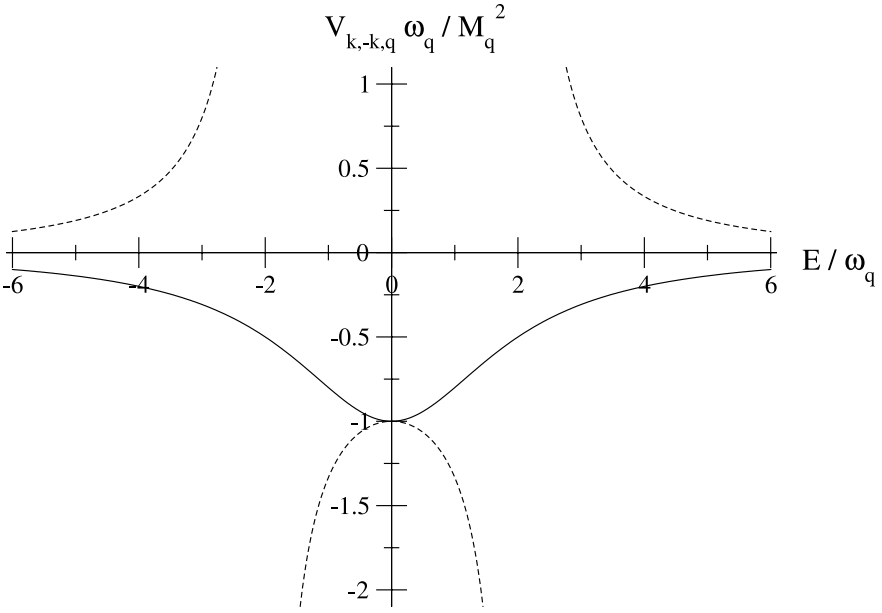

Fig. 4.7. Effective electron–electron interaction as a function of the energy transfer $E = 2(\epsilon_{\boldsymbol{k}+\boldsymbol{q}} - \epsilon_{\boldsymbol{k}})$. The full line is the flow equation result (4.323) and the dashed line the classic result (4.322) of the Fröhlich transformation

flow equation result shows less singular behavior can be traced back to (4.320) with its energy denominator consisting of a sum of squares.[27]

At this point the question arises which result is "better", the Fröhlich result for the effective electron–electron interaction or the flow equation result. One criterion would be to look at the neglected higher-order terms in (4.316) and (4.321), and in particular to require that they do not become large due to vanishing energy denominators. With respect to this criterion the flow equation result seems "better". We have seen many times in the previous chapters the importance of energy scale separation in order to arrive at controlled results. The key principle of the flow equation method is just to avoid vanishing energy denominators in each iterative step.[28]

The main advantage of a controlled expansion using the flow equation method is that the effective electron–electron interaction (4.320) correctly

[27] Similar results for the effective electron–electron interaction with a sharp cutoff in energy transfer have been obtained by Becker et al. [38] using related schemes. Our observations hold for their results as well.

[28] From a pragmatic point of view it can also be observed that the flow equation result (4.321) can be used to determine very accurately the superconducting transition temperature of realistic materials within BCS-theory, even for strong electron–phonon coupling. This has been demonstrated by Mielke [39, 40].

describes retardation effects, which are absent in the Fröhlich result (4.317). Since this point is of fundamental importance, we want to discuss it in some detail.

Retardation plays a very important role in many metallic superconductors. The key observation is that the phonon induced attractive electron–electron interaction is not instantaneous in time due to the exchange of a virtual phonon. On the other hand, the Coulomb repulsion of electrons can be considered instantaneous and therefore, in the conventional picture, less effective for destroying the pairing instability. As is traditional, let λ denote the dimensionless attractive electron–electron interaction and μ the dimensionless Coulomb repulsion (that is both couplings are multiplied with the density of states ρ_F). Then the superconducting transition temperature is given by [41]

$$T_c \propto \omega_D \, \exp\left(-\frac{1}{\lambda - \mu^*}\right) \, , \tag{4.324}$$

with the "renormalized" Coulomb repulsion

$$\mu^* = \frac{\mu}{1 + \mu \, \ln(D/\omega_D)} \, . \tag{4.325}$$

Here ω_D is the Debye frequency and D is the conduction band width. $\lambda > \mu^*$ is a necessary condition for the applicability of (4.324), otherwise there is no pairing instability. One observes that for $D/\omega_D \gg 1$ (as is the case in many metallic superconductors with ratios up to 1000), the Coulomb repulsion is strongly renormalized in (4.325). Only because of this renormalization can it in many real materials be overcome by the weak effective attractive electron–electron interaction. This raises the question how such retardation effects can be described within a Hamiltonian framework with a time-independent interaction. It is sometimes asserted that such a Hamiltonian theory can only be phenomenological and must miss the essential physics of retardation [41].

However, a careful analysis shows that this argument is incorrect. Let us introduce the total energy transfer of the electron–electron scattering process (4.321),

$$E = \epsilon_{\boldsymbol{k}_1+\boldsymbol{q}} + \epsilon_{\boldsymbol{k}_2-\boldsymbol{q}} - \epsilon_{\boldsymbol{k}_1} - \epsilon_{\boldsymbol{k}_2} \, , \tag{4.326}$$

and the partial energy transfer

$$E_{\text{part}} = \epsilon_{\boldsymbol{k}_2-\boldsymbol{q}} - \epsilon_{\boldsymbol{k}_2} \, . \tag{4.327}$$

We can rewrite the flow equation result for the effective interaction (4.320) in terms of these parameters:

$$V^{(\text{feq})}(E, E_{\text{part}}) = M_{\boldsymbol{q}}^2 \left[\frac{-E_{\text{part}} - \omega_{\boldsymbol{q}} + E/2}{(E_{\text{part}} + \omega_{\boldsymbol{q}})^2 + (E - E_{\text{part}} - \omega_{\boldsymbol{q}})^2} + \frac{E_{\text{part}} - \omega_{\boldsymbol{q}} - E/2}{(E_{\text{part}} - \omega_{\boldsymbol{q}})^2 + (E - E_{\text{part}} + \omega_{\boldsymbol{q}})^2} \right] . \tag{4.328}$$

The Fröhlich effective interaction (4.317) takes the following form:

$$V^{(\mathrm{Fr})}(E, E_{\mathrm{part}}) = M_{\boldsymbol{q}}^2 \left[\frac{\omega_q/2}{E_{\mathrm{part}}^2 - \omega_q^2} + \frac{\omega_q/2}{(E - E_{\mathrm{part}})^2 - \omega_q^2} \right] . \tag{4.329}$$

The behavior of these two effective interactions is depicted in Fig. 4.8. One notices the main difference that the flow equation effective interaction vanishes for $|E| \gg \omega_{\boldsymbol{q}}$, while the Fröhlich result does not have this property. Going from energy to time this means that $V^{(\mathrm{feq})}(E, E_{\mathrm{part}})$ describes an interaction that only contributes for scattering processes on a time scale $\Delta t \gg 1/\omega_{\boldsymbol{q}}$. But this is just what we mean by retardation; the induced attractive interaction is only present on a time scale larger than the inverse Debye frequency. On the other hand, the Fröhlich result in Fig. 4.8 describes an instantaneous interaction, which is physically wrong.

Now we would like to show that this interpretation of retardation in $V^{(\mathrm{feq})}(E, E_{\mathrm{part}})$ is consistent with the "renormalization" of the Coulomb repulsion through retardation effects as described by (4.325). In order to do this we study the flow of the electron–electron interaction

$$H_{\mathrm{int}}(B) = \frac{1}{\Omega} \sum_{\boldsymbol{k}_1, \boldsymbol{k}_2, \boldsymbol{q}} U_{\boldsymbol{k}_1, \boldsymbol{k}_2, \boldsymbol{q}}(B) \; : c^\dagger_{\boldsymbol{k}_1 + \boldsymbol{q}, \uparrow} c^\dagger_{\boldsymbol{k}_2 - \boldsymbol{q}, \downarrow} c_{\boldsymbol{k}_2 \downarrow} c_{\boldsymbol{k}_1 \uparrow} : \tag{4.330}$$

under the canonical generator. For a local Coulomb repulsion U the initial condition of the flow equations is then

$$U_{\boldsymbol{k}_1, \boldsymbol{k}_2, \boldsymbol{q}}(B = 0) = U + V^{(\mathrm{feq})}_{\boldsymbol{k}_1, \boldsymbol{k}_2, \boldsymbol{q}}(B = \infty) \; , \tag{4.331}$$

with $V^{(\mathrm{feq})}_{\boldsymbol{k}_1, \boldsymbol{k}_2, \boldsymbol{q}}(B = \infty)$ according to (4.320). In the sequel, we neglect the flow of the electron and phonon single-particle energies, which is justified for weak electron–phonon interaction. Taking these flows into account is important for calculating transition temperatures for strong electron–phonon coupling as shown by Mielke in [39].

In the BCS-channel we can use the IR-parametrization

$$U_{\boldsymbol{k}, -\boldsymbol{k}, \boldsymbol{q}}(B) = g_{\mathrm{BCS}}(B)\, \mathrm{e}^{-4B(\epsilon_{\boldsymbol{k}+\boldsymbol{q}} - \epsilon_{\boldsymbol{k}})^2} \; , \tag{4.332}$$

where $g_{\mathrm{BCS}}(B)$ is determined from the behavior at the Fermi surface with small momentum transfer $\boldsymbol{q}$. From (4.284) one can then easily derive the following flow equation in the BCS-channel:

$$\frac{\mathrm{d} g_{\mathrm{BCS}}(\Lambda_{\mathrm{feq}})}{\mathrm{d} \ln \Lambda_{\mathrm{feq}}} = \rho_F \, g^2_{\mathrm{BCS}} \; . \tag{4.333}$$

This scaling equation has already been deduced in [24] by conventional scaling methods (see also [42] for its relation to (4.325)). If we plug in the initial condition (4.331) we need to remember that the induced interaction $V^{(\mathrm{feq})}_{\boldsymbol{k}_1, \boldsymbol{k}_2, \boldsymbol{q}}$

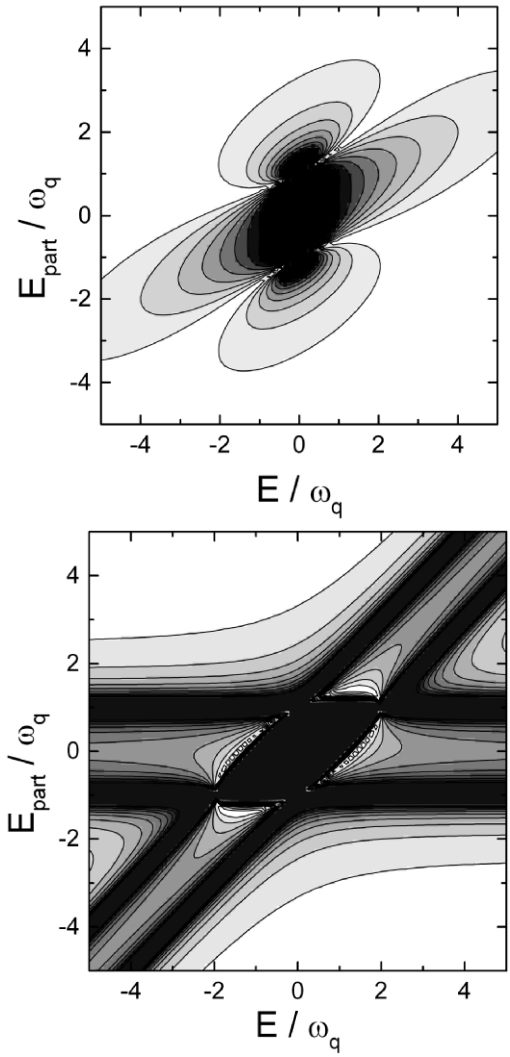

Fig. 4.8. Modulus of the effective electron–electron interaction as a function of its two parameters: the total energy transfer E of the scattering process, and the energy transfer of one of the involved electrons E_{part} (see (4.327)). Dark areas indicate large values of $|V(E, E_{\mathrm{part}})|$, light areas smaller values. The upper diagram shows the effective interaction (4.328) as derived from the flow equation method, the lower diagram the classic result (4.329) of the Fröhlich transformation. Notice that the Fröhlich result is divergent along the lines $E_{\mathrm{part}} = \pm\omega_{\boldsymbol{q}}$ and $E - E_{\mathrm{part}} = \pm\omega_{\boldsymbol{q}}$. The flow equation result describes a retarded interaction since $|V^{(\mathrm{feq})}(E, E_{\mathrm{part}})|$ decays to zero everywhere for large total energy transfer E, which is not the case for the Fröhlich effective interaction

is absent for energy transfer $|E| \gg \omega_D$. Therefore we have to integrate (4.333) from $\Lambda_{\rm feq} = D$ (conduction band width) to $\Lambda_{\rm feq} = \omega_D$ with the initial value $g_{\rm BCS}(B = 0) = U$. This leads to

$$g_{\rm BCS}(\Lambda_{\rm feq} = \omega_D) = \frac{U}{1 + \rho U \, \ln(D/\omega_D)} \; . \tag{4.334}$$

Since we have obtained scaling equations with respect to energy-diagonality $\Lambda_{\rm feq}$, the second part of (4.331) starts to contribute too once $\Lambda_{\rm feq} \approx \omega_D$. At this scale we can replace

$$g_{\rm BCS}(\Lambda_{\rm feq} = \omega_D) \quad \longrightarrow \quad \frac{U}{1 + \rho U \, \ln(D/\omega_D)} - \frac{M_D^2}{\omega_D} \; . \tag{4.335}$$

Here the second term is the induced electron–electron interaction in the BCS-channel (4.323).[29] If we integrate (4.333) further down starting at $\Lambda_{\rm feq} = \omega_D$, the running coupling constant $g_{\rm BCS}(\Lambda_{\rm feq})$ diverges at the scale

$$\Lambda_{\rm feq} = T_c \propto \omega_D \, \exp\left(\frac{1}{g^*_{\rm BCS}}\right) \tag{4.336}$$

if

$$g^*_{\rm BCS} = g_{\rm BCS}(\Lambda_{\rm feq} = \omega_D) = -\frac{M_D^2}{\omega_D} + \frac{U}{1 + \rho U \, \ln(D/\omega_D)} \tag{4.337}$$

is negative.[30] This shows the retardation effect by renormalizing the Coulomb repulsion as discussed in (4.325). Other effects of retardation can be seen in dynamical correlation functions. However, these are conceptually easy to understand from the transformation of observables similar to the discussion of the spin–boson model in Sect. 4.3. For example see [43] where the phonon damping due to the electron–phonon interaction is discussed within the flow equation framework.

Notice that there is no contradiction between our description with an effective Hamiltonian and the more conventional framework of an effective retarded action obtained from integrating out the phonon degrees of freedom in a path integral framework: the latter can no longer be mapped to a Hamiltonian due to its non-instantaneous interactions. The resolution of this apparent conflict is the observation that the degrees of freedom in these two effective theories differ: the physical electrons still appear in the effective action description, while the fermionic operators in the effective Hamiltonian description are not in one to one correspondence with the physical electrons.

[29] For clarity we assume that only the phonon modes at the Debye frequency are important, which is often a good assumption anyway.

[30] An alternative way for obtaining the superconducting transition temperature would be to use the mapping to a Hamiltonian of molecular-field type as discussed in Sect. 4.4.2.

Therefore no direct mapping between these two effective theories need to exist without extending the Hilbert space to include the phonon degrees of freedom.

The above observations regarding the construction of effective interactions using flow equations seem to be generic and occur in other models as well. Another case discussed in the literature is the Schrieffer–Wolff transformation for mapping the Anderson impurity model to an effective Kondo model [44]. The comparison with the flow equation result worked out in [45] shows similar features to the electron–phonon problem with no divergences in the induced interactions due to quadratic terms in the denominator (4.320). For the Schrieffer–Wolff transformation it is also explicitly clear by comparison with exact Bethe ansatz results that the flow equation result is "better" (for details see the discussion in [45]). Other applications of the flow equation method to construct effective Hamiltonians can be found in the literature (e.g. for spin chains [46], for the mapping of the Hubbard model to the $t-J$-model [47], in the field of cold atom physics when analyzing Feshbach resonances [48] and boson–fermion models [49, 50], etc.) Since the derivation of effective interactions is a common topic in many-particle physics, it should be very interesting to re-analyze other many-body problems using the flow equation method.

4.5.2 Block-Diagonal Hamiltonians

In many physical problems the Hamiltonian has a "banded" structure with respect to some counting operator Q. For example, in interacting fermion systems one can introduce the number of quasiparticles, that is the number of particles above the Fermi surface plus the number of holes below the Fermi surface:

$$Q = \sum_{\boldsymbol{k},\alpha} \mathrm{sgn}(|\boldsymbol{k}| - k_F) \; : c^\dagger_{\boldsymbol{k}\alpha} c_{\boldsymbol{k}\alpha} : \; . \tag{4.338}$$

A two-particle interaction term can change Q by $0, \pm 2, \pm 4$. It would certainly be desirable to have a scheme such that the final Hamiltonian conserves Q,

$$[H(B = \infty), Q] = 0 \; , \tag{4.339}$$

while at the same time the interaction terms in $H(B)$ retain their banded structure during the flow. That is Q changes only by $0, \pm 2, \pm 4$. A general way to achieve this was first introduced by Mielke for band-diagonal matrices [35], and later generalized to many-body problems by Uhrig and coworkers [51, 52].[31] However, this route is often not as robust as Wegner's original approach as we will see in a moment.

Let us denote the states in the many-particle Hilbert space that are eigenstates of Q with eigenvalue q_i by $|i, \lambda_i\rangle$. We can then express the Hamiltonian

[31] This scheme has been called the CUT method by Uhrig et al.

in terms of its matrix elements with respect to a basis constructed from these states,

$$H_{(i\lambda_i)(j\lambda_j)} \stackrel{\text{def}}{=} \langle \mathrm{i}, \lambda_i | H | j, \lambda_j \rangle \ . \tag{4.340}$$

Notice that in general the subspace with a given value of q_i will be more than one-dimensional, therefore the need for an additional quantum number λ_i. In order to keep the notation compact, we will, however, suppress these additional quantum numbers subsequently. One chooses the following generator [35, 51]

$$\eta_{ij}(B) \stackrel{\text{def}}{=} \mathrm{sgn}(q_i(B) - q_j(B))\, H_{ij}(B) \tag{4.341}$$

and finds the flow equation:

$$\begin{aligned} \frac{\mathrm{d}H_{ij}}{\mathrm{d}B} &= -\mathrm{sgn}(q_i - q_j) \left(H_{ii} H_{ij} - H_{ij} H_{jj} \right) \\ &\quad + \sum_{k \neq i,j} \left(\mathrm{sgn}(q_i - q_k) + \mathrm{sgn}(q_j - q_k) \right) H_{ik}\, H_{kj} \ . \end{aligned} \tag{4.342}$$

It is easy to verify that this choice of the generator leads to the desired structure (4.339). In particular, if the maximum change of Q in the initial Hamiltonian is N, then $H(B)$ has the same property for all B. However, one can notice a potential danger when $H_{ii} < H_{jj}$ while $q_i > q_j$: this leads to contributions to matrix elements H_{ij} that (initially) grow exponentially and can make the method uncontrollable. Therefore the generator (4.341) does in general not respect energy scale separation and has to be used with some caution. Situations where the above scheme can be applied successfully are when the number of excitations correlates well with the energy, so that no such instabilities can occur. This has been employed by Uhrig and coworkers in a number of very interesting papers on spin chains [53, 54, 55, 56, 57]. One advantage of this scheme in these models is that the structure of the Hamiltonian stays simpler during the flow than with the canonical generator, so that one can computerize the generation of flow equations and calculate them to higher orders.[32]

References

1. G.C. Wick, Phys. Rev. **80**, 268 (1950)
2. F.G. Scholtz, B.H. Bartlett, and H.B. Geyer, Phys. Rev. Lett. **91**, 080602 (2003)
3. J.N. Kriel, A.Y. Morozov, and F.G. Scholtz, J. Phys. A **38**, 205 (2005)
4. E. Körding and F. Wegner, J. Phys. A **39**, 1231 (2006)
5. K.W. Becker, A. Hübsch, and T. Sommer, Phys. Rev. B **66**, 235115 (2002)
6. A. Hübsch and K.W. Becker, Phys. Rev. B **71**, 155116 (2005)

[32] The flow equation method as a tool to systematically extend perturbation theory has also been used in numerous other publications, see for example [58, 59, 60, 61, 62, 63, 64, 65].

7. W. Hofstetter and S. Kehrein, Phys. Rev. B **63**, 140402 (2001)
8. S. Kehrein, Phys. Rev. Lett. **95**, 056602 (2005)
9. A.C. Hewson: *The Kondo Problem to Heavy Fermions*, 1st edn (Cambridge University Press, Cambridge 1993)
10. D. Withoff and E. Fradkin, Phys. Rev. Lett. **64**, 1835 (1990)
11. M. Vojta and R. Bulla, Phys. Rev. B **65**, 014511 (2002)
12. L. Fritz and M. Vojta, Phys. Rev. B **70**, 214427 (2004)
13. A.J. Leggett, S. Chakravarty, A.T. Dorsey, M.P.A. Fisher, A. Garg, and W. Zwerger, Rev. Mov. Phys. **59**, 1 (1987)
14. U. Weiss: *Quantum Dissipative Systems*, 2nd edn (World Scientific, Singapore 1999)
15. S. Kehrein and A. Mielke, Ann. Phys. (Leipzig) **6**, 90 (1997)
16. S. Kehrein and A. Mielke, J. Stat. Phys. **90**, 889 (1998)
17. T. Stauber and A. Mielke, J. Phys. A **36**, 2707 (2003)
18. T. Stauber, Phys. Rev. B **68**, 125102 (2003)
19. S. Kleff, S. Kehrein, and J. von Delft, Phys. Rev. B **70**, 014516 (2004)
20. F. Wegner, Ann. Phys. (Leipzig) **3**, 77 (1994)
21. A. Kabel and F. Wegner, Z. Phys. B **103**, 555 (1997)
22. T. Stauber, Phys. Rev. B **69**, 113315 (2004)
23. P. Nozières: *Theory of Interacting Fermi Systems*, 1st edn (Benjamin, New York 1964)
24. R. Shankar, Rev. Mod. Phys. **66**, 129 (1994)
25. I. Grote, E. Körding and F. Wegner, J. Low Temp. Phys. **126**, 1385 (2002)
26. V. Hankevych, I. Grote, and F. Wegner, Phys. Rev. B **66**, 094516 (2002)
27. V. Hankevych and F. Wegner, Acta Phys. Pol. B **34**, 497 (2003); Erratum **34**, 1591 (2003)
28. V. Hankevych and F. Wegner, Eur. Phys. J. B **31**, 497 (2003)
29. M. Salmhofer, Comm. Math. Phys. **194**, 249 (1998)
30. C. Honerkamp and M. Salmhofer, Phys. Rev. B **64**, 184516 (2001)
31. S. Andergassen, T. Enss, V. Meden, W. Metzner, U. Schollwöck, and K. Schönhammer, Phys. Rev. B **70**, 075102 (2004)
32. C.J. Halboth and W. Metzner, Phys. Rev. B **61**, 7364 (2000)
33. C.J. Halboth and W. Metzner, Phys. Rev. Lett. **85**, 5162 (2000)
34. H. Fröhlich, Proc. Roy. Soc. A **215**, 291 (1952)
35. A. Mielke, Eur. Phys. J. B **5**, 605 (1998)
36. D.Z. Anderson, R.W. Brockett, and N. Nuttall, Phys. Rev. Lett. **82**, 1418 (1999)
37. P. Lenz and F. Wegner, Nucl. Phys. B[FS] **482**, 693 (1996)
38. A. Hübsch and K.W. Becker, Eur. Phys. J. **33**, 391 (2003)
39. A. Mielke, Europhys. Lett. **40**, 195 (1997)
40. A. Mielke, Ann. Phys. (Leipzig) **6**, 215 (1997)
41. P.B. Allen and B. Mitrović, Theory of Superconducting T_c.. In: *Solid State Physics*, vol 37, ed by H. Ehrenreich, F. Seitz, D. Turnbull (Academic Press, New York 1982), pp 1–92
42. E.W. Carlson, V.J. Emery, S.A. Kivelson, and D. Orgad, Concepts in High Temperature Superconductivity. In: *The Physics of Superconductors*, vol 2, ed by K.H. Bennemann, J.B. Ketterson (Springer, Berlin Heidelberg New York 2004), pp 275–452
43. M. Ragwitz and F. Wegner, Eur. Phys. J. B **8**, 9 (1999)

44. J.R. Schrieffer and P.A. Wolff, Phys. Rev. **149**, 491 (1966)
45. S. Kehrein and A. Mielke, Ann. Phys. (NY) **252**, 1 (1996)
46. C. Raas, A. Bühler, and G.S. Uhrig, Eur. Phys. J. B **21**, 369 (2001)
47. A. Reischl, E. Müller–Hartmann, and G.S. Uhrig, Phys. Rev. B **70**, 245124 (2004)
48. T. Domanski, Phys. Rev. A **68**, 013603 (2003)
49. T. Domanski and J. Ranninger, Phys. Rev. B **63**, 134505 (2001)
50. T. Domanski and J. Ranninger, Phys. Rev. Lett. **91** 255301 (2003)
51. C. Knetter and G.S. Uhrig, Eur. Phys. J. B **13**, 209 (2000)
52. C.P. Heidbrink and G.S. Uhrig, Eur. Phys. J. B **30**, 443 (2002)
53. C. Knetter, K.P. Schmitt, and G.S. Uhrig, Eur. Phys. J. B **36**, 525 (2004)
54. K.P. Schmidt, H. Monien, and G.S. Uhrig, Phys. Rev. B **67**, 184413 (2003)
55. K.P. Schmidt and G.S. Uhrig, Phys. Rev. Lett. **90**, 227204 (2003)
56. K.P. Schmidt, Ch. Knetter, and G.S. Uhrig, Phys. Rev. B **69**, 104417 (2004)
57. Ch. Knetter and G.S. Uhrig, Phys. Rev. Lett. **92**, 027204 (2004)
58. J. Stein, J. Stat. Phys. **88**, 487 (1997)
59. J. Stein, Eur. Phys. J. B **5**, 193 (1998)
60. S. Dusuel and J. Vidal, Phys. Rev. Lett. **93**, 237204 (2004)
61. S. Dusuel and J. Vidal, Phys. Rev. B **71**, 224420 (2005)
62. S. Dusuel and J. Vidal, Phys. Rev. A **71**, 060304 (2005)
63. W. Brenig, Phys. Rev. B **67**, 064402 (2003)
64. A.B. Bylev and H.J. Pirner, Phys. Lett. B **428**, 329 (1998)
65. D. Cremers and A. Mielke, Physica D **126**, 123 (1999)

5 Modern Developments

In this final chapter we discuss three developments of the flow equation approach that promise to be particularly fruitful directions for future applications:

- Strong-coupling models (Sect. 5.1)
- Non-equilibrium problems (Sect. 5.2)
- Real time evolution (Sect. 5.3)

These problems are often difficult to treat with conventional analytical many-body techniques, while first applications of the flow equation method have shown remarkable success. We discuss one model application in each of these categories – and hope that readers of this book will contribute to the future development of these ideas.

5.1 Strong-Coupling Behavior: Sine–Gordon Model

Many of the most interesting many-body systems are strong-coupling models, which means that the scaling flow drives the interaction couplings to larger and larger values in the physically relevant scaling limit. Famous examples are the Kondo model in condensed matter physics, or QCD in high-energy theory. Since the scaling equations themselves are derived perturbatively, strong-coupling behavior implies that we are eventually leaving the region of applicability of our scaling equations. While one can still obtain valuable information about the low-energy physics from the scaling equations, like the scaling invariants which determine the relevant low-energy scales, it is generally not possible to say what kind of physics takes place at these energy scales. A good example is the Kondo model, where the perturbative scaling equations identify the Kondo temperature, which corresponds to the energy scale where the impurity spin is screened into a Kondo singlet. However, what we really need to know in order to describe low-temperature experiments is the response of the Fermi sea to the formation of this Kondo singlet, which is out of reach for the perturbative scaling analysis.

Flow equations have turned out to be a tool that can go beyond these limitations of conventional scaling analysis for *some* strong-coupling models. Examples discussed so far in the literature are the sine–Gordon model [1, 2]

Stefan Kehrein: *The Flow Equation Approach to Many-Body Problems*
STMP **217**, 137–168 (2006)

and the Kondo model [3]. The key feature of these applications is that the expansion parameter of the flow equation approach turns out to be different from the running coupling constant, and in fact remains finite during the entire flow from weak to strong coupling. However, in order to make use of such an expansion parameter one cannot work with the canonical generator η, which in turn makes it clear that these ideas cannot be generalized to all strong-coupling models. We will see below what kind of conditions seem necessary to make strong-coupling problems amenable to a flow equation analysis with a controlled expansion parameter.

It is also worthwhile to remark that both the Kondo model and the sine–Gordon model can be solved exactly using integrable model methods [4]. However, as usual such techniques are limited to linear dispersion relations and other integrability constraints. These limitations do not appear in the flow equation strong-coupling analysis. For example, based on the flow equation solution of the Kondo model [3] it has been possible to discuss time-dependent Kondo physics [5] and Ising-coupled Kondo impurities [6], both of which have so far not been solved by exact analytical methods. This observation that the flow equation solution does not rely on integrability constraints is one key motivation for studying such strong-coupling models using flow equations. Since we have already looked at numerous impurity models in the past chapters, we will here outline the flow equation diagonalization of the sine–Gordon model.

5.1.1 Sine–Gordon Model

The sine–Gordon model describes a one-dimensional translation-invariant system of interacting bosons,

$$H = \int \mathrm{d}x \left(\frac{1}{2} \Pi^2(x) + \frac{1}{2} \left(\frac{\partial \phi}{\partial x} \right)^2 + g \, \Lambda^2 \, \cos(\beta \phi(x)) \right) . \tag{5.1}$$

Here $\phi(x)$ is a bosonic field and $\Pi(x)$ its conjugate momentum field with the canonical commutator

$$[\Pi(x), \phi(y)] = -i\delta(x-y) . \tag{5.2}$$

The sine–Gordon model (5.1) is of paradigmatic importance in condensed matter theory and describes a large number of physical systems like the one-dimensional Hubbard model, the spin-1/2 X-Y-Z chain , the Thirring model or the two-dimensional Coulomb gas [4]. Its behavior is determined by the coupling constant $g > 0$ and the parameter β. Λ in (5.1) is the UV-cutoff, which is also implicitly cutting off all momentum sums that occur in the mode expansion of the Hamiltonian.

A perturbative scaling analysis in the coupling constant leads to the following two scaling equations upon varying the cutoff [4]:

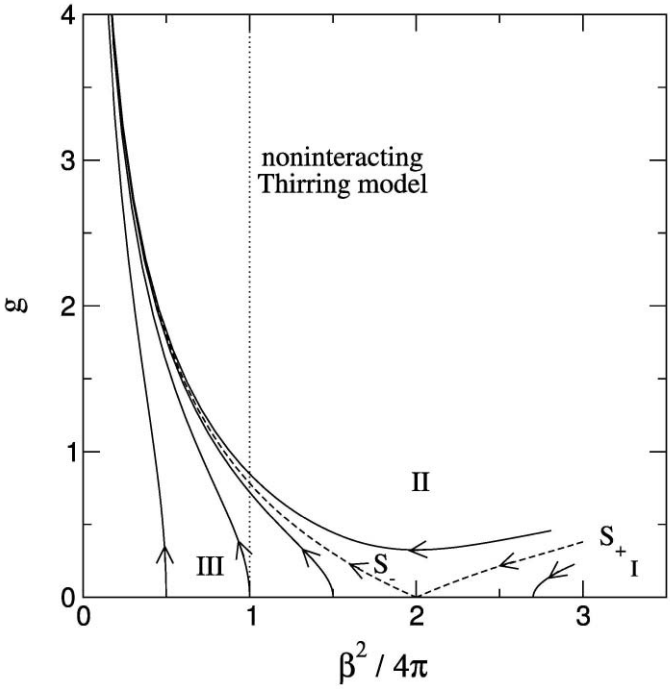

Fig. 5.1. Perturbative scaling flow and phase diagram of the sine–Gordon model. The strong-coupling phase is to the *left* and/or above the Kosterlitz–Thouless transition line S_+, the weak-coupling phase lies below S_+. The *dotted line* for $\beta^2 = 4\pi$ corresponds to the noninteracting Thirring model, see text

$$\begin{aligned} \frac{\mathrm{d}\beta^{-2}}{\mathrm{d}\ln \Lambda_{\mathrm{RG}}} &= -\frac{g^2}{4\pi} + O(g^3) \\ \frac{\mathrm{d}g}{\mathrm{d}\ln \Lambda_{\mathrm{RG}}} &= \left(\frac{\beta^2}{4\pi} - 2\right) g + O(g^2) \ . \end{aligned} \tag{5.3}$$

The resulting scaling flow is depicted in Fig. 5.1. In the weak-coupling phase I below the line S_+ (that is for sufficiently large values of $\beta^2/4\pi$) the running coupling constant g flows to zero in the infrared limit and we can trust our scaling equations (5.3) along the entire flow. On the other hand, in the strong-coupling regimes II and III the running coupling constant becomes larger and larger, which shows that the perturbative scaling approach eventually breaks down. The separatrix S_+ between the weak- and strong-coupling phase describes a Kosterlitz–Thouless phase transition.

From the exact inverse scattering solution [4] we know that a mass gap M opens in the spectrum of the sine–Gordon model in the strong-coupling phase. For example for $1 - \beta^2/8\pi \gg g$ one derives

$$M \propto \Lambda \left(\frac{g}{2 - \beta^2/4\pi} \right)^{1/(2-\beta^2/4\pi)} , \tag{5.4}$$

which is also a scaling invariant of the equations (5.3). We next derive the flow equation generalization of (5.3), which allows us to see how this mass gap develops and what the low-energy excitations above the mass gap are. This kind of information cannot be inferred from the conventional perturbative scaling picture.

5.1.2 Flow Equation Analysis

Our discussion of the flow equation diagonalization of the sine–Gordon Hamiltonian (5.1) follows closely the presentation in [2], to which we refer the reader for more details. The main purpose of this presentation is to outline the essential steps and ideas without going into the technical and somehow lengthy steps of the full calculation. For this reason we also quote many results without giving a self-contained derivation.

First we need to rewrite the Hamiltonian (5.1) in a form that is better suited for the flow equation approach. We expand the fields in normal modes:

$$\begin{aligned} \phi(x) &= -\frac{\mathrm{i}}{\sqrt{4\pi}} \sum_{k>0} \frac{1}{\sqrt{k}} \left(\mathrm{e}^{-\mathrm{i}kx} \left(a_l^\dagger(k) + a_r(-k) \right) - \mathrm{e}^{\mathrm{i}kx} \left(a_l(k) + a_r^\dagger(-k) \right) \right) \\ \Pi(x) &= \frac{1}{\sqrt{4\pi}} \sum_{k>0} \sqrt{k} \left(\mathrm{e}^{-\mathrm{i}kx} \left(a_l^\dagger(k) - a_r(-k) \right) + \mathrm{e}^{\mathrm{i}kx} \left(a_l(k) - a_r^\dagger(-k) \right) \right) . \end{aligned} \tag{5.5}$$

Here and in the sequel all sums over wavevectors are to be understood as

$$\sum_k \stackrel{\mathrm{def}}{=} \frac{2\pi}{L} \sum_{n=-\infty}^{\infty} , \tag{5.6}$$

where $k = 2\pi n/L$. L is the system size which we keep finite until the very end of the calculation (when we can send it to infinity) in order to avoid infrared problems. The operators $a_t^\dagger(k), a_t(k)$ with $t = l, r$ correspond to left- and right-movers, resp. The only nonvanishing commutators are

$$[a_t(k), a_{t'}^\dagger(k')] = \delta_{tt'} \, \delta_{kk'} \, \frac{L}{2\pi} . \tag{5.7}$$

The bosonic vacuum is annihilated by

$$a_l(k)|\Omega\rangle = a_r(-k)|\Omega\rangle = 0 \tag{5.8}$$

for $k > 0$. The Hamiltonian (5.1) can be rewritten in the following way:

$$H = \sum_{k>0} k \left(a_l^\dagger(k) a_l(k) + a_r^\dagger(-k) a_r(-k) \right) \tag{5.9}$$
$$+ \frac{g}{2\pi a^2} \left(\frac{2\pi a}{L} \right)^{\alpha^2} \int \mathrm{d}x \left(V_l(\alpha; x)\, V_r(-\alpha; x) + V_r(\alpha; x)\, V_l(-\alpha; x) \right) .$$

Here we have used the identification

$$\alpha \stackrel{\text{def}}{=} \frac{\beta}{\sqrt{4\pi}} . \tag{5.10}$$

In (5.9) $a \propto \Lambda^{-1}$ plays the role of the inverse UV-cutoff, which now only appears inside the vertex operators:

$$V_l(\alpha; x) \stackrel{\text{def}}{=} :\exp\left(\alpha \sum_{k>0} \mathrm{e}^{-ak/2} \frac{1}{\sqrt{k}} \left(\mathrm{e}^{-\mathrm{i}kx}\, a_l^\dagger(k) - \mathrm{e}^{\mathrm{i}kx}\, a_l(k) \right) \right): \tag{5.11}$$
$$V_r(\alpha; x) \stackrel{\text{def}}{=} :\exp\left(\alpha \sum_{k>0} \mathrm{e}^{-ak/2} \frac{1}{\sqrt{k}} \left(\mathrm{e}^{-\mathrm{i}kx}\, a_r(-k) - \mathrm{e}^{\mathrm{i}kx}\, a_r^\dagger(-k) \right) \right): .$$

Vertex Operators

We sum up some fundamental properties of vertex operators before we continue with our derivation. Vertex operators are essentially normal-ordered exponentials of bosonic fields like (5.11).[1] For more details and the derivation of these properties one can for example consult [7].

The operator product expansion of two left-moving vertex operators leads to:

$$V_l(\alpha; x)\, V_l(-\alpha; y) = \left(\frac{L/2\pi}{i(y-x) + a} \right)^{\alpha^2} \tag{5.12}$$
$$\times \left(1 + i\alpha(y-x) \sum_{k>0} \mathrm{e}^{-ak/2} \sqrt{k} \left(\mathrm{e}^{-\mathrm{i}kx}\, a_l^\dagger(k) + \mathrm{e}^{\mathrm{i}kx}\, a_l(k) \right) + O((y-x)^2) \right)$$

Likewise for the right-movers:

$$V_r(\alpha; x)\, V_r(-\alpha; y) = \left(\frac{L/2\pi}{i(x-y) + a} \right)^{\alpha^2} \tag{5.13}$$
$$\times \Bigg(1 + i\alpha(x-y) \sum_{k>0} \mathrm{e}^{-ak/2} \sqrt{k} \left(\mathrm{e}^{-\mathrm{i}kx}\, a_r(-k) + \mathrm{e}^{\mathrm{i}kx}\, a_r^\dagger(-k) \right)$$
$$+ O((y-x)^2) \Bigg) .$$

[1] Remember that normal-ordering with respect to the bosonic vacuum just amounts to commuting all annihilation operators to the right, see (4.20).

Using the representation of the δ-function

$$\lim_{a\to 0}\left(\frac{1}{i(y-x)+a}+\frac{1}{i(x-y)+a}\right)=2\pi\,\delta(x-y)\;, \tag{5.14}$$

one can immediately deduce the following anticommutation relation from (5.12) and (5.13) for $\alpha=1$:

$$\{V_t(1;x),V_t(-1;y)\}=L\,\delta(x-y)\;. \tag{5.15}$$

This holds without any higher order terms if we take the limit $a\to 0$. For $\alpha=1$ the vertex operators therefore behave like fermions. In fact, they are fermionic solitons made up of bosonic excitations [8].

We will later also need the following normalized Fourier transforms of vertex operators:

$$P_t(\alpha;k)\stackrel{\text{def}}{=}\left(\frac{\Gamma(\alpha^2)}{2\pi L}\,\left(\frac{L\,|k|}{2\pi}\right)^{1-\alpha^2}\right)^{1/2}\int \mathrm{d}x\,\mathrm{e}^{-\mathrm{i}kx}\,V_t(-\alpha;x)\;. \tag{5.16}$$

These operators act like soliton creation and annihilation operators for left and right movers with the properties

$$\begin{aligned} P_l\,(\alpha;k)|\Omega\rangle=P_l^\dagger(\alpha;-k)|\Omega\rangle=0\quad&\text{for } k>0\\ P_r\,(\alpha;-k)|\Omega\rangle=P_r^\dagger(\alpha;k)|\Omega\rangle=0\quad&\text{for } k>0 \end{aligned} \tag{5.17}$$

and

$$\begin{aligned} \langle P_l\,(\alpha;k)\,P_l^\dagger(\alpha;k')\rangle=\langle P_r^\dagger(\alpha;k')\,P_r\,(\alpha;k)\rangle=\delta_{kk'}\,\Theta(k)\,\frac{L}{2\pi}\\ \langle P_l^\dagger(\alpha;k')\,P_l\,(\alpha;k)\rangle=\langle P_r\,(\alpha;k)\,P_r^\dagger(\alpha;k')\rangle=\delta_{kk'}\,\Theta(-k)\,\frac{L}{2\pi} \end{aligned} \tag{5.18}$$

with respect to the bosonic vacuum.

Generator (Part 1)

The elimination of interaction matrix elements that couple modes with large energy differences implies that the interaction in (5.9) becomes nonlocal. Of course, translation invariance is preserved, which leads us to the following ansatz for the flowing Hamiltonian:

$$H(B)=H_0+H_{\text{int}}(B) \tag{5.19}$$

with

$$H_0=\sum_{k>0}k\,\left(a_l^\dagger(k)a_l\,(k)+a_r^\dagger(-k)a_r(-k)\right) \tag{5.20}$$

$$H_{\text{int}}(B)=\int \mathrm{d}x\,\mathrm{d}y\,u(y;B)\left(V_l(\alpha;x)\,V_r(-\alpha;x-y)+V_r(\alpha;x-y)\,V_l(-\alpha;x)\right) \tag{5.21}$$

Here

$$u(y; B = 0) = \frac{1}{2\pi a^2} \left(\frac{2\pi a}{L}\right)^{\alpha^2} g\, \delta(y) \ , \tag{5.22}$$

where g is the initial dimensionless coupling constant from (5.1). One can easily verify:

$$\begin{aligned} \left[\sum_{k>0} k\, a_l^\dagger(k) a_l(k), V_l(\alpha; x)\right] &= i\partial_x\, V_l(\alpha; x) \\ \left[\sum_{k>0} k\, a_r^\dagger(-k) a_r(-k), V_r(\alpha; x)\right] &= -i\partial_x\, V_r(\alpha; x) \ . \end{aligned} \tag{5.23}$$

The canonical generator follows as:

$$\begin{aligned} \eta^{(1)}(B) &\stackrel{\text{def}}{=} [H_0, H_{\text{int}}(B)] \\ &= -2i \int \mathrm{d}x\, \mathrm{d}y\, \frac{\partial u(y; B)}{\partial y} \Big(V_l(\alpha; x)\, V_r(-\alpha; x - y) + \text{h.c.} \Big). \end{aligned} \tag{5.24}$$

From $[\eta^{(1)}(B), H_0]$ we can now deduce the linear part of the flow equations:

$$\begin{aligned} [\eta^{(1)}(B), H_0] &= 4 \int \mathrm{d}x\, \mathrm{d}y\, \frac{\partial^2 u(y; B)}{\partial y^2} \Big(V_l(\alpha; x)\, V_r(-\alpha; x - y) + \text{h.c.} \Big) \\ \Rightarrow \quad \frac{\partial u(y; B)}{\partial B} &= 4\, \frac{\partial^2 u(y; B)}{\partial y^2} \ . \end{aligned} \tag{5.25}$$

The solution with the initial condition (5.22) is:

$$u(y; B) = \frac{1}{2\pi a^2} \left(\frac{2\pi a}{L}\right)^{\alpha^2} g\, \frac{\mathrm{e}^{-y^2/16B}}{\sqrt{16\pi B}} \ . \tag{5.26}$$

We are working in position space instead of the more familiar momentum representation. This turns out to be the more convenient notation for the operator product expansion that we encounter later on. However, these two representations are, of course, fully equivalent.

Commutator $[\eta^{(1)}, H_{\text{int}}]$

The commutator $[\eta^{(1)}, H_{\text{int}}]$ is as usual the centerpiece of the calculation. A typical term that enters here is[2]

$$[V_l(\alpha; x_1)\, V_r(-\alpha; x_1 - y_1), V_r(\alpha; x_2)\, V_l(-\alpha; x_2 - y_2)] \ . \tag{5.27}$$

[2] $[\eta^{(1)}, H_{\text{int}}]$ generates another term with only scaling dimensions $+\alpha$ or $-\alpha$ in (5.27). However, such commutators lead to terms with larger scaling dimensions in the OPE, which we can neglect later on anyway [2].

Since vertex operators are complicated exponentials of bosonic operators, such commutators produce new interactions that were not previously contained in the interaction Hamiltonian. Our usual procedure to organize the resulting expansion was normal-ordering. However, it is easy to see that normal-ordering of products of vertex operators leads to non-local vertex operators. Therefore we will be less ambitious than usual and introduce a simplified procedure that only subtracts the ground state expectation values. We denote this by $*O*$ to avoid confusion with the usual normal-ordering prescription,

$$*\,O* \stackrel{\text{def}}{=} O - \langle O \rangle \tag{5.28}$$

for any composite operator O. Inserting this in (5.27) leads to

$$\begin{aligned}
&[V_l(\alpha;x_1)\,V_r(-\alpha;x_1-y_1), V_r(\alpha;x_2)\,V_l(-\alpha;x_2-y_2)] \\
&= \langle V_l(\alpha;x_1)V_l(-\alpha;x_2-y_2)\rangle\,\langle V_r(-\alpha;x_1-y_1)V_r(\alpha;x_2)\rangle \\
&\quad -\langle V_l(-\alpha;x_2-y_2)V_l(\alpha;x_1)\rangle\,\langle V_r(\alpha;x_2)V_r(-\alpha;x_1-y_1)\rangle \\
&\quad +\langle V_l(\alpha;x_1)V_l(-\alpha;x_2-y_2)\rangle\ *V_r(-\alpha;x_1-y_1)V_r(\alpha;x_2)* \\
&\quad + *V_l(\alpha;x_1)V_l(-\alpha;x_2-y_2)*\ \langle V_r(-\alpha;x_1-y_1)V_r(\alpha;x_2)\rangle \\
&\quad -\langle V_l(-\alpha;x_2-y_2)V_l(\alpha;x_1)\rangle\ *V_r(\alpha;x_2)V_r(-\alpha;x_1-y_1)* \\
&\quad - *V_l(-\alpha;x_2-y_2)V_l(\alpha;x_1)*\ \langle V_r(\alpha;x_2)V_r(-\alpha;x_1-y_1)\rangle \\
&\quad +R
\end{aligned} \tag{5.29}$$

with

$$\begin{aligned}
R = &*V_l(\alpha;x_1)V_l(-\alpha;x_2-y_2)*\ *V_r(-\alpha;x_1-y_1)V_r(\alpha;x_2)* \\
&- *V_l(-\alpha;x_2-y_2)V_l(\alpha;x_1)*\ *V_r(\alpha;x_2)V_r(-\alpha;x_1-y_1)*\ .
\end{aligned} \tag{5.30}$$

Even if the reader skips the remaining somehow technical aspects of the calculation, it is recommended to go through the following argument that explains the essential difference between conventional scaling and the flow equation approach in this model.

The only terms that are structurally more complicated than the terms originally contained in the Hamiltonian consist of products of four vertex operators and enter via the R-term in (5.29). In the R-term we now use the operator product expansions (5.12) and (5.13) and neglect all higher order terms that consist of more than two bosonic operators.[3] After some algebra [2] this yields

$$[\eta^{(1)}, H_{\text{int}}] \;\longrightarrow\; -2\psi(B) \sum_{k>0} k \left(a_l^\dagger(k)a_r^\dagger(-k) + a_r(-k)a_l(k)\right) \tag{5.31}$$

with

[3] In the language of conventional RG this amounts to neglecting irrelevant operators.

$$\psi(B) = -\frac{32}{a^2}\left(\frac{32B}{a^2}\right)^{1-\alpha^2} g^2 \frac{\alpha^2}{4\Gamma(\alpha^2-1)} \tag{5.32}$$

for small momenta $|k| \ll B^{-1/2}$. This operator product expansion in the R-term is the only step in the calculation where we are forced to use an approximation. The key observation of our calculation is the Γ-function in the denominator of (5.32), which implies that the R-term itself vanishes for $\alpha^2 = 1$. This is easy to understand since for $\alpha = \pm 1$ the vertex operator describe fermions which obey the usual anticommutation relations (5.15). Therefore according to (2.93) no higher order terms are generated in a commutator of the structure (5.29), and we are able to solve the unitary flow on the line $\alpha = 1$ (corresponding to $\beta^2 = 4\pi$) exactly. This line $\beta^2 = 4\pi$ corresponds to the non-interacting Thirring model. From our discussion here we can therefore already conclude that the scaling flow deduced from the flow equation method will *not cross* the line $\beta^2 = 4\pi$ in Fig. 5.1.

New diagonal term $H_{\mathrm{diag}}(B)$

Before we deal with the R-term (5.31), let us look at the terms in the third to sixth line of (5.29) that are generated even for $\alpha = 1$. They are not contained in the original Hamiltonian and we take them into account by introducing a new term

$$H_{\mathrm{diag}}(B) = \sum_{k>0} \omega_k(B) \Big(P_l\,(\alpha;-k)\, P_l^\dagger(\alpha;-k) + P_l^\dagger(\alpha;k)\, P_l\,(\alpha;k) + P_r^\dagger(\alpha;-k)\, P_r\,(\alpha;-k) + P_r\,(\alpha;k)\, P_r^\dagger(\alpha;k)\Big) \tag{5.33}$$

with a differential equation for $\omega_k(B)$. Of course, one also needs to calculate $[\eta^{(1)}(B), H_{\mathrm{diag}}(B)]$. One arrives at the following system of differential equations (for $|a\,k| \ll 1$, for details see [2]):

$$\frac{\mathrm{d}\omega_k(B)}{\mathrm{d}B} = -\frac{4g^2}{a^3\Gamma^2(\alpha^2)}\Big(\cos(\pi\alpha^2)\,(ak)^{2\alpha^2-1}\, v_k^2(B) + \frac{\Gamma(\alpha^2/2)}{2\pi}\,\sin(\pi\alpha^2)\,(ak)^{\alpha^2-1}\left(\frac{8B}{a^2}\right)^{-\alpha^2/2}\Big) \tag{5.34}$$

$$\frac{dv_k(B)}{dB} = -4k^2\, v_k(B) - 4k\,\omega_k(B)\, v_k(B)\ . \tag{5.35}$$

The initial conditions are $\omega_k(B=0) = 0$, $v_k(B=0) = 1$. Notice that

$$[H_0, H_{\mathrm{diag}}(B)] = 0\ , \tag{5.36}$$

therefore it is appropriate to consider $H_{\mathrm{diag}}(B)$ part of the diagonal Hamiltonian which cannot be removed through unitary transformations.

Generator (Part 2)

Next we need to deal with the newly generated term (5.31). At this point we depart from the usual choice of the canonical generator in order to simplify our calculation. We add another part to the previous generator, $\eta(B) = \eta^{(1)}(B) + \eta^{(2)}(B)$, with

$$\eta^{(2)}(B) \stackrel{\text{def}}{=} -\psi(B) \sum_{k>0} \left(a_l^\dagger(k) a_r^\dagger(-k) - a_r(-k) a_l(k) \right) . \tag{5.37}$$

It is easy to verify that the commutator

$$[\eta^{(2)}(B), H_0] \tag{5.38}$$

exactly cancels the term (5.31). Notice that $\eta^{(2)}(B)$ is still a well-behaved generator without low-energy divergences in its matrix elements. We therefore expect our expansion to be controlled without small-energy denominator problems, as will indeed be the case.

Now we need to investigate the effect of $\eta^{(2)}(B)$ on $H_{\text{int}}(B)$.[4] The key part of this calculation is the transformation of the bosonic fields:

$$\begin{aligned} \mathrm{e}^{\eta^{(2)}(B)}\, a_l(k)\, \mathrm{e}^{-\eta^{(2)}(B)} &= a_l(k)\, \cosh(\psi(B)) + a_r^\dagger(-k)\, \sinh(\psi(B)) \\ \mathrm{e}^{\eta^{(2)}(B)}\, a_r(k)\, \mathrm{e}^{-\eta^{(2)}(B)} &= a_r(k)\, \cosh(\psi(B)) + a_l^\dagger(-k)\, \sinh(\psi(B)) . \end{aligned} \tag{5.39}$$

From this it is easy to show (in leading order of the operator product expansion)

$$\begin{aligned} \mathrm{e}^{\eta^{(2)}(B)}\, H_{\text{int}}(B)\, \mathrm{e}^{-\eta^{(2)}(B)} = \left(\frac{2\pi s \sqrt{B}}{L} \right)^{2\psi\alpha^2} \int \mathrm{d}x\, \mathrm{d}y\, u(y;B) \\ \times \left(V_l(\alpha(1+\psi);x)\, V_r(-\alpha(1+\psi);x-y) + \text{h.c.} \right) , \end{aligned} \tag{5.40}$$

where the prefactor appears due to normal-ordering of the vertex operators. s is a constant of order 1.

5.1.3 Conventional Scaling vs. Flow Equations

The shift in the scaling dimension of the vertex operators in (5.40) can be interpreted as a flow of α (or β), while the prefactor leads to a flow of the coupling constant g. After some algebra one finds:

$$\frac{\mathrm{d}\beta^{-2}}{\mathrm{d}\ln \Lambda_{\text{feq}}} = -\frac{g^2 + O(g^3)}{4\pi \Gamma(-1+\beta^2/4\pi)} \tag{5.41}$$

$$\frac{\mathrm{d}g}{\mathrm{d}\ln \Lambda_{\text{feq}}} = \left(\frac{\beta^2}{4\pi} - 2 \right) g + O(g^2) . \tag{5.42}$$

[4] The effect of $\eta^{(2)}(B)$ on $H_{\text{diag}}(B)$ vanishes in leading order of the operator product expansion [2].

These scaling equations should be compared with the scaling equations (5.3) from the conventional scaling approach. The main difference is the Γ-function in the denominator of (5.41), which can be directly traced back to the structure of the R-term (5.32). The resulting flow diagram is depicted in Fig. 5.2. Its key difference from the conventional scaling picture Fig. 5.1 is the *strong-coupling fixed line* for $\beta^2 = 4\pi$ that attracts the flow in the strong-coupling phase. Since the R-term vanishes exactly for $\beta^2 = 4\pi$, we can even say that this fixed line is stable to all orders in the expansion. The structure of (5.41) also explains why it is a futile exercise to try to find this strong-coupling fixed line by expanding around $g = 0$ and $\beta^2 = 8\pi$: the correct pole in the Γ-function can only emerge after summing up all orders in the expansion around $\beta^2 = 8\pi$.

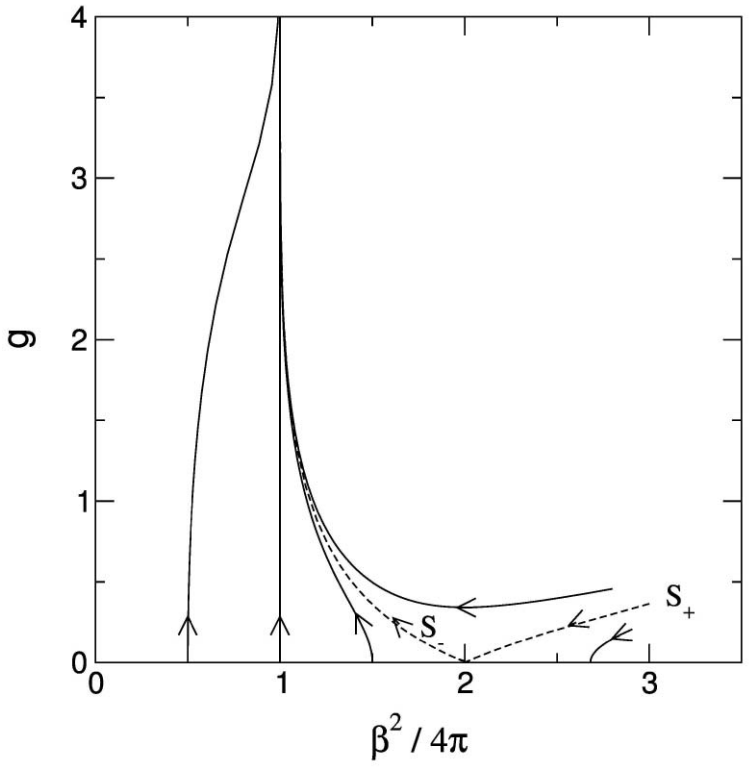

Fig. 5.2. Flow equation flow diagram of the sine–Gordon model: Notice that the scaling flow in the strong-coupling phase approaches the noninteracting Thirring model $\beta^2 = 4\pi$. This is the main difference from the conventional perturbative scaling flow depicted in Fig. 5.1 and allows for a finite expansion parameter (5.43) of the flow equation solution

Expansion Parameter

From Fig. 5.2 one concludes that the running coupling constant $g(\Lambda_{\rm feq})$ still diverges in the strong-coupling phase, which makes one wonder about the reliability of our expansion. However, all the approximations that we encountered along the way were triggered by the nonvanishing R-term (5.32), implying that our expansion parameter is actually the prefactor of this term and not simply the running coupling constant. We therefore identify the dimensionless combination

$$\epsilon(\Lambda_{\rm feq}) = g^2(\Lambda_{\rm feq})\,\frac{\beta^2/4\pi}{\Gamma(-1+\beta^2/4\pi)} \tag{5.43}$$

from (5.32) as the genuine expansion parameter of the flow equation solution of the sine–Gordon model:

- In the weak-coupling phase the running coupling constant eventually vanishes and so does the expansion parameter, which makes the results asymptotically exact.
- In the strong-coupling phase the running coupling constant diverges. However, the flow of β^2 approaches the strong-coupling fixed line much faster, so that the expansion parameter 5.43 becomes small again. This behavior is depicted in Fig. 5.3. Notice that these are universal curves in units of the mass gap M (compare (5.4)), therefore the error in our approximation always becomes largest on the energy scale set by the mass gap. Since the expansion parameter $\epsilon(\Lambda_{\rm feq})$ remains finite throughout the whole crossover from weak to strong coupling, we expect that the present order of the calculation gives reliable results, which can be systematically improved by going to higher orders.

Low-Energy Excitations

Since we have performed a controlled approximate diagonalization of the sine–Gordon Hamiltonian, we can now try to learn something about its low-energy physics. We have seen before that

$$H(B=\infty) = H_0 + H_{\rm diag}(B=\infty) \tag{5.44}$$

with:

$$H_0 = \sum_{k>0} k\,\left(a_l^\dagger(k)a_l(k) + a_r^\dagger(-k)a_r(-k)\right) \tag{5.45}$$

$$\begin{aligned} &H_{\rm diag}(B=\infty) = \\ &= \sum_{k>0}\omega_k(B=\infty)\,\Big(P_l\,(\alpha_k;-k)\,P_l^\dagger(\alpha_k;-k) + P_l^\dagger(\alpha_k;k)\,P_l\,(\alpha_k;k) \\ &\qquad + P_r^\dagger(\alpha_k;-k)\,P_r\,(\alpha_k;-k) + P_r\,(\alpha_k;k)\,P_r^\dagger(\alpha_k;k)\Big)\,. \end{aligned} \tag{5.46}$$

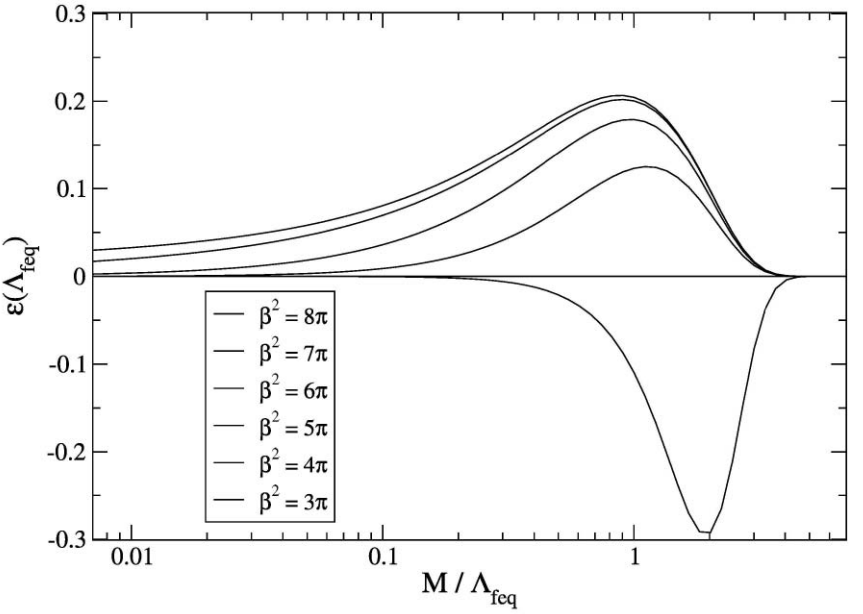

Fig. 5.3. Universal curves for the expansion parameter (5.43) of the flow equation solution in the strong-coupling phase of the sine–Gordon model. M denotes the mass gap and the curves are labeled from top to bottom with their initial parameter β^2. Notice that $\epsilon(\Lambda_{\rm feq}) \equiv 0$ for $\beta^2 = 4\pi$

Here α_k is the scaling dimension on the energy scale where this particular contribution to $H_{\rm diag}$ has been generated,

$$\alpha_k = \frac{\beta\Big(\Lambda_{\rm feq} = (k^4 + k^2\, M^2)^{1/4}\Big)}{\sqrt{4\pi}}\ . \tag{5.47}$$

Single bosonic creation and annihilation operators are not ladder operators of $H(B = \infty)$ anymore. One can verify that they are replaced by (again in leading order of an operator product expansion):

$$\begin{aligned}
[H(B=\infty), P_l^\dagger(\alpha_k;-k)] &= E_k\, P_l^\dagger(\alpha_k;-k)\\
[H(B=\infty), P_l\,(\alpha_k;k)] &= E_k\, P_l\,(\alpha_k;k)\\
[H(B=\infty), P_r^\dagger(\alpha_k;k)] &= E_k\, P_r^\dagger(\alpha_k;k)\\
[H(B=\infty), P_r\,(\alpha_k;-k)] &= E_k\, P_r\,(\alpha_k;-k)
\end{aligned} \tag{5.48}$$

with $E_k = k + \omega_k(B = \infty)$. Here $P_l^\dagger(\alpha_k;-k)$, $P_l\,(\alpha_k;k)$, $P_r^\dagger(\alpha_k;k)$ and $P_r\,(\alpha_k;-k)$ generate left moving solitons/antisolitons and right moving solitons/antisolitons, resp. From (5.34) and (5.34) one can verify that their dispersion relation is to very good accuracy given by [2]:

$$E_k = \sqrt{k^2 + M^2} \tag{5.49}$$

with the mass gap

$$M = \frac{1}{a} \lim_{\Lambda_{\mathrm{feq}} \to 0} \left[g(\Lambda_{\mathrm{feq}})\, \Lambda_{\mathrm{feq}}^{2-\beta^2(\Lambda_{\mathrm{feq}})/4\pi} \right] . \tag{5.50}$$

We see that the low-energy excitations are fermionic solitons and antisolitons with a finite mass M that depends nonperturbatively on the initial parameters, compare (5.4). Notice that eventually for $\Lambda_{\mathrm{feq}} \to 0$

$$g(\Lambda_{\mathrm{feq}}) \propto \frac{1}{\Lambda_{\mathrm{feq}}} , \tag{5.51}$$

therefore the expression (5.50) for M is finite and nonzero. Relation (5.50) also shows that a diverging dimensionless coupling constant is physically necessary and unavoidable in a scaling framework since the system exhibits a nonzero mass gap. The scaled Hamiltonian $H(\Lambda_{\mathrm{feq}})$ has to describe the same mass gap irrespective of Λ_{feq}, even in the limit $\Lambda_{\mathrm{feq}} \ll M$. Therefore its dimensionless coupling constant has to diverge according to (5.51) in order to produce a constant dimensionful product $M \propto g(\Lambda_{\mathrm{feq}})\, \Lambda_{\mathrm{feq}}$.

For this reason the search for a scaling expansion without such a strong-coupling divergence, e.g. with a critical point in the RG β-function for g, is a futile exercise. What one can realistically achieve is an approximation scheme with a finite expansion parameter that is not the running coupling constant, as we have demonstrated in this chapter.

Perspectives and Limitations

Strong-coupling models with diverging coupling constants play an important role in modern theoretical physics. It is a natural question to ask whether our flow equation calculation for the sine–Gordon model can be generalized to other models. Looking back at the key ingredients of our solution we can identify two essential points:

- The existence of a point in the parameter space where the Hamiltonian becomes simple and can be solved exactly. This is the noninteracting Thirring model in Fig. 5.1. Notice that the Hamiltonian becomes "simple" in complex objects, namely fermionic solitons and antisolitons. However, this is no problem for the flow equation machinery since we only need to know the fundamental commutators or anticommutators.
- The fact that the scaling flow drives us to this exactly solvable line in the parameter space (Fig. 5.2). In particular, this approach to the exactly solvable line turns out to be fast enough to yield a finite expansion parameter (5.43).

These conditions are very specific and do not hold for all strong-coupling problems, e.g. certainly not for QCD. One important case where the sine–Gordon calculation can be carried over is the Kondo model [3]. Here the exactly solvable line in the parameter space is the famous Toulouse line.[5]

5.2 Steady Non-Equilibrium: Kondo Model with Voltage Bias

Our current understanding of many-body physics is strongly focused on equilibrium properties or near-to-equilibrium, i.e. linear response properties. This is mainly due to a lack of suitable analytical and numerical methods that can deal with quantum many-body systems out of equilibrium. One of the main reasons for this is that typically many energy scales contribute to the behavior far out of equilibrium, while e.g. conventional RG methods only focus on the low energy degrees of freedom. Since the flow equation method does not eliminate parts of the Hilbert space, it turns out to be a very useful tool for studying quantum systems in steady non-equilibrium states beyond the linear response regime. We will discuss this below for the Kondo model with voltage bias.

5.2.1 Kondo Model in Non-Equilibrium

Recent theoretical interest in the Kondo model with voltage bias has grown largely out of experiments on quantum dots in the Coulomb blockade regime. We will leave the experimental realization aside in our discussion here, and start immediately with the suitable Hamiltonian that describes a spin-1/2 degree of freedom coupled to conduction electrons in a left (l) and a right (r) lead:

$$H = \sum_{a,p,\alpha} (\epsilon_p - \mu_a) c^\dagger_{ap\alpha} c_{ap\alpha} + \sum_{a',a} J_{a'a} \sum_{p',p} : \boldsymbol{S} \cdot \boldsymbol{s}_{(a'p')(ap)} : \ . \tag{5.52}$$

Here $a', a = l, r$ label the two leads and p', p are momentum labels, otherwise the notation is like in Sect. 4.2. We are interested in the steady non-equilibrium state that develops when we have a potential difference voltage V between the two leads: we take the chemical potentials as $\mu_{l,r} = \pm V/2$. The

[5] It is possible that other models with a mass gap can also be solved in a controlled way using flow equations even without such an exactly solvable point. The key idea would be that a mass gap can eliminate IR-divergences, which one could try to employ to obtain a controlled expansion in combination with the ideas in Sect. 4.1.5. This is similar in spirit to the symmetry-broken normal ordering prescription used in [9], and it would be very worthwhile to explore such ideas in more detail.

couplings $J_{a'a}$ describe the exchange interaction with the localized spin degree of freedom ($J_{lr} = J_{rl}$ for hermiticity). If the quantum dot can be derived from an underlying Anderson single-impurity model with tunneling rates $\Gamma_{l,r}$ from the left/right lead, the coupling constants of the effective Kondo model are related by: [10, 11]

$$\begin{aligned} J_{lr}^2 &= J_{ll} J_{rr} \\ r &\stackrel{\text{def}}{=} J_{ll}/J_{rr} = \Gamma_l/\Gamma_r \ . \end{aligned} \tag{5.53}$$

Here r is the asymmetry parameter of the model.

The fundamental theoretical problem when analyzing the Hamiltonian (5.52) is that it is unbounded from below. By moving electrons from the left to the right lead we can lower the total energy indefinitely. However, for a non-equilibrium problem like this we are not interested in the ground state, but rather in the *steady state* that develops when we start the time evolution with some given initial state (here, e.g., the noninteracting Fermi seas in the left and right leads) and then wait long enough.

Still, from the flow equation point of view nothing much changes in the analysis of (5.52) as compared to the equilibrium discussion in Sect. 4.2. We attempt to make the Hamiltonian (5.52) energy-diagonal through suitable infinitesimal unitary transformations. An approximation scheme is introduced through normal-ordering with respect to the noninteracting ground state like before in Sect. 4.2.[6] Essentially we can take over the whole system of flow equations derived in Sect. 4.2 without any additional work and just re-analyze it in a non-equilibrium setting. This is a significant advantage as compared to Keldysh-based diagrammatic calculations which need to be derived from scratch without the benefit of re-using parts of a previous calculation in a similar manner.

Before starting with the flow equation analysis, we can simplify the Hamiltonian (5.52) somewhat by making use of the relations (5.53). We introduce the following linear combination of left and right lead fermion operators

$$f_{p\alpha} \stackrel{\text{def}}{=} \frac{1}{\sqrt{1+r}}\, c_{rp\alpha} + \frac{1}{\sqrt{1+r^{-1}}}\, c_{lp\alpha} \ , \tag{5.54}$$

which obey the usual anticommutation relations $\{f_{p\alpha}, f^\dagger_{p'\beta}\} = \delta_{pp'}\delta_{\alpha\beta}$. The Kondo Hamiltonian (5.52) can then be rewritten as

$$H = \sum_{p,\alpha} \epsilon_p\, f^\dagger_{p\alpha} f_{p\alpha} + J \sum_{p',p} : \boldsymbol{S} \cdot \boldsymbol{s}_{p'p} : \ , \tag{5.55}$$

where now the conduction band spin operators $\boldsymbol{s}_{p'p} = \frac{1}{2}\sum_{\alpha,\beta} f^\dagger_{p'\alpha} \boldsymbol{\sigma}_{\alpha\beta} f_{p\beta}$ are defined for the f-operators. The antisymmetric combination

[6] We remind the reader that this is a consistent procedure up to two-loop order, see the discussion following (4.156).

$$\frac{1}{\sqrt{1+r^{-1}}}\, c_{rp\alpha} - \frac{1}{\sqrt{1+r}}\, c_{lp\alpha} \tag{5.56}$$

decouples from the impurity spin and can be ignored when deriving the flow equations. The coupling constant in (5.55) is given by $J = J_{ll} + J_{rr}$, and the zero temperature Fermi distribution function for our new f-operators follows from the original fermions in (5.52):

$$\begin{aligned} n_f(p) &= \langle f^\dagger_{p\alpha} f_{p\alpha}\rangle \\ &= \frac{1}{1+r}\,\langle c^\dagger_{rp\alpha} c_{rp\alpha}\rangle + \frac{1}{1+r^{-1}}\,\langle c^\dagger_{lp\alpha} c_{lp\alpha}\rangle \\ &= \begin{cases} 0 & \epsilon_p > \frac{V}{2} \\ \dfrac{1}{1+r^{-1}} & |\epsilon_p| \leqq \frac{V}{2} \\ 1 & \epsilon_p < -\frac{V}{2}\ . \end{cases} \end{aligned} \tag{5.57}$$

5.2.2 Flow Equation Analysis

The analysis presented here follows [12]. The starting point is the system of flow equations (4.143) and (4.144) derived previously:

$$\begin{aligned} \frac{\mathrm{d}J_{p'p}}{\mathrm{d}B} &= -(\epsilon_{p'}-\epsilon_p)^2 J_{p'p} \\ &\quad + \sum_q (\epsilon_{p'}+\epsilon_p-2\epsilon_q) J_{p'q} J_{qp}\,(n_f(q)-1/2) \\ &\quad + \frac{1}{2}\sum_{q',q} (2\epsilon_q - 2\epsilon_{q'} + \epsilon_p - \epsilon_{p'})\, J_{q'q}(K_{q'q,p'p} - K_{p'p,q'q}) \\ &\qquad \times \big(n_f(q')\,(1-n_f(q)) + n_f(q)\,(1-n_f(q'))\big) \\ &\quad + O(J^4) \end{aligned} \tag{5.58}$$

$$\begin{aligned} \frac{\mathrm{d}K_{p'p,q'q}}{\mathrm{d}B} &= -(\epsilon_{p'}+\epsilon_{q'}-\epsilon_p-\epsilon_q)^2\, K_{p'p,q'q} \\ &\quad + (\epsilon_{p'}-\epsilon_p) J_{p'p} J_{q'q} + O(J^3) \end{aligned} \tag{5.59}$$

with the initial conditions $J_{p'p}(B=0) = J_{ll} + J_{rr}$ and $K_{p'p,q'q}(B=0) = 0$.

We could now proceed directly with the numerical solution of these equations and for example work out the phase diagram of the non-equilibrium Kondo model. However, we can gain valuable analytical insights by using the diagonal parametrization,

$$\rho J_{p'p}(B) = g_{\overline{p'p}}(B)\, \mathrm{e}^{-B(\epsilon_{p'}-\epsilon_p)^2}\ . \tag{5.60}$$

Notice that here the IR-parametrization would not be a suitable approach since the coupling constants $g_{\overline{p'p}}(B)$ develop a strong and complicated dependence on the energy scale due to the presence of two Fermi surfaces. On the

other hand, we will later see by comparison with the full numerical solution that the diagonal parametrization (5.60) yields an excellent approximation.

Inserting the diagonal parametrization into (5.58) for $p' = p$ results in:

$$\begin{aligned}\frac{\mathrm{d}g_p}{\mathrm{d}B} = \frac{g_p^2}{2B}\Big(\frac{1}{1+r}\,\mathrm{e}^{-2B(-\epsilon_p - V/2)^2} + \frac{1}{1+r^{-1}}\,\mathrm{e}^{-2B(-\epsilon_p + V/2)^2}\Big) \\ -2\int \mathrm{d}\epsilon_{q'}\,\mathrm{d}\epsilon_q\,(\epsilon_{q'} - \epsilon_q)^2\, g_q\,\mathrm{e}^{-2B(\epsilon_{q'} - \epsilon_q)^2} \\ \times n_f(q')\,(1 - n_f(q))\int_0^B \mathrm{d}B'\, g_p(B')\, g_q(B')\ .\end{aligned} \tag{5.61}$$

Because $n_f(q')\,(1 - n_f(q)) \neq 0$ for all energies $|\epsilon_{q'}|, |\epsilon_q| \leqq V/2$, this whole range of energies contributes to the integral in the second line of (5.61). This is the main difference from the equilibrium case where $V = 0$. It turns out that we can replace these couplings by their average over the window $[-V/2, V/2]$ (which is responsible for transport) with very good accuracy,

$$g_t(B) \stackrel{\mathrm{def}}{=} \frac{1}{V}\int_{-V/2}^{V/2} \mathrm{d}\epsilon_q\, g_q(B)\ . \tag{5.62}$$

We insert this in (5.61) and average both sides over $\epsilon_p \in [-V/2, V/2]$, which gives a closed equation for $g_t(B)$:

$$\begin{aligned}\frac{\mathrm{d}g_t}{\mathrm{d}B} = \frac{g_t^2(B)}{2B}\,\frac{\sqrt{\pi}}{\sqrt{8B}V}\,\mathrm{erf}(\sqrt{2B}V) \\ -\frac{g_t(B)}{4B^2}\,\frac{1}{(1+r)(1+r^{-1})}\int_0^B \mathrm{d}B'\, g_t^2(B') \\ \times\Big(r + r^{-1} + 2\mathrm{e}^{-2BV^2} + \sqrt{2\pi B}V\,\mathrm{erf}(\sqrt{2B}V)\Big)\ .\end{aligned} \tag{5.63}$$

Of particular importance are the running coupling constants at the left and right Fermi surfaces,

$$g_l\,(B) \stackrel{\mathrm{def}}{=} g_{\epsilon_p = V/2}(B)\ , \quad g_r(B) \stackrel{\mathrm{def}}{=} g_{\epsilon_p = -V/2}(B)\ , \tag{5.64}$$

which determine the behavior of the quasiparticle resonances (Kondo peaks) and the phase diagram. Their flow equations follow immediately from (5.61):

$$\begin{aligned}\frac{\mathrm{d}g_l}{\mathrm{d}B} = \frac{g_l^2(B)}{2B}\Big(\frac{1}{1+r^{-1}} + \frac{1}{1+r}\,\mathrm{e}^{-2BV^2}\Big) \\ -\frac{g_t(B)}{4B^2}\,\frac{1}{(1+r)(1+r^{-1})}\int_0^B \mathrm{d}B'\, g_l(B')\, g_t(B') \\ \times\Big(r + r^{-1} + 2\mathrm{e}^{-2BV^2} + \sqrt{2\pi B}V\,\mathrm{erf}(\sqrt{2B}V)\Big)\end{aligned} \tag{5.65}$$

$$\frac{\mathrm{d}g_r}{\mathrm{d}B} = \frac{g_r^2(B)}{2B}\Big(\frac{1}{1+r} + \frac{1}{1+r^{-1}}\,\mathrm{e}^{-2BV^2}\Big) \qquad (5.66)$$
$$-\frac{g_t(B)}{4B^2}\,\frac{1}{(1+r)(1+r^{-1})}\int_0^B \mathrm{d}B'\, g_r(B')\, g_t(B')$$
$$\times\Big(r + r^{-1} + 2\mathrm{e}^{-2BV^2} + \sqrt{2\pi B}V\,\mathrm{erf}(\sqrt{2B}V)\Big)\ .$$

Before proceeding with an analytical analysis of (5.63), (5.65) and (5.66), we should verify that the solutions of these differential equations agree sufficiently accurately with the full numerical solution of the original system of differential equations (5.58) and (5.59). This step serves as an a posteriori justification of the diagonal parametrization and is important in the flow equation analysis of a complicated many-body system. Figure 5.4 contains such a comparison and shows that the approximations leading from (5.58) and (5.59) to (5.63)–(5.66) were indeed very reliable.

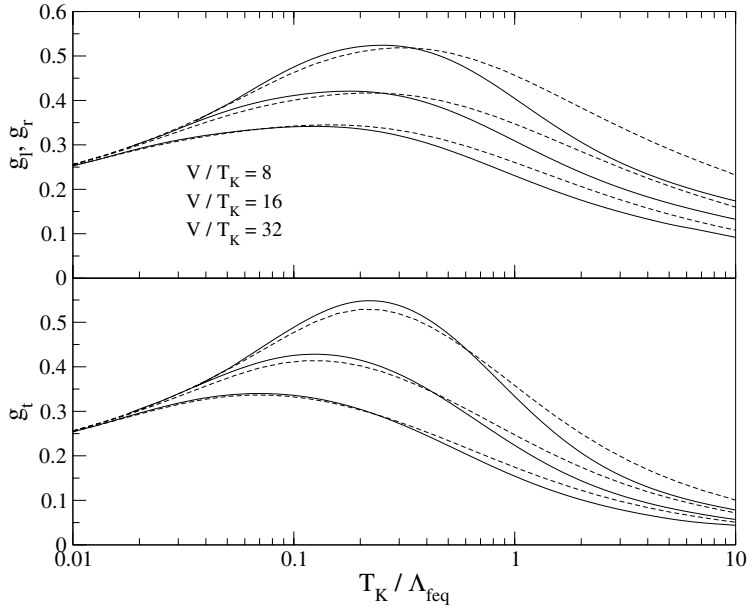

Fig. 5.4. Comparison of the flow of the coupling constants g_l and g_t from the full numerical solution of (5.58) and (5.59) with the effective equations (5.63) and (5.65). Depicted here is a symmetric Kondo dot (therefore $g_l = g_r$). The full lines refer to the full numerical solution and the dashed lines to the effective equations. Results are shown for various ratios V/T_K labeling the pairs of curves from top to bottom

Scaling Analysis

After confirming that (5.63)–(5.66) provide an accurate description of the flow, we continue with an analytical analysis. First of all, one notices that all three differential equations coincide for $\Lambda_{\rm feq} \gg V$ ($B^{-1/2} \gg V$),

$$\frac{{\rm d}g_a}{{\rm d}\Lambda_{\rm feq}} = -\frac{g_a^2}{\Lambda_{\rm feq}} + \frac{g_a^3}{2\Lambda_{\rm feq}} \tag{5.67}$$

with $a = l, r, t$. As expected one finds the conventional 2-loop scaling equation for the Kondo model (4.154) in this initial phase of the flow where the voltage bias plays no role.

Once the flow parameter is smaller than the voltage bias, $\Lambda_{\rm feq} \ll V$, the scaling equations take a different structure. The effective transport coupling obeys:

$$\frac{{\rm d}g_t}{{\rm d}\Lambda_{\rm feq}} = g_t^3 \, \frac{V}{\Lambda_{\rm feq}^2} \sqrt{\frac{\pi}{2}} \, \frac{1}{(1+r)(1+r^{-1})} \ . \tag{5.68}$$

We notice that the strong-coupling growth from the second order term has disappeared since there is no Fermi discontinuity for energy-diagonal transport processes with energy transfer $\lesssim V$. This equation has a striking (and not accidental) similarity to (4.162) for the Kondo model at finite temperature once $\Lambda_{\rm feq} \ll T$. We can therefore use the solution (4.164):

$$g_t(\Lambda_{\rm feq}) = \frac{g_*}{\sqrt{1 + \Gamma_{\rm rel}/\Lambda_{\rm feq}}} \tag{5.69}$$

for $\Lambda_{\rm feq} \ll V$. Here

$$\Gamma_{\rm rel} \stackrel{\rm def}{=} \sqrt{2\pi}\, g_*^2 \, V \, \frac{1}{(1+r)(1+r^{-1})} \tag{5.70}$$

and g_* is the running coupling constant on the scale $\Lambda_{\rm feq} = V$. From the solution of (5.67) we then find

$$g_* = g_t(\Lambda_{\rm feq} = V) = \frac{1}{\ln(V/T_{\rm K})} \ , \tag{5.71}$$

with the Kondo temperature defined from the equilibrium model:

$$\rho\, T_{\rm K} = \sqrt{\rho J_{ll} + \rho J_{rr}}\, {\rm e}^{-1/(\rho J_{ll} + \rho J_{rr})} \ . \tag{5.72}$$

Like for the case of the finite temperature Kondo model, $\Gamma_{\rm rel}$ is interpreted as a spin decoherence rate (see the results below for the spin-spin correlation function). The main difference is that here $\Gamma_{\rm rel}$ is due to the Schottky noise produced by the non-equilibrium current. One can show that for $V \gg T_{\rm K}$ the current is given by [11]

$$I = \frac{\mathrm{e}^2}{h}\,\frac{3\pi^2}{2}\,g_*^2\,V\,\frac{1}{(1+r)(1+r^{-1})}\ , \tag{5.73}$$

and therefore indeed

$$\Gamma_{\mathrm{rel}} \propto I \tag{5.74}$$

with a proportionality factor independent of V, T_{K} and r.

This spin decoherence rate has an important effect in the scaling equations for the couplings at the Fermi surfaces. For $\Lambda_{\mathrm{feq}} \ll V$ (5.65) takes the following form:

$$\frac{\mathrm{d}g_l}{\mathrm{d}\Lambda_{\mathrm{feq}}} = -\frac{1}{1+r^{-1}}\,\frac{g_l^2}{\Lambda_{\mathrm{feq}}} + g_l\,g_t^2\,\frac{V}{\Lambda_{\mathrm{feq}}^2}\,\sqrt{\frac{\pi}{2}}\,\frac{1}{(1+r)(1+r^{-1})}\ . \tag{5.75}$$

This leads to

$$\begin{aligned}\frac{\mathrm{d}g_l}{\mathrm{d}\ln\Lambda_{\mathrm{feq}}} &= -\frac{g_l^2}{1+r^{-1}} + g_l\,\frac{\mathrm{d}\ln g_t}{\mathrm{d}\ln\Lambda_{\mathrm{feq}}} \\ &= g_l\left(-\frac{g_l}{1+r^{-1}} + \frac{1}{2}\,\frac{\Gamma_{\mathrm{rel}}}{\Lambda_{\mathrm{feq}}+\Gamma_{\mathrm{rel}}}\right)\ ,\end{aligned} \tag{5.76}$$

where we have inserted the solution (5.69) for $g_t(\Lambda_{\mathrm{feq}})$. Likewise at the right Fermi surface:

$$\frac{\mathrm{d}g_r}{\mathrm{d}\ln\Lambda_{\mathrm{feq}}} = g_r\left(-\frac{g_r}{1+r} + \frac{1}{2}\,\frac{\Gamma_{\mathrm{rel}}}{\Lambda_{\mathrm{feq}}+\Gamma_{\mathrm{rel}}}\right)\ . \tag{5.77}$$

We observe an interesting *competition* between strong-coupling second order terms due to inter-lead scattering processes, and the spin decoherence effects due to the current [12]. When the running coupling constants have not become too large at the energy scale set by the decoherence rate, $\Lambda_{\mathrm{feq}} \approx \Gamma_{\mathrm{rel}}$, then the second terms on the right hand sides of (5.76) and (5.77) take over and the couplings g_l and g_r eventually decay to zero. This is depicted in Fig. 5.4 for some examples.

Phase Diagram

We can now determine the phase diagram of the Kondo model with voltage bias that is generated by the competition between strong-coupling coherence effects and non-equilibrium decoherence. We define the weak-coupling regime to be the part of parameter space where the couplings g_l and g_r remain smaller than 0.75 during the entire flow. Likewise, if at least one of these couplings becomes larger we are in the strong-coupling regime. The crossover line actually hardly depends on the specific value 0.75. The choice of this specific value is motivated by the observation that then the T-matrix reaches its unitarity limit in second order perturbation theory at the respective Fermi surface. The crossover line therefore indicates the breakdown of

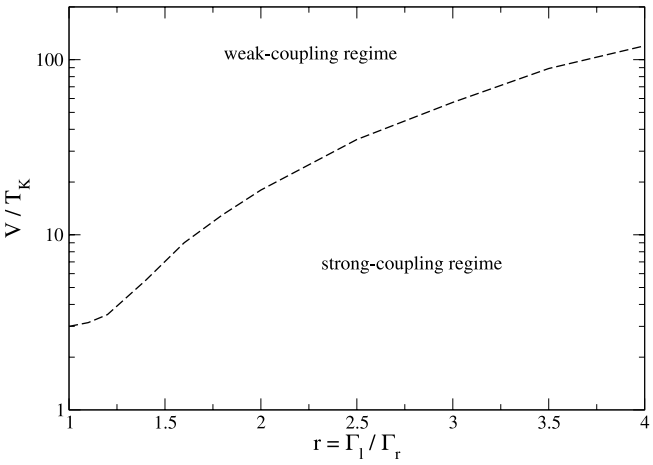

Fig. 5.5. Phase diagram of the non-equilibrium Kondo model as a function of asymmetry $r = \Gamma_l/\Gamma_r$ and voltage bias. The dashed line separates the weak-coupling regime from the strong-coupling regime, see text

the perturbative expansion in the running coupling constants, but also that the quasiparticle resonance reaches its Friedel limit. This is the physical interpretation of the crossover line, i.e. it does not indicate a phase transition. The phase diagram determined in this way from the full numerical solution of the flow equations is depicted in Fig. 5.5.

Flow Equations vs. Conventional Scaling

One important observation in the phase diagram Fig. 5.5 is that one needs to go to rather large values of the voltage bias for asymmetrically coupled Kondo dots in order to find weak-coupling physics. This is due to the suppression of the current and therefore the spin decoherence rate (5.70) for $r \neq 1$. However, in order to work out the resulting phase diagram quantitatively one needs to be able to quantitatively investigate the competition of coherence and decoherence effects in (5.76) and (5.77). We have just seen that this is straightforward in the flow equation framework, and it is worthwhile to understand this better since it is a major difference to the conventional scaling approach,

First of all, the reason why we could analyze the effect of non-equilibrium decoherence in a controlled way (that is for small running coupling constants) is the appearance of the decoherence term in linear order of the coupling constant in (5.76) and (5.77). This term was originally a third order contribution in the running coupling constant. Its remarkable *transmutation* to a first order term is due to the $V/\Lambda_{\rm feq}^2$-factor in (5.68). Similar to the finite temperature Kondo model (4.161) and (4.162), this factor is due to the phase

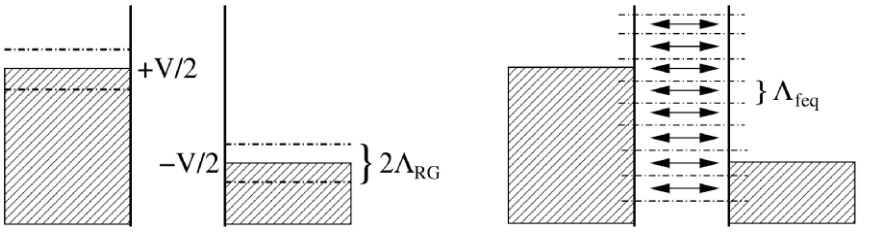

Fig. 5.6. *Left*: Conventional scaling picture where states are integrated out around the two Fermi surfaces with voltage bias V (here depicted for cutoff $\Lambda_{\rm RG} < V$). *Right*: Flow equation approach. Here all interaction matrix elements with energy transfer $|\Delta E| \lesssim \Lambda_{\rm feq}$ are retained in $H(\Lambda_{\rm feq})$

space proportional to V open for energy-diagonal processes even in the limit $\Lambda_{\rm feq} \to 0$ in the second line of (5.61). However, once this prefactor V appears, the $1/\Lambda_{\rm feq}^2$-dependence follows immediately for dimensional reasons.

The key difference between the conventional scaling approach and flow equations can then be summed up in Fig. 5.6. In the conventional scaling approach one integrates out degrees of freedom around the two Fermi surfaces. Once $\Lambda_{\rm RG} \ll V$ the Hamiltonian $H(\Lambda_{\rm RG})$ *cannot* produce a phase space factor V anymore since the energy window available for transport processes is only proportional to $\Lambda_{\rm RG}$. On the other hand, since all sufficiently energy-diagonal scattering processes are retained in the flow equation Hamiltonian $H(\Lambda_{\rm feq})$, the phase space factor V emerges naturally (see Fig. 5.6).

On a technical level the difference is that in the conventional scaling approach one purports to be able to eliminate energy-diagonal and nearly energy-diagonal scattering elements between the left and the right lead in Fig. 5.6. Even for small coupling constants this is not possible in a controlled way. Therefore a term like the one on the right hand side of (5.68) is necessarily absent and one cannot study the competition of coherence and decoherence with the scaling equations. We have thereby come full circle to our matrix picture Fig. 1.1 in the introduction where we have emphasized the difference between

- flow equations, where we retain energy-diagonal processes with $|\Delta E| \lesssim \Lambda_{\rm feq}$, and
- conventional scaling equations, where we retain states with an *absolute* energy smaller than the cutoff, $|E| < \Lambda_{\rm RG}$.

5.2.3 Correlation Functions in Non-Equilibrium: Spin Dynamics

In Chap. 3 we have worked out how to evaluate equilibrium expectation values and correlation functions within the flow equation framework. This needs to be reanalyzed now in a non-equilibrium setting like the Kondo model with voltage bias. As mentioned previously, the key problem of non-equilibrium

many-particle physics is that unlike in equilibrium one has no variational construction principle for a steady non-equilibrium state. Therefore we are forced to "construct" the steady state dynamically. Let us assume that the system is prepared in an initial state $|\Psi_i\rangle$ at time $t = 0$. In our example this is the ground state of the free electron system when the Kondo dot is not coupled to the leads. Then a correlation function in the steady state is given by

$$C_{\rm neq}(t) \stackrel{\rm def}{=} \lim_{t_w\to\infty} C(t,t_w)\ , \tag{5.78}$$

where

$$\begin{aligned} C(t,t_w) &\stackrel{\rm def}{=} \langle\Psi_i|\, O(t+t_w)\, O(t_w)\, |\Psi_i\rangle \\ &= \langle\Psi_i|\, {\rm e}^{{\rm i}H(t+t_w)}\, O\, {\rm e}^{-{\rm i}H(t+t_w)}\, {\rm e}^{{\rm i}Ht_w}\, O\, {\rm e}^{-{\rm i}Ht_w}\, |\Psi_i\rangle\ . \end{aligned} \tag{5.79}$$

Here the thermodynamic limit needs to be taken before sending the waiting time t_w for the measurement to infinity.[7] If we now insert the diagonalizing unitary transformation everywhere (like in going from (3.24) to (3.26)), we obtain

$$C(t,t_w) = \langle\Psi_i|\, U^\dagger(B=\infty)\, {\rm e}^{{\rm i}\tilde{H}(t+t_w)}\, \tilde{O}\, {\rm e}^{-{\rm i}\tilde{H}t}\, \tilde{O}\, {\rm e}^{-{\rm i}\tilde{H}t_w}\, U(B=\infty)\, |\Psi_i\rangle\ . \tag{5.80}$$

Here $\tilde{H}$ and $\tilde{O}$ are the unitarily transformed Hamiltonian and observable, resp. The basic difference from our analysis in Sect. 3.2 is that now $U(B = \infty)\,|\Psi_i\rangle$ *is not* the ground state of the diagonal Hamiltonian $\tilde{H}$. However, the difference

$$C(t,t_w) - \langle\Psi_i|\, {\rm e}^{{\rm i}\tilde{H}(t+t_w)}\, \tilde{O}\, {\rm e}^{-{\rm i}\tilde{H}t}\, \tilde{O}\, {\rm e}^{-{\rm i}\tilde{H}t_w}\, |\Psi_i\rangle \propto O(g) \tag{5.81}$$

is proportional to the running coupling constant since (loosely speaking) $U(B = \infty)$ differs from the identity operator in order the running coupling constant. So in our specific problem at hand we are left with the easier task of evaluating

$$\langle{\rm FS}|\, {\rm e}^{{\rm i}\tilde{H}(t+t_w)}\, \tilde{O}\, {\rm e}^{-{\rm i}\tilde{H}t}\, \tilde{O}\, {\rm e}^{-{\rm i}\tilde{H}t_w}\, |{\rm FS}\rangle \tag{5.82}$$

to leading order in the coupling constant. Here $|{\rm FS}\rangle$ is the noninteracting Fermi sea in the left and right lead since we took the Kondo dot to be decoupled from the leads for $t < 0$. The diagonal Hamiltonian itself takes the form

$$\tilde{H} = \sum_{p,\alpha} \epsilon_p\, f^\dagger_{p\alpha} f_{p\alpha} + i \sum_{p',p,q',q} K_{p'p,q'q}(B=\infty)\ :\boldsymbol{S}\cdot(\boldsymbol{s}_{p'p}\times\boldsymbol{s}_{q'q}):\ , \tag{5.83}$$

where $K_{p'p,q'q}(B = \infty)$ is nonvanishing only for energy-diagonal processes. If we replace $\tilde{H}$ by the free conduction electron part H_0, we are again neglecting terms in order the running coupling constant. We can say

[7] Notice that in general $C_{\rm neq}(t)$ could depend on the initial state $|\Psi_i\rangle$. However, similar to the Keldysh approach we assume that this is not the case for a "reasonable" initial state $|\Psi_i\rangle$.

$$C_{\rm neq}(t) - C^{(0)}_{\rm neq}(t) \propto O(g) \tag{5.84}$$

with

$$\begin{aligned} C^{(0)}_{\rm neq}(t) &= \langle {\rm FS}|\, {\rm e}^{{\rm i}H_0(t+t_w)}\, \tilde{O}\, {\rm e}^{-{\rm i}H_0 t}\, \tilde{O}\, {\rm e}^{-{\rm i}H_0 t_w}\, |{\rm FS}\rangle \\ &= \langle {\rm FS}|\, {\rm e}^{{\rm i}H_0 t}\, \tilde{O}\, {\rm e}^{-{\rm i}H_0 t}\, \tilde{O}\, |{\rm FS}\rangle \ . \end{aligned} \tag{5.85}$$

Notice that (5.85) does not depend on the waiting time anymore since $|{\rm FS}\rangle$ is an eigenstate of H_0. To leading order the calculation of a correlation function in the steady state therefore reduces to the same expression as in the equilibrium case. It should be mentioned that there are observables where the leading order $C^{(0)}_{\rm neq}(t)$ vanishes exactly. The most important example for this is the current across the Kondo dot. Then one has to work out the above terms in $O(g)$ explicitly, which turn out to give the leading contributions.[8]

Spin Dynamics

Let us use the above considerations to work out to the symmetrized spin-spin correlation function $C(\omega)$ and the imaginary part of the response function $\chi''(\omega)$ to leading order. We can use the expressions from the previous equilibrium calculation (4.192):

$$\begin{aligned} C(\omega) = \frac{\pi}{4} \sum_u \gamma^2_{\epsilon_u+\omega,\epsilon_u}(B=\infty) \\ \times \big(n_f(\epsilon_u)\,(1-n_f(\epsilon_u+\omega)) + n_f(\epsilon_u+\omega)\,(1-n_f(\epsilon_u)) \big) \end{aligned} \tag{5.86}$$

$$\begin{aligned} \chi''(\omega) = \frac{\pi}{4} \sum_u \gamma^2_{\epsilon_u+\omega,\epsilon_u}(B=\infty) \\ \times \big(n_f(\epsilon_u)\,(1-n_f(\epsilon_u+\omega)) - n_f(\epsilon_u+\omega)\,(1-n_f(\epsilon_u)) \big) \ . \end{aligned} \tag{5.87}$$

Notice that here we need to calculate $C(\omega)$ and $\chi''(\omega)$ individually since they will in general not be related by the fluctuation–dissipation theorem (3.40). Remember that the fluctuation–dissipation theorem does in general only hold for the ground state or the equilibrium finite temperature mixed state, whereas here we are interested in a steady non-equilibrium state.

We can use the results (4.185) and (4.186) for the coefficients:

$$\rho\, \gamma_{\epsilon+\omega,\epsilon}(B=\infty) \sim \begin{cases} \dfrac{g(B=\omega^{-2})}{\omega} & \text{for } |\omega| \gtrsim \Gamma_{\rm rel} \\ \dfrac{g_*}{\Gamma_{\rm rel}\, {\rm sgn}(\omega)} & \text{for } |\omega| \lesssim \Gamma_{\rm rel} \ , \end{cases} \tag{5.88}$$

where $\Gamma_{\rm rel}$ is given by (5.70). It is easy to work out the qualitative behavior for the spin-spin correlation function and the dynamical spin susceptibility from (5.86) and (5.87):

[8] A detailed discussion of these issues is beyond the scope of this book and the reader should consult recent research publications.

$$C(\omega) \sim \begin{cases} \dfrac{1}{\Gamma_{\rm rel}} & \text{for } |\omega| \lesssim \Gamma_{\rm rel} \\ \dfrac{\Gamma_{\rm rel}}{\omega^2} & \text{for } \Gamma_{\rm rel} \lesssim |\omega| \lesssim \dfrac{V}{(1+r)(1+r^{-1})} \\ \dfrac{g^2(\Lambda_{\rm feq}=|\omega|)}{\omega} & \text{for } |\omega| \gtrsim \dfrac{V}{(1+r)(1+r^{-1})} \end{cases} \tag{5.89}$$

$$\chi''(\omega) \sim \begin{cases} \dfrac{g_*^2}{\Gamma_{\rm rel}^2}\,\omega & \text{for } |\omega| \lesssim \Gamma_{\rm rel} \\ \dfrac{g^2(\Lambda_{\rm feq}=|\omega|)}{\omega} & \text{for } |\omega| \gtrsim \Gamma_{\rm rel}\ , \end{cases} \tag{5.90}$$

The spin-spin correlation function has a zero frequency peak of width $\Gamma_{\rm rel}$, which confirms our previous interpretation of $\Gamma_{\rm rel}$ as a spin relaxation rate. The dynamical spin susceptibility has its maximum at $\omega \approx \Gamma_{\rm rel}$,

$$\chi''(\omega = \Gamma_{\rm rel}) \sim \frac{(1+r)(1+r^{-1})}{V}\ . \tag{5.91}$$

Some quantitative results obtained from the full numerical solution of the flow equations are shown in Fig. 5.7.

Static Spin Susceptibility

The comparison of (5.89)–(5.91) with the corresponding results for the equilibrium Kondo model at finite temperature shows that the non-equilibrium Kondo model effectively looks like the equilibrium model at the temperature

$$T_{\rm eff} = \frac{V}{(1+r)(1+r^{-1})}\ . \tag{5.92}$$

This is also precisely the relation that maps the two decoherence rates (4.165) and (5.70) in equilibrium and non-equilibrium onto one another. It is therefore not surprising that the static spin susceptibility (4.201)

$$\chi_0 = \frac{2}{\pi}\int_0^\infty {\rm d}\omega\ \frac{\chi''(\omega)}{\omega} \tag{5.93}$$

obeys

$$V\,\chi_0(V) = \frac{(1+r)(1+r^{-1})}{4} \tag{5.94}$$

for $V \gg T_{\rm K}$.[9] A large voltage bias therefore suppresses the static spin susceptibility in the characteristic way (5.94), which can be interpreted as replacing the $1/4T$-Curie law by a $(1+r)(1+r^{-1})/4V$-behavior.

[9] More accurately one should actually put the stronger constraint $\Gamma_{\rm rel} \gg T_{\rm K}$. For the discussion of logarithmic corrections in (5.94) the reader should consult the recent research literature.

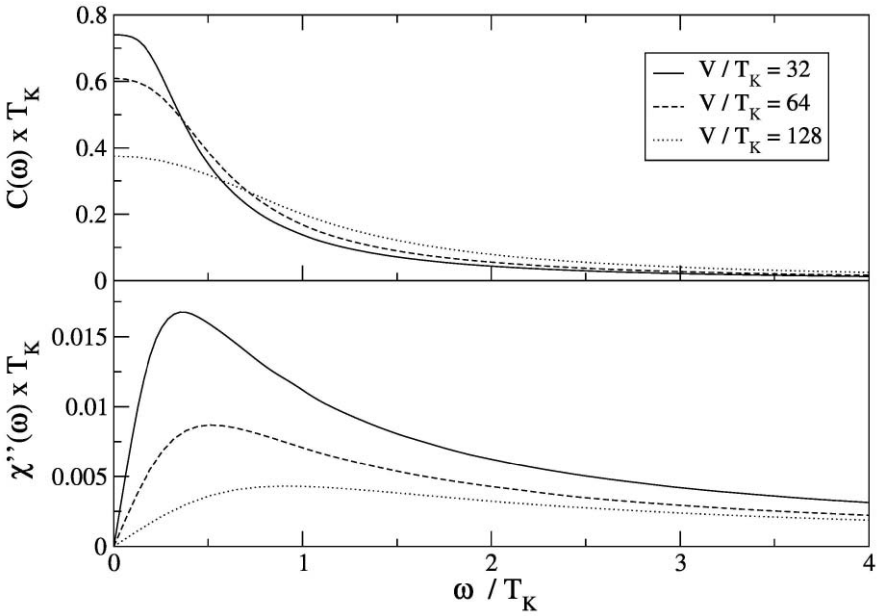

Fig. 5.7. Universal curves for the spin-spin correlation function $C(\omega)$ and the imaginary part of the dynamical spin susceptibility $\chi''(\omega)$ obtained from the full numerical solution of the flow equations (symmetric model $r = 1$) for various values of the voltage bias at zero temperature. The fluctuation–dissipation theorem (3.40) is clearly not fulfilled for these curves since we are investigating a non-equilibrium steady state

It is worthwhile to mention that this result is highly nontrivial in the framework of conventional expansion methods since it differs in zeroth order of the coupling constant from the noninteracting case, i.e. the static susceptibility of a free spin-1/2 degree of freedom. This makes it necessary to carefully reconsider perturbative expansions, and the nonequilibrium calculation is substantially more complicated than the equilibrium calculation [13]. For a very enlightening discussion of this point the reader should consult [14]. On the other hand, the derivation of (5.94) within the flow equation framework was straightforward. In fact, we could essentially just carry over the calculation for the equilibrium model at nonzero temperature.

5.3 Real Time Evolution: Spin–Boson Model

In the previous section we discussed a steady non-equilibrium situation generated by a nonzero voltage bias of the external leads. Another class of nonequilibrium problems is related to the real time evolution of a quantum system that is not prepared in its ground state, or that contains time-dependent

external parameters. Such situations occur very naturally in physical systems, and are far less well understood than equilibrium many-body systems.

The flow equation method also offers an interesting new tool for studying this class of non-equilibrium models. The key observation is that the flow equation diagonalization amounts to being able to solve the Heisenberg equations of motion for observables in an interacting system in a controlled approximation. Once one has worked out the time evolution of an operator, the time-dependent expectation value can be evaluated with respect to a given quantum state. This can be the equilibrium ground state, but also some non-equilibrium initial state. The key difference from conventional many-body techniques is that we are not following the time evolution of the quantum state (Schrödinger picture), but rather the time evolution of the operators (Heisenberg picture). In the flow equation formalism, the latter is independent of the quantum state and we can carry over the equilibrium calculation.[10] The new part of the non-equilibrium calculation is to express the initial state in the diagonal basis, or to evaluate matrix elements of the initial state with respect to the diagonal flow equation basis.

As a pedagogical example we will here study the real time evolution of the spin–boson model with an external field that is suddenly switched off at time $t = 0$. The spin–boson model in equilibrium has already been discussed in Sect. 4.3. We generalize the Hamiltonian in the following way:

$$H(t) = h(t)\,\sigma_z - \frac{\Delta}{2}\,\sigma_x + \frac{1}{2}\,\sigma_z \sum_k \lambda_k\,(a_k + a_k^\dagger) + \sum_k \omega_k\, a_k^\dagger a_k\ . \tag{5.95}$$

We take

$$h(t) = \begin{cases} h_0 & \text{for } t \leqq 0 \\ 0 & \text{for } t > 0 \end{cases} \tag{5.96}$$

and assume that at time $t = 0$ the system is in its ground state $|\Psi_i\rangle$ with respect to the nonvanishing external field h_0. One quantity of immediate interest is the subsequent decay of the spin expectation value

$$P(t) \stackrel{\text{def}}{=} \langle \Psi_i | \sigma_z(t) | \Psi_i \rangle \tag{5.97}$$

at zero temperature.

The structure of this non-equilibrium situation allows a very straightforward solution based on the flow equation diagonalization obtained in Sect. 4.3. Neglecting all higher-order terms, we deduce from (4.236) and (4.250) that $H(t)$ takes the following form in the diagonal basis for $t > 0$:

$$\tilde{H}(t) = h(t)\,\sigma_x \sum_k \chi_k(B = \infty)\,(a_k^\dagger + a_k) - \frac{\Delta_r}{2}\,\sigma_x + \sum_k \omega_k\, a_k^\dagger a_k\ . \tag{5.98}$$

[10] However, it should be mentioned that approximations are of course done with respect to a certain state. Therefore initial quantum states that are "very different" from the ground state can make the approach more complicated. This is a subject for future research.

The time-evolved observable $\sigma_z(t)$ for $t > 0$ is given by the following expression in the diagonal basis:

$$\tilde{\sigma}_z(t) = \sigma_x \sum_k \chi_k(B=\infty)\,(\mathrm{e}^{\mathrm{i}\omega_k t}\, a_k^\dagger + \mathrm{e}^{-\mathrm{i}\omega_k t}\, a_k)\ , \tag{5.99}$$

which leads to

$$P(t) = \sum_k \chi_k(B=\infty)\,\left(\mathrm{e}^{\mathrm{i}\omega_k t}\,\langle\Psi_i|a_k^\dagger|\Psi_i\rangle + \mathrm{e}^{-\mathrm{i}\omega_k t}\,\langle\Psi_i|a_k|\Psi_i\rangle\right)\ . \tag{5.100}$$

We need to find the ground state of (5.98) for $t < 0$ in order to extract these matrix elements. Clearly $\langle\Psi_i|\sigma_x|\Psi_i\rangle = 1$ for $\Delta_r > 0$, and therefore $\tilde{H}(t \leqq 0)$ can be rewritten as the quadratic form

$$\sum_k \omega_k \left(a_k^\dagger + \frac{h_0\chi_k(B=\infty)}{\omega_k}\right)\left(a_k + \frac{h_0\chi_k(B=\infty)}{\omega_k}\right) \tag{5.101}$$

plus an uninteresting constant. We need to find the ground state of (5.101). This is a trivial exercise:

$$a_k\,|\Psi_i\rangle = -\frac{h_0\chi_k(B=\infty)}{\omega_k}\,|\Psi_i\rangle\ , \tag{5.102}$$

and we find in (5.100):

$$P(t) = -2h_0 \sum_k \frac{\chi_k^2(B=\infty)}{\omega_k}\,\cos(\omega_k\, t)\ . \tag{5.103}$$

Interestingly, the Fourier transform can be expressed in a straightforward way through the equilibrium correlation function $C_{zz}^{(\mathrm{sym})}(\omega)$ from (4.248):

$$P(\omega) = -2\,\frac{h_0}{\omega}\,C_{zz}^{(\mathrm{sym})}(\omega)\ . \tag{5.104}$$

Universal curves for an Ohmic bath with various dissipation strengths are depicted in Fig. 5.8. Notice that $P(\omega = 0) \neq 0$ for an Ohmic bath, which indicates an exponential decay of the spin oscillations. The non-equilibrium preparation of the spin–boson system therefore leads to a different long-time behavior. According to (4.255) the long-time decay of the equilibrium spin-spin correlation function was algebraic, $C_{zz}^{(\mathrm{sym})}(t) \propto t^{-2}$.

Notice that it was straightforward to solve this non-equilibrium problem based on the previous equilibrium solution, while e.g. in a Keldysh-type perturbation expansion it is quite nontrivial to recover the exponential long-time decay. In the real time domain this amounts to a resummation of all powers of the system-bath coupling.

One key reason why the flow equation solution worked so easily is that we used the same flow equation diagonalization for the system with and

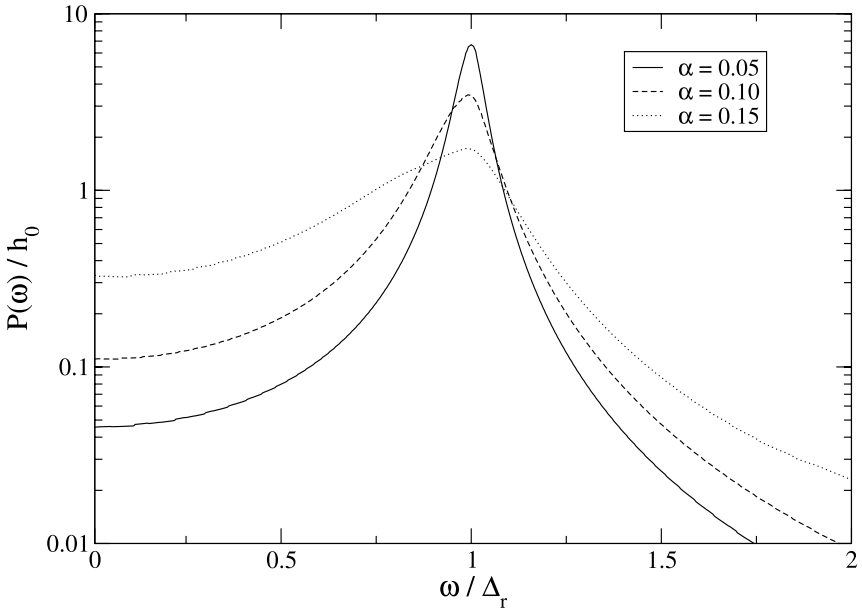

Fig. 5.8. Zero temperature decay of the spin expectation value $P(t)$ for the non-equilibrium spin–boson model (5.95) with an Ohmic bath (4.241) for various dissipation strengths α

without external field in going from (5.95) to (5.98). This is not a good approximation for large external fields (when $|h_0| \ll \Delta_r$ does no longer hold) since then $h_0\,\sigma_z$ should be considered as part of the diagonal Hamiltonian and the unitary diagonalizing transformation is different. In addition, one then needs to reconsider the ansatz for the transformation of the observable σ_z to make sure that the sum rule (4.253) is fulfilled with good accuracy also with respect to the ground state for nonzero field h_0.

Therefore the results obtained in this chapter are restricted to the regime of small fields, $|h_0| \ll \Delta_r$. Flow equation calculations for large fields and product initial states can be found in [5], where the time-dependent Kondo model has been studied using the ideas outlined above. The main difference is that the evaluation of the matrix elements in (5.100) becomes more complicated.

In conclusion, we have seen in the previous two chapters about the non-equilibrium Kondo and spin–boson model that the flow equation method allowed a very straightforward roadmap from the equilibrium model to the non-equilibrium model. While the flow equation diagonalization can be hard work for an equilibrium many-body problem as compared to conventional many-body methods, it is precisely this additional information encoded in the diagonalization procedure that permits us to go beyond equilibrium physics without much extra effort.

5.4 Outlook and Open Questions

The flow equation approach is under active development and many topics still need to be addressed and answered. I want to end this book by listing some questions and suggestions for future research:

1. The transformation of observables in a generic many-body problem needs to be better understood. Are there new considerations to be taken into account in non-equilibrium problems? Both in equilibrium and in non-equilibrium, in particular the effect of higher order terms in the flow equation expansion should be studied in more detail. What can one say about the spectral weight of these higher order terms as compared to the leading order ones? In principle it might even be possible that all the spectral weight is moved into higher and higher orders of the transformed operator expansion in an interacting many-body system.[11] Also it would be very desirable to develop reliable analytical methods for solving the flow equations for an operator that decays completely for $B \to \infty$, so that one can gain more analytical insights.
2. It would be desirable to put the relation between the flow equation approach and renormalization group methods on a more formal footing, especially the notions of relevant, marginal and irrelevant operators. What is the role of the flow equation transformation of observables and possible complete decay into a different structure in this context? What is the relation of the flow equation approach to other functional renormalization group frameworks [15, 16, 17, 18] developed recently?
3. The construction of effective theories plays a major role in many models. We have seen in Sect. 4.5.1 that contrary to conventional wisdom, Hamiltonian theories are capable of describing retardation effects in such effective theories. It would be interesting to see in which other models this observation can be useful.
4. The possibility to have a well-behaved expansion parameter in the flow equation approach which is different from the running coupling constant played a pivotal role in the strong-coupling model applications in Sect. 5.1. In what other strong-coupling models can one find similar well-behaved expansion parameters? Is it possible to use the observation that the interacting ground state can be very different from the non-interacting one to construct better behaved expansions in certain strong-coupling models, along the lines mentioned in Sect. 4.1.5 and [9]?
5. One of the most promising future applications of the flow equation method are non-equilibrium problems, both for steady states like discussed in Sect. 5.2, and for the time evolution of some initial state like in Sect. 5.3. In particular, it would be very interesting to see whether these ideas can also be used in a controlled way in strong-coupling models.

[11] Although this would not necessarily affect the results when actually evaluating correlation functions.

6. The choice of the generator is at the heart of the flow equation method. While the canonical generator seems to be the best choice from a mathematical point of view, we have sometimes encountered modifications to keep the number of newly generated terms small (for example in Sect. 4.3). Such modifications can become unavoidable in the numerical implementation of flow equations beyond the leading order calculation, since higher order interactions carry many indices and therefore lead to many differential equations. I believe that such modifications of the generator that violate energy scale separation are allowed if one deals with interactions that are quadratic (i.e., potential scattering terms) or irrelevant in the conventional scaling sense. It would be very desirable to gain a better understanding of this issue.

I hope that this book has equipped and motivated its readers to contribute to these and other developments.

References

1. S. Kehrein, Phys. Rev. Lett. **83**, 4914 (1999)
2. S. Kehrein, Nucl. Phys. B[FS] **592**, 512 (2001)
3. W. Hofstetter and S. Kehrein, Phys. Rev. B **63**, 140402 (2001)
4. A.O. Gogolin, A.A. Nersesyan, and A.M. Tsvelik: *Bosonization and Strongly Correlated Systems*, 1st edn (Cambridge University Press, Cambridge 1998)
5. D. Lobaskin and S. Kehrein, Phys. Rev. B **71**, 193303 (2005)
6. M. Garst, S. Kehrein, Th. Pruschke, A. Rosch, and M. Vojta, Phys. Rev. B **69**, 214413 (2004)
7. J. von Delft and H. Schoeller, Ann. Phys. (Leipzig) **4**, 225 (1998)
8. S. Mandelstam, Phys. Rev. D **11**, 3026 (1975)
9. E. Körding and F. Wegner, J. Phys. A **39**, 1231 (2006)
10. A. Kaminski, Yu.V. Nazarov, and L.I. Glazman, Phys. Rev. Lett. **83**, 384 (1999)
11. A. Kaminski, Yu.V. Nazarov, and L.I. Glazman, Phys. Rev. B **62**, 8154 (2000)
12. S. Kehrein, Phys. Rev. Lett. **95**, 056602 (2005)
13. J. Paaske, A. Rosch, J. Kroha, and P. Wölfle, Phys. Rev. B **70**, 155301 (2004)
14. O. Parcollet and C. Hooley, Phys. Rev. B **66**, 085315 (2002)
15. S. Andergassen, T. Enss, V. Meden, W. Metzner, U. Schollwöck, and K. Schönhammer, Phys. Rev. B **70**, 075102 (2004)
16. J. Berges, N. Tetradis, and C. Wetterich, Phys. Rep. **363**, 223 (2002)
17. C. Honerkamp and M. Salmhofer, Phys. Rev. B **64**, 184516 (2001)
18. M. Salmhofer, Comm. Math. Phys. **194**, 249 (1998)

Index

Springer Tracts in Modern Physics

177 **Applied Asymptotic Expansions in Momenta and Masses**
By Vladimir A. Smirnov 2002. 52 figs. IX, 263 pages

178 **Capillary Surfaces**
Shape – Stability – Dynamics, in Particular Under Weightlessness
By Dieter Langbein 2002. 182 figs. XVIII, 364 pages

179 **Anomalous X-ray Scattering for Materials Characterization**
Atomic-Scale Structure Determination
By Yoshio Waseda 2002. 132 figs. XIV, 214 pages

180 **Coverings of Discrete Quasiperiodic Sets**
Theory and Applications to Quasicrystals
Edited by P. Kramer and Z. Papadopolos 2002. 128 figs., XIV, 274 pages

181 **Emulsion Science**
Basic Principles. An Overview
By J. Bibette, F. Leal-Calderon, V. Schmitt, and P. Poulin 2002. 50 figs., IX, 140 pages

182 **Transmission Electron Microscopy of Semiconductor Nanostructures**
An Analysis of Composition and Strain State
By A. Rosenauer 2003. 136 figs., XII, 238 pages

183 **Transverse Patterns in Nonlinear Optical Resonators**
By K. Staliūnas, V. J. Sánchez-Morcillo 2003. 132 figs., XII, 226 pages

184 **Statistical Physics and Economics**
Concepts, Tools and Applications
By M. Schulz 2003. 54 figs., XII, 244 pages

185 **Electronic Defect States in Alkali Halides**
Effects of Interaction with Molecular Ions
By V. Dierolf 2003. 80 figs., XII, 196 pages

186 **Electron-Beam Interactions with Solids**
Application of the Monte Carlo Method to Electron Scattering Problems
By M. Dapor 2003. 27 figs., X, 110 pages

187 **High-Field Transport in Semiconductor Superlattices**
By K. Leo 2003. 164 figs.,XIV, 240 pages

188 **Transverse Pattern Formation in Photorefractive Optics**
By C. Denz, M. Schwab, and C. Weilnau 2003. 143 figs., XVIII, 331 pages

189 **Spatio-Temporal Dynamics and Quantum Fluctuations in Semiconductor Lasers**
By O. Hess, E. Gehrig 2003. 91 figs., XIV, 232 pages

190 **Neutrino Mass**
Edited by G. Altarelli, K. Winter 2003. 118 figs., XII, 248 pages

191 **Spin-orbit Coupling Effects in Two-dimensional Electron and Hole Systems**
By R. Winkler 2003. 66 figs., XII, 224 pages

192 **Electronic Quantum Transport in Mesoscopic Semiconductor Structures**
By T. Ihn 2003. 90 figs., XII, 280 pages

193 **Spinning Particles – Semiclassics and Spectral Statistics**
By S. Keppeler 2003. 15 figs., X, 190 pages

194 **Light Emitting Silicon for Microphotonics**
By S. Ossicini, L. Pavesi, and F. Priolo 2003. 206 figs., XII, 284 pages

195 **Uncovering *CP* Violation**
Experimental Clarification in the Neutral K Meson and B Meson Systems
By K. Kleinknecht 2003. 67 figs., XII, 144 pages

196 **Ising-type Antiferromagnets**
Model Systems in Statistical Physics and in the Magnetism of Exchange Bias
By C. Binek 2003. 52 figs., X, 120 pages

Springer Tracts in Modern Physics

197 **Electroweak Processes in External Electromagnetic Fields**
By A. Kuznetsov and N. Mikheev 2003. 24 figs., XII, 136 pages

198 **Electroweak Symmetry Breaking**
The Bottom-Up Approach
By W. Kilian 2003. 25 figs., X, 128 pages

199 **X-Ray Diffuse Scattering from Self-Organized Mesoscopic Semiconductor Structures**
By M. Schmidbauer 2003. 102 figs., X, 204 pages

200 **Compton Scattering**
Investigating the Structure of the Nucleon with Real Photons
By F. Wissmann 2003. 68 figs., VIII, 142 pages

201 **Heavy Quark Effective Theory**
By A. Grozin 2004. 72 figs., X, 213 pages

202 **Theory of Unconventional Superconductors**
By D. Manske 2004. 84 figs., XII, 228 pages

203 **Effective Field Theories in Flavour Physics**
By T. Mannel 2004. 29 figs., VIII, 175 pages

204 **Stopping of Heavy Ions**
By P. Sigmund 2004. 43 figs., XIV, 157 pages

205 **Three-Dimensional X-Ray Diffraction Microscopy**
Mapping Polycrystals and Their Dynamics
By H. Poulsen 2004. 49 figs., XI, 154 pages

206 **Ultrathin Metal Films**
Magnetic and Structural Properties
By M. Wuttig and X. Liu 2004. 234 figs., XII, 375 pages

207 **Dynamics of Spatio-Temporal Cellular Structures**
Henri Benard Centenary Review
Edited by I. Mutabazi, J.E. Wesfreid, and E. Guyon 2005. approx. 50 figs., 150 pages

208 **Nuclear Condensed Matter Physics with Synchrotron Radiation**
Basic Principles, Methodology and Applications
By R. Röhlsberger 2004. 152 figs., XVI, 318 pages

209 **Infrared Ellipsometry on Semiconductor Layer Structures**
Phonons, Plasmons, and Polaritons
By M. Schubert 2004. 77 figs., XI, 193 pages

210 **Cosmology**
By D.-E. Liebscher 2005. Approx. 100 figs., 300 pages

211 **Evaluating Feynman Integrals**
By V.A. Smirnov 2004. 48 figs., IX, 247 pages

213 **Parametric X-ray Radiation in Crystals**
By V.G. Baryshevsky, I.D. Feranchuk, and A.P. Ulyanenkov 2006. 63 figs., IX, 172 pages

214 **Unconventional Superconductors**
Experimental Investigation of the Order-Parameter Symmetry
By G. Goll 2006. 67 figs., XII, 172 pages

215 **Control Theory in Physics and other Fields of Science**
Concepts, Tools, and Applications
By M. Schulz 2006. 46 figs., X, 294 pages

216 **Theory of the Muon Anomalous Magnetic Moment**
By K. Melnikov, A. Vainshtein 2006. 33 figs., XII, 176 pages

217 **The Flow Equation Approach to Many-Particle Systems**
By S. Kehrein 2006. 24 figs., XII, 170 pages